AD-A046 862 CINCINNATI ELECTRONICS CORP OHIO F/G 9/1
VHF MANPACK CENTERFED WHIP ANTENNA.(U)
JUN 77 J E BRUNNER DAAB07-76-C-0109
UNCLASSIFIED 80045-URC92/777 NL

2 OF 2
AD
AD A046862

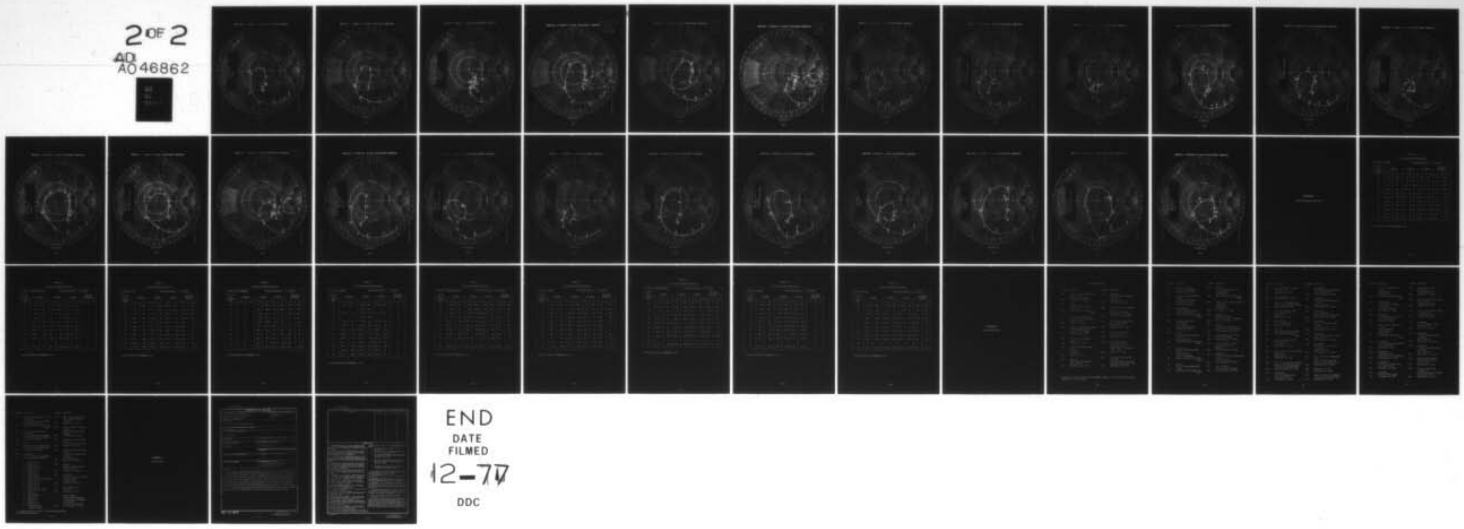

END
DATE FILMED
12-77
DDC

IMPEDANCE COORDINATES — 50-OHM CHARACTERISTIC IMPEDANCE

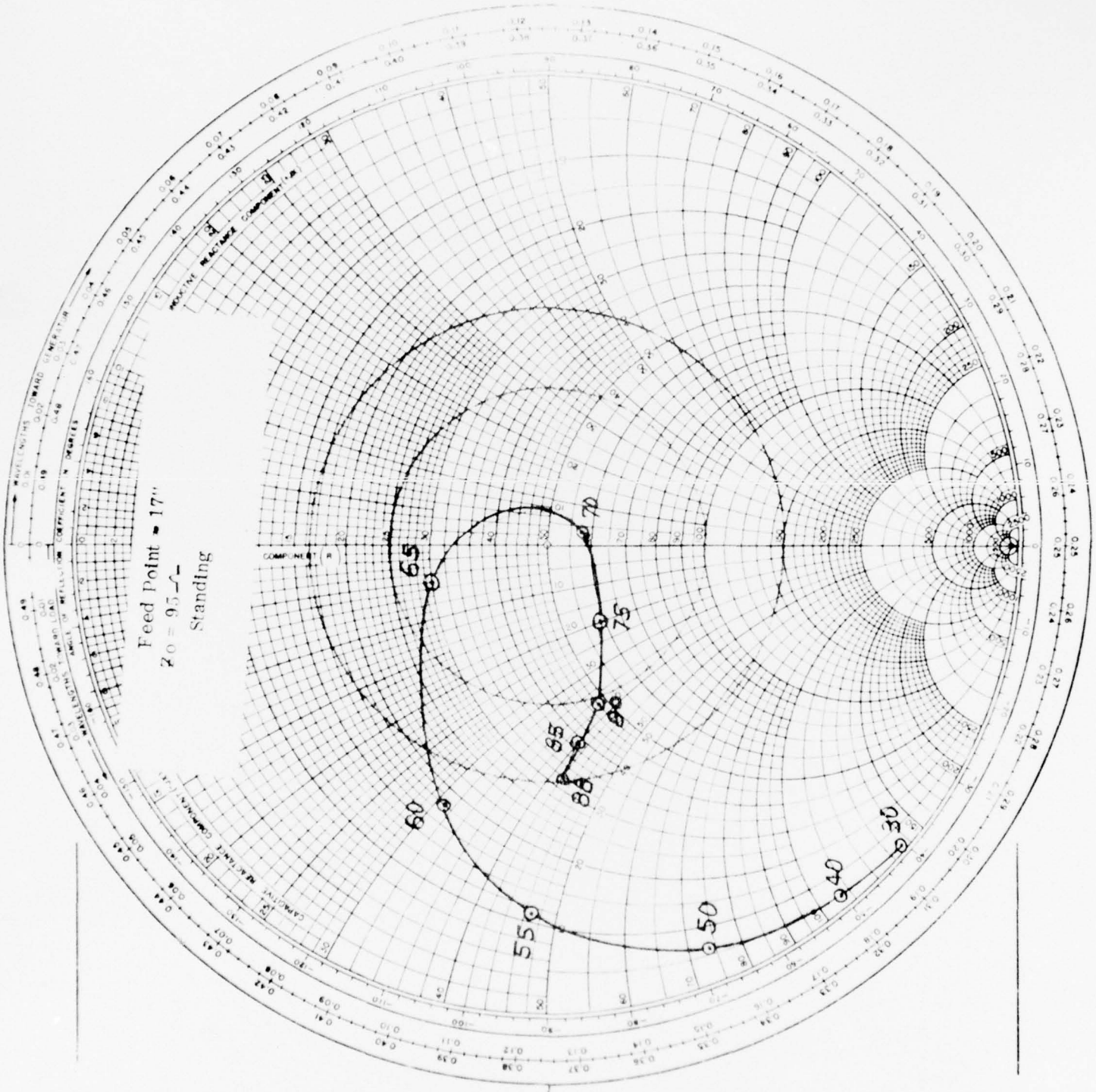

FIGURE B-4

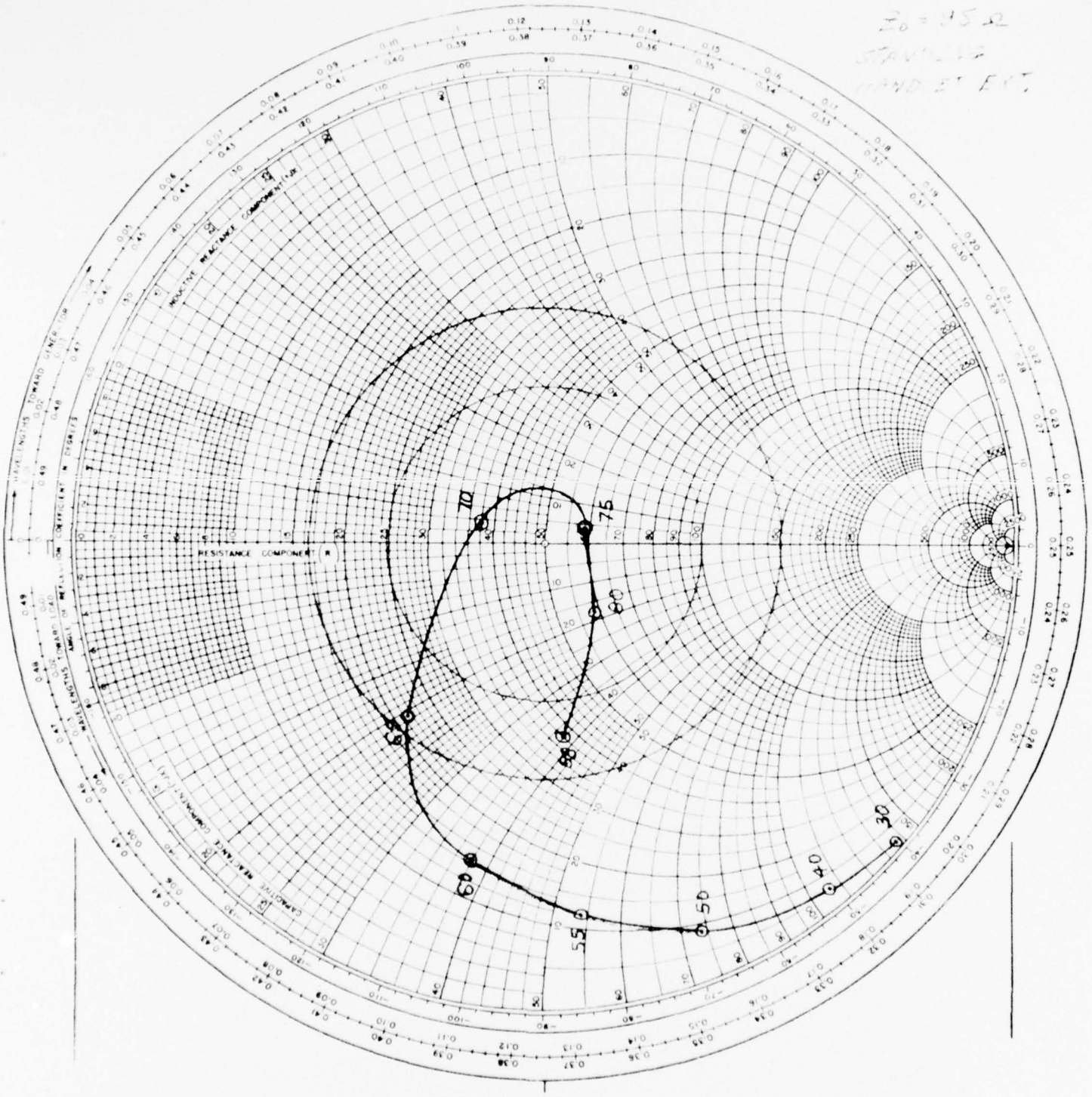
IMPEDANCE COORDINATES - 50-OHM CHARACTERISTIC IMPEDANCE
RESISTANCE COMPONENT (R)
INDUCTIVE REACTANCE COMPONENT (+jX)
70
75
80
85
60
55
50
40
30

FIGURE B-5

IMPEDANCE COORDINATES—50-OHM CHARACTERISTIC IMPEDANCE

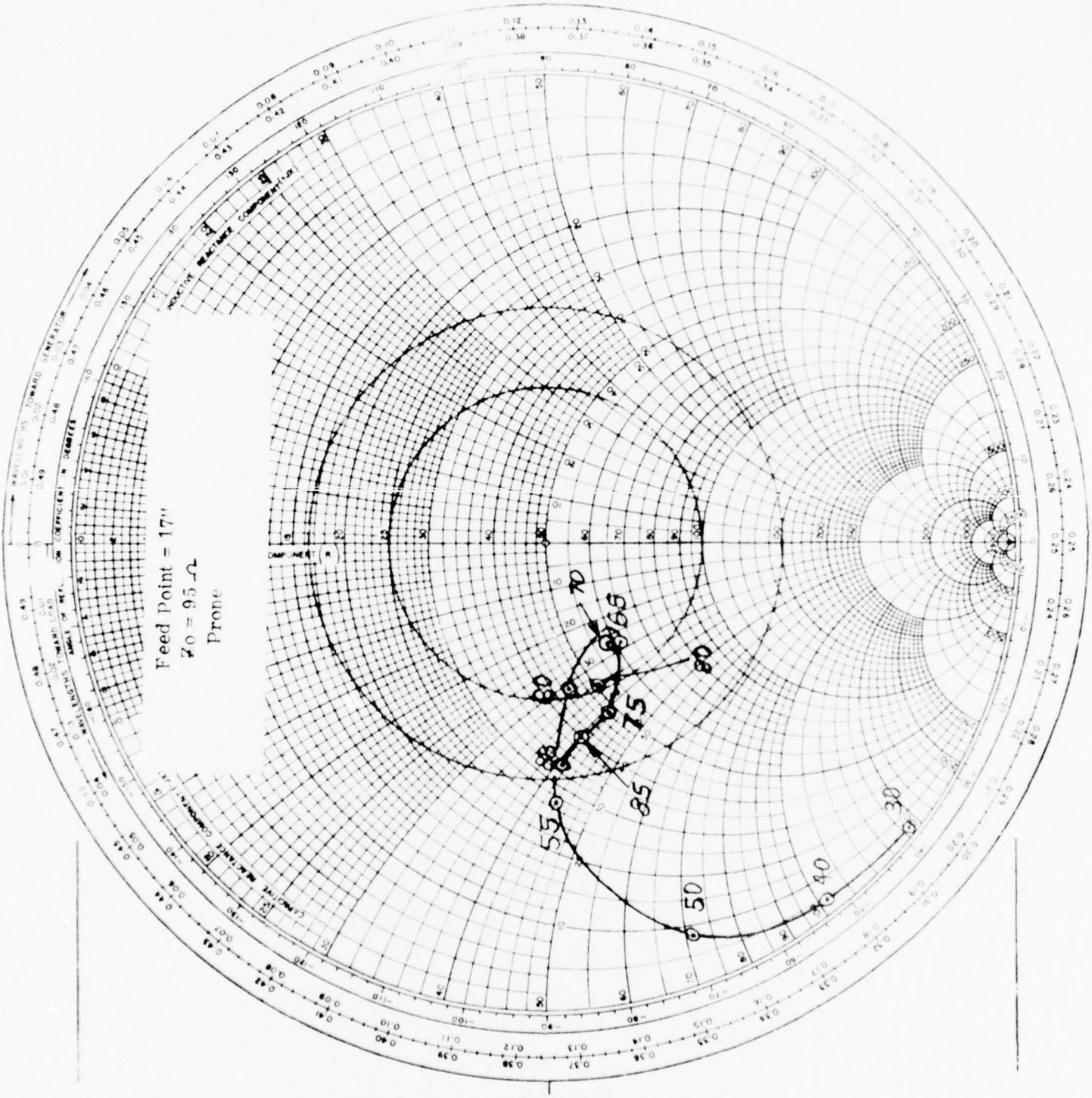

FIGURE B-6

ENG DEV. MODEL

IMPEDANCE COORDINATES—50-OHM CHARACTERISTIC IMPEDANCE $F_P = 17"$

$Z_0 = 125\Omega$

STANLING

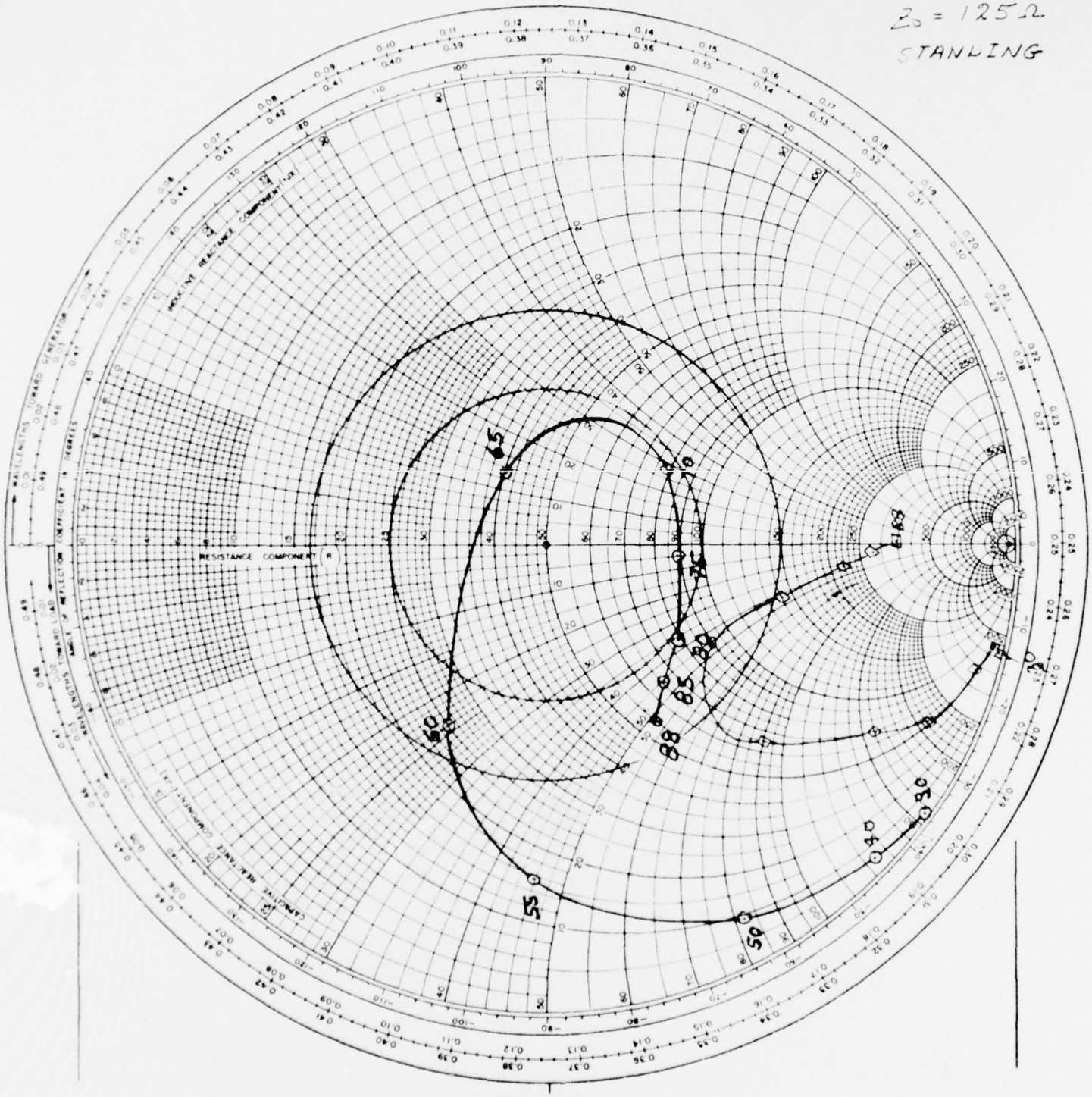

FIGURE B-7

IMPEDANCE COORDINATES — 50-OHM CHARACTERISTIC IMPEDANCE

EXP. DEV. MODEL
F.P. = 17°
Z_0 = 125 Ω
STANDING
HANDSET EXT.

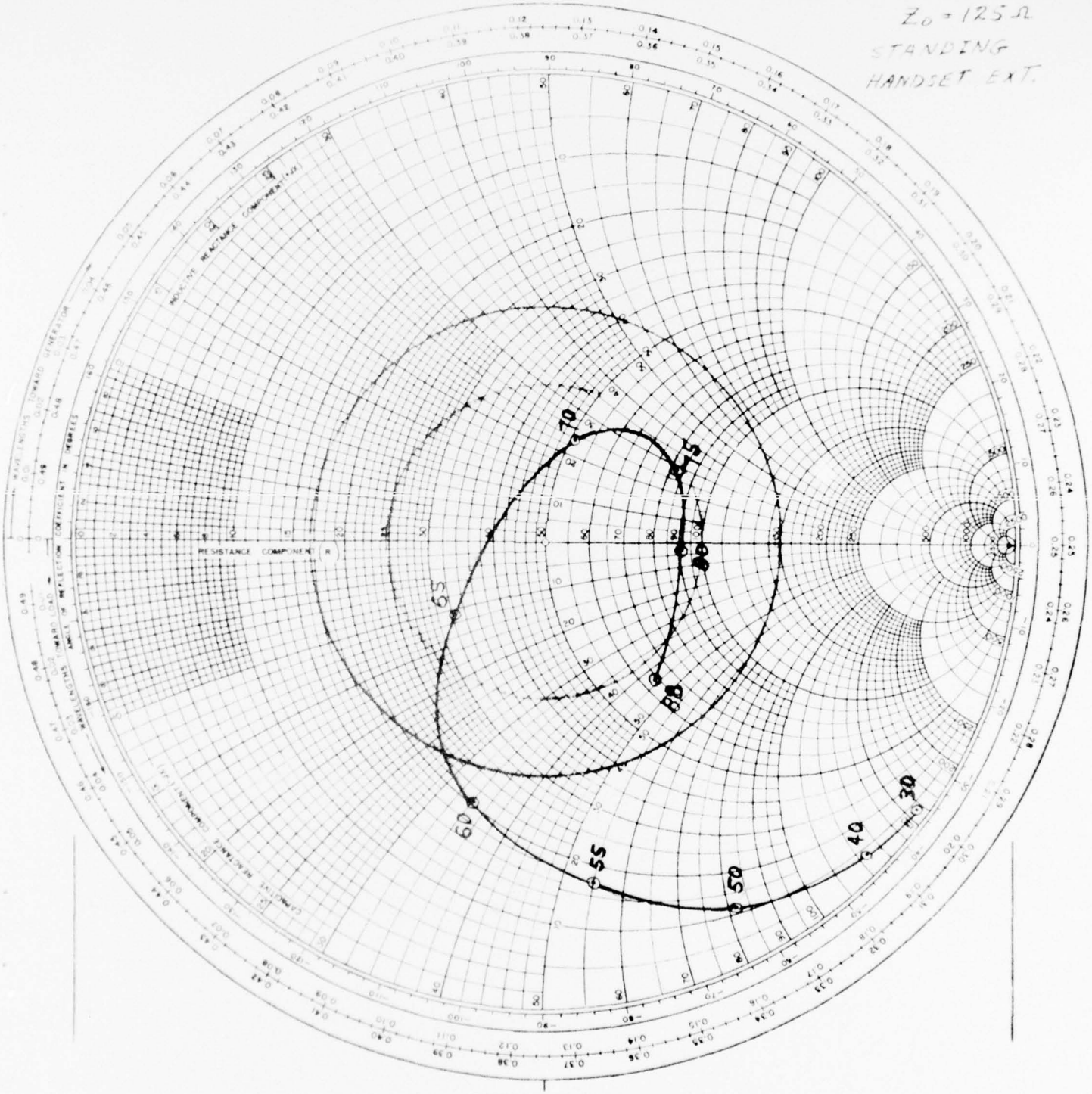

FIGURE B-8

IMPEDANCE COORDINATES — 50-OHM CHARACTERISTIC IMPEDANCE

DEVELOPMENT MODEL
FP = 17"
Z_0 = 125 Ω
PRONE

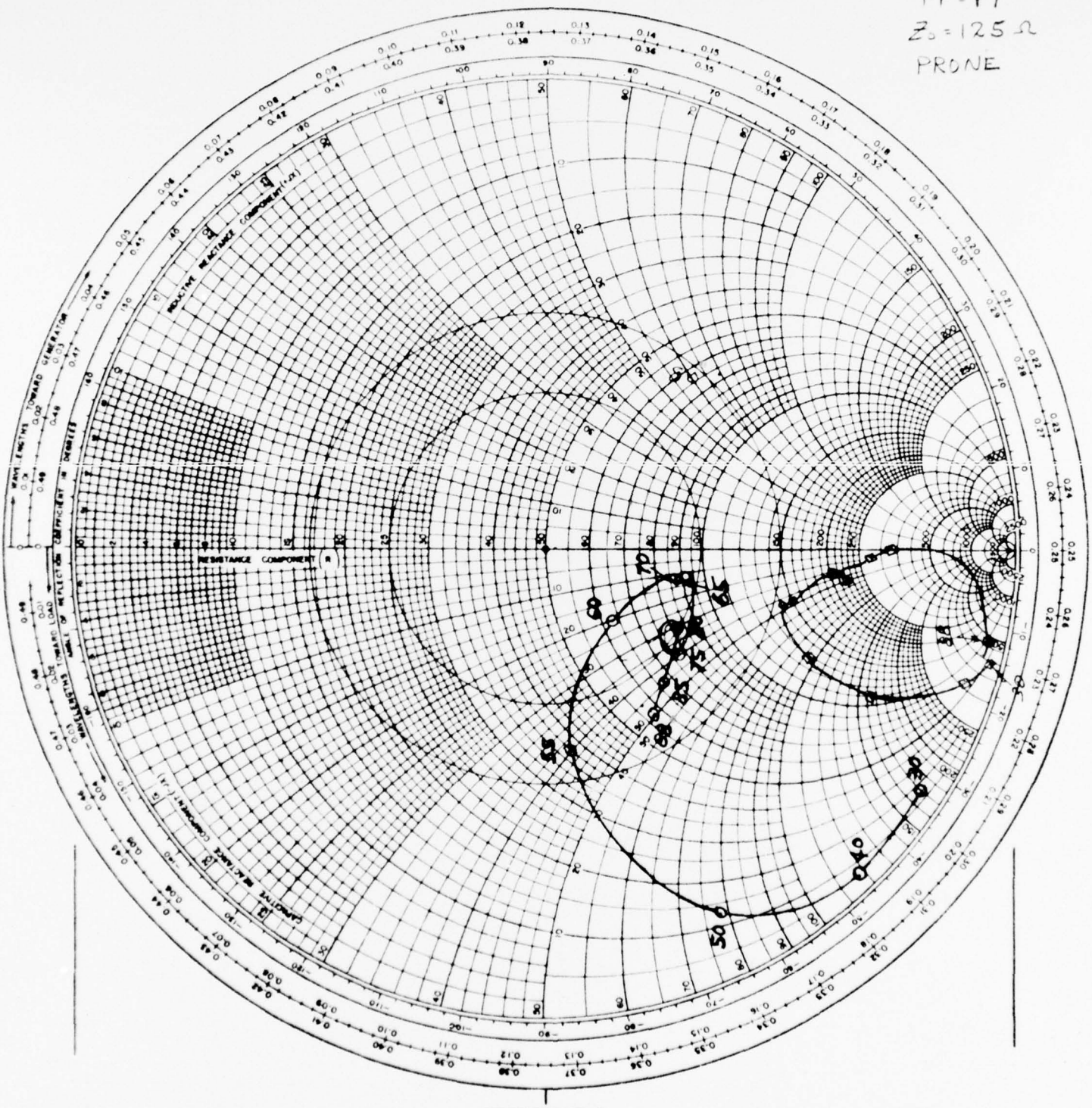

FIGURE B-9

IMPEDANCE COORDINATES — 50 OHM CHARACTERISTIC IMPEDANCE

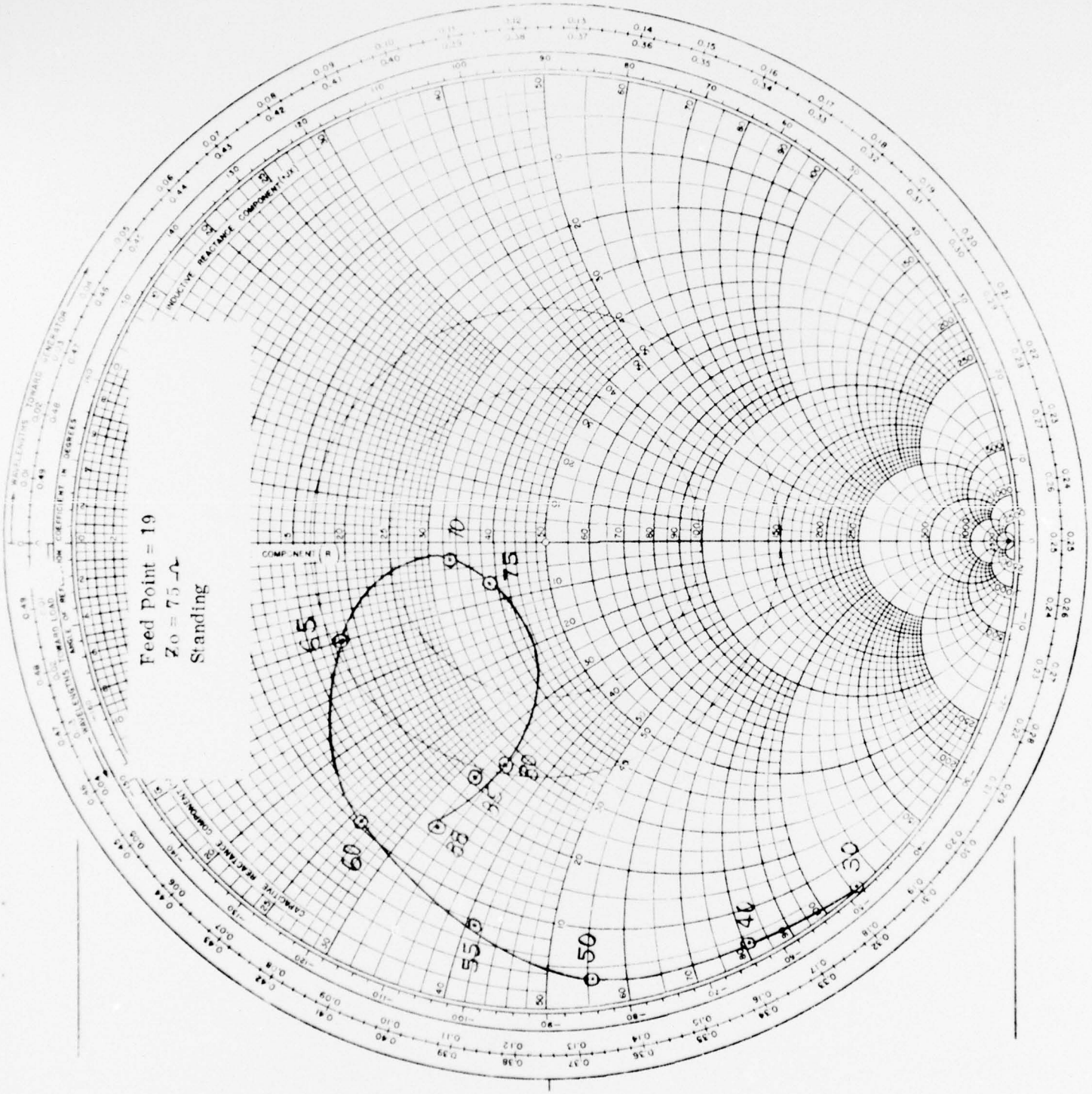

FIGURE B-10

IMPEDANCE COORDINATES — 50 OHM CHARACTERISTIC IMPEDANCE

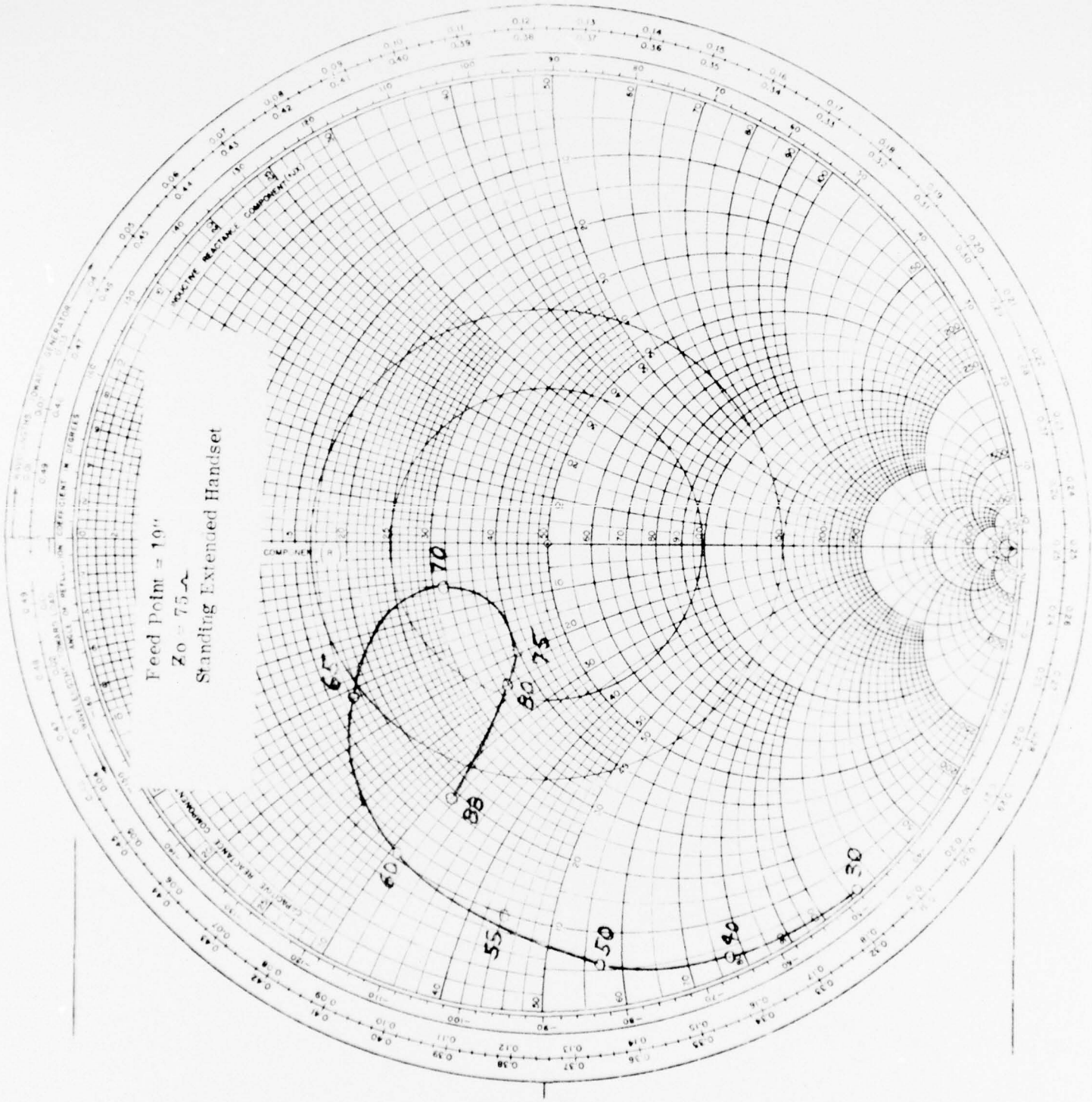

FIGURE B-11

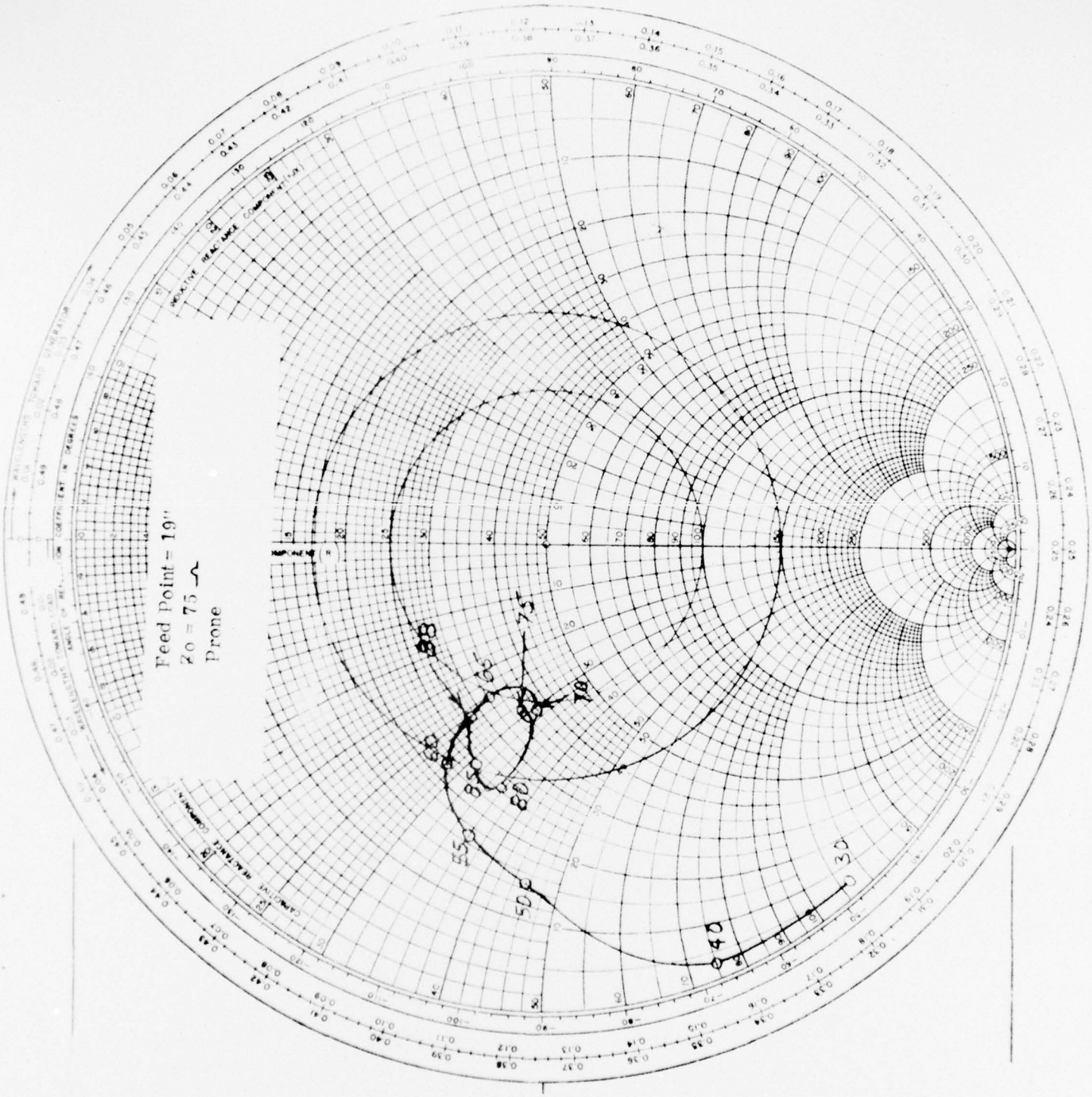
IMPEDANCE COORDINATES — 50 OHM CHARACTERISTIC IMPEDANCE
Feed Point – 19"
Zo = 75 Ω
Prone

FIGURE B-12

IMPEDANCE COORDINATES—50-OHM CHARACTERISTIC IMPEDANCE

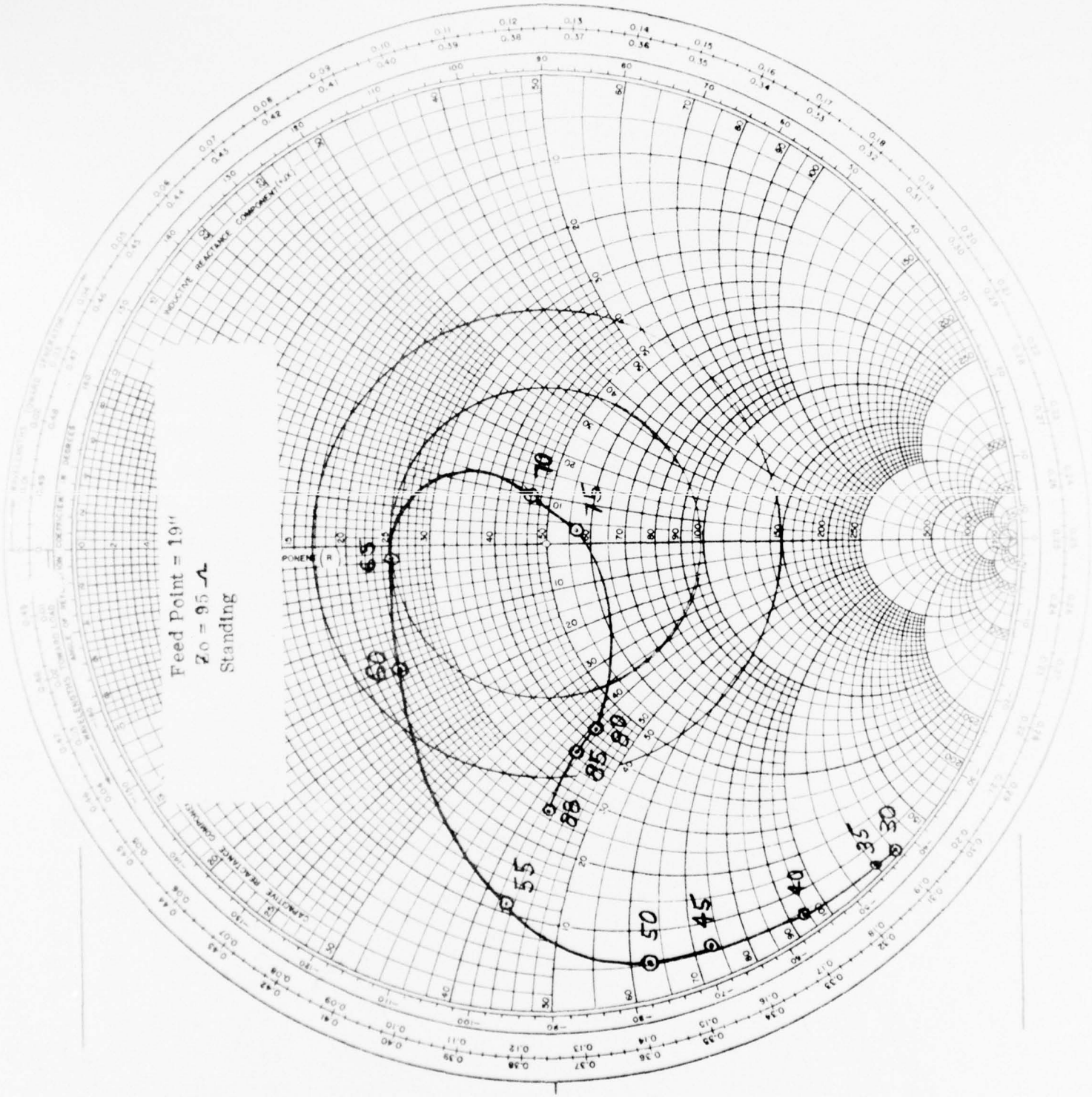

FIGURE B-13

IMPEDANCE COORDINATES — 50-OHM CHARACTERISTIC IMPEDANCE

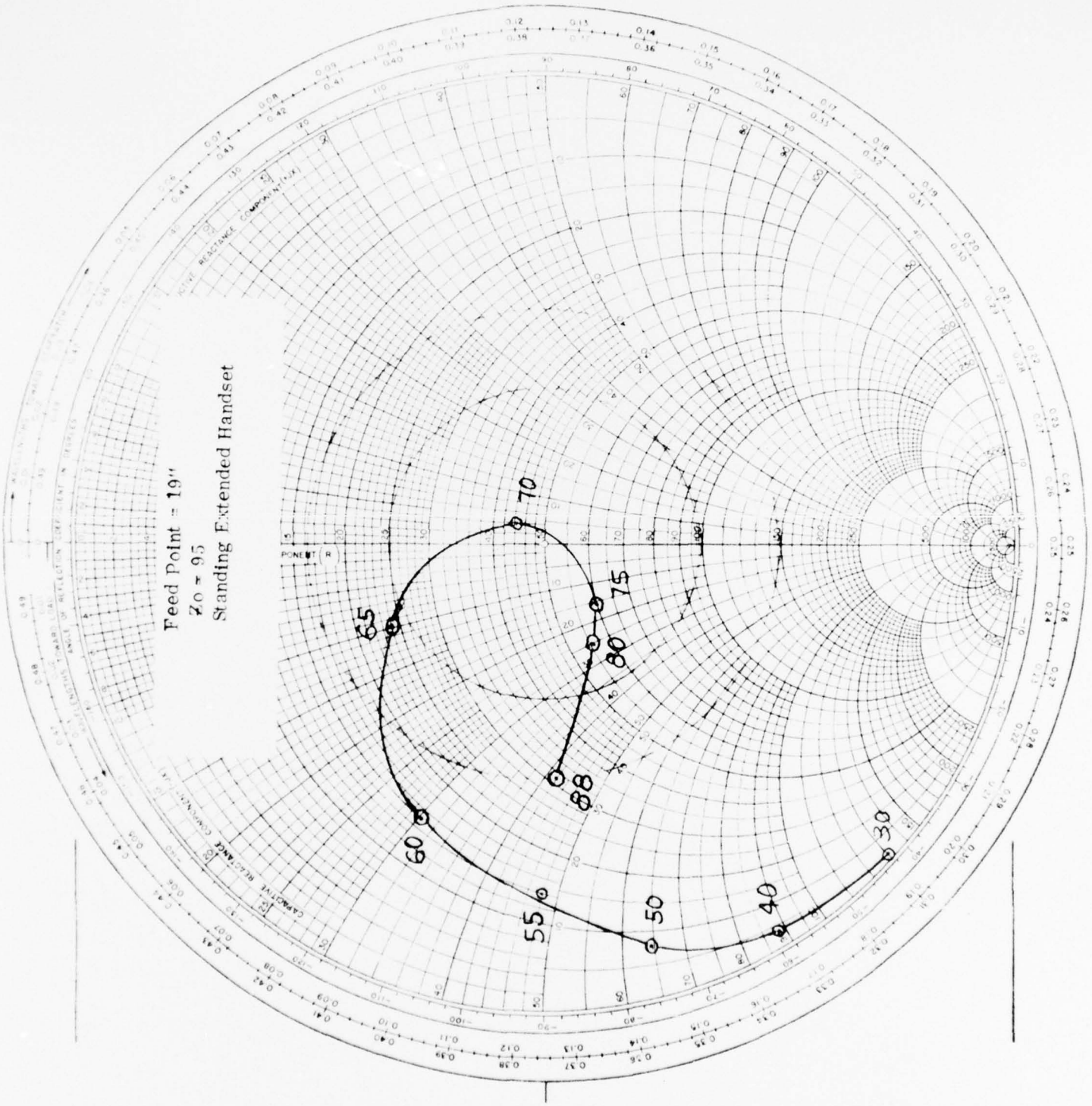

FIGURE B-14

IMPEDANCE COORDINATES—50-OHM CHARACTERISTIC IMPEDANCE

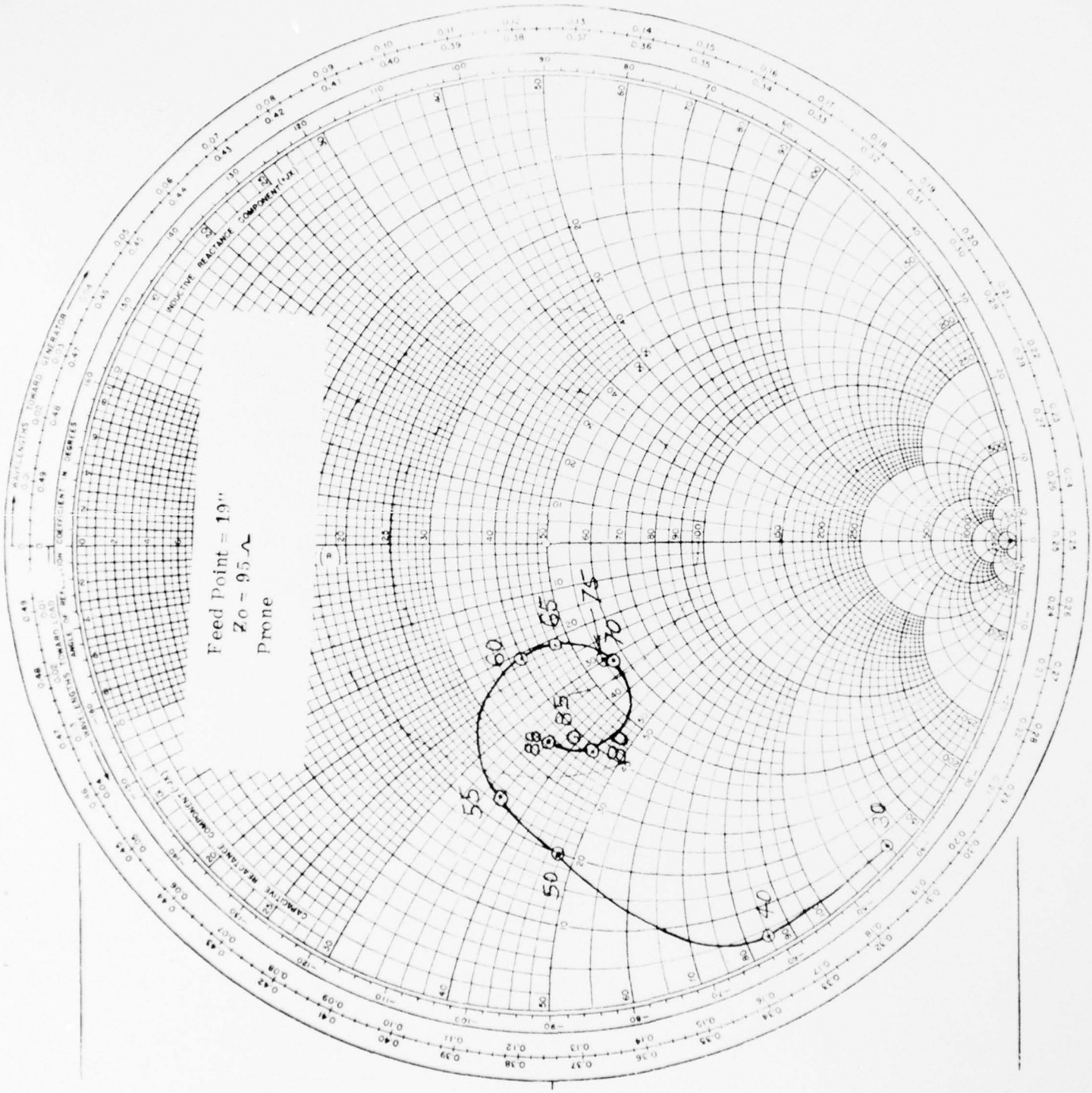

FIGURE B-15

IMPEDANCE COORDINATES – 50-OHM CHARACTERISTIC IMPEDANCE

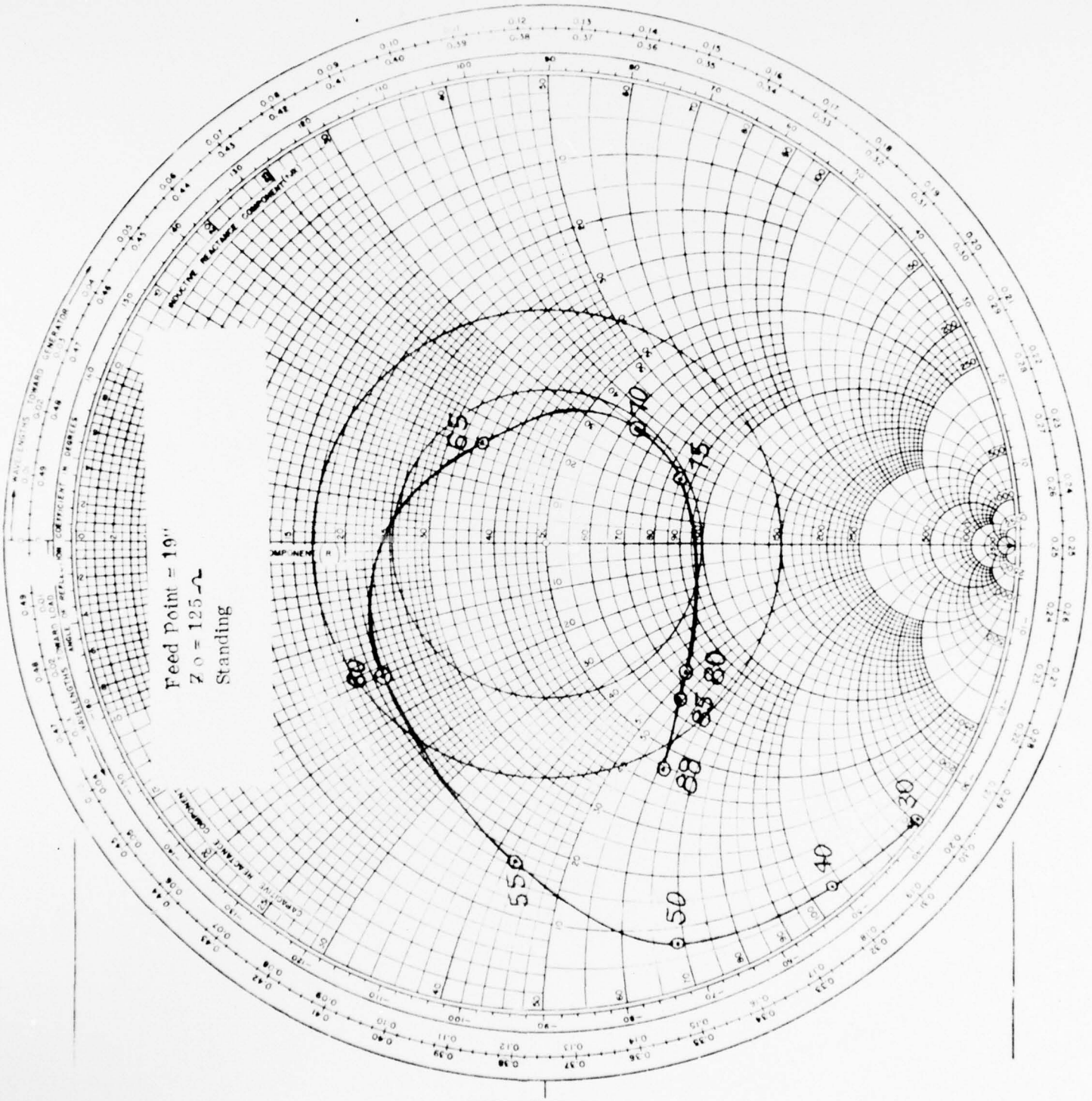

FIGURE B-16

IMPEDANCE COORDINATES — 50 OHM CHARACTERISTIC IMPEDANCE

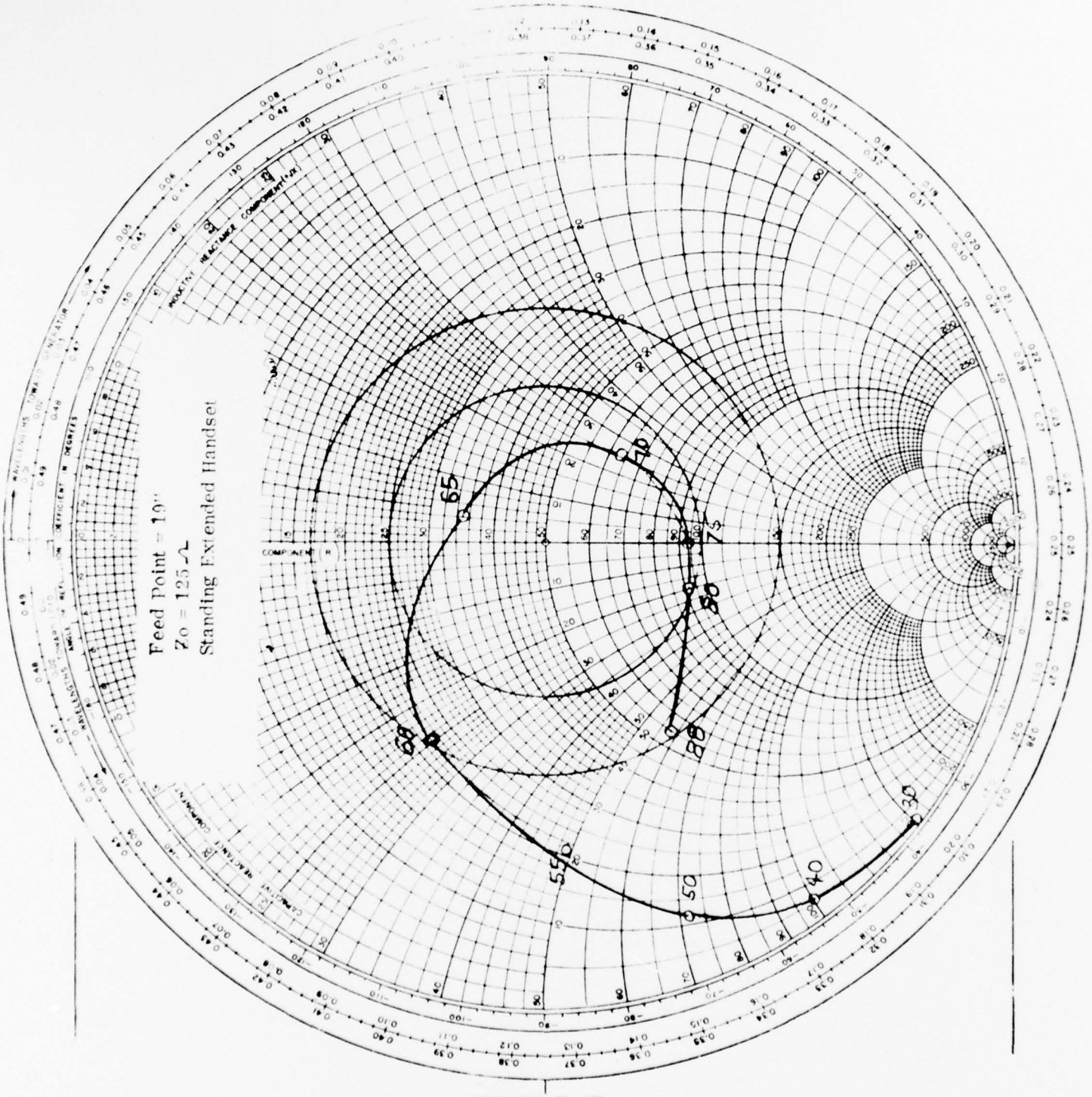

FIGURE B-17

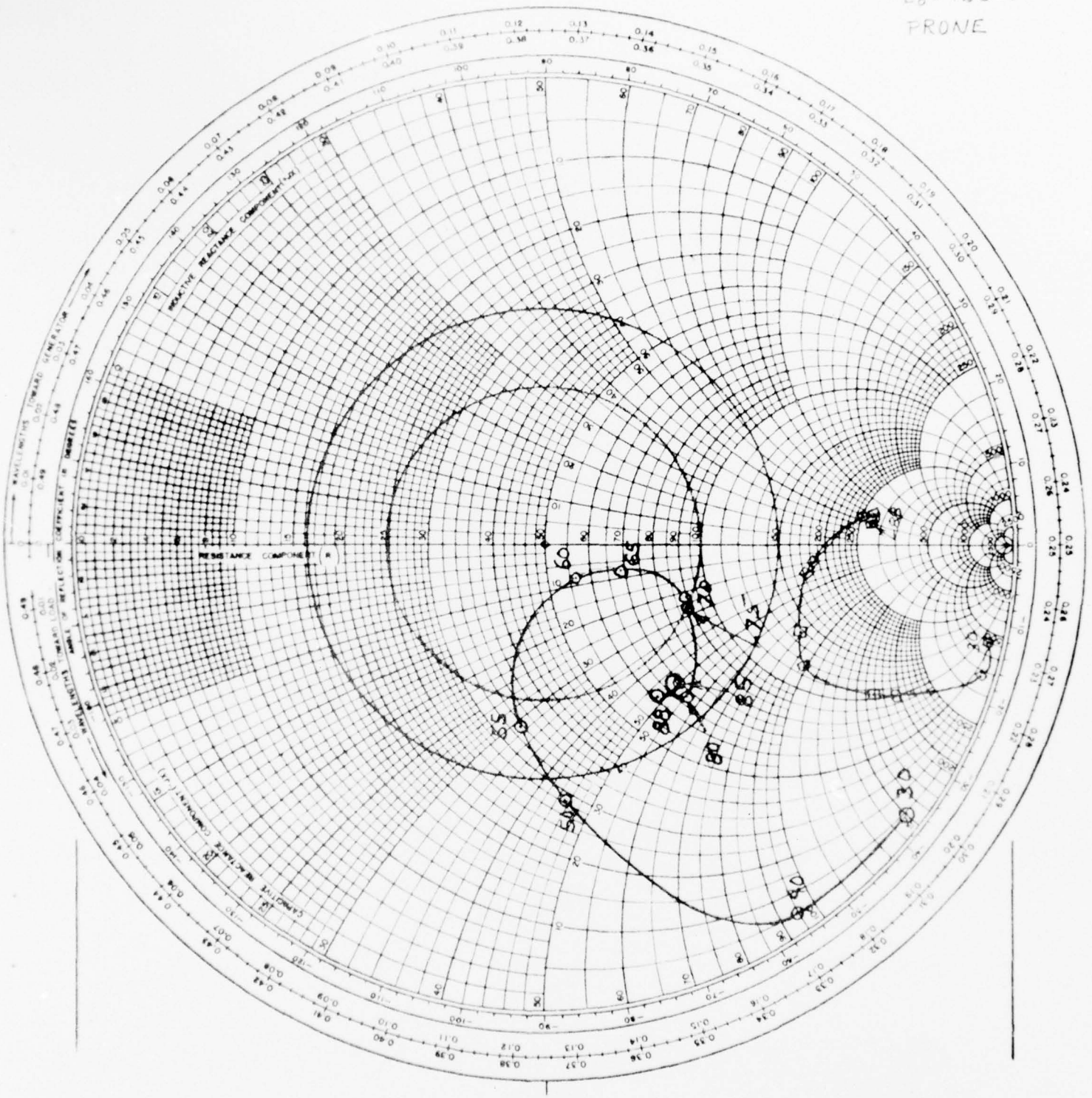
IMPEDANCE COORDINATES — 50-OHM CHARACTERISTIC IMPEDANCE
MODEL XD-2
FP = 19"
Z_0 = 125 Ω
PRONE

FIGURE B-18

IMPEDANCE COORDINATES—50-OHM CHARACTERISTIC IMPEDANCE

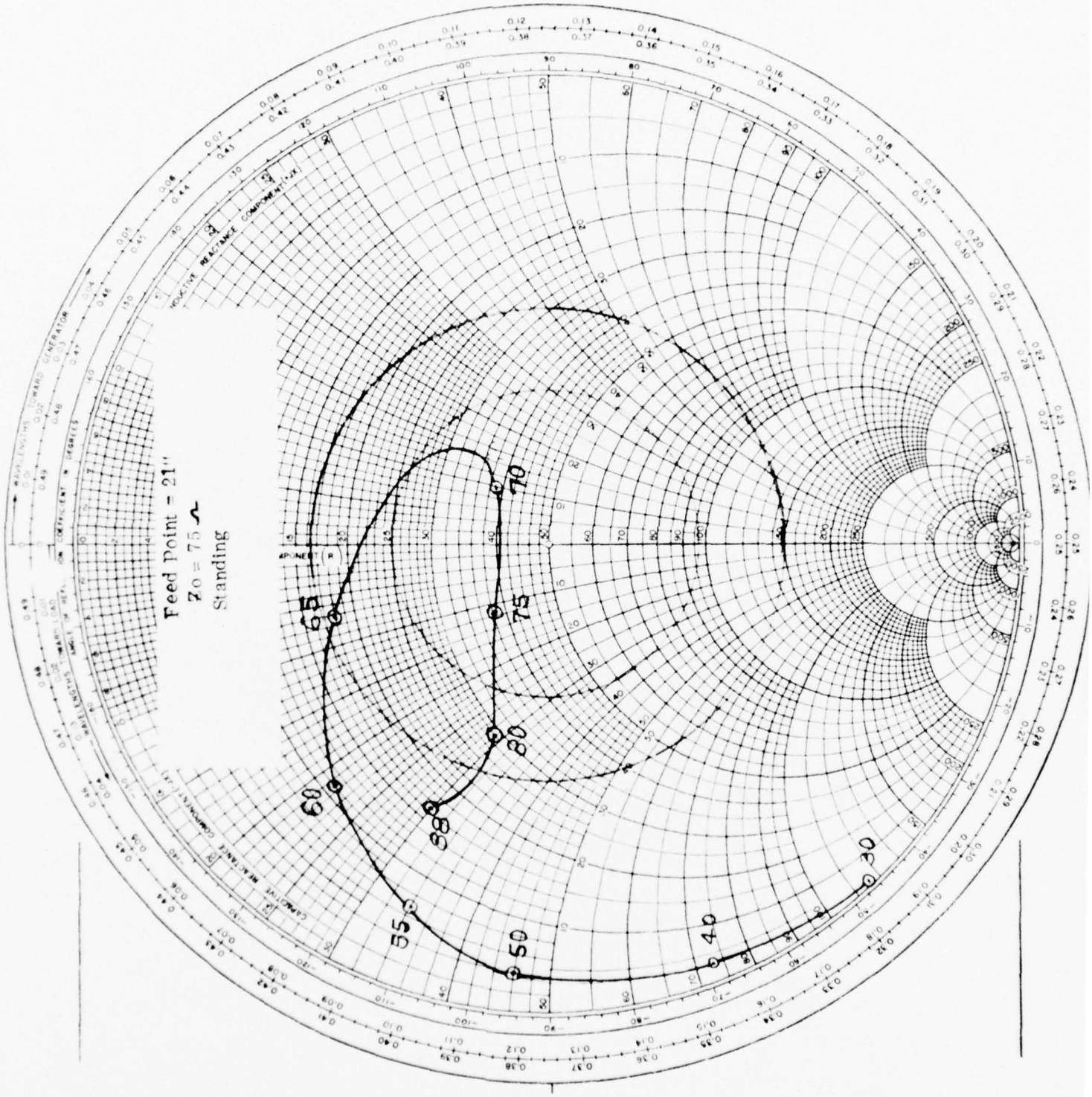

FIGURE B-19

IMPEDANCE COORDINATES — 50 OHM CHARACTERISTIC IMPEDANCE

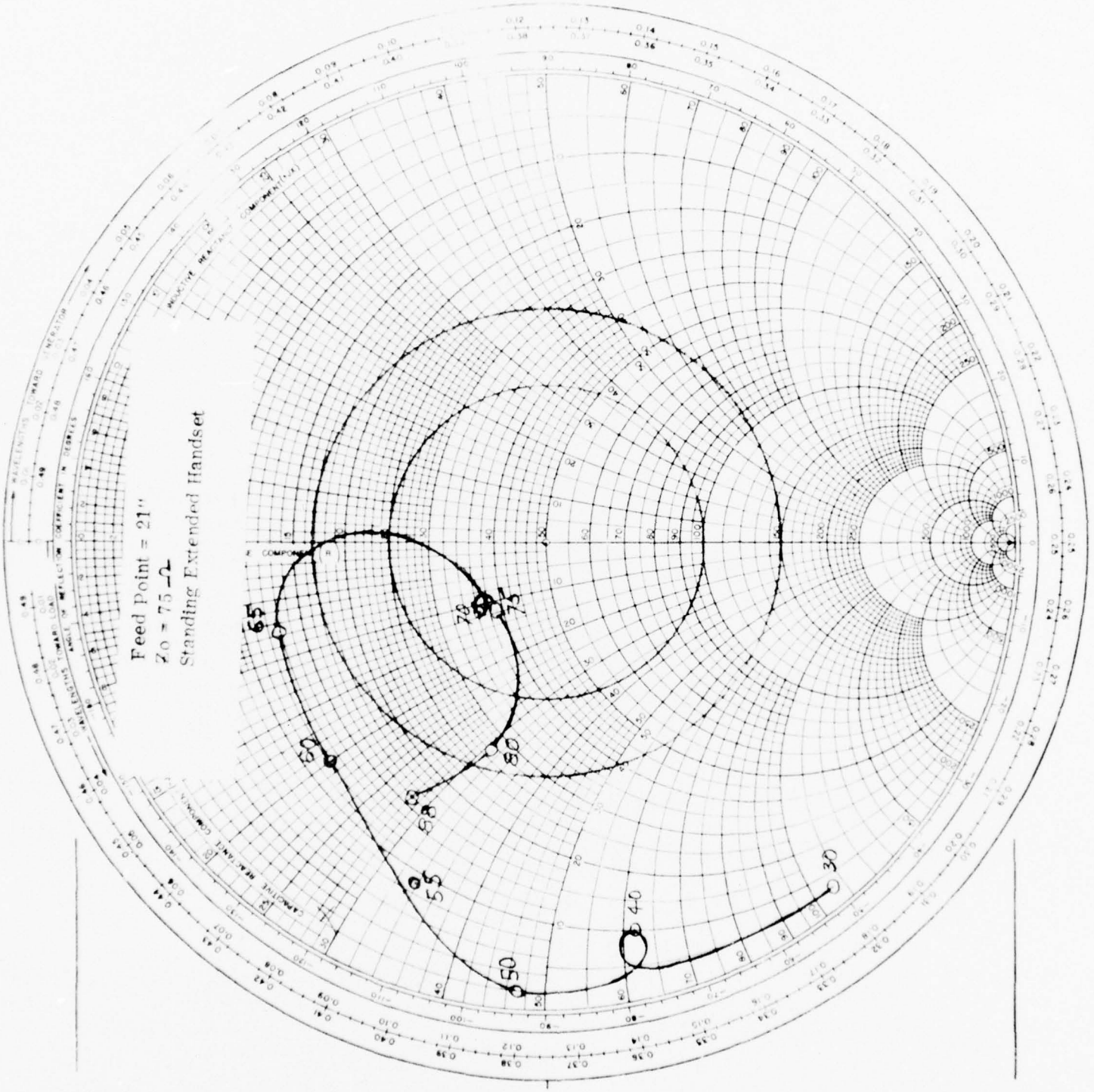

FIGURE B-20

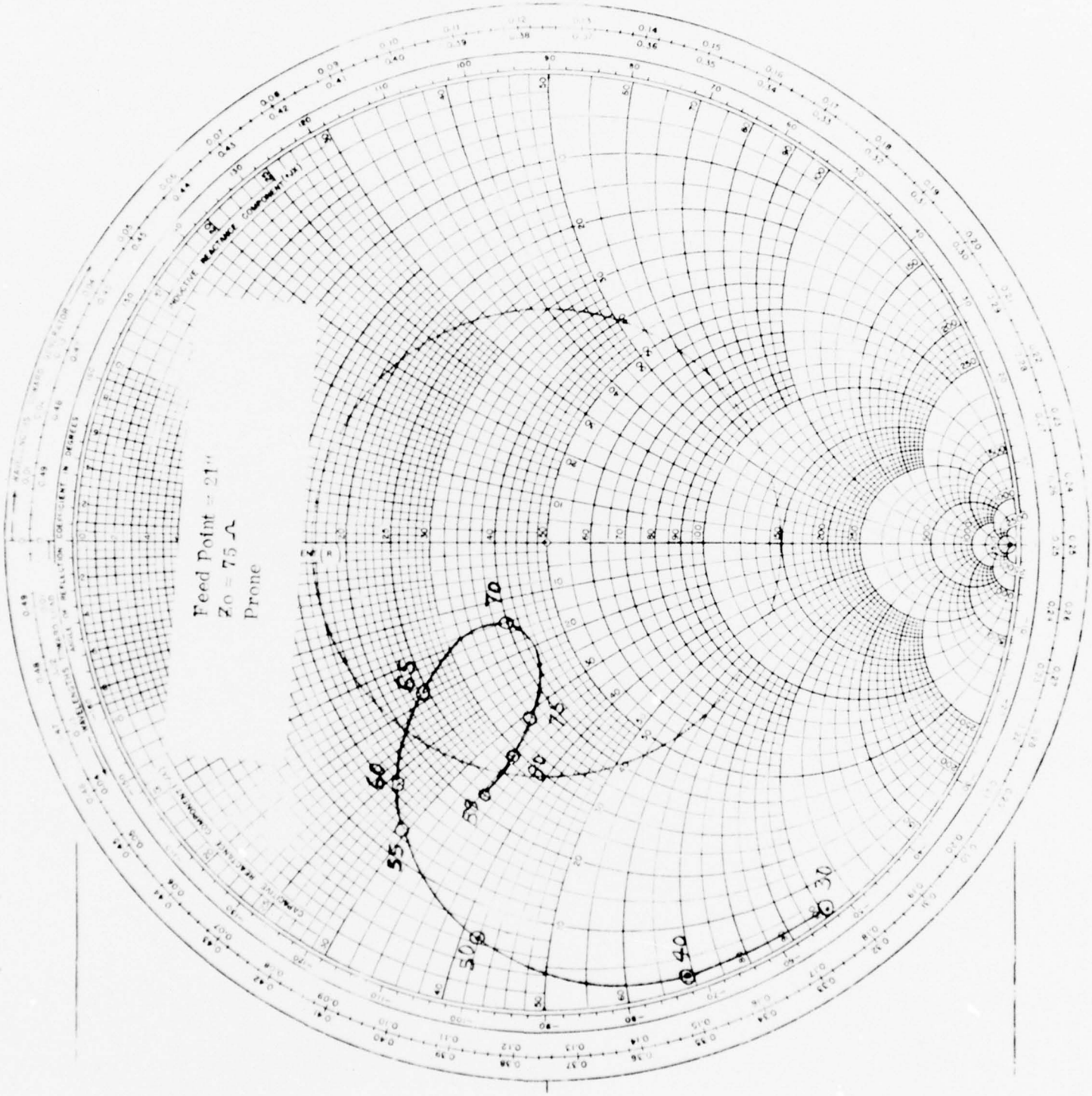
IMPEDANCE COORDINATES – 50 OHM CHARACTERISTIC IMPEDANCE
Feed Point = 21°
Zo = 75 Ω
Prone
70
65
60
55
50
75
80
40
30

FIGURE B-21

IMPEDANCE COORDINATES—50-OHM CHARACTERISTIC IMPEDANCE

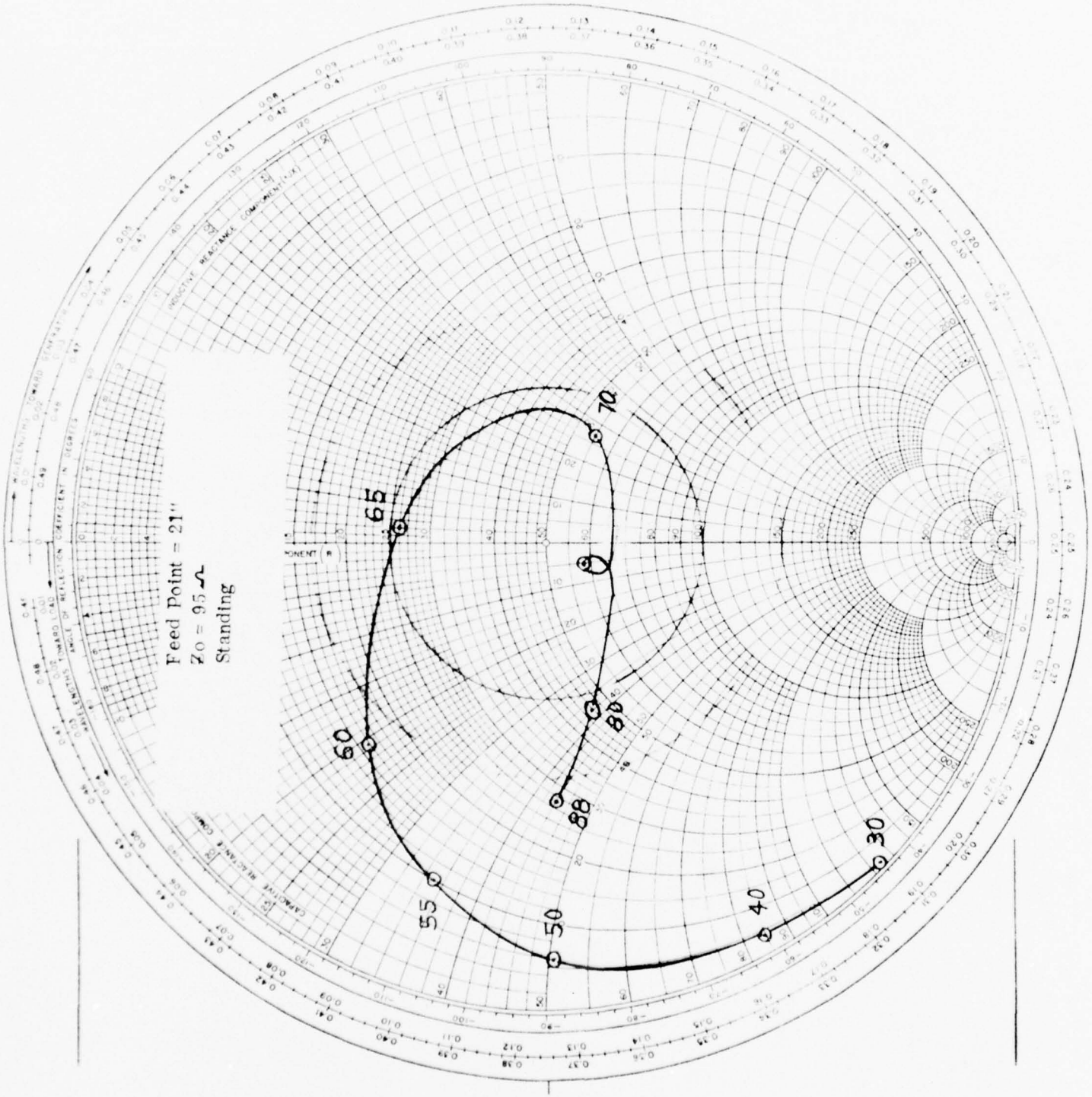

FIGURE B-22

IMPEDANCE COORDINATES — 50-OHM CHARACTERISTIC IMPEDANCE

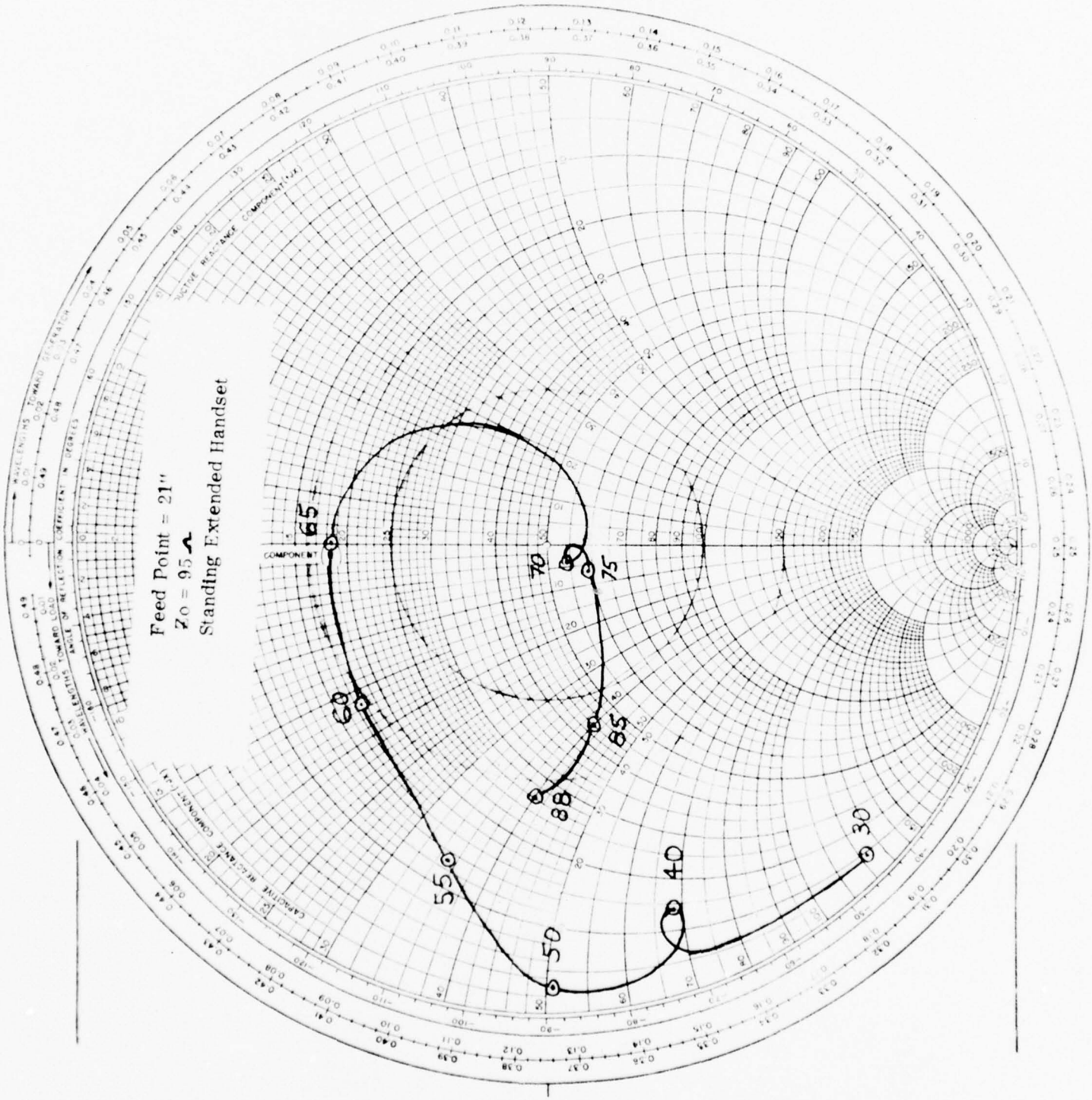

FIGURE B-23

IMPEDANCE COORDINATES—50-OHM CHARACTERISTIC IMPEDANCE

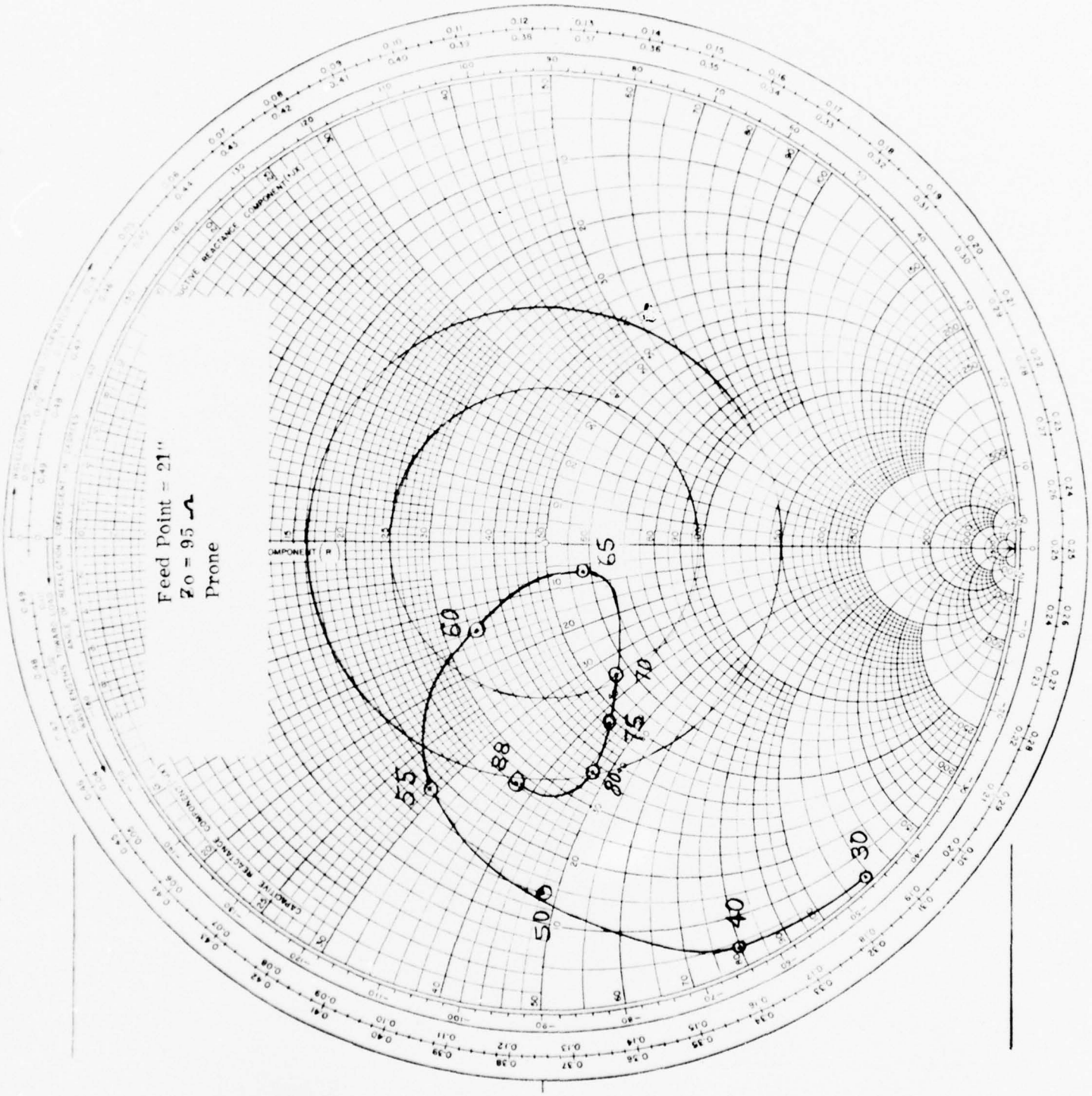

FIGURE B-24

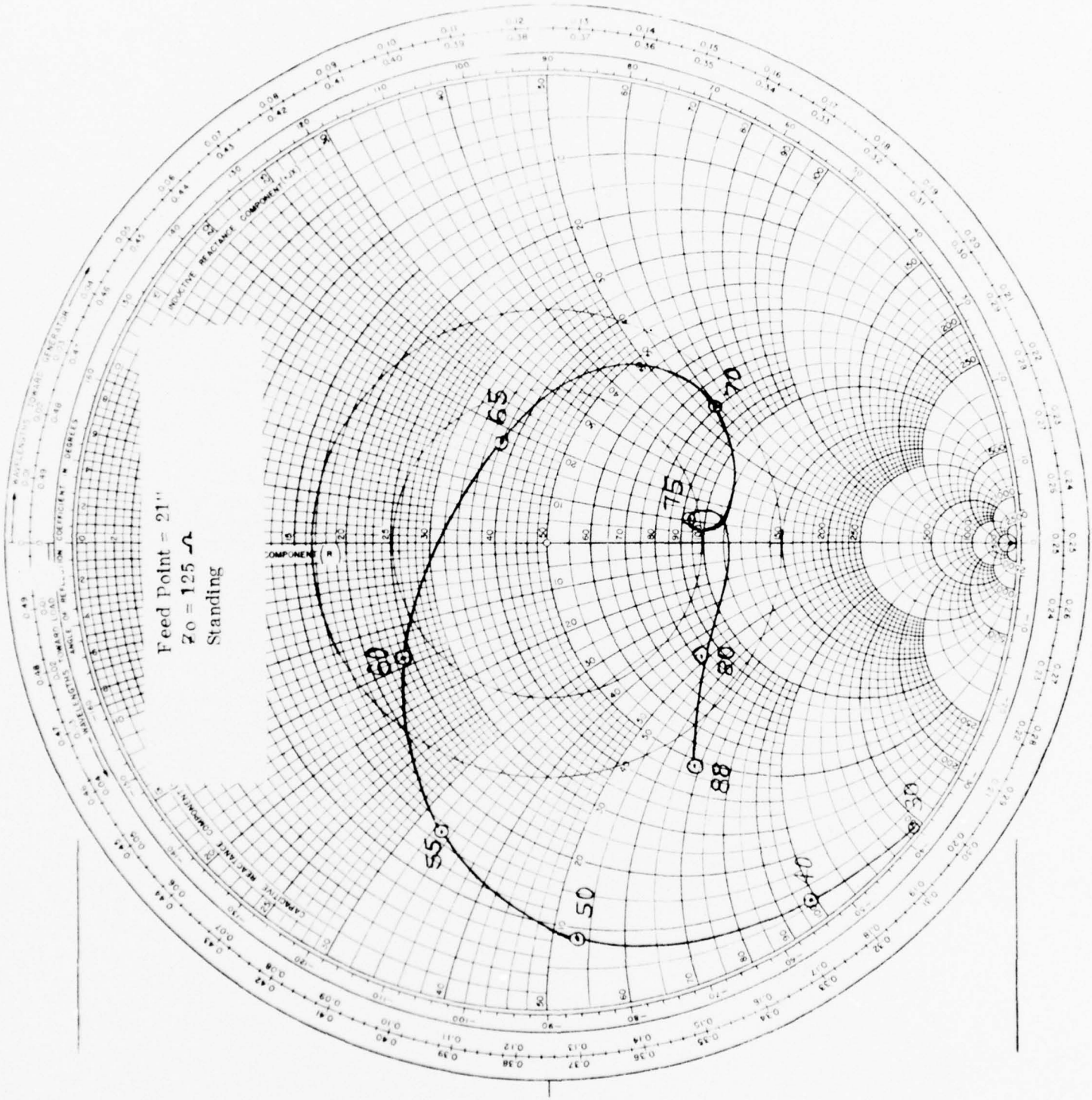
IMPEDANCE COORDINATES 50 OHM CHARACTERISTIC IMPEDANCE
Feed Point = 21"
Zo = 125 Ω
Standing
INDUCTIVE REACTANCE COMPONENT
CAPACITIVE REACTANCE COMPONENT
50
55
60
65
70
75
80
88
90
100

FIGURE B-25

IMPEDANCE COORDINATES—50-OHM CHARACTERISTIC IMPEDANCE

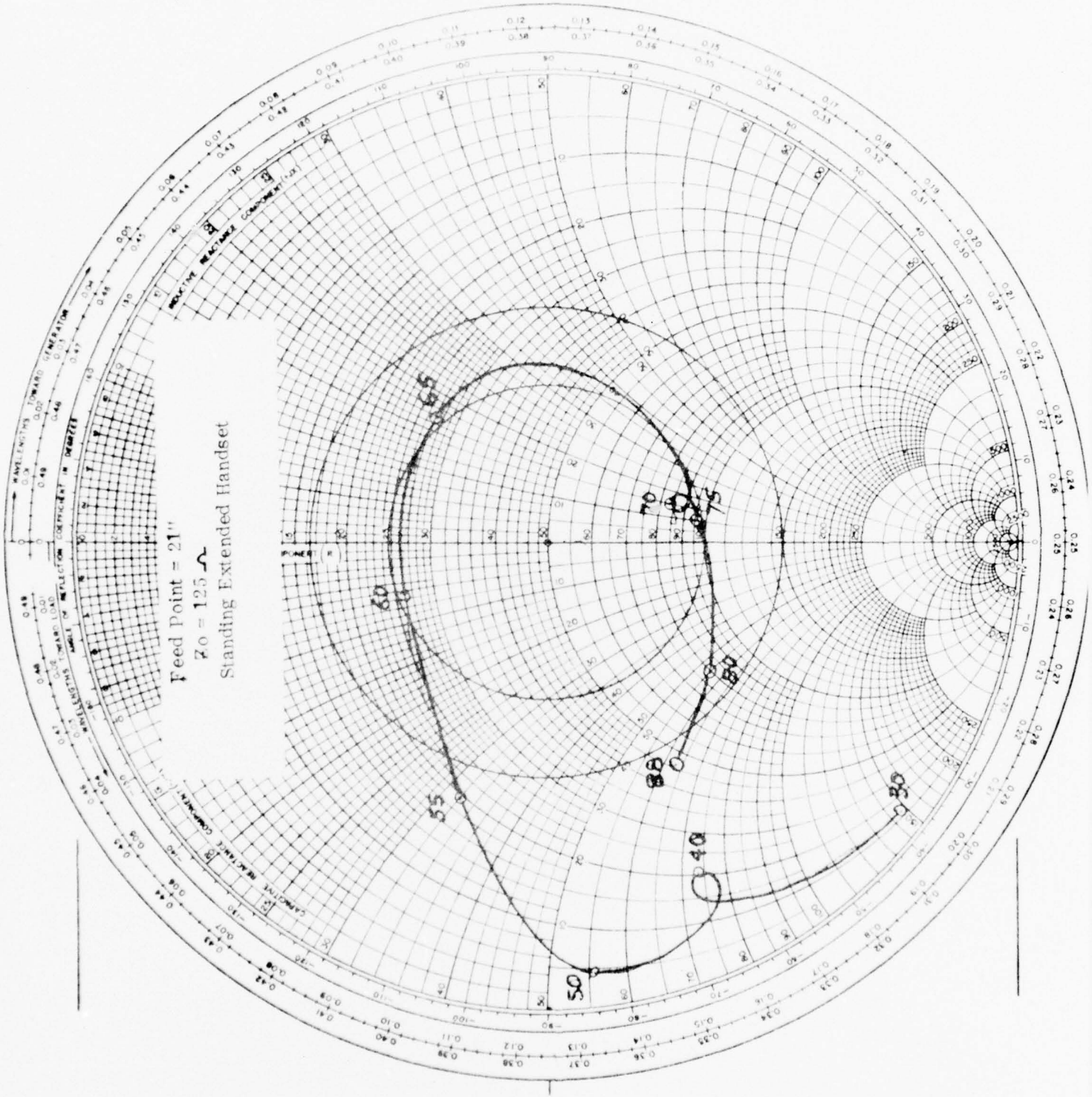

FIGURE B-26

IMPEDANCE COORDINATES — 50-OHM CHARACTERISTIC IMPEDANCE

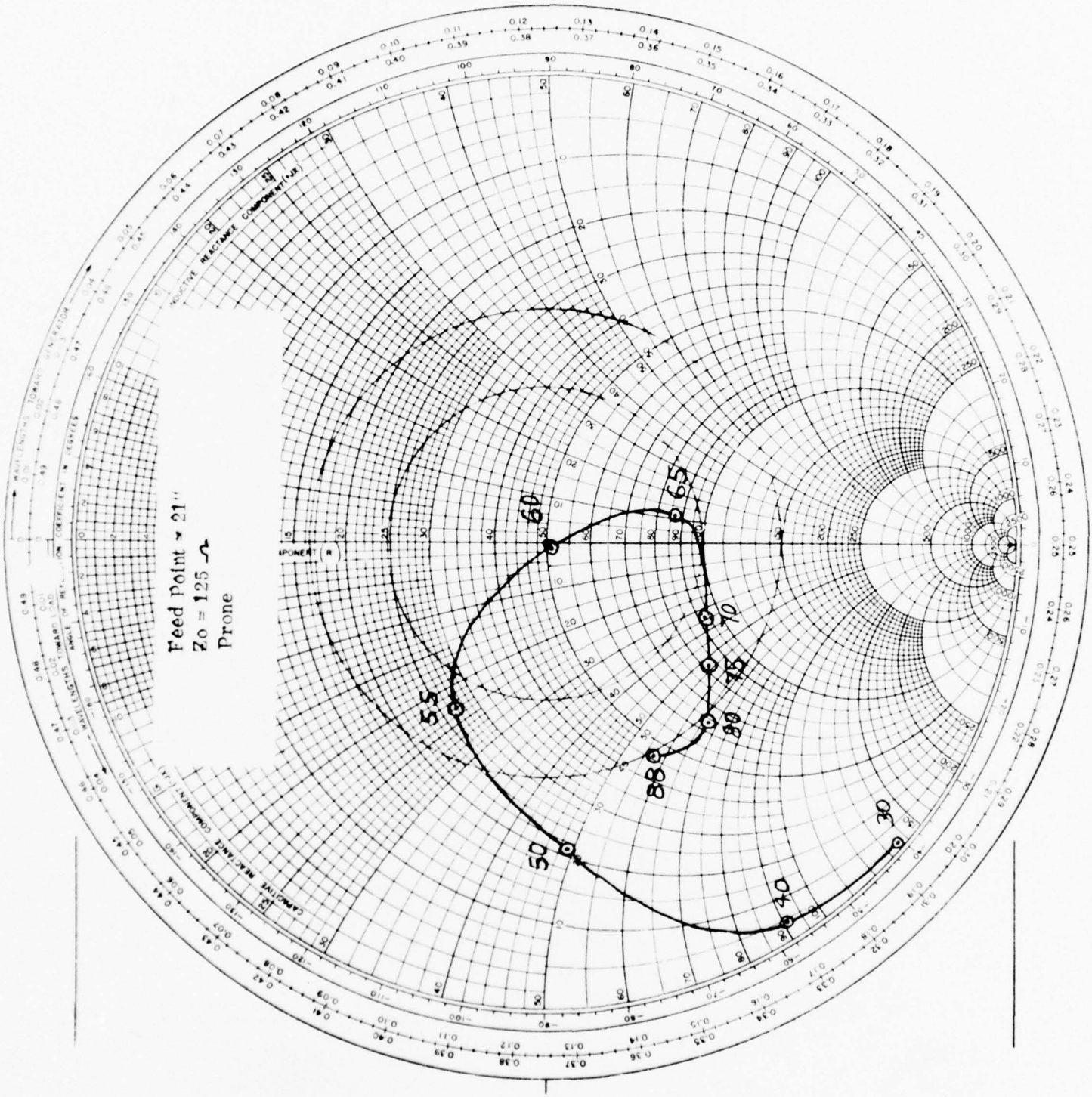

FIGURE B-27

APPENDIX C

TABULATED IMPEDANCE DATA

TABLE C1

CENTERFED WHIP IMPEDANCE

Condition - Standing					Feed Point Location 17 - Inches			
Feed Line Zo	75 Ohms		95 Ohms		125 Ohms		Feed Point Impedance	
Frequency MHz	R	X	R	X	R	X	R	X
30	1.40	-118.8	1.92	-136	2.67	-155	12.5	-413
40	2.88	-92	4.10	-107	6.0	-124	39.7	-433
50	4.5	-65	6.42	-73.7	9.42	-82	55	-335
55	7.94	-45	11.0	-47	15.5	-45	54.6	-210.6
60	13.1	-32.6	18	-31	25.2	-24	69	-160.5
65	22.6	-13.0	30	-4.6	40.2	+12.8	65	-91
70	43.0	-9.0	58	+3	78.3	+27.8	89.3	-46
75	40.5	-24.7	59	-20	88.1	-4.9	140.5	-44.4
80	31.1	-34	48	-37	77.8	-35.7	216.7	-36.6
85	24.7	-34	39	-40	65.5	-45.3	277.4	-20.5
88	20.0	-34.3	32	-42	54.8	-51.6	343	9.6

Feed Line Velocity of Propagation = 71%.

TABLE C2

CENTERFED WHIP IMPEDANCE

Condition - Handset Extended Feed Point Location 17 - Inches

Feed Line Zo	75 Ohms		95 Ohms		125 Ohms		Feed Point Impedance	
Frequency MHz	R	X	R	X	R	X	R	X
30	1.60	-119	2.2	-137	3.0	-157		
40	3.59	-92	5.1	-107	7.5	-12.4		
50	5.75	-65	8.2	-74	12.0	-82.2		
55	8.52	-50	12	-54	17.3	-55		
60	10.2	-37.5	14.3	-38	20.4	-34		
65	16.3	-32	23	-21	32.4	-10.4		
70	28.3	-7.1	38	+3.4	51.5	+24.6		
75	42.6	-8.0	59	+3.8	82.3	+29		
80	39.9	-21.8	59.2	-17.4	90.6	-2.5		
85	-	-	-	-	-	-		
88	23.9	-32	38	-38.2	64.4	-44.2		

Feed Line Velocity of Propagation = 71%.

TABLE C3

CENTERFED WHIP IMPEDANCE

Condition - Prone					Feed Point Location 17 - Inches.			
Feed Line Zo	75 Ohms		95 Ohms		125 Ohms		Feed Point Impedance	
Frequency MHz	R	X	R	X	R	X	R	X
30	7.8	-125	3.1	-145	15.3	-168	84	-468
40	3.0	-89	4.2	-102	6.10	-116	34.8	-389
50	6.2	-63	8.8	-71	12.8	-78	67.7	-308
55	19.5	-43	26.8	-44	37.5	-40	108.2	-163
60	32.7	-34	45	-31	62.7	-20	128	-94
65	43.9	-33	62	-28	88.4	-13.2	141	-46
70	40.7	-31	58.8	-27	86.7	-13.7	148	-48
75	31.5	-38	48	-41	76.4	-39.5	218	-50
80	33	-32.5	50.7	-34.5	81.5	-31.1	201	-35
85	25.1	-33.8	39.6	-39.5	66.4	-44.3	272	-22
88	21.0	-33.6	33.5	-40.8	57.2	-49.4	325	+1.3

Feed Line Velocity of Propagation = 71%.

TABLE C4

CENTERFED WHIP IMPEDANCE

Condition - Free Standing					Feed Point Location 19 - Inches			
Feed Line Zo	75 Ohms		95 Ohms		125 Ohms		Feed Point Impedance	
Frequency MHz	R	X	R	X	R	X	R	X
30			2.0	-140	2.9	-165	22.7	-562
40			3.0	-93.8	4.44	-108	31.8	-423
50			3.43	-65	5.2	-72	36.2	-360
55			4.80	-50	4.2	-53	25	-305
60			5.90	-35.5	8.81	-33	42	-251
65			9.0	-31	13.4	-13	49	-202
70			20.5	+13	28.7	+36	44.4	-99
75			57.0	+5	84.3	+29	103	-51
80			52.0	-10	82.6	+3.5	149	-52
85			60.0	-4	96.8	+12.1	135	-35
88			45.0	-33	78.1	-40.9	221	-41.9

Feed Line Velocity of Propagation = 71%.

TABLE C5

CENTERFED WHIP IMPEDANCE

Condition - Standing					Feed Point Location 19 - Inches			
Feed Line Zo	75 Ohms		95 Ohms		125 Ohms		Feed Point Impedance	
Frequency MHz	R	X	R	X	R	X	R	X
30	1.39	-112	1.95	-130	2.80	-151		
35			3.67	-124				
40	2.96	-81	4.17	-94	6.3	-108		
45			5.81	-72.7				
50	3.58	-56	5.18	-63	7.74	-69		
55	7.89	-41	11.27	-43.7	16.6	-43		
60	10.4	-25.8	14.6	-23.2	21.0	-14.6		
65	18.23	-9.7	25.1	-1.3	35.2	+16.4		
70	32.87	-2.3	45.6	+9.8	64.2	+34.5		
75	39.2	-7.1	56.9	+2.92	84.6	+26		
80	26.7	-33.8	42.8	-41.2	73.5	-49.4		
85	22.97	-32.1	37.2	-41.2	65.1	-54		
88	15.4	-32.2	25.1	-43.2	44.5	-61		

Feed Line Velocity of Propagation = 71%.

TABLE C6

CENTERFED WHIP IMPEDANCE

Condition - Handset Extended					Feed Point Location 19 - Inches			
Feed Line Zo	75 Ohms		95 Ohms		124 Ohms		Feed Point Impedance	
Frequency MHz	R	X	R	X	R	X	R	X
30	1.36	-112	1.90	-130	2.73	-151	16.4	-463
40	2.68	-77	3.80	-88.3	5.54	-100	33.1	-370
50	5.31	-57	7.70	-64.6	11.55	-72	78	-345
55	9.7	-44	14.0	-48.0	20.8	-49	106	-258
60	10.5	-30.8	15.0	-30.4	22.0	-25	81	-199
65	17.3	-15.9	24.3	-10.0	34.9	+4.1	79	-128
70	31.6	-6.5	44.4	+3.70	63.6	+25.7	92	-73
75	39.9	-19.8	60	-15.5	93.5	-0.9	143	-35
80	35.7	-24.3	55.6	-25	91.6	-19.8	177	-15
85	-	-	-	-	-	-	-	-
88	18.9	-31.6	30.8	-42	54.5	-58.5	286	+135

Feed Line Velocity of Propagation = 71%.

TABLE C7

CENTERFED WHIP IMPEDANCE

Condition - Prone — Feed Point Location 19 - Inches

Feed Line Zo	75 Ohms		95 Ohms		125 Ohms		Feed Point Impedance	
Frequency MHz	R	X	R	X	R	X	R	X
30	4.8	-112	6.71	-130	9.6	-151	57	-458
40	2.4	-75	3.35	-84.8	5.1	-95	27.5	-341
50	14.6	-45	20.26	-47.5	28.9	-45.8	100	-197
55	16.7	-36	23.4	-36.3	33.6	-31	106	-171
60	28.4	-25	39.8	-20.8	56.7	-8.2	117	-99
65	32.4	-24.6	46.7	-20.6	68.9	-7.9	129	-79
70	37.7	-30.8	57.1	-30.6	89.8	-22.6	174	-31
75	35.8	-29.2	55.3	-30.4	89.8	-25.5	184	-19
80	24.5	-35.7	39.4	-44.4	68.2	-55.5	276	+151
85	24.7	-30.9	39.9	-39.1	69.5	-50	255	+59.6
88	21.8	-28.3	35.2	-36.4	61.5	-48.2	276	+75

Feed Line Velocity of Propagation = 71%.

TABLE C8

CENTERFED WHIP IMPEDANCE

Condition - Handset Extended					Feed Point Location 21 - Inches			
Feed Line Zo	75 Ohms		95 Ohms		125 Ohms		Feed Point Impedance	
Frequency MHz	R	X	R	X	R	X	R	X
30	6.4	-105	9.2	-123	13.6	-144	101	-496
40	10.1	-61	14.2	-68	20.4	-73	91.4	-268
50	1.9	-47	2.7	-51.7	4.1	-55	26.7	-326
55	8.9	-34	12.86	-34.7	19.3	-31.8	88.5	-234
60	12.2	-20	17.5	-16.5	25.9	-6.3	80.2	-169
65	12.9	-7.7	18.4	0	27.1	+16.8	62.3	-137
70	36.1	-11	53.6	-3.8	82.5	+14.6	126.3	-55.6
75	38.7	-11.4	59.2	-6.0	94.8	+9.9	136	-36
80	27.2	-30.9	44.4	-40.4	77.9	-54.3	213	+79.7
85	-	-	-	-	-	-	-	-
88	15.7	-28.1	25.7	-40.4	45.7	-62.6	200	+198

Feed Line Velocity of Propagation = 71%.

TABLE C9

CENTERFED WHIP IMPEDANCE

Condition - Standing					Feed Point Location 21 - Inches			
Feed Line Zo	75 Ohms		95 Ohms		125 Ohms		Feed Point Impedance	
Frequency MHz	R	X	R	X	R	X	R	X
30	1.39	-106	2.0	-12.4	2.95	-146		
40	2.88	-73	4.2	-84.7	6.33	-98		
50	4.02	-46	5.84	-50.5	8.25	-53		
55	6.89	-34	10.0	-35.4	15.0	-33		
60	10.9	-23	15.8	-21.4	23.7	-13.7		
65	18.2	-7.2	26.0	+1.0	38.1	+18.9		
70	39.2	+9.95	55.0	+26.7	78.5	+59.7		
75	38.2	-10.7	58.3	-4.9	93.1	+11.4		
80	28.7	-29.2	46.6	-37.5	81.7	-48.8		
85	-	-	-	-	-	-		
88	16.4	-30.3	26.8	-4.40	47.9	-68.9		

Feed Line Velocity of Propagation = 71%.

TABLE C10

CENTERFED WHIP IMPEDANCE

Condition - Prone					Feed Point Location 21 - Inches			
Feed Line Zo	75 Ohms		95 Ohms		125 Ohms		Feed Point Impedance	
Frequency MHz	R	X	R	X	R	X	R	X
30	1.84	-102	2.60	-118	3.78	-136	24.9	-439
40	2.15	-69.7	3.1	-80	4.61	-91	32.3	-388
50	9.69	-44.2	14.0	-48	20.9	-49.2	108	-261
55	12.7	-29.7	18.1	-28.8	26.6	-22.7	93.9	-187
60	24.5	-19	35.0	-13.9	51.3	-0.52	115	-110
65	40.1	-14.6	58.4	-6.9	87	+12.8	121	-47
70	35.6	-31.2	56.0	-34.7	93.2	-33.8	191	+3.4
75	29.2	-34.1	4.2	-42	82.3	-53.4	221	+58
80	21.9	-34.7	35.9	-47.0	64.1	-67.1	226	+137
85	-	-	-	-	-	-	-	-
88	15.8	-26.1	25.8	-37.1	45.7	-56.7	228	+192

Feed Line Velocity of Propagation = 71%.

APPENDIX D

DISTRIBUTION LIST

DISTRIBUTION LIST

COPIES	RECIPIENT
101	Defense Documentation Center Attn: DDC-TCA Cameron Station (Bldg 5)
*012	Alexandria, VA 22314
102	Director National Security Agency Attn: TDL
001	Fort George G. Meade, MD 20755
103	Code R123, Tech Library DCA Defense Comm Engrg Ctr 1860 Wiehle Ave.
001	Reston, VA 22090
104	Defense Communications Agency Technical Library Center Code 205 (P.A. Tolovi)
001	Washington, DC 20305
200	Office of Naval Research Code 427
001	Arlington, VA 22217
203	Gidep Engineering & Support Dept. TE Section PO Box 398
001	Norco, CA 91760
205	Director Naval Research Laboratory Attn: Code 2627
001	Washington, DC 20375
206	Commander Naval Electronics Laboratory Center Attn: Library
001	San Diego, CA 92152
207	CDR, Naval Surface Weapons Center White Oak Laboratory Attn: Library, Code WX-21
001	Silver Spring, MD 20910
210	Commandant, Marine Corps Hq, US Marine Corps Attn: Code LMC
002	Washington, DC 20380
211	Hq. US Marine Corps Attn: Code INTS
001	Washington, DC 20380
212	Command, Control & Communications Div Development Center Marine Corps Development & Educ Comd
001	Quantico, VA 22134
215	Naval Telecommunications Command Technical Library, Code 91L 4401 Massachusetts Ave., NW
001	Washington, DC 20390

* Decrease to 2 copies if report is not releasable to public. See ECOMR 70-31 for types of reports not to be sent to DDC.

COPIES	RECIPIENT
438	HQDA (DAMA-ARP/ Dr. F.D. Verderame)
001	Washington, DC 20310
470	Director of Combat Developments US Army Armor Center Attn: ATZK-CD-MS
002	Fort Knox, KY 40121
473	Commandant US Army Ordnance School Attn: ATSL-CD-OR
002	Aberdeen Proving Ground, MD 21005
475	CDR, Harry Diamond Laboratories Attn: Library 2800 Powder Mill Road
001	Adelphi, MD 20783
477	Director US Army Ballistic Research Labs Attn: DRXBR-LB
001	Aberdeen Proving Ground, MD 21005
478	Director US Army Ballistic Research Labs Attn: DRXBR-CA (Dr. L. Vandekieft)
001	Aberdeen Proving Ground, MD 21005
479	Director US Army Human Engineering Labs
001	Aberdeen Proving Ground, MD 21005
482	Director US Army Materiel Systems Analysis Acty Attn: DRXSY-T
001	Aberdeen Proving Ground, MD 21005
507	CDR, US Army Aviation Systems Command Attn: DRSAV-G PO Box 209
001	St. Louis, MO 63166
512	Commander Picatinny Arsenal Attn: SARPA-ND-A-4 (Bldg 95)
001	Dover, NJ 07801
514	Director Joint Comm Office (TRI-TAC) Attn: TT-AD (Tech Docu Cen)
001	Fort Monmouth, NJ 07703
515	Project Manager, REMBASS Attn: DRCPM-RBS
002	Fort Monmouth, NJ 07703
516	Project Manager, NAVCON Attn: DRCPM-NC-TM Bldg 2539
001	Fort Monmouth, NJ 07703
517	Commander US Army Satellite Communications Agcy Attn: DRCPM-SC-3
002	Fort Monmouth, NJ 07703
518	TRI-TAC Office Attn: CSS (Dr. Pritchard)
001	Fort Monmouth, NJ 07703

COPIES	RECIPIENT
217	Naval Air Systems Command Code: AIR-5332
004	Washington, DC 20360
300	AUL/LSE 64-285
001	Maxwell AFB, AL 36112
301	Rome Air Development Center Attn: Documents Library (TILD)
001	Griffiss AFB, NY 13441
304	Air Force Geophysics Lab L.G. Hanscom AFB Attn: LIR
001	Bedford, MA 01730
307	Hq. ESD (DRI) L.G. Hanscom AFB
001	Bedford, MA 01731
310	Hq, AFCS Attn: EPECRW Mail Stop 105B
001	Richards-Gebaur AFB, MO 64030
312	Hq, Air Force Electronic Warfare Center Attn: SURP
002	San Antonio, TX 78243
314	Hq, Air Force Systems Command Attn: DLCA Andrews AFB
001	Washington, DC 20331
403	CDR, US Army Missile Command Redstone Scientific Info Center Attn: Chief, Document Section
002	Redstone Arsenal, AL 35809
406	Commandant US Army Aviation Center Attn: ATZQ-D-MA
003	Fort Rucker, AL 36362

COPIES	RECIPIENT
408	Commandant US Army Military Police School Attn: ATSJ-CD-M-C
003	Fort McClellan, AL 36201
417	Commander US Army Intelligence Center & School Attn: ATSI-CD-MD
002	Fort Huachuca, AZ 85613
418	Commander Hq. Fort Huachuca Attn: Technical Reference Div.
001	Fort Huachuca, AZ 85613
419	Commander US Army Electronic Proving Ground Attn: STEEP-MT
002	Fort Huachuca, AZ 85613
420	Commander USASA Test & Evaluation Center Attn: IAO-CDR-T
001	Fort Huachuca, AZ 85613
421	Commander Hq US Army Communications Command Attn: CC-OPS-SM
001	Fort Huachuca, AZ 85613
432	Dir, US Army Air Mobility R&D Lab Attn: T. Gossett, Bldg 207-5 NASA Ames Research Center
001	Moffett Field, CA 94035
436	HQDA (DAMO-TCE)
002	Washington, DC 20310
437	Deputy for Science & Technology Office, Assist Sec Army (R&D)
001	Washington, DC 20310

COPIES	RECIPIENT
531	CDR, US Army Research Office Attn: DRXRO-IP PO Box 12211 Research Triangle Park, NC 07709
533	Commandant US Army Inst for Military Assistance Attn: ATSU-CTD-MO Fort Bragg, NC 28307
536	Commander US Army Arctic Test Center Attn: STEAC-TD-MI APO Seattle 98733
537	CDR, US Army Tropic Test Center Attn: STETC-MO-A (Tech Library) Drawer 942 Fort Clayton, Canal Zone 09827
542	Commandant US Army Field Artillery School Attn: ATSFA-CTD Fort Sill, OK 73503
548	Commander Frankford Arsenal Attn: PDS 64-4 (J. L. Helfrich) Philadelphia, PA 19137
554	Commandant US Army Air Defense School Attn: ATSA-CD-MC Fort Bliss, TX 79916
555	Commander US Army Nuclear Agency Fort Bliss, TX 79916
563	Commander, DARCOM Attn: DRCDE 5001 Eisenhower Ave Alexandria, VA 22333
564	CDR, US Army Security Agency Attn: IARDA-IT Arlington Hall Station Arlington, VA 22212
566	CDR, US Army Security Agency Attn: IARDA-AQ Arlington Hall Station Arlington, VA 22212
572	Commander US Army Logistics Center Attn: ATCL-MC Fort Lee, VA 22801
575	Commander US Army Training & Doctrine Command Attn: ATCD-TEC Fort Monroe, VA 23651
577	Commander US Army Training & Doctrine Command Attn: ATCD-TM Fort Monroe, VA 23651
578	CDR, US Army Garrison Vint Hill Farms Station Attn: IAVAAF Warrenton, VA 22186
602	Director, Night Vision Laboratory US Army Electronics Command Attn: DRSEL-NV-D Fort Belvoir, VA 22060

COPIES	RECIPIENT
603	CDR/DIR, Atmospheric Sciences Laboratory US Army Electronics Command Attn: DRSEL-BL-SY-S
001	White Sands Missile Range, NM 88002
605	Chief, Aviation Electronics Div (SIMO) US Army Electronics Command Attn: DRSEL-SI-AE, PO Box 209
001	St. Louis, MO 63166
606	Chief Intel Materiel Dev & Support Ofc Electronic Warfare Lab, ECOM
001	Fort Meade, MD 20755
680	Commander US Army Electronics Command
000	Fort Monmouth, NJ 07703
1	DRSEL-PL-ST
1	DRSEL-VL-D
1	DRSEL-PP-I-PI
1	DRSEL-WL-D
1	DRSEL-TL-D
3	DRSEL-CT-D
1	DRSEL-BL-D
*3	DRSEL-NL-RN
1	DRSEL-NL-D (Ofc of Record)
1	DRSEL-SI-CM
1	DRSEL-MA-MP
**2	DRSEL-MS-TI
1	DRSEL-GG-TD
1	DRSEL-CG (Mr. Doxey)
2	DRSEL-PA
1	DRCPM-AA
1	DRCPM-TDS-SE
1	USMC-LNO
1	DRSEL-GS-H
1	DRSEL-RD
1	TRADOC-LNO
25	Originating Office (DRSEL-NL-RH)

COPIES	RECIPIENT
701	MIT - Lincoln Laboratory Attn: Library (RM A-082) PO Box 73
002	Lexington, MA 02173
703	NASA Scientific & Tech Info Facility Baltimore/Washington Intl Airport
001	PO Box 8757, MD 21240
705	Advisory Group on Electron Devices 201 Varick Street, 9th Floor
002	New York, NY 10014
706	Advisory Group on Electron Devices Attn: Secy, Working Group D (Lasers) 201 Varick Street
002	New York, NY 10014
707	TACTEC Battelle Memorial Institute 505 King Avenue
001	Columbus, OH 43201
710	Ketron, Inc. Attn: Mr. Frederick Leuppert 1400 Wilson Blvd, Architect Bldg
002	Arlington, VA 22209
71?	R.C. Hansen, Inc. PO Box 215
001	Tarzana, CA 91356
	Project Manager Single Channel Ground & Airborne Radio Subsystem (SINCGARS) Attn: DRCOM-GARS-TM
003	Ft. Monmouth, NJ 07703

* Or number specified in contract. Add COTR's mail symbol.

** Unclassified reports only.

APPENDIX E

FORM DD 1473

UNCLASSIFIED

Security Classification

DOCUMENT CONTROL DATA - R&D

(Security classification of title, body of abstract and indexing annotation must be entered when the overall report is classified)

1 ORIGINATING ACTIVITY (Corporate author) Cincinnati Electronics Corporation 2630 Glendale-Milford Road Cincinnati, Ohio 45241	2a REPORT SECURITY CLASSIFICATION Unclassified 2b GROUP

3 REPORT TITLE

VHF Manpack Centerfed Whip Antenna

4 DESCRIPTIVE NOTES (Type of report and inclusive dates)

Final Report

5 AUTHOR(S) (Last name, first name, initial)

J. E. Brunner

6 REPORT DATE	7a TOTAL NO. OF PAGES	7b NO. OF REFS
June 1977	123	3

8a CONTRACT OR GRANT NO. DAAB07-76-C-0109 b PROJECT NO. CLIN 0004 c d	9a ORIGINATOR'S REPORT NUMBER(S) 80045-URC92/777 9b OTHER REPORT NO(S) (Any other numbers that may be assigned this report)

10 AVAILABILITY/LIMITATION NOTICES

DISTRIBUTION STATEMENT A
Approved for public release;
Distribution Unlimited

11 SUPPLEMENTARY NOTES	12 SPONSORING MILITARY ACTIVITY
	U.S. Army Electronics Command Fort Monmouth, New Jersey

13 ABSTRACT

Historically, manpack radios operating in the VHF military communications band, have been equipped with basefed whip antennas requiring electrically small manpack radio-case to serve as a counterpoise. Since the manpack case is in rather close contact with the carrier's body, antenna performance is affected by body positions (standing, prone, etc.) and by the degree of coupling to the carrier's body as determined by clothing and body conductivity. The objective of the work presented in this report is to develop a 30-88 MHz manpack whip antenna exhibiting impedance, efficiency and radiation pattern characteristics which are less sensitive to body proximity and position. A further objective is to achieve a radiating structure which can be matched to a 50 ohm source, under all operating conditions, employing no more than six fixed-tuned matching networks.

DD FORM 1 JAN 64 1473

UNCLASSIFIED

Security Classification

14 KEY WORDS	LINK A		LINK B		LINK C	
	ROLE	WT	ROLE	WT	ROLE	WT

INSTRUCTIONS

1. ORIGINATING ACTIVITY: Enter the name and address of the contractor, subcontractor, grantee, Department of Defense activity or other organization *(corporate author)* issuing the report.

2a. REPORT SECURITY CLASSIFICATION: Enter the overall security classification of the report. Indicate whether "Restricted Data" is included. Marking is to be in accordance with appropriate security regulations.

2b. GROUP: Automatic downgrading is specified in DoD Directive 5200.10 and Armed Forces Industrial Manual. Enter the group number. Also, when applicable, show that optional markings have been used for Group 3 and Group 4 as authorized.

3. REPORT TITLE: Enter the complete report title in all capital letters. Titles in all cases should be unclassified. If a meaningful title cannot be selected without classification, show title classification in all capitals in parenthesis immediately following the title.

4. DESCRIPTIVE NOTES: If appropriate, enter the type of report, e.g., interim, progress, summary, annual, or final. Give the inclusive dates when a specific reporting period is covered.

5. AUTHOR(S): Enter the name(s) of author(s) as shown on or in the report. Enter last name, first name, middle initial. If military, show rank and branch of service. The name of the principal author is an absolute minimum requirement.

6. REPORT DATE: Enter the date of the report as day, month, year, or month, year. If more than one date appears on the report, use date of publication.

7a. TOTAL NUMBER OF PAGES: The total page count should follow normal pagination procedures, i.e., enter the number of pages containing information.

7b. NUMBER OF REFERENCES: Enter the total number of references cited in the report.

8a. CONTRACT OR GRANT NUMBER: If appropriate, enter the applicable number of the contract or grant under which the report was written.

8b, 8c, & 8d. PROJECT NUMBER: Enter the appropriate military department identification, such as project number, subproject number, system numbers, task number, etc.

9a. ORIGINATOR'S REPORT NUMBER(S): Enter the official report number by which the document will be identified and controlled by the originating activity. This number must be unique to this report.

9b. OTHER REPORT NUMBER(S): If the report has been assigned any other report numbers *(either by the originator or by the sponsor)*, also enter this number(s).

10. AVAILABILITY/LIMITATION NOTICES: Enter any limitations on further dissemination of the report, other than those imposed by security classification, using standard statements such as:

(1) "Qualified requesters may obtain copies of this report from DDC."

(2) "Foreign announcement and dissemination of this report by DDC is not authorized."

(3) "U. S. Government agencies may obtain copies of this report directly from DDC. Other qualified DDC users shall request through _____."

(4) "U. S. military agencies may obtain copies of this report directly from DDC. Other qualified users shall request through _____."

(5) "All distribution of this report is controlled. Qualified DDC users shall request through _____."

If the report has been furnished to the Office of Technical Services, Department of Commerce, for sale to the public, indicate this fact and enter the price, if known.

11. SUPPLEMENTARY NOTES: Use for additional explanatory notes.

12. SPONSORING MILITARY ACTIVITY: Enter the name of the departmental project office or laboratory sponsoring *(paying for)* the research and development. Include address.

13. ABSTRACT: Enter an abstract giving a brief and factual summary of the document indicative of the report, even though it may also appear elsewhere in the body of the technical report. If additional space is required, a continuation sheet shall be attached.

It is highly desirable that the abstract of classified reports be unclassified. Each paragraph of the abstract shall end with an indication of the military security classification of the information in the paragraph, represented as *(TS), (S), (C), or (U)*.

There is no limitation on the length of the abstract. However, the suggested length is from 150 to 225 words.

14. KEY WORDS: Key words are technically meaningful terms or short phrases that characterize a report and may be used as index entries for cataloging the report. Key words must be selected so that no security classification is required. Identifiers, such as equipment model designation, trade name, military project code name, geographic location, may be used as key words but will be followed by an indication of technical context. The assignment of links, rules, and weights is optional.

GPO 886-551

AD-A046 862 CINCINNATI ELECTRONICS CORP OHIO F/G 9/1
VHF MANPACK CENTERFED WHIP ANTENNA.(U)
JUN 77 J E BRUNNER DAAB07-76-C-0109
UNCLASSIFIED 80045-URC92/777 NL

1 OF 2
AD
AD 46862

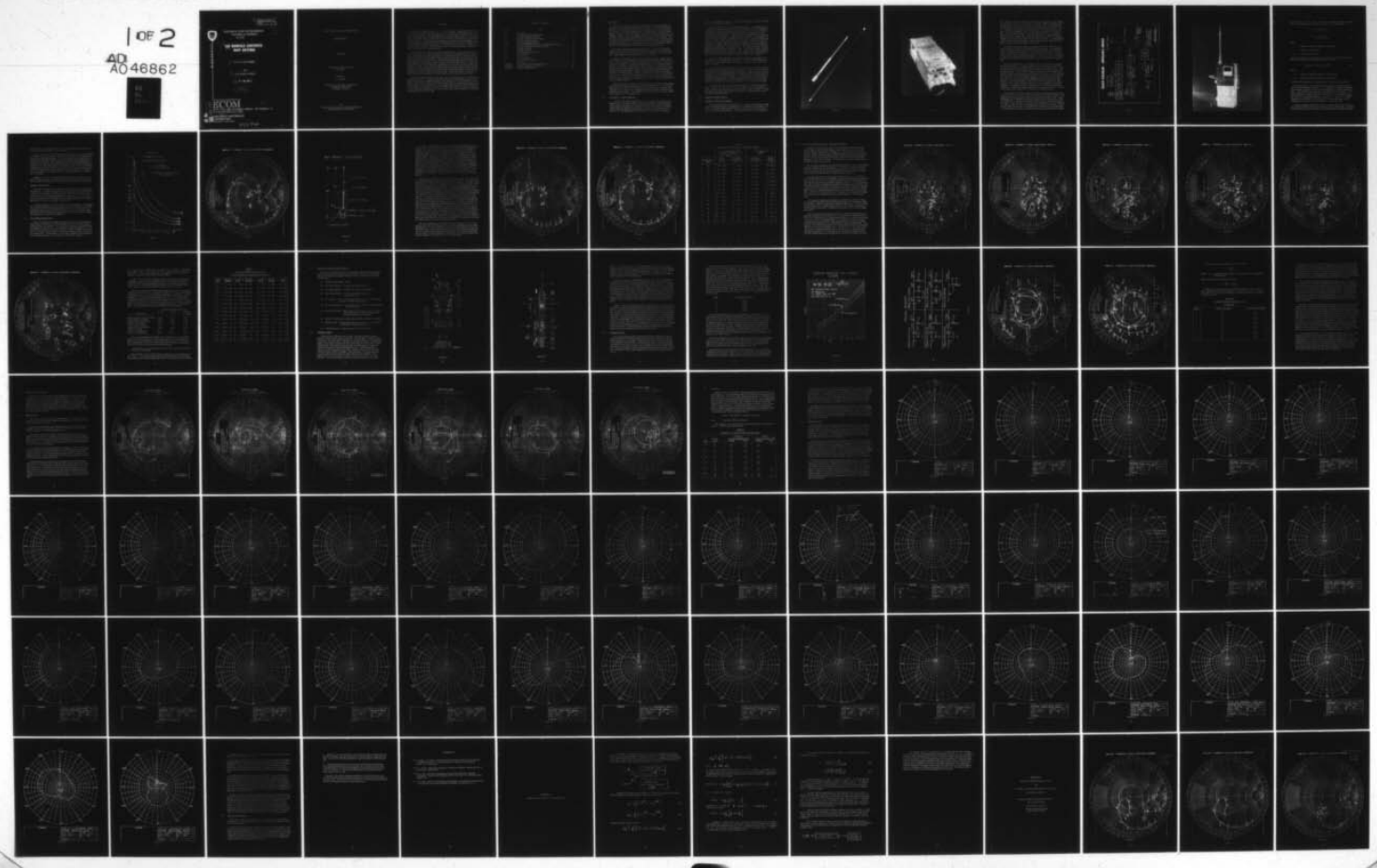

(14) 80045-URC92/777

AD

(12)

RESEARCH AND DEVELOPMENT
TECHNICAL REPORT
ECOM-

(6) VHF MANPACK CENTERFED WHIP ANTENNA.

(9) FINAL REPORT.

BY

(10) J.E. BRUNNER

(11) JUNE 1977

(12) 133 p.

ECOM

UNITED STATES ARMY ELECTRONICS COMMAND · FORT MONMOUTH, N.J.

CONTRACT (15) DAAB07-76-C-0109

CINCINNATI ELECTRONICS CORPORATION
CINCINNATI, OHIO 45241

Q1

1473

H07944

AB

VHF MANPACK CENTERFED WHIP ANTENNA

FINAL REPORT

JUNE 1977

CONTRACT DAAB07-76-C-0109
CLIN-0004

Prepared by

J. E. Brunner

CINCINNATI ELECTRONICS CORPORATION
2630 Glendale-Milford Road
Cincinnati, Ohio 45241

For

UNITED STATES ARMY ELECTRONICS COMMAND
FORT MONMOUTH, NEW JERSEY

ABSTRACT

Historically, manpack radios operating in the VHF military communications band, have been equipped with basefed whip antennas requiring electrically small manpack radio-case to serve as a counterpoise. Since the manpack case is in rather close contact with the carrier's body, antenna performance is affected by body positions (standing, prone, etc.) and by the degree of coupling to the carrier's body as determined by clothing and body conductivity. The objective of the work presented in this report is to develop a 30-88 MHz manpack whip antenna exhibiting impedance, efficiency and radiation pattern characteristics which are less sensitive to body proximity and position. A further objective is to achieve a radiating structure which can be matched to a 50 ohm source, under all operating conditions, employing no more than six fixed-tuned matching networks.

To achieve the above objectives, electrical characteristics of a 4-foot whip antenna, fed 17-21 inches above its point of connection to an AN/URC-78 manpack radio, were investigated. The elevated feed point approach causes a larger portion of the antenna current to return to the generator via the outer conductor of the feed coax rather than via the carrier's body, thus reducing proximity effects. Although the feed point is not at the physical center of the radiator, the structure is referred to as a Centerfed Whip Antenna. Various feed point locations, feed-line characteristic impedances and feed-line electrical lengths were examined in terms of input impedance characteristics as related to the various operational conditions. Operational conditions explored include: standing, standing with handset extended and prone; also measurements were conducted with the antenna-manpack combination free standing on a dielectric support 5-foot above ground. Finally, performance characteristics of the optimal centerfed antenna are compared with a basefed whip of the same length.

Results show that when the feed point is located at the electrical center of the whip and packset assembly, the centerfed antenna can be matched, for all conditions, using fewer subbands than required for the basefed antenna. Also, efficiency of the centerfed whip is several dB better than the basefed whip over the lower portion of the 30-88 MHz band and about equal to the basefed efficiency above 50 MHz. The azimuth radiation patterns of both configurations are reasonably omnidirectional over the 30-50 MHz range; however, significant anomalies occur in the basefed whip pattern at 60 MHz; whereas, the centerfed whip shows reasonably well behaved patterns up to 80 MHz.

TABLE OF CONTENTS

1.0 Introduction

This report describes the design and development of an asymmetrically fed whip antenna and associated matching network circuitry. The antenna is intended for future use with tactical manpack radios operating in the 30-88 MHz portion of the VHF band. The subject whip antenna is generally called a "Centerfed" whip because the whip is fed, via a coax line, at a point which is the electrical center of the radiating structure. The total radiating structure is considered to be the whip and associated manpack radio case, including the metal battery-pack container. Since the radio case is an important part of the radiating structure, a URC-78 radio and associated battery pack was used in conjunction with the whip antenna throughout the development program. The 4-foot whip mounted on the URC-78 manpack radio results in an overall radiating structure length of approximately five feet.

The subject program was executed in two phases. Phase I entailed design, fabrication and test of exploratory-optimization models in order to establish optimum design parameters. In Phase II the design was finalized, advanced development models fabricated and final performance tests conducted.

During the first phase, a battery powered impedance bridge, capable of being housed within a URC-78 Radio case, was designed and fabricated so that measurement of antenna impedance could be accomplished without perturbing connections to external test equipment. Several experimental whips were then fabricated and extensive measurements, using the battery powered bridge were performed in order to determine optimal feed point location, electrical length of the feed-line and feed-line characteristic impedance. These measurements were conducted for three conditions: 1) manpack carrier standing, 2) standing with handset extended approximately three feet and held by a second person and 3) carrier in the prone position. Also, measurements were performed with the radio and antenna combination mounted 5-foot above ground level on a dielectric stand. This is referred to hereafter as the free standing condition.

During Phase II of the program mechanical design of the centerfed whip antenna was finalized based upon the parameters determined during Phase I. Also, matching networks covering the 30-88 MHz range in six subbands were designed, fabricated and tested. Three URC-78 Manpack Radios were modified to accept the new matching network modules. The modules were designed to fit in the space occupied by the original URC-78 matching network.

1.1 Description of Final Configuration

The final 4-foot whip configuration is fed 17 inches above the point where the whip connects to the manpack radio. Since the total length of the whip and radio case assembly is 60-inches, the 17-inch feed point location results in excitation of the composite structure one-inch below its center. The feed line is a 95 ohm coax incorporating expanded teflon dielectric, having a relative dielectric constant of 1.23. This low dielectric constant allows the feed line outer diameter

to be kept small without requiring an excessively small center conductor to realize the 95 ohm characteristic impedance.

Figure 1 shows the final centerfed whip configuration. As indicated, a screw type coupling, similar to a type-N connector, is provided to secure the antenna to the radio case. A section of flexible steel tubing six-inches long and 0.45 inch in diameter is provided at the base of the whip assembly to allow a 90° bend when operating in the prone position. The feed coax runs through the flex section and an 8.4-inch length of 0.19-inch O.D. rigid stainless teel tubing. At the feed point, a short section of 0.31-inch O.D. fiberglass tubing is used to support the upper whip section. The upper whip section is attached to the lower section via a screw connection; thus, the upper whip can be removed to facilitate packaging in a field kit. In addition, the upper section is made of spring stainless steel 0.10 inch diameter at the base and tapering to 0.040 inch at the tip. This allows bending into a rather tight loop without permanent deformation. Also, a one-half inch diameter teardrop-shaped tip is provided for eye protection. The eye protector tip is molded plastic foam and can be removed by crushing to reduce visibility under combat conditions. Figure 2 shows a URC-78 Radio with a matching network module installed.

Performance characteristics of the final centerfed whip configuration, as described above, are presented under paragraph 4.0. These include: impedance at the matching network input, efficiency relative to a half-wave dipole and azimuth radiation patterns.

For comparison, similar measurements were also performed with a 4-foot basefed whip mounted on the URC-78 manpack radio case. These measurements were performed for the free standing condition and with the manpack on a carrier's back. In general, the basefed whip exhibited a much higher impedance than the centerfed configuration over the 30-50 MHz range. At the higher end of the band impedance characteristics were similar. However, impedance variations over the range of operational conditions were noted to be significantly less for the centerfed whip than for the basefed whip. This was particularly true at the low end of the band.

Smith Chart plots of the measured impedance data, for all antenna configurations, is presented. This data is also listed in tabular form (see Appendix C) since resolution on the charts is poor over the lower portion of the band. The tables also indicate the feed point impedances as derived by transformation of the measured input impedance values.

2.0 Initial Investigation (Phase I)

2.1 Impedance Measurement Technique

Accurate measurement of the impedance of a manpack antenna requires a high degree of isolation between the radiating system and impedance measuring instruments. In general, cable connections between antenna and test instruments represent the major perturbing factor. Previous investigators, such as Krupka[1],

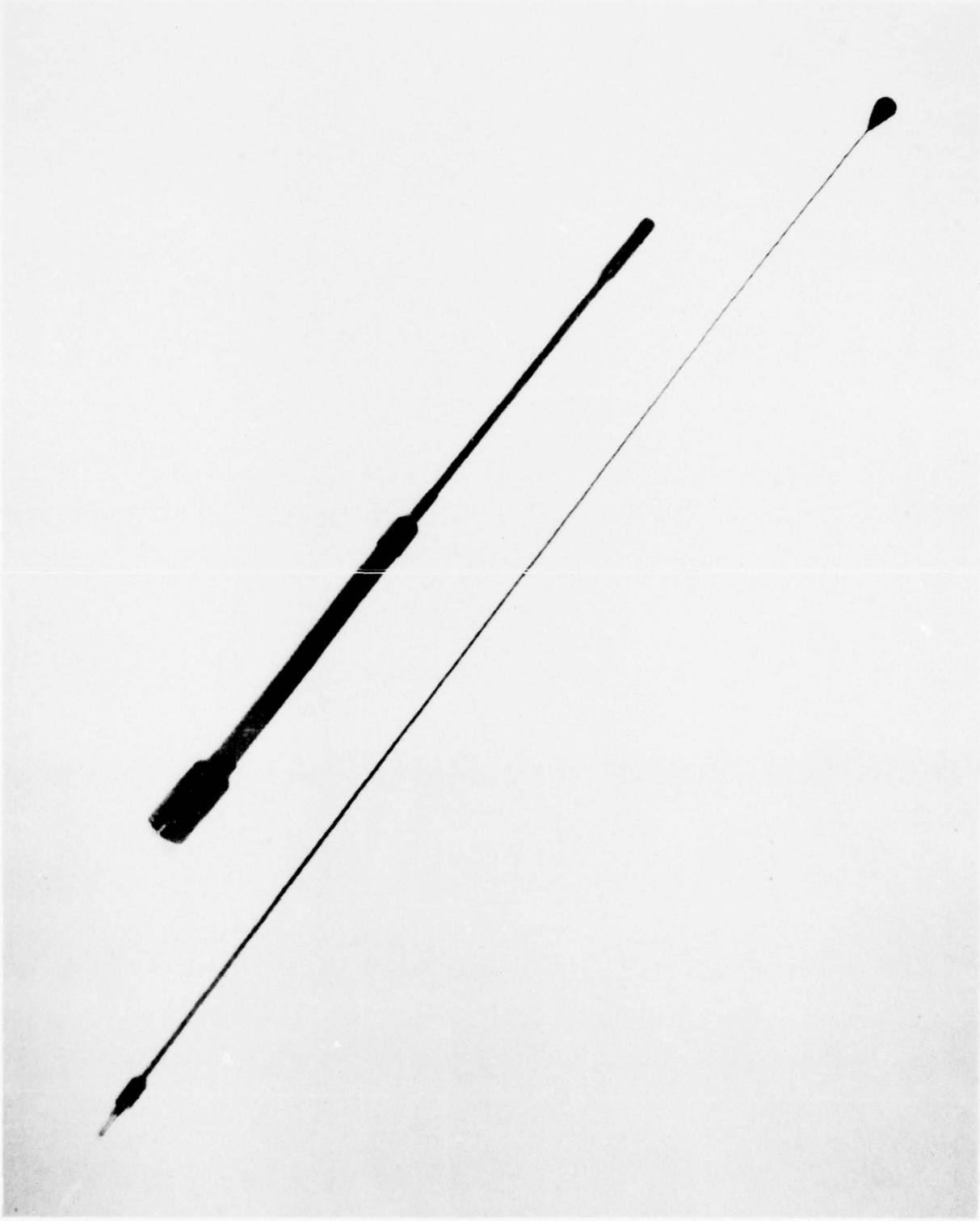

FIGURE 1

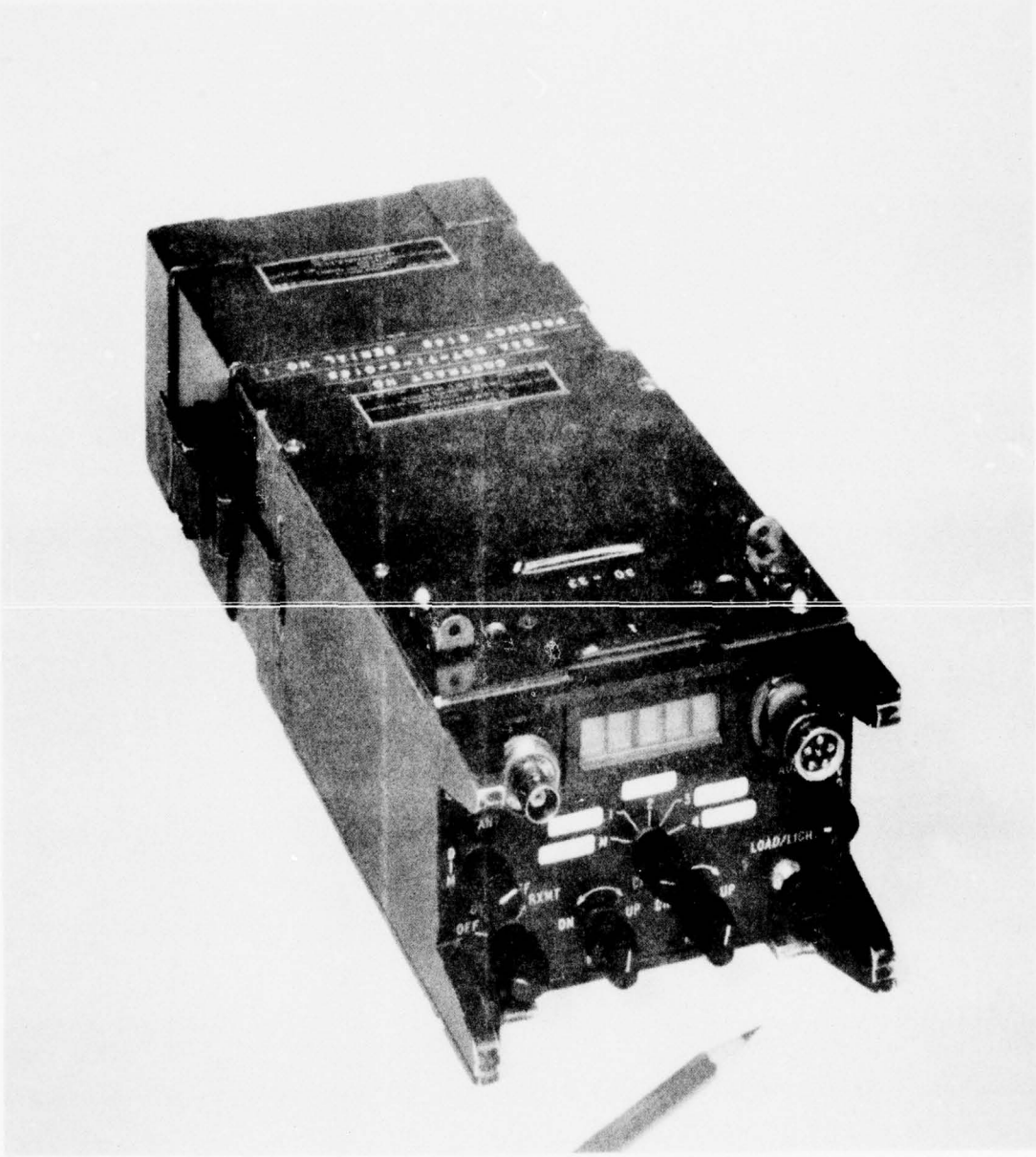

FIGURE 2

have employed RF chokes in the interconnecting lines. Such devices reduce directly conducted RF currents but have no effect on mutual coupling between the driven antenna and the line on the test-instrument side of the choke. For example, the mutual impedance between two resonant colinear half wave dipoles spaced 0.01λ is $(26 + j18)$; hence, if one dipole is driven and the other shorted the current at the center of the shorted dipole is only 7 dB below that at the center of the driven dipole. Also, the input impedance of the driven dipole becomes $(67 - j13)$ rather than the 72 ohm free space value. In this example the 0.01λ spacing between dipole ends may be considered an infinite-impedance perfect choke, yet significant coupling occurs and is reflected in the driven dipole impedance. To avoid the above problem a battery powered impedance bridge, having the block diagram shown in figure 3, was used for all impedance measurements.

The circuitry indicated in figure 3 was housed in a URC-78 Radio case and powered by batteries housed in a standard URC-78 battery box. The impedance test set assembly is shown in figure 4. The bridge was balanced by remotely adjusting the variable load, using a 12-foot long tapered fiberglass tube as a tuning wand, so that the person operating the bridge did not affect the antenna impedance. Proximity of the person operating the bridge was observed to be least critical over the 30-50 MHz range; in general, proximity was most critical between 60 and 75 MHz.

An Anzac Model HH-107 180°-hybrid was used as the impedance comparator element in the bridge. As indicated in figure 3, the whip antenna is connected to one arm of the hybrid and a variable load is connected to the opposite arm. A null is obtained, at the hybrid difference port, when the load impedance is equal to the antenna impedance. When a null is obtained the impedance of the variable load is measured using a Hewlett Packard network analyzer. When the system is adjusted for a null, any power not absorbed by the loads is reflected back to the hybrid sum port; therefore, a 6 dB pad and buffer amplifier are used to isolate the tunable oscillator. This prevents frequency pulling and forward power variation under high sum - port VSWR conditions. Also, the RF Source is modulated at 1 kHz and the detected modulation at the hybrid difference port is amplified via a bandpass amplifier. The amplifier provides 70 dB gain and a 14 Hz bandwidth centered at 1 kHz; hence, interferring signals coupled in by the antenna are rejected. The system provides a null sensitivity of 40 to 45 dB over the band of interest.

The variable reference load provides a reflection coefficient magnitude range of 0.966 to 0.06 ($1.13 < \text{VSWR} < 58$) by adjustment of the variable attenuator. The capacitor and inductor provide variation of the reflection coefficient angle. Series combination of the variable attenuator and reactors provide a wide range of reflection coefficient, or impedance, variation. However, when measuring an antenna impedance of large reactance to resistance ratio significant error in the measured R-component value can result, even though a good bridge null is achieved. This is caused by finite insertion loss associated with the variable attenuator which limits the maximum value of reflection coefficient-magnitude achievable with the variable

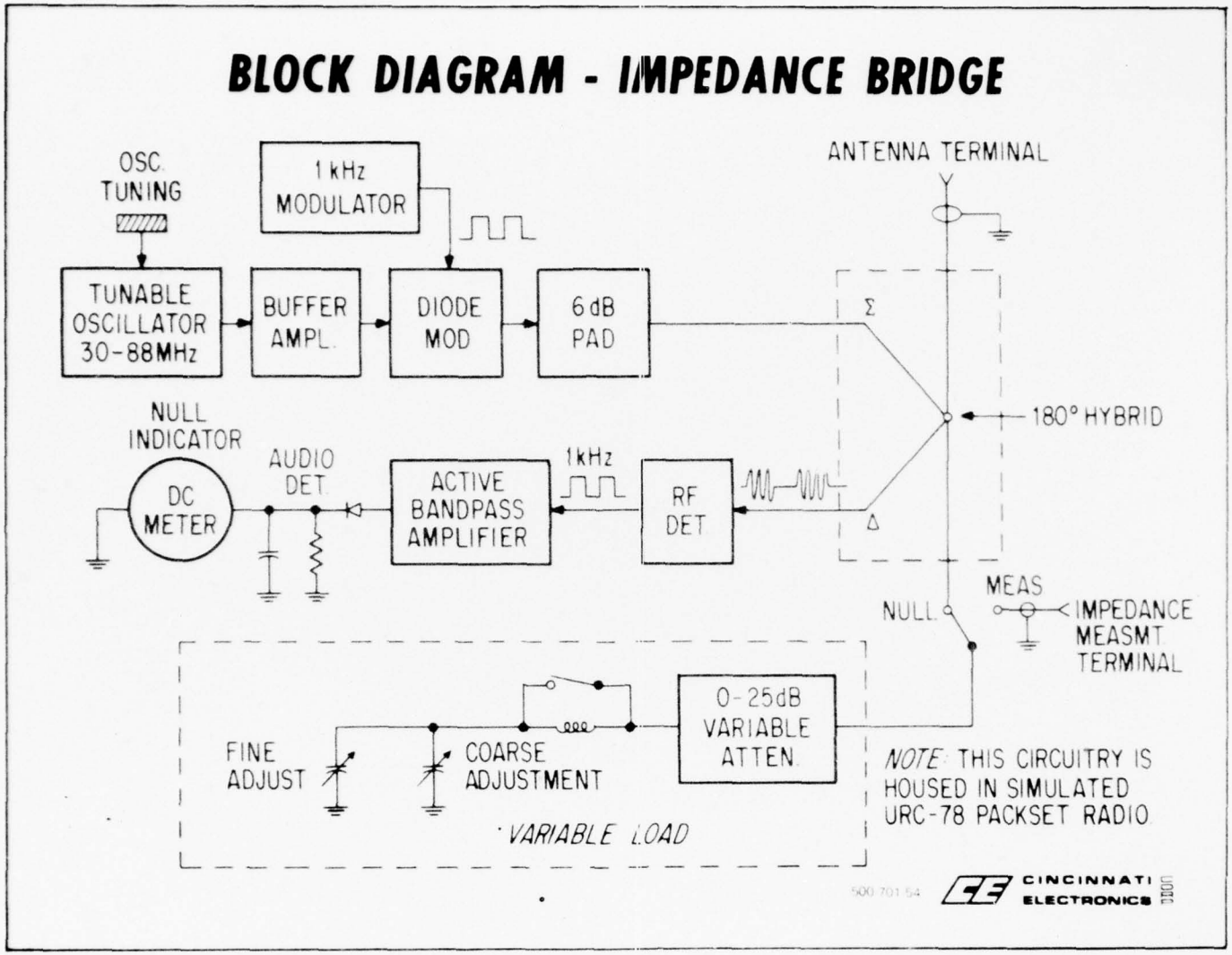
BLOCK DIAGRAM - IMPEDANCE BRIDGE
OSC. TUNING
1 kHz MODULATOR
ANTENNA TERMINAL
TUNABLE OSCILLATOR 30-88MHz
BUFFER AMPL.
DIODE MOD
6 dB PAD
Σ
180° HYBRID
NULL INDICATOR
DC METER
AUDIO DET.
ACTIVE BANDPASS AMPLIFIER
1kHz
RF DET
Δ
MEAS
NULL
IMPEDANCE MEASMT. TERMINAL
0-25dB VARIABLE ATTEN.
FINE ADJUST
COARSE ADJUSTMENT
VARIABLE LOAD
NOTE: THIS CIRCUITRY IS HOUSED IN SIMULATED URC-78 PACKSET RADIO
500-701-54
CINCINNATI ELECTRONICS

FIGURE 3

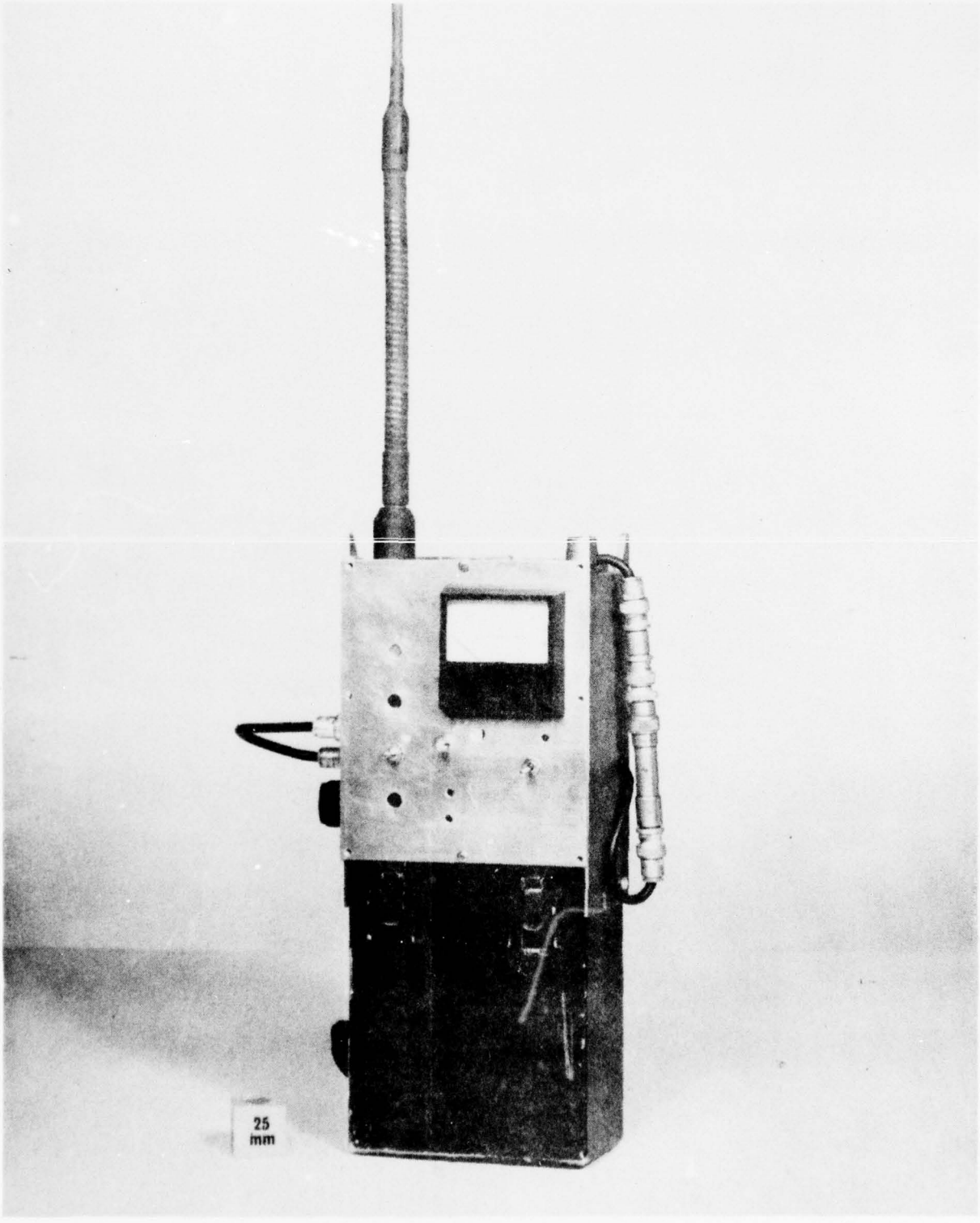

FIGURE 4

reference load. Using the standard expression for reflection coefficient, the R & X values corresponding to polar reflection coefficient ($\Gamma \angle \phi$) are given by:

$$R = \frac{(1 - \Gamma^2)\, Z_o}{(1 + \Gamma^2) - 2\Gamma \cos\phi} \tag{1}$$

$$X = \frac{2\Gamma\, Z_o \sin\phi}{(1 + \Gamma^2) - 2\Gamma \cos\phi} \tag{2}$$

where:

Γ = reflection coefficient magnitude (Voltage Ratio)

ϕ = reflection coefficient angle

Z_o = characteristic impedance

Also, if the reflection coefficient angle of the reference load is equal to that of the unknown load, the maximum null depth obtainable is given by:

$$\text{Null (dB)} = 20 \log_{10} \left| \frac{\Gamma r - \Gamma x}{2} \right| \tag{3}$$

where:

Γr = reflection coefficient magnitude of reference load

Γx = reflection coefficient magnitude of unknown load

In general, the equal reflection coefficient angle condition is easily satisfied.

If the insertion loss of the variable attenuator limits the maximum value of reference load reflection coefficient to $\Gamma r = -0.30$ dB and the unknown load reflection coefficient is actually -0.20 dB, the null obtainable is -45 dB per equation (3) above. This would be considered a very good null; however, inserting $\Gamma r = -0.30$ dB into equations (1) and (2), with angle ϕ assumed to be -45°, results in an apparent value for the unknown load of R = 5.88 ohms, X = -120.47 ohms. Substitution of the true unknown load reflection coefficient $\Gamma x = -0.20$ dB, $\phi = -45°$ into equations (1) and (2) yields: R = 3.93 ohms, X = -120.60 ohms; hence, the R-component error is 49.6% and the X-component error is only 0.11 %.

The above example shows that a large R-component measurement error may occur if the attenuator setting must be reduced to zero to obtain a null, even though the null depth is very good. However, the good null results from accurate match-

ing of reflection coefficient angles which yields an accurate reactance value provided the reflection coefficient magnitude is large.

Error in measurement of the R-component, under large X to R ratio conditions, is avoided by inserting an inductor of known reactance and Q in series with the antenna prior to balancing the bridge. This transforms the antenna impedance to a lower reflection coefficient which can be accommodated by an attenuation value exceeding the insertion loss of the variable attenuator. The antenna impedance is obtained by correcting the measured variable load impedance using the previously measured R & X values of the added series inductor. Moreover, the X-component of antenna impedance thus obtained can be checked by measurement with the series inductor removed, since direct measurement of the X-component is less than 1% in error as indicated in the above example. The above approach was used in the 30-45 MHz range.

Appendix A presents a discussion of bridge accuracy considerations. Also, figure 5 shows the minimum R-value which can be accurately measured as a function of reflection coefficient angle, for several values of attenuator insertion loss.

2.2 Impedance Characteristics

Impedance measurements were performed using the battery powered bridge discussed above. Initially, measurements were conducted with the manpack-whip combination free standing on a dielectric support which placed the bottom of the radio approximately five feet above ground level. All other measurements were conducted with the manpack-whip combination on a carrier's back. Measurements were taken with the carrier standing, prone and standing with the handset extended approximately three feet and held by a second person.

Feed point locations of 17, 19 and 21 inches were investigated. Also feed line characteristic impedances of 50, 75, 95 and 125 ohms were explored. Only limited investigation of the 50 and 75 ohm impedance levels was carried out since it was immediately apparent that these values resulted in very low R-component values. Smith Chart plots of all impedance characteristics are presented; also, corresponding tabulated data is given in the Appendix B.

2.2.1 Free Standing Characteristics

Figure 6 shows the free standing impedance characteristics of the centerfed whip-manpack combination for feed line impedance of 95 and 125 ohms with the feed point located at 19 inches. Unless otherwise specified, the feed-line velocity of propagation for all data is 71%, corresponding to solid teflon dielectric. Also, the impedances plotted are referred to the base or input of the whip (see figure 7), hence, the feed line length is equal to the feed point position relative to the top of the manpack radio. The impedance at the feed point, obtained by transforming the measured input impedance to the feed-point, is also plotted in figure 6.

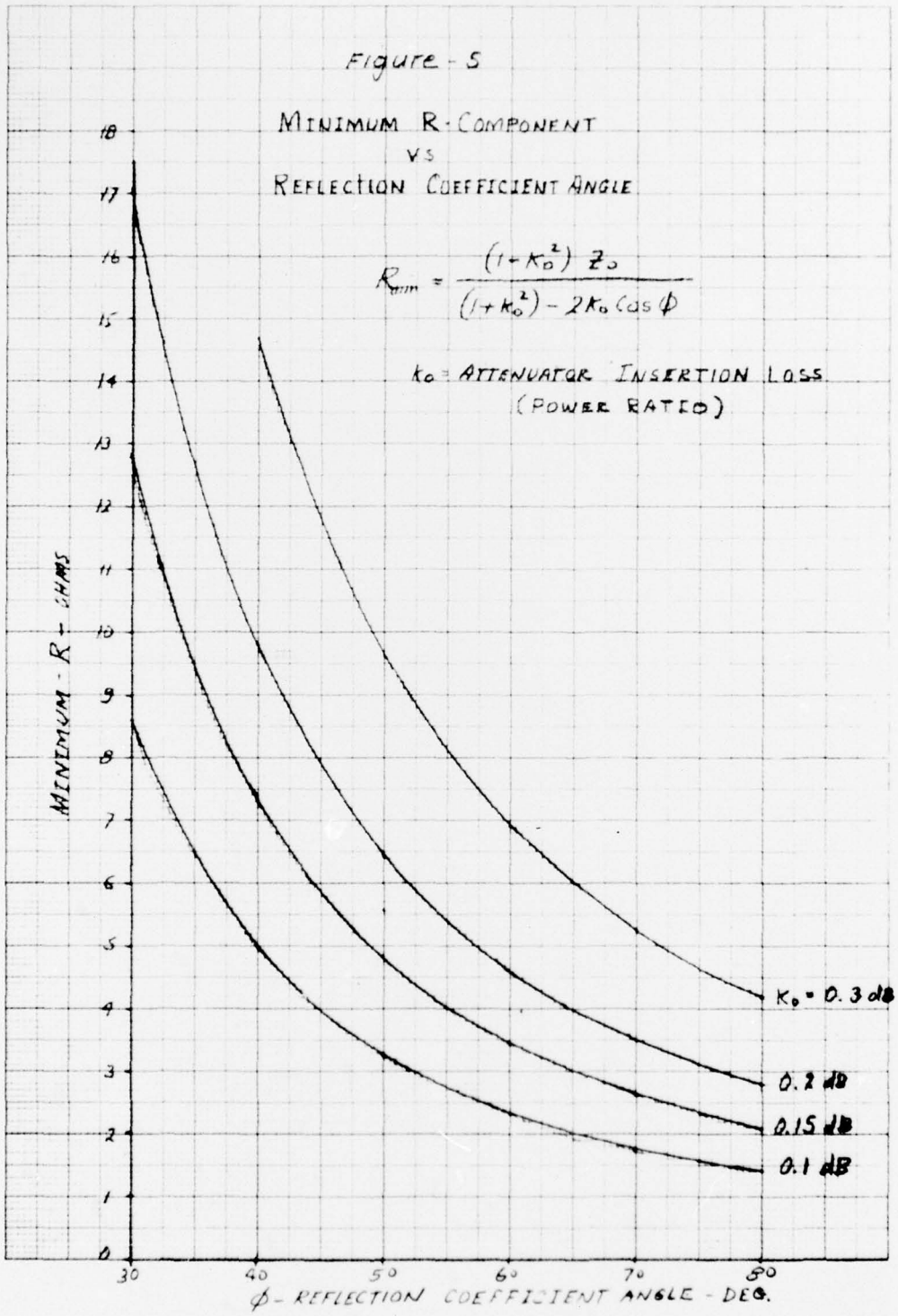
Figure - 5
MINIMUM R-COMPONENT
VS
REFLECTION COEFFICIENT ANGLE
$R_{min} = \frac{(1+K_0^2)\,Z_0}{(1+K_0^2) - 2K_0 \cos\phi}$
K_0 = ATTENUATOR INSERTION LOSS (POWER RATIO)
MINIMUM - R - OHMS
0
1
2
3
4
5
6
7
8
9
10
11
12
13
14
15
16
17
18
30
40
50
60
70
80
ϕ - REFLECTION COEFFICIENT ANGLE - DEG.
K_0 = 0.3 dB
0.2 dB
0.15 dB
0.1 dB

FIGURE 5

IMPEDANCE COORDINATES — 50 OHM CHARACTERISTIC IMPEDANCE

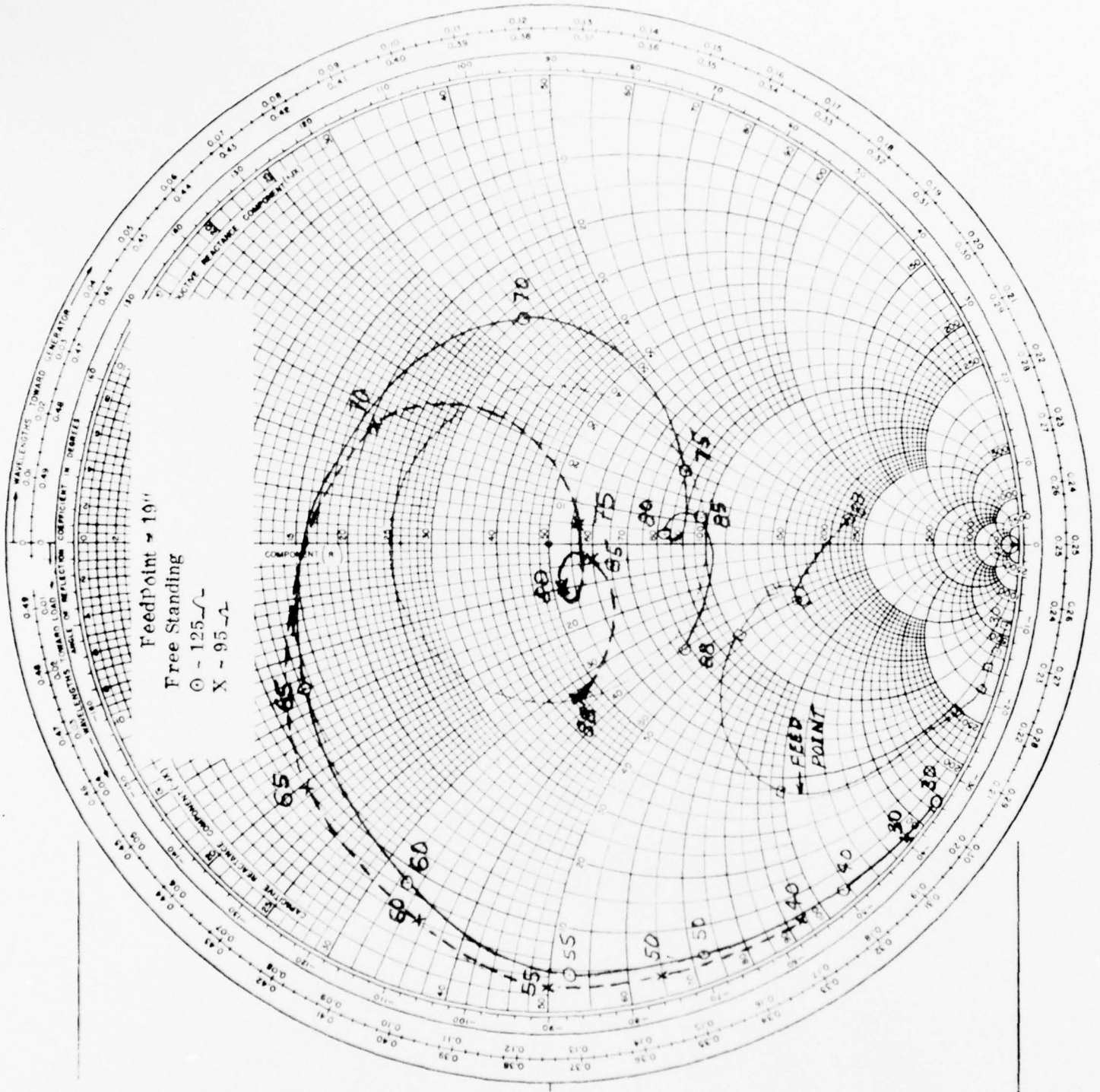

FIGURE 6

WHIP - MANPACK CONFIGURATION

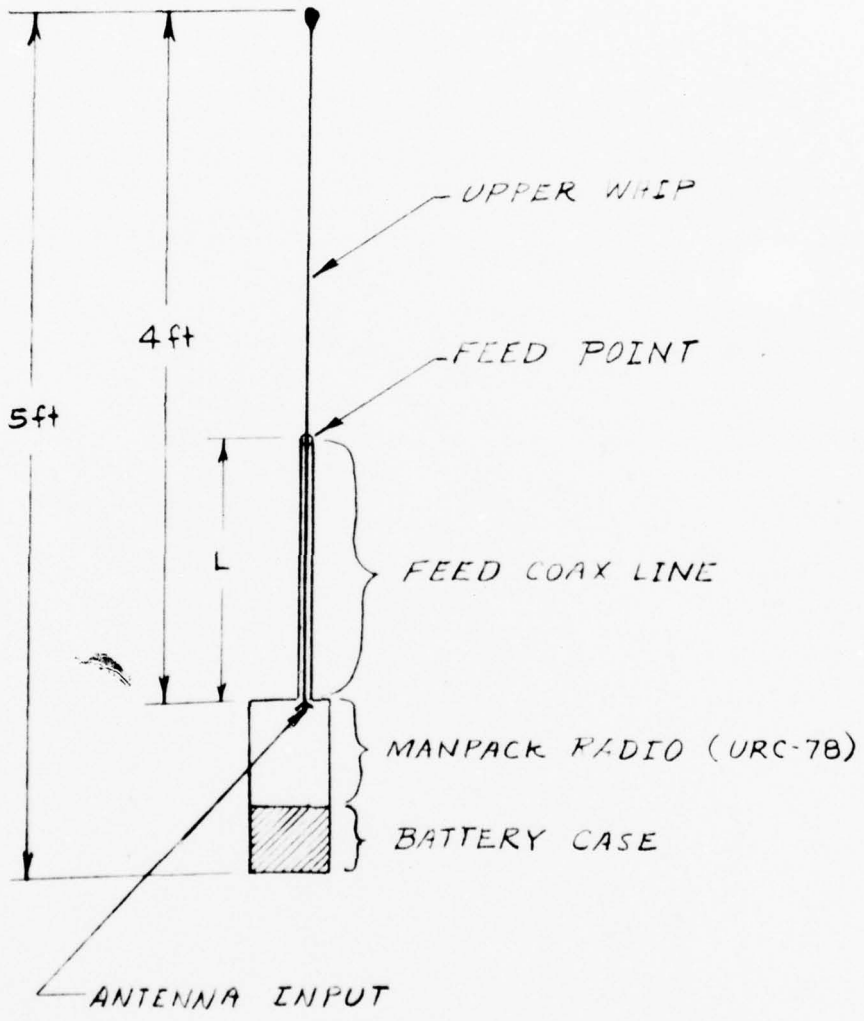

FIGURE 7

For the free standing condition, the whip-manpack combination may be considered a dipole type structure driven at the feed point with one end loaded by the manpack case. Therefore, the feed point impedance characteristic should be similar to a dipole of the same overall length and driven at the same point. To establish confidence in the measured data this theory was explored. The feed point impedance of an off-center fed dipole having an overall length of 60-inches (Length of whip + manpack) was computed using the method developed by King & Harrison[2]. For comparison with measured data, the computed feed point impedance of the dipole was transformed through a 19 inch length of 95 ohm coax as used to feed the actual antenna. The impedance characteristic thus computed is plotted in figure 8 along with measured points for the whip-manpack combination. The computed characteristic is quite similar to the measured data, except the reactance at corresponding frequencies is less for the measured points. This is probably due to the fact that the end loading effect of the manpack case was not included in the computation. Figure 9 shows the same data for the 125 ohm feed line case.

Impedance characteristics for a basefed whip, driven against the URC-78 manpack case, are shown in Table I for the free standing condition. The whip in this case was four feet long and tapered from 0.10-inch in diameter at the base to 0.040-inch in diameter at the tip. For comparison, the free standing impedances of the centerfed configuration are also listed in Table I along with impedance measured for each antenna when on a carrier's back. Examination of the data in Table I shows the centerfed configuration to be reasonably independent of carrier proximity. This is particularly true over the 30-50 MHz range. Conversely, the basefed whip R-component increases significantly when the manpack is on the carrier's back; moveover, the increase is greatest within the low frequency portion of the band. The large R-component increase may be interpreted to indicate large dissipative losses caused by coupling to the carrier's body; to a degree this is certainly true. However, it is well known that the impedance of a linear radiator is a first order function of current distribution and this distribution is most certainly altered, relative to the free-standing condition, by the carrier's body. Therefore, one cannot conclude that the increase in R-component is totally due to power dissipated in the carrier's body. Also, some alteration of the basefed whip current distribution is indicated by change in the reactive component. Efficiency measurements, as discussed under paragraph 4.2, show the efficiency of the centerfed configuration to be considerably better than the basefed configuration at the lower end of the band, but the improvement is not as great as obtained by assuming the total basefed R-component increase to be due to dissipative losses.

The most significant factors indicated by the data in Table I are: 1) The impedance (both R and X Components) of the centerfed configuration does not change significantly due to carrier proximity; thus the current distribution is not greatly altered and 2) the reactive component at the lower end of the band is smaller and the rate of change is less than for the basefed whip. The second factor is important in terms of matching bandwidth; in other words, the reactance spread is less when the impedance is transformed by the matching network.

IMPEDANCE COORDINATES—50-OHM CHARACTERISTIC IMPEDANCE

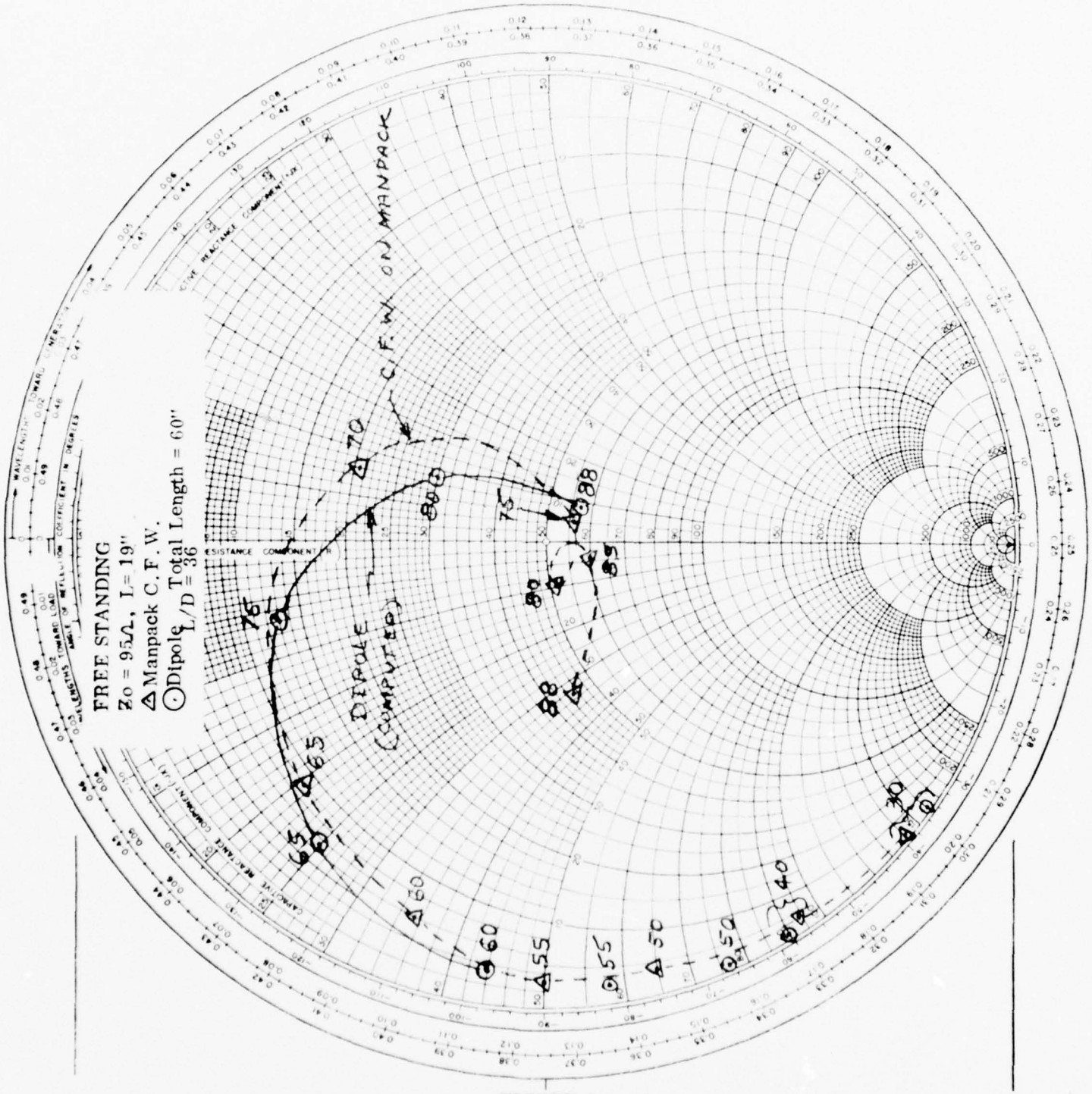

FIGURE 8

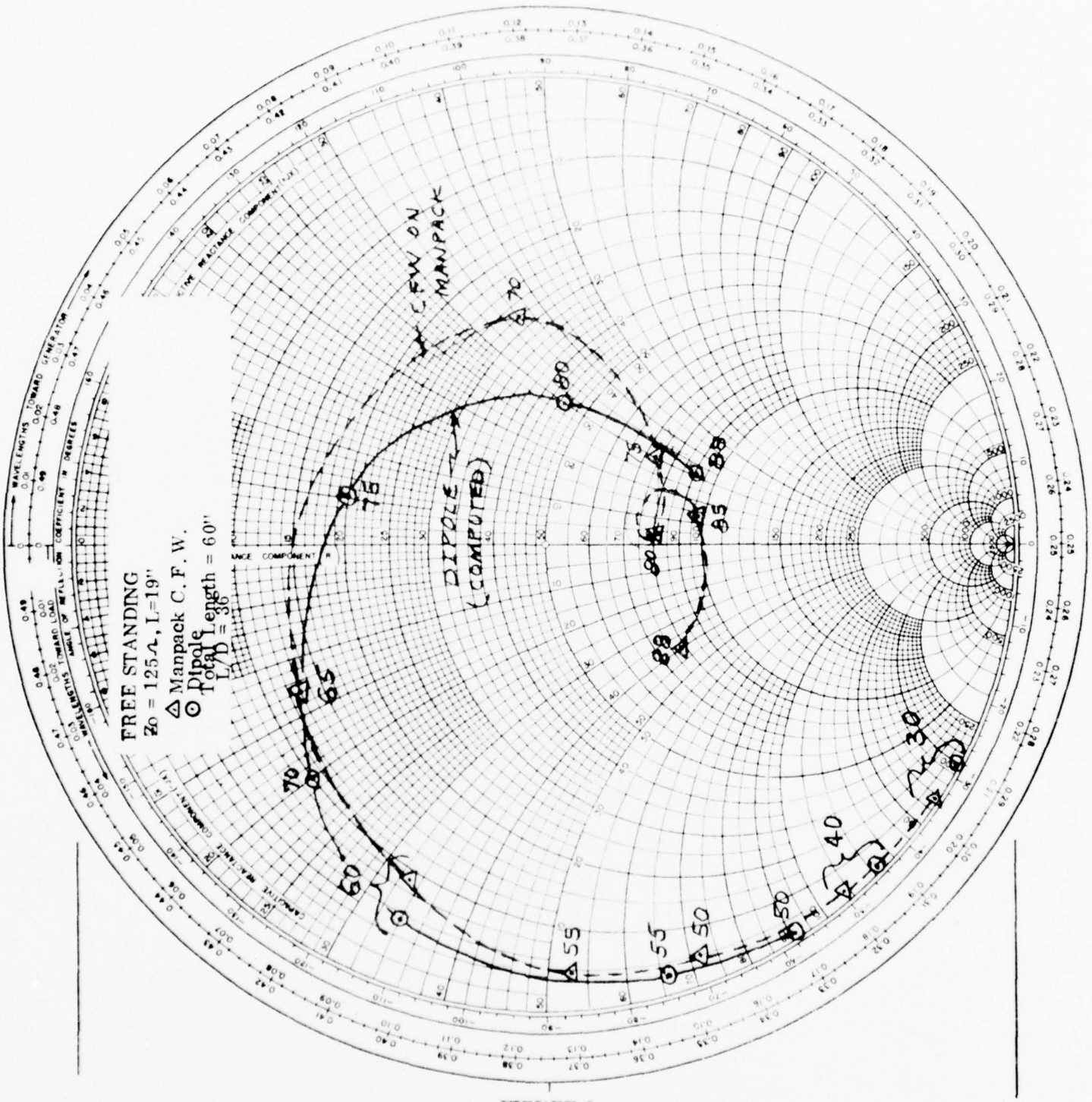
IMPEDANCE COORDINATES—50-OHM CHARACTERISTIC IMPEDANCE
FREE STANDING
Zo = 125Ω, L=19"
△ Manpack C. F. W.
⊙ Dipole
Total Length = 6.0"
L/D = 36
C.F.W. ON MANPACK
DIPOLE (COMPUTED)

FIGURE 9

TABLE I

IMPEDANCE OF CENTERFED AND BASEFED WHIPS

	4-FT CENTERFED WHIP FEEDPOINT POSITION L = 19" Z_o = 95 ohms , ϵ_r = 2		4-FT BASEFED WHIP	
FREQUENCY (MHz)	FREE STANDING R + jX	STANDING CARRIERS BACK R + jX	STANDING CARRIERS BACK R + jX	FREE STANDING R + jX
30	1.95 - J130	2 - j140	30 - j340	1.9 - j493
33	2.6 - j119	2.3 - j126	32 - j310	2.8 - j443
36	3.3 - j108	2.6 - j112	33 - j280	3.9 - j387
40	4.2 - j94	3.0 - j94	34 - j255	7.2 - j330
41	4.3 - j91	3.2 - j91	34 - j246	8.0 - j314
47	4.9 - j72	3.2 - j74	35 - j198	11.4 - j240
50	5.2 - j63	3.4 - j65	35 - j176	13.1 - j190
55	11.3 - j44	4.8 - j50	35 - j146	16 - j100
60	15 - j23	5.9 - j36	35 - j112	18 - j73
65	25 - j1.3	9.0 - j31	45 - j31	23 - j47
70	46 - j9.8	21 + j13	45 - j23	28 - j20
75	57 + j3	57 + j3	58 + j25	34 - j3
80	43 - j41	52 - j10	117 + j21	41 + j14
85	37 - j41	60 - j4	122 - j8	63 + j20
88	25 - j43	45 - j33	118 - j35	85 + j10

2.2.2 Centerfed Whip Characteristics - Operational Conditions

Impedance characteristics of the centerfed whip antenna under three operational conditions, with the whip-manpack combination on a carrier's back, are shown in Appendix B, figures B-1 through B-27. The conditions are: carrier standing, standing with second person holding the handset extended 3-feet and with the carrier prone. Characteristics for these conditions are shown for feed point locations of 17 inches, 19 inches and 21 inches and for feed line characteristic-impedances of 75, 95 and 125 ohms. The data is also presented in tabular form in Appendix B, Tables B1 through B9.

The variation of impedance, at corresponding frequencies, for each operational condition is shown in figures 10 through 15. These figures are plots of the same data shown in figures B1 through B-27; however, points for all three operational conditions are plotted on the same chart with each chart corresponding to a particular feed point location and feed coax characteristic impedance.

In general, the points are most tightly grouped between 30 and 50 MHz (the most critical region in terms of matching) and begin to spread at higher frequencies. Note that some care must be exercised in evaluating the plotted data because the Smith Chart is compressed in the higher impedance region. The 17 inch feed point data shows the tightest grouping in the critical low frequency range; therefore, the 17-inch location was chosen for the final design even though the reactive component is slightly greater than for higher feed points. It may be noted; however, that the higher reactance is primarily a function of feed-coax length rather than feed point height relative to the top of the radio case. Therefore, tight grouping of the points is considered the most important factor governing selection of the feed point location.

From inspection of figures 10 through 15, it is further noted that the impedance spread is reasonably small in the standing position with and without the handset extended, for all feed point locations and cable impedances. On the other hand, the prone points are more widely spread relative to the standing condition points. Fortunately this occurs above 50 MHz where the antenna Q is lower and matching less critical.

Since the feed point impedance is constant for a given feed point position, the whip input impedance becomes a function of the transformation properties of the feed coax as determined by its characteristic impedance "Z_o" and electrical length. At the low end of the band (high feedpoint X to R ratio) the transformed X and R components increase as Z_o of the coax is increased; however, the R-component increases more rapidly than the X-component for a given electrical length. As an example, if the feed point impedance is 5 - j150 and the line length is 16 electrical degrees the transformed impedance for Z_o = 80 ohms is 2.28 - j83.3 and for Z_o = 140 ohms the components increase to 3.17 - j84.06. It may be noted that the R-component increased by 26.5%; whereas, the X-component increased by only 1%. If the line length is increased to 24-degrees the transformed impedance becomes

IMPEDANCE COORDINATES — 50-OHM CHARACTERISTIC IMPEDANCE

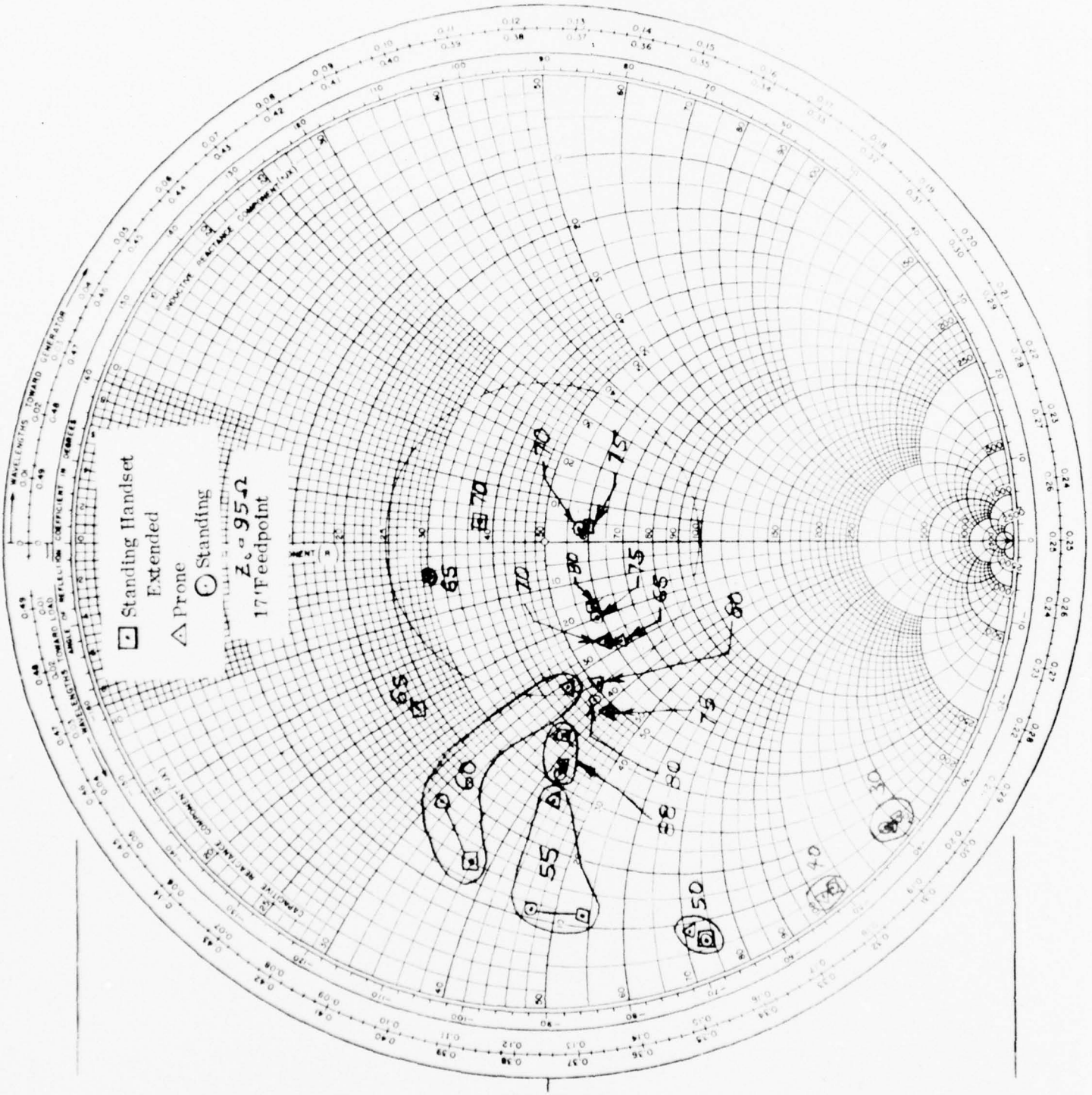

FIGURE 10

IMPEDANCE COORDINATES — 50-OHM CHARACTERISTIC IMPEDANCE

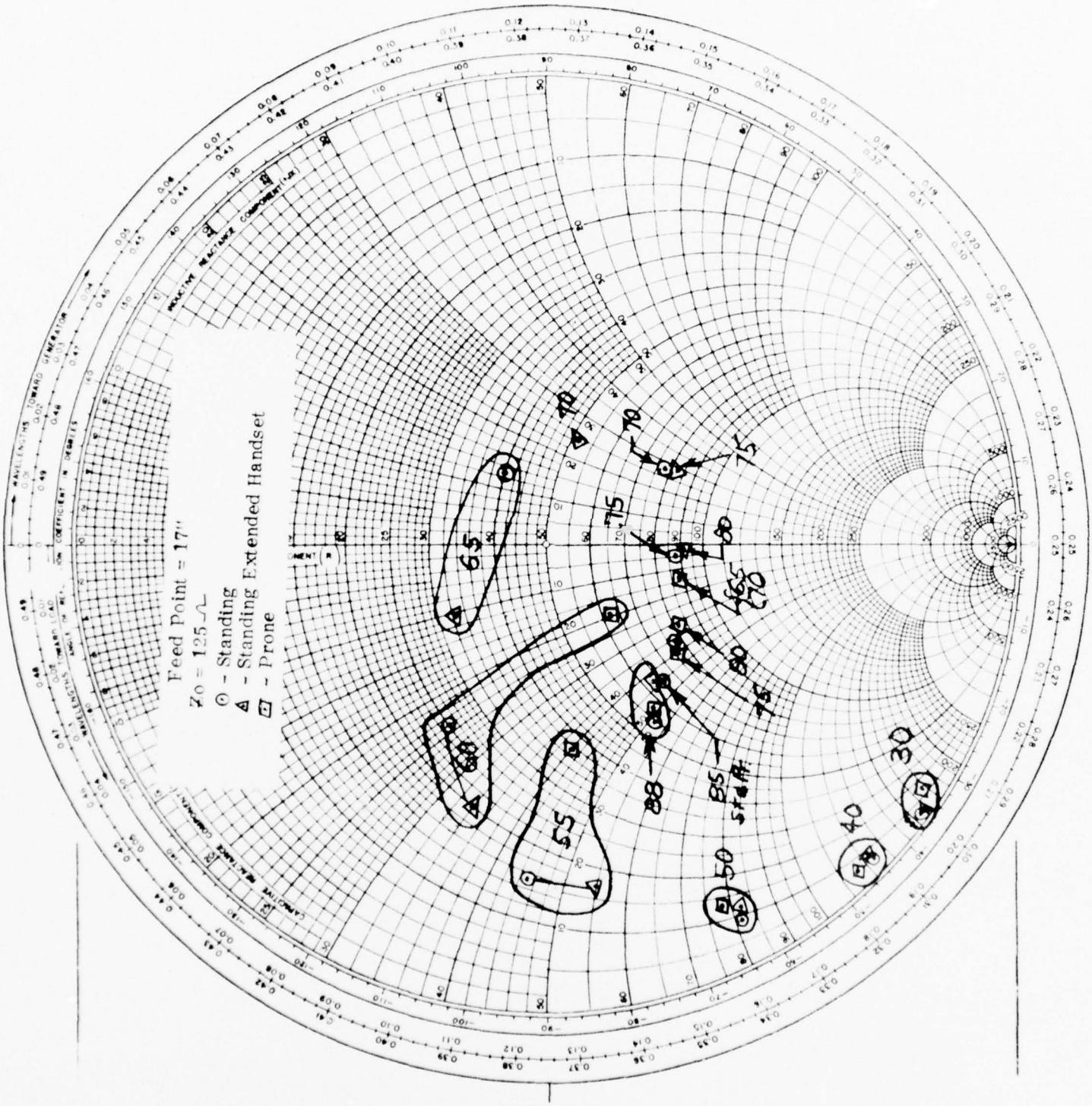

FIGURE 11

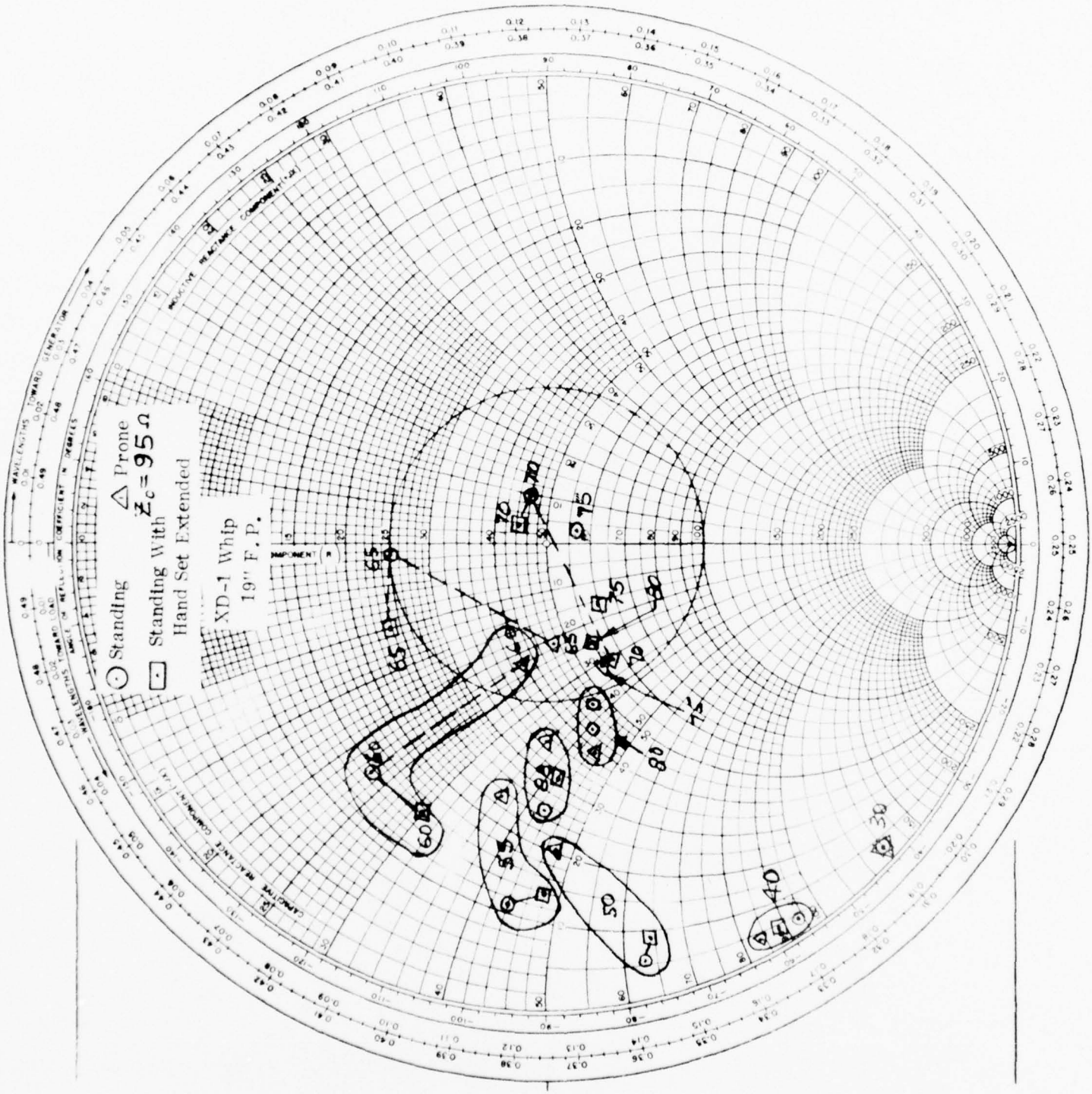
IMPEDANCE COORDINATES — 50-OHM CHARACTERISTIC IMPEDANCE
Standing
Prone
Standing With $Z_c = 95\ \Omega$
Hand Set Extended
XD-1 Whip
19" F. P.

FIGURE 12

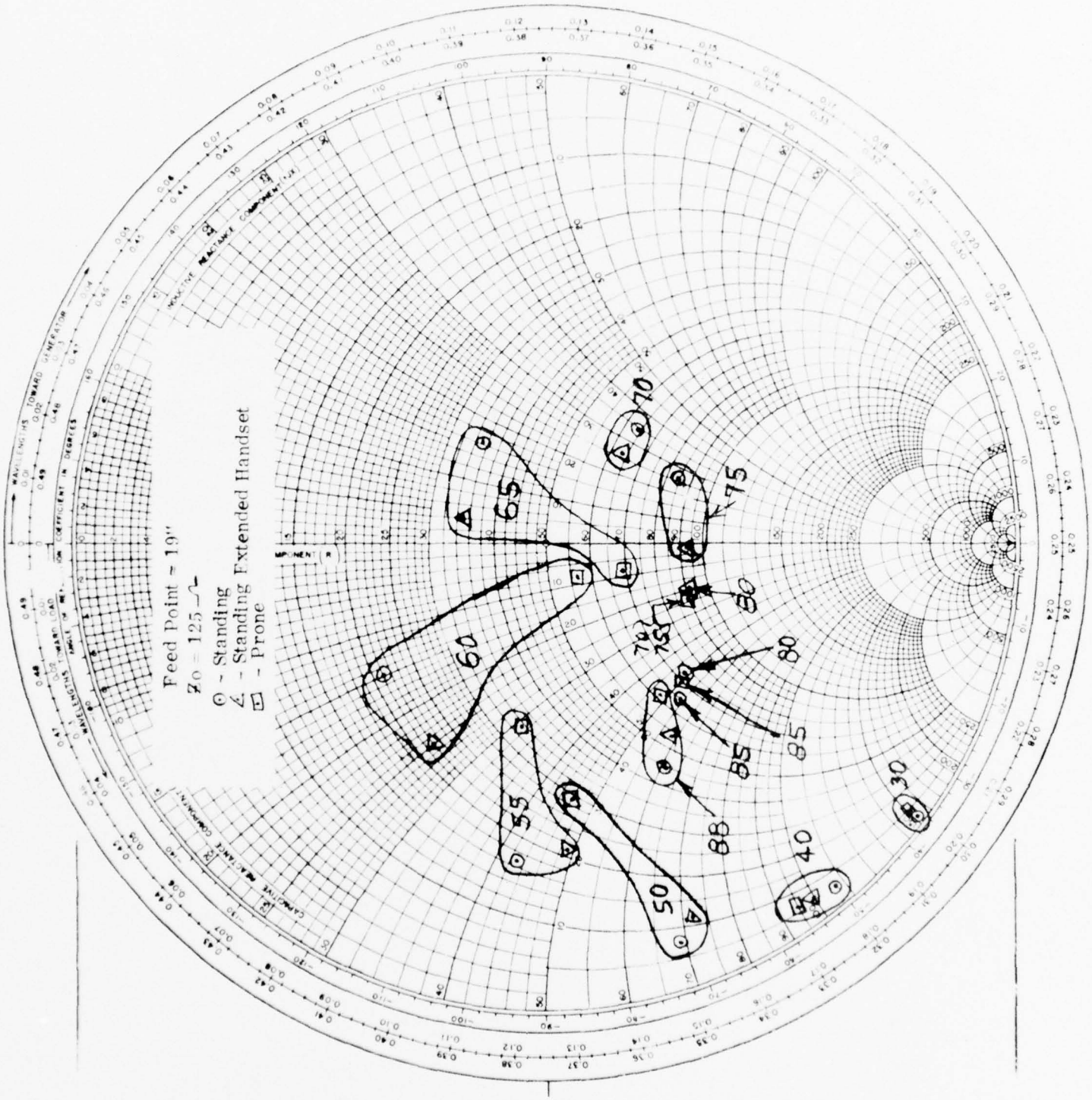
IMPEDANCE COORDINATES — 50-OHM CHARACTERISTIC IMPEDANCE
Feed Point = 19"
Z0 = 125 Ω
⊙ - Standing
∠ - Standing Extended Handset
⊡ - Prone
70
75
80
80
85
85
88
30
40
50
55
60
65

FIGURE 13

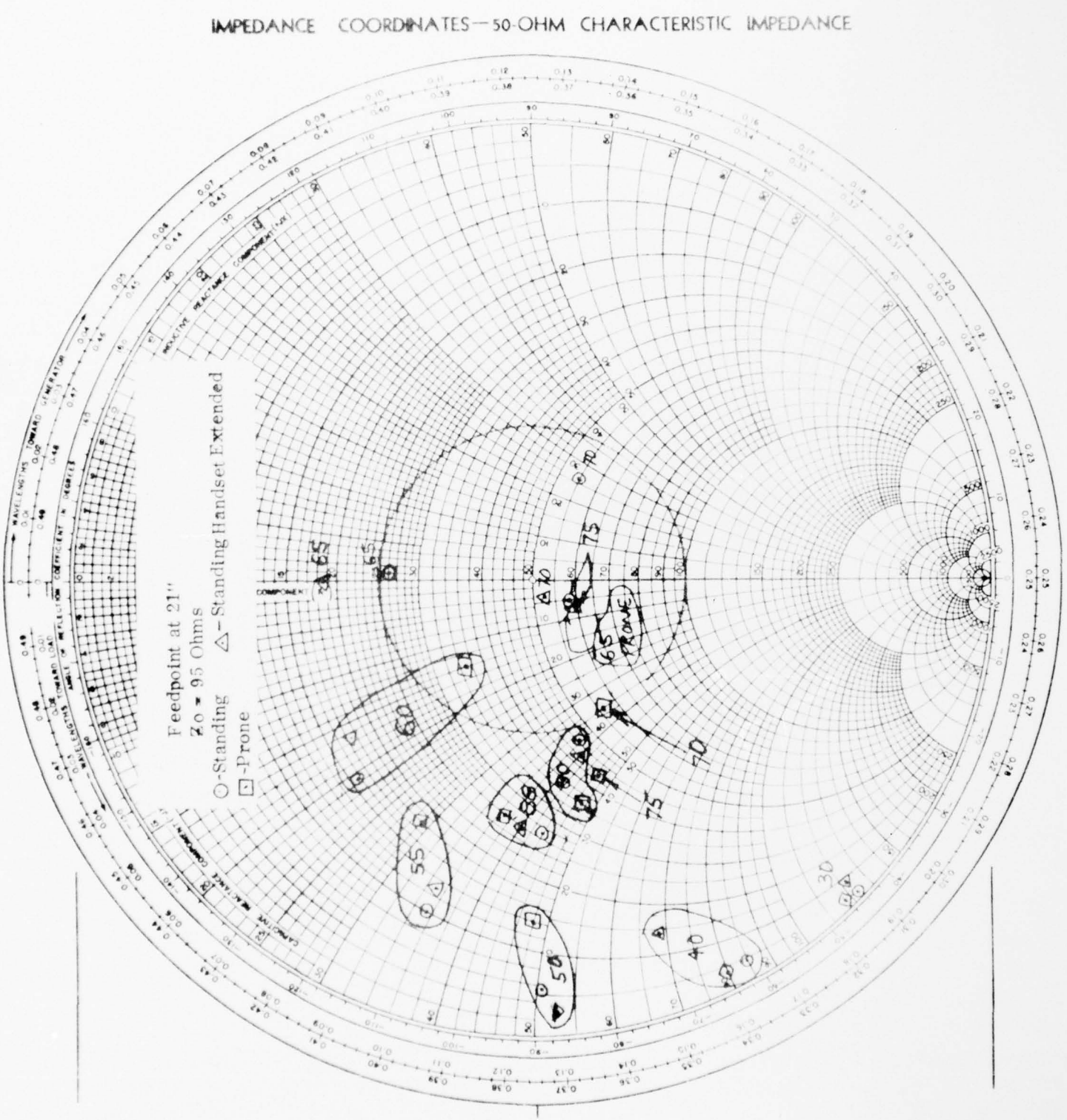
IMPEDANCE COORDINATES—50-OHM CHARACTERISTIC IMPEDANCE
Feedpoint at 21"
Zo = 95 Ohms
○-Standing △-Standing Handset Extended
□-Prone

FIGURE 14

IMPEDANCE COORDINATES—50-OHM CHARACTERISTIC IMPEDANCE

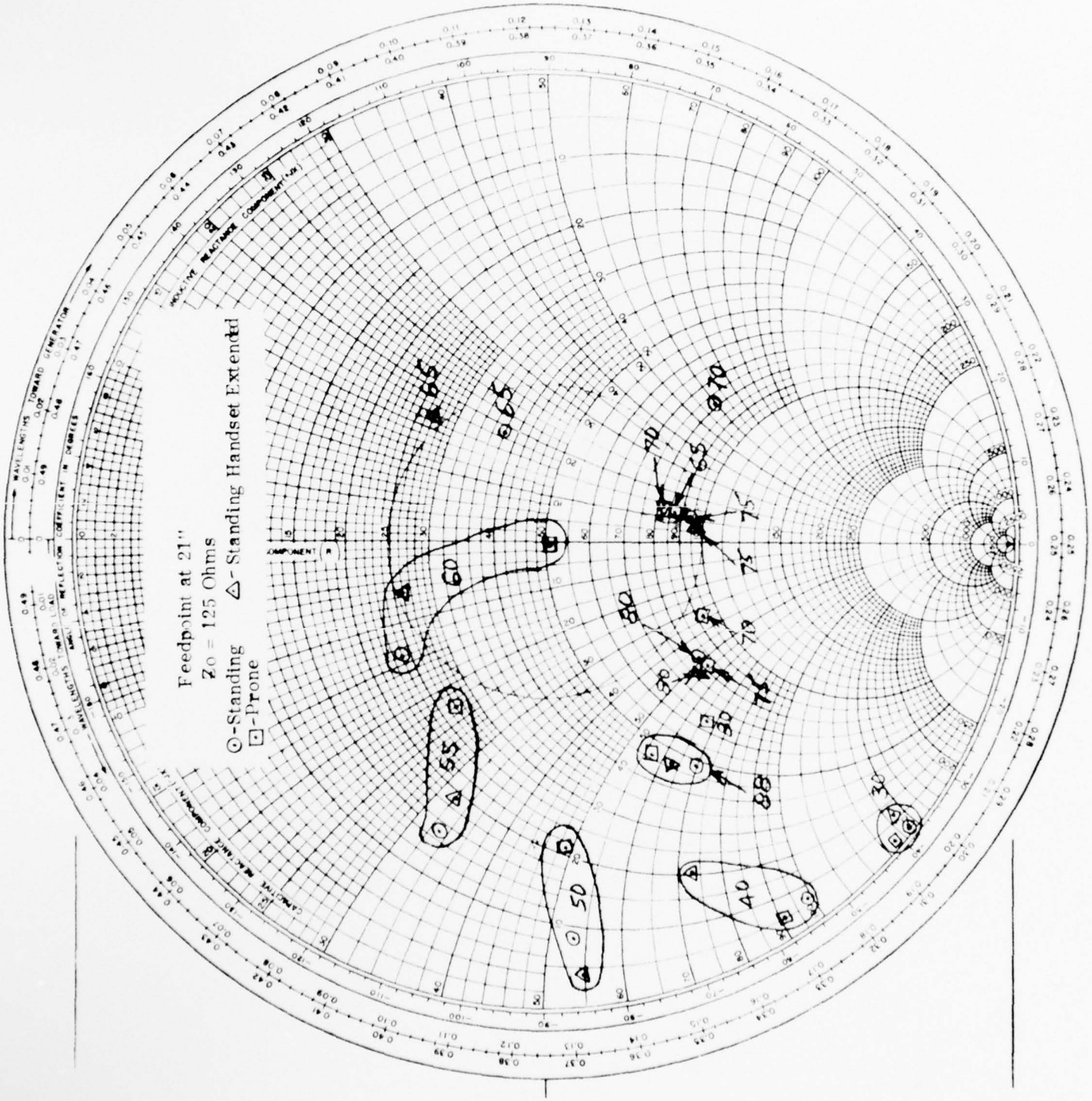

FIGURE 15

1.77 - j62.36 for Z_o = 80 ohms and 2.75 - j59.4 for Z_o = 140 ohms. These impedances exhibit a slightly lower X to R ratio which is generally desirable, however, the smaller R-Values are undesirable since the magnitude of "R" has a greater influence on overall antenna-matching network efficiency.

In view of the above facts, a high Z_o feed line, of minimum electrical length, is desirable. Moreover, the line should be as small in diameter as possible to minimize visibility of the lower portion of the whip. The requirement of small outer diameter in combination with high impedance is somewhat incompatible; because, the coax center conductor diameter becomes extremely small.

In an effort to satisfy the above feed coax requirement a survey of coax cable manufacturers was conducted. It was found that cable of the desired characteristics is manufactured by W. L. Gore & Associates of Minneapolis, Minnesota. The Gore designs achieve high characteristic impedance and small overall diameter while maintaining a reasonable center conductor diameter. This is accomplished by employing an expanded teflon dielectric which exhibits a relative dielectric constant of 1.23; the low dielectric constant also reduces electrical length for a given physical length. Typical parameters of two Gore expanded teflon cables, 95 ohm and 125 ohm, are as listed below; along with Standard RG-195U for comparison.

PARAMETER	CHARACTERISTIC IMPEDANCE 95 ohm	125 ohm	(95 ohm) RG-195/U
Center Conductor Diameter (inches)	0.012	0.012	0.012
Center Conductor Stranding	7/38	7/38	7/38
Dielectric Diameter (inches)	0.068	0.118	0.102
Diameter Over Braded Outer Conductor (inches)	0.082	0.132	0.124
Diameter Over Teflon Jacket	0.096	0.146	0.155
Dielectric Constant	1.23	1.23	2.10
Velocity of Propagation %	90	90	71
Dielectric Strength (Volts)	1000	1500	2000

In terms of matching network efficiency the 125 ohm cable is most desirable; however, the quoted delivery time (180 days) was excessive for the subject program; hence, the low dielectric constant 95 ohm cable was used. This was available in small quantity from stock. Table II shows the measured input impedances for the 95 ohm cable used in the final centerfed whip design.

For comparison, the input impedances for the RG-195U coax and the 125 ohm (ϵ = 1.23) coax are also listed.

Input impedance for the 125 ohm coax was computed from data measured with the 95 ohm ϵ = 1.23 cable by transforming measured impedances to the feed point and transforming the feed point impedances back to the input using a Z_o of 125 ohms.

TABLE II

CENTERFED WHIP INPUT IMPEDANCE

(17-inch Feedpoint Location and 17-inch Feed Line)

FREQ (MHz)	$Z_o = 95$ $\epsilon = 1.23$		$Z_o = 125$ $\epsilon = 1.23$		$Z_o = 95$ $\epsilon = 2.1$	
	Standing	Prone	Standing	Prone	Standing	Prone
30	2.5 - 156	4 - 174	3.3 - 175	5.5 - 199	1.9 - 136	3.1 - 145
33	3.3 - 150	4.4 - 160	4.5 - 170	6.1 - 184	2.4 - 129	2.5 - 138
36	4.2 - 143	4.9 - 146	5.0 - 163	6.8 - 167	3.6 - 117	3.8 - 122
40	5.4 - 134	5.4 - 127	7.7 - 154	7.5 - 144	4.1 - 107	4.2 - 102
41	5.6 - 130	5 - 124	8.0 - 149	8.4 - 141	5.0 - 96	5.6 - 90
47	7.3 - 113	9.4 - 103	10.5 - 130	13.2 - 115	5.8 - 84	7.2 - 78
50	8.1 - 97	11.1 - 93	11.5 - 109	15.6 - 103	6.4 - 74	8.8 - 71
55	13.1 - 66	31.5 - 61	17.8 - 68	42 - 50	11.0 - 47	27 - 44
60	19.6 - 43	51 - 45	25.8 - 38	67 - 36	18 - 31	45 - 31
65	31.4 - 20	70 - 39	39.9 - 7.1	93 - 25	30 - 4.6	62 - 28
70	58.6 - 8	67 - 39	73.7 - 12.5	92 - 25	58 - 3	59 - 27
75	65.9 - 35	59 - 60	92 - 20.9	89 - 89	59 - 20	48 - 41
80	59.2 - 56	62 - 52	90.9 - 54.1	94 - 47	48 - 37	51 - 35
85	49.9 - 64	51 - 63	81 - 71	83 - 69	39 - 40	40 - 40
88	42 - 69	44 - 67	70.5 - 83	73 - 79	32 - 42	33.5 - 41

3.0 Advanced Development Antenna (Phase II)

Based upon the Phase I investigation, examination of the Exploratory Development Antenna models and conclusions reached during the Design Review Meeting, design on an Advanced Development Model proceeded. Parameters of this model are listed below:

(a) Antenna Overall Length — 4-feet.

(b) Feed Point Location — 17-inches above input connector.

(c) Feed Coax Impedance — 95 ohms, 90% velocity of propagation.

(d) Upper Whip Diameter — 0.10-inch at feed point tapering to 0.045-inch at tip.

(e) Eye Protector — Tip to be fitted with 1/2-inch diameter Teardrop shaped protector of crushable foam material.

(f) Two Piece Construction — Upper whip to be detachable from lower section by screw coupling.

(g) Connection To Radio — Input connector to be similar to Type-N and provide for twisting motion without damage of flex section or BNC portion of connector.

(h) Material — Stainless steel construction should be used wherever possible.

(i) Flexible Section — Shall maintain whip in 90° position for prone operation and not exceed 0.45 inch in diameter.

(j) Feed Coax Section — Shall not exceed 5/16-inch in diameter.

3.1 Mechanical Design

Figures 16 and 17 illustrate critical areas of the whip mechanical design. Figure 38 shows the input connector assembly. This assembly is composed of four basic ports: 1) the outer sleeve (reference No. 21) which engages the threaded boss on the radio, 2) an inner sleeve (reference 4) into which is pressed a modified BNC Connector (reference 8) which mates with the BNC Connector on the radio, 3) Slip-clutch bushing (17 and 18) and 4) Spring washer (16) which applies 18 pounds of axial force between the conical clutch busing surfaces. Clutch bushing (18) is slotted to accept the pins on the radio BNC-connector and is therefore held rotationally fixed once the BNC is engaged. Also, dimensions are adjusted such that the main connector thread cannot be engaged until the slots in bushing (18) are aligned with the pins on the BNC connector. This prevents damage of the radio BNC pins. The clutch assembly is provided to allow the antenna to rotate when

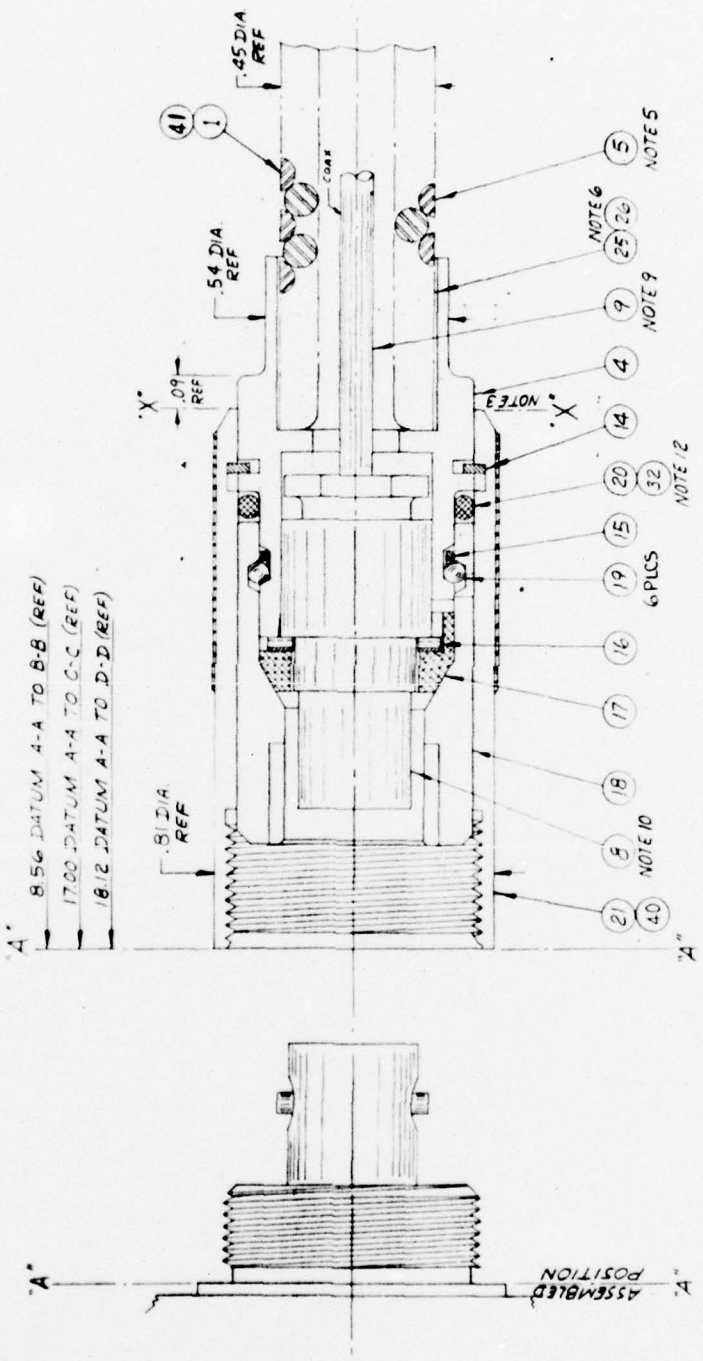
.45 DIA REF
41
1
COAT
5
NOTE 5
NOTE 6
25
26
.54 DIA REF
9
NOTE 9
.09 REF
"X"
4
NOTE 3
"X"
14
20
32
NOTE 12
15
19
6 PLCS
16
17
18
.81 DIA REF
6
NOTE 10
21
40
"A"
8.56 DATUM A-A TO B-B (REF)
17.00 DATUM A-A TO C-C (REF)
18.12 DATUM A-A TO D-D (REF)
"A"
"A"
ASSEMBLED POSITION
"A"

FIGURE 16

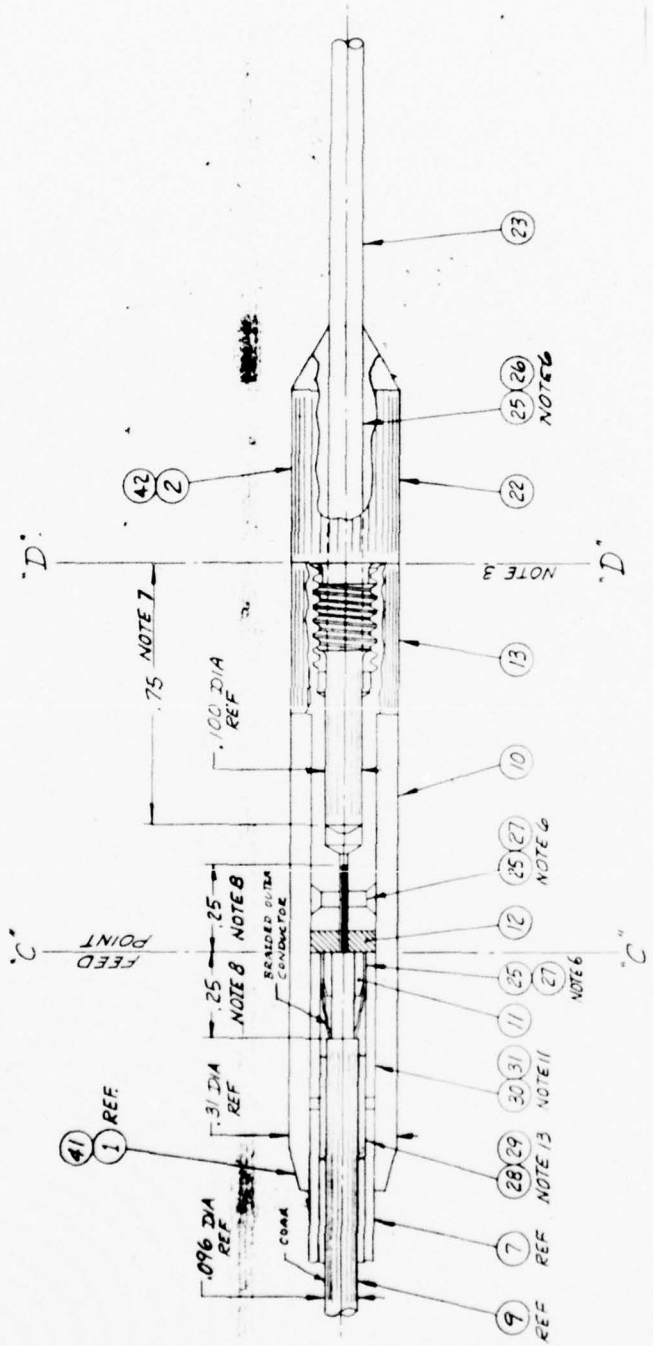
23
25 26 NOTE 6
42 2
22
D'
D"
NOTE 3
.75 NOTE 7
.100 DIA REF
13
10
25 27 NOTE 6
12
C'
FEED POINT
.25 NOTE 8
BRAIDED OUTER CONDUCTOR
C"
25 27 NOTE 6
11
.31 DIA REF
30 31 NOTE 11
41 1 REF
28 29 NOTE 13
.096 DIA REF
COAX
7 REF
9 REF

FIGURE 17

flexed 90° for prone operation. The frictional torque provided by the clutch was designed to maintain the whip in a vertical position, but still allow rotation without damaging the flex section. Although the flex section is capable of limited compound bending, excessive twisting, when already flexed 90° in one plane, would most certainly result in permanent damage. This has been a problem with AN/PRC-77 whips, which utilize the same flex tubing.

To minimize wear, the clutch bushings are held in place by six ball bearings (19) which are inserted by compressing spring (16). Also, the slip clutch cone-angle was chosen as a compromise between frictional torque and wear. The clutch was designed to provide 7.4 inch-pounds of torque, which is sufficient to keep the whip in an upright position in a 50 MPH wind. However, after assembly the torque was found to be less than desired. Since the 18 pound spring force was checked, it is believed that the 0.70 coefficient of friction between brass bushing (17) and stainless bushing (18), as given by Mark's Mechanical Engineering Handbook, was in error. Although not experimentally investigated, it is believed that replacement of bushing (17) with a hard polyurethane bushing would result in the desired torque. However, the wear properties of polyurethane for a slip clutch application are not known.

Figure 17 shows the feed point assembly. The braided outer conductor of the feed coax is terminated by soldering it betweenbushing (11) and outer stainless steel tube (7). The inner conductor of the feed coax extends through teflon washer (12) and is soldered to part (13) which is a bronze section incorporating a screw thread for connection to the upper stainless steel whip (reference 23). It should be noted that a long lead is provided on the upper whip screw thread to insure proper thread alignment. The threaded bronze section (13) is secured to the lower whip tubular section (7), by fiberglass sleeve (10) which is secured by epoxy bonding. The coax feed line is sealed against moisture intrusion, at the input end, via the standard gaskets in the BNC connector. At the feed point end, any moisture entering through the flex section is blocked by injection of a silastic compound (reference 28) just below the feed point. The injection holes are covered by fiberglass sleeve (10), which seals the remaining portion of the feed point assembly.

3.2 Matching Networks

Based on measured impedance data derived from the Advanced Development Model, matching networks were designed to cover the 30-88 MHz band. Several design approaches were initially investigated in an effort to determine the maximum bandwidth achievable within a VSWR no greater than 3:1, while maintaining reasonable network insertion loss. The VSWR upper limit of 3:1 was based upon the automatic level control circuitry associated with the AN/URC-78 power amplifier. The power amplifier is protected from high VSWR overloads via an ALC circuit which begins to reduce power output when the load VSWR is between 3 and 3.5 to one.

Initial subband choice was based upon the work of Tanner[2] & Fano[3], who developed the curves shown in figure 18. These curves relate the maximum bandwidth "Δf" which can be achieved within a given VSWR using an N-element matching network. As indicated in figure 18, the curves are based on the absolute value of load reactance at the band center frequency, reactance change over the band, bandwith desired and magnitude of the average R-component over the band. It was found that this approach is somewhat useful but represents only a rough guide line and that bandwidths thus determined tend to be optimistic. This is possibly due to the fact that the curves assume that all points on the transformed or matched impedance characteristic lie on the maximum allowable VSWR circle. Theoretically this condition results in the maximum possible bandwidth for a given VSWR. However, this optimum condition is not readily achieved in practice. The above approach indicated that the 30-88 MHz range could be covered in 5 subbands; however, subsequent calculations shown at 6-bands were necessary. The final subbands are as listed below:

Band	Frequency Range MHz
1	30-33
2	33-36
3	36-41
4	41-47
4	47-55
6	55-88

The matching network schematic for each subband is shown in figure 19. Component values are those originally computer based on antenna impedance; however, due to stray reactance and some error in measured antenna impedance it was necessary to tune some of the reactors but the general circuit configuration remained as originally designed. As indicated in figure 19, the same circuit configuration was used to match bands 1, 2 and 3. Figure 20 illustrates the general approach used to match the first three bands; transformations obtained by addition of each element are indicated by separate loci. A similar diagram, figure 21, shows the general approach used to match bands 4 and 5; it may be noted that band 4 and 5 networks are essentially the same except for component values and the input series capacitor in the band 4 network.

In band 6 all impedances are capacitive and have a relatively large R-component, hence, the series inductor transforms the higher frequency points symmetrically about the 50 ohm point. The shunt resonant circuit, which is resonant below the band, acts as a shunt inductor for transformation of the 55 to 60 MHz points and appears as a virtual open circuit over the remainder of the band.

Insertion loss of the matching networks was computed based on a Q of 100 for all inductors and 1000 for the capacitors. The Q of the rather small inductors, used in the band 4 and 5 parallel resonant circuits, was determined by measuring the resistance across the parallel combination at resonance and also the capacitor value.

OPTIMUM MATCHING WITH N-ELEMENT NETWORK

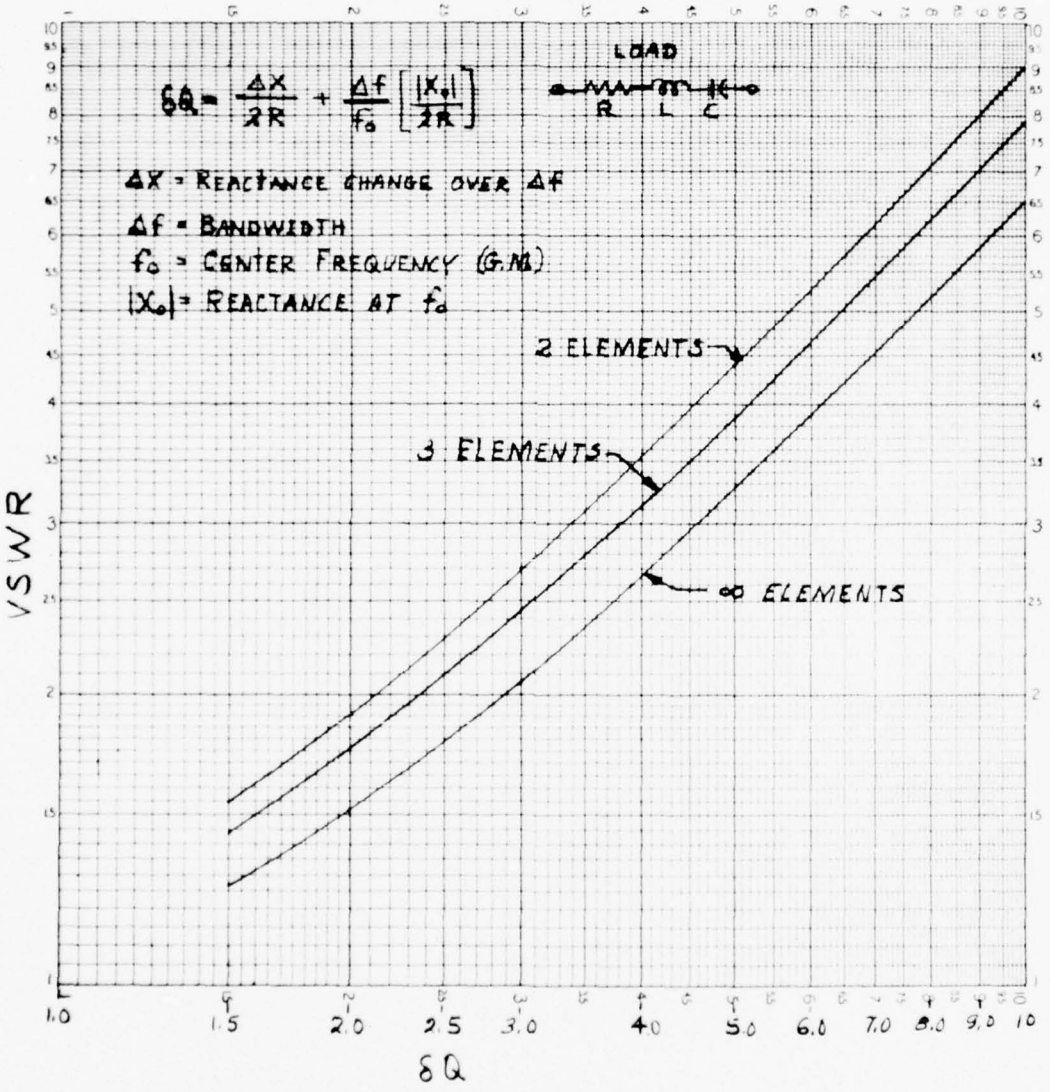

FIGURE 18

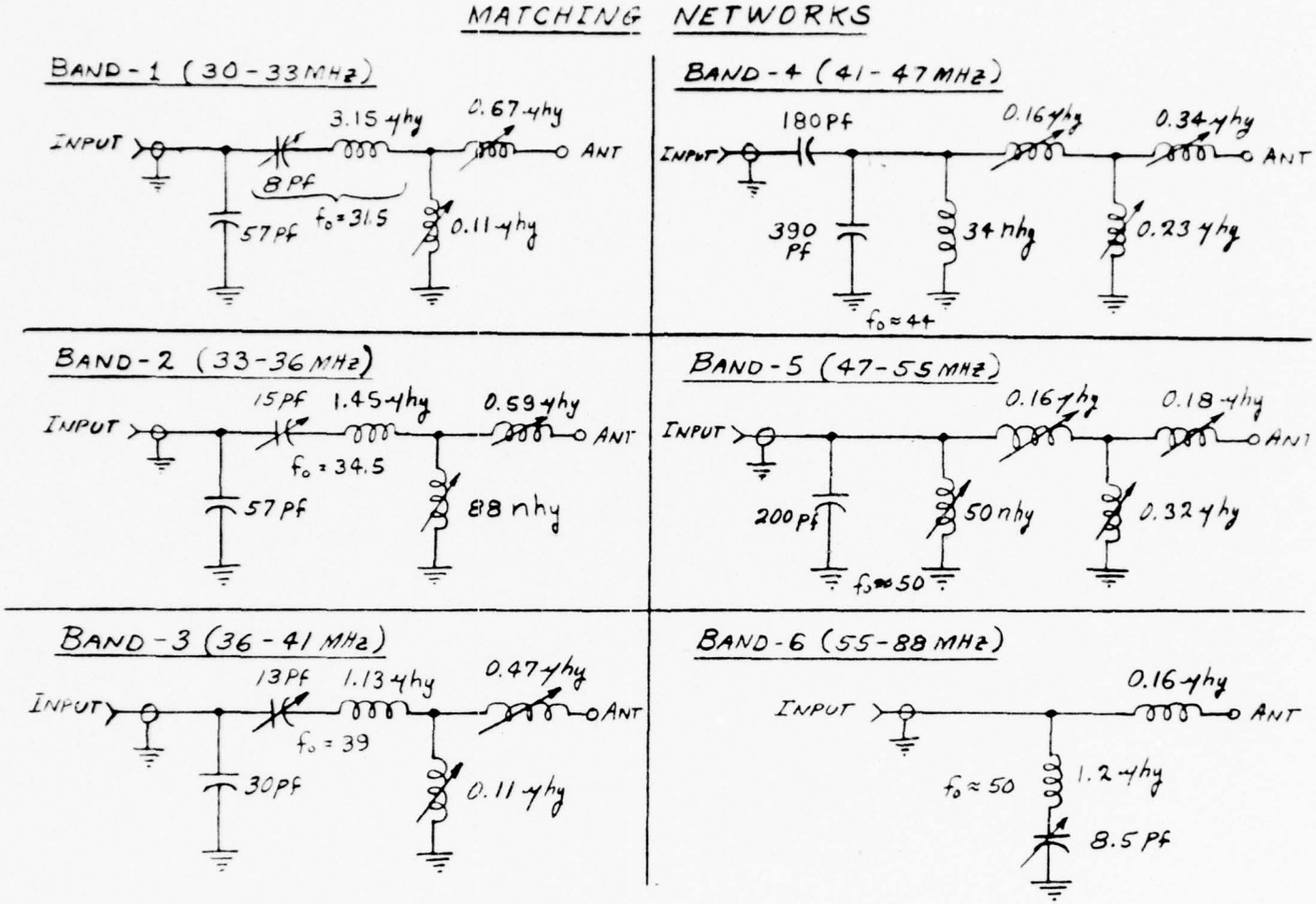
MATCHING NETWORKS
BAND-1 (30-33MHz)
INPUT
3.15 μhy
0.67 μhy
ANT
8 Pf
57 Pf
f_o = 31.5
0.11 μhy
BAND-4 (41-47MHz)
180 Pf
0.16 μhy
0.34 μhy
INPUT
ANT
390 Pf
34 nhy
0.23 μhy
f_o ≈ 44
BAND-2 (33-36MHz)
15 Pf
1.45 μhy
0.59 μhy
INPUT
ANT
f_o = 34.5
57 Pf
88 nhy
BAND-5 (47-55MHz)
0.16 μhy
0.18 μhy
INPUT
ANT
200 Pf
50 nhy
0.32 μhy
f_o ≈ 50
BAND-3 (36-41MHz)
13 Pf
1.13 μhy
0.47 μhy
INPUT
ANT
f_o = 39
30 Pf
0.11 μhy
BAND-6 (55-88MHz)
0.16 μhy
INPUT
ANT
f_o ≈ 50
1.2 μhy
8.5 Pf

FIGURE 19

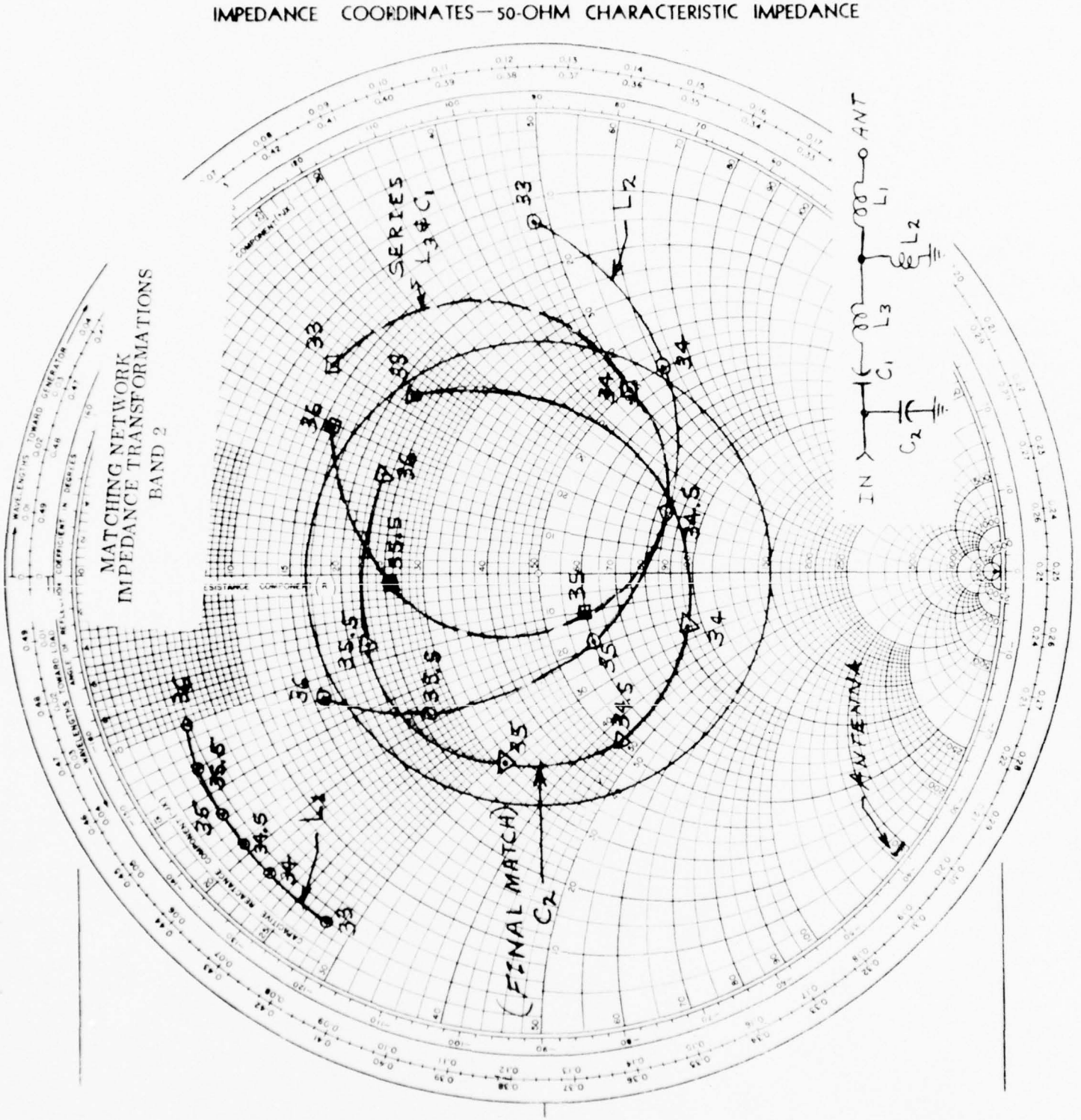
IMPEDANCE COORDINATES—50-OHM CHARACTERISTIC IMPEDANCE
MATCHING NETWORK
IMPEDANCE TRANSFORMATIONS
BAND 2
SERIES L3 & C1
L2
L1
L3
C1
C2
IN
ANT
ANTENNA
(FINAL MATCH) C2

FIGURE 20

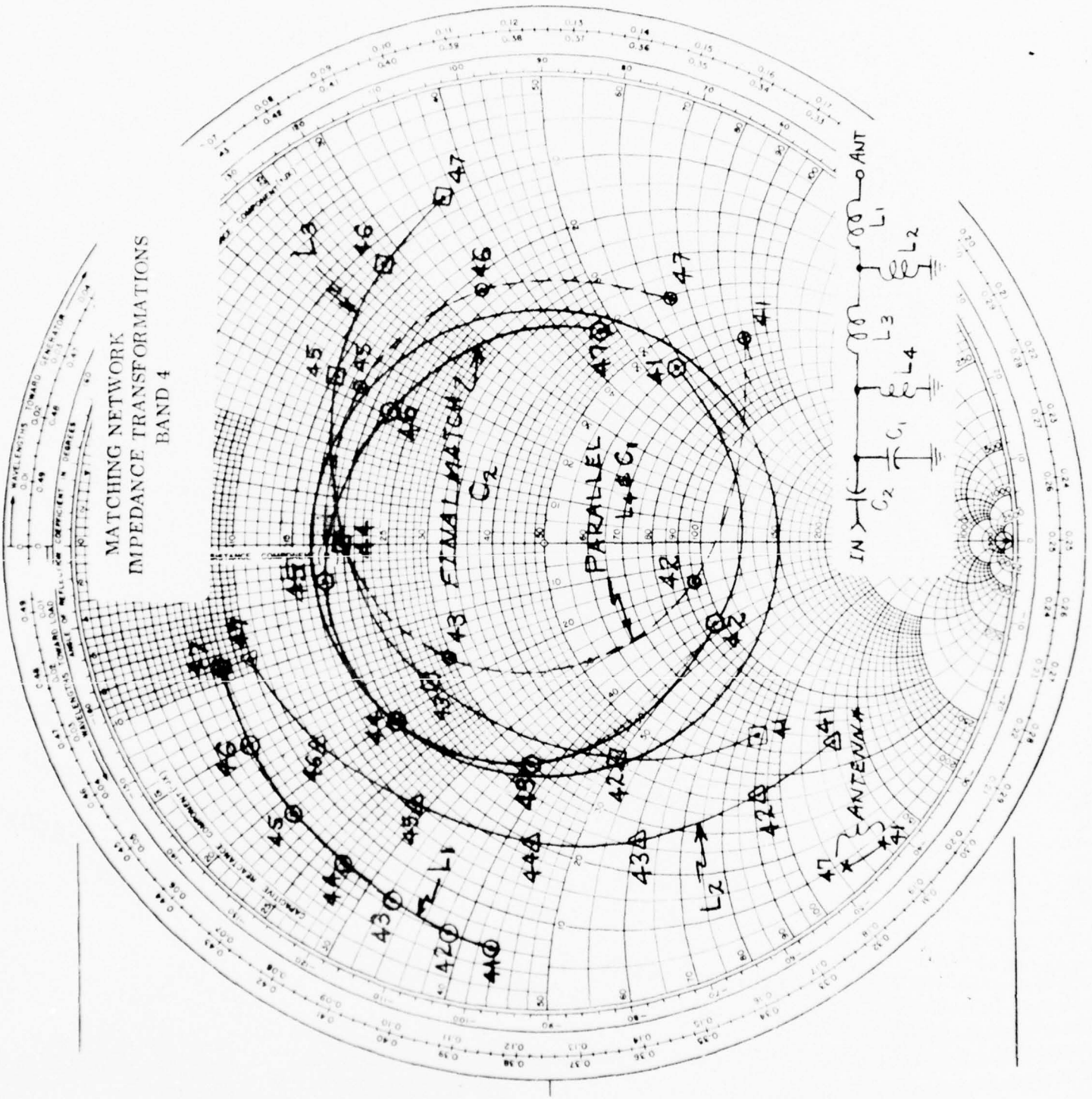
IMPEDANCE COORDINATES—50-OHM CHARACTERISTIC IMPEDANCE
MATCHING NETWORK
IMPEDANCE TRANSFORMATIONS
BAND 4
ANT
L1
L2
L3
L4
C1
C2
IN
FINAL MATCH
PARALLEL
ANTENNA

FIGURE 21

The series resistance of the inductor at "ω_o" is given by:

$$R = R_p \left(\frac{L}{C} \right)$$

where: R_p = measured circuit resistance at resonance and ω_o is the resonant radian frequency.

thence, the inductor Q at resonance is given by:

$$Q = \frac{\omega_o L}{R} = \omega_o R_p C$$

Using the above method, the Q of the small value inductors used in the band 4 and 5 resonant circuits were determined to be 88 and 97 respectively. These Q's were used in the insertion loss computations. Computed Network insertion loss is as listed in Table III.

TABLE III

MATCHING NETWORK INSERTION LOSS

(COMPUTED)

BAND	FREQUENCY (MHz)	INSERTION LOSS (dB)
1	30	-3.57
	33	-3.00
2	33	-2.60
	36	-2.00
3	36	-1.80
	41	-1.61
4	41	-1.08
	47	-1.14
5	47	-0.66
	55	-0.92
6	55	-0.76
	88	-0.92

Final tuning of the matching networks proved to be very difficult because point-by-point impedance measurements had to be performed after each adjustment, because direct connection of test equipment alters the antenna impedance. Initially, each network was tuned on the bench by placing a short across the antenna terminal and adjusting the input impedance, at low, mid and high frequencies, to the impedance computed using the theoretical network component values, but with the antenna replaced by a short. This approach proved to be unsatisfactory, even when networks which had been tuned point-by-point in the radio were used as standards.

A second approach to direct bench tuning, involving measurement of the network transfer function (Amplitude and Phase), was tried. In this case, a HP Network Analyzer was used for the transfer function measurement; hence, the antenna terminal was terminated in 50 ohms by the analyzer test input. Again using theoretical-design circuit component values, the transfer function of the matching network was computed with 50 ohms across the antenna terminal. The matching network transfer function was then displayed using the HP Network Analyzer and component values were adjusted to yield a characteristic as close as possible to the computed transfer function. This approach also failed to yield the desired result; namely a reasonable match across the subband when the network was checked point-by-point in the radio.

The tuning method which proved most satisfactory was accomplished by initially connecting the composite manpack-antenna assembly to a network analyzer and, ignoring the perturbing effect of the cables, the network was adjusted for the best possible VSWR characteristic by sweeping across the particular subband under test while observing the polar impedance display. Once this was accomplished, a minor point-by-point adjustment generally resulted in a good match across the band. These final adjustments were done using a reflectometer circuit consisting of a miniature bidirectional coupler, diode detectors and a microammeter mounted externally on the manpack to indicate forward and reflected power. The reflectometer circuit was mounted on a PC board which could be inserted in a matching network module; hence, no external connections were required. To isolate the radio power-amp from high VSWR during tuning of the matching network, a 4 dB pad was inserted ahead of the bidirectional coupler. Also, calibration curves were generated so that the ammeter readings could be converted to forward and reflected power.

For large quantity production, it is believed the networks could be tuned on the bench by using dummy loads to simulate the antenna. The best procedure for establishing the dummy load impedances would be to initially develop a set of standard networks, accurately tuned by the laborious point-by-point method. The input impedance of these networks, with the manpack free standing, would then be carefully measured at the low, mid and high frequency points of each subband. A set of dummy loads could then be fabricated and adjusted to yield the measured input impedance when connected to the standard networks. All other networks could then be bench adjusted using the loads thus established.

4.0 Performance Characteristics

Measurements of VSWR, efficiency and radiation patterns were made on the centerfed antenna mounted on the AN/URC-78 Radio Set. A similar set of measurements was carried out on a 4-foot basefed whip mounted on the same radio. A stainless steel whip 0.120-inch at the base and tapering to 0.040-inch at the tip was used for the basefed measurements. Simple narrowband matching networks were used to match the basefed whip at frequencies corresponding to the upper and lower end of each sub-band associated with the centerfed whip. Therefore, insertion loss of the basefed networks may have been slightly lower than the broadband centerfed networks.

4.1 Input Impedance

The impedance characteristic of the centerfed whip, at the input of the matching network associated with each subband, is shown in figures 22 through 27; for both standing and prone positions.

In the standing position the input VSWR is generally 3:1 or less across each subband; this insures full output of the AN/URC-78 transmitter since ALC loop action is initiated at a VSWR of approximately 3.5:1.

In the prone position, the VSWR exceed 3:1 over a portion of the lower subbands 1 through 4. However, in bands 2, 3 and 4 the prone impedance characteristic does not show extreme variations and a large percentage of each of these subbands is within the 3:1 VSWR circle. Band 1 (30-33 MHz) presented the most difficult problem due to the larger value of antenna reactance and rather rapid excursion of this reactance with frequency.

The matching networks associated with each subband, as shown in figure 19, were designed based on measured impedances in the standing and prone positions; however, optimization for both conditions in the lower frequency range proved somewhat difficult in terms of both theoretical design and final adjustment of components in the field. Rough adjustments were made via sweep frequency measurements and fine adjustments point-by-point.

Although difficulty was encountered in matching the centerfed whip simultaneously for both standing and prone conditions, over the lower portion of the 30-88 MHz range; it is certain that this problem would be greatly magnified in the case of the basefed whip. Examination of the 4-foot basefed whip impedance, in only the standing position, indicates that at least nine matching networks would be required to accommodate the standing position due to the much higher and rapidly varying reactive component at the lower end of the band. In other words, several networks covering narrower bands would have to be added at the lower end of the band.

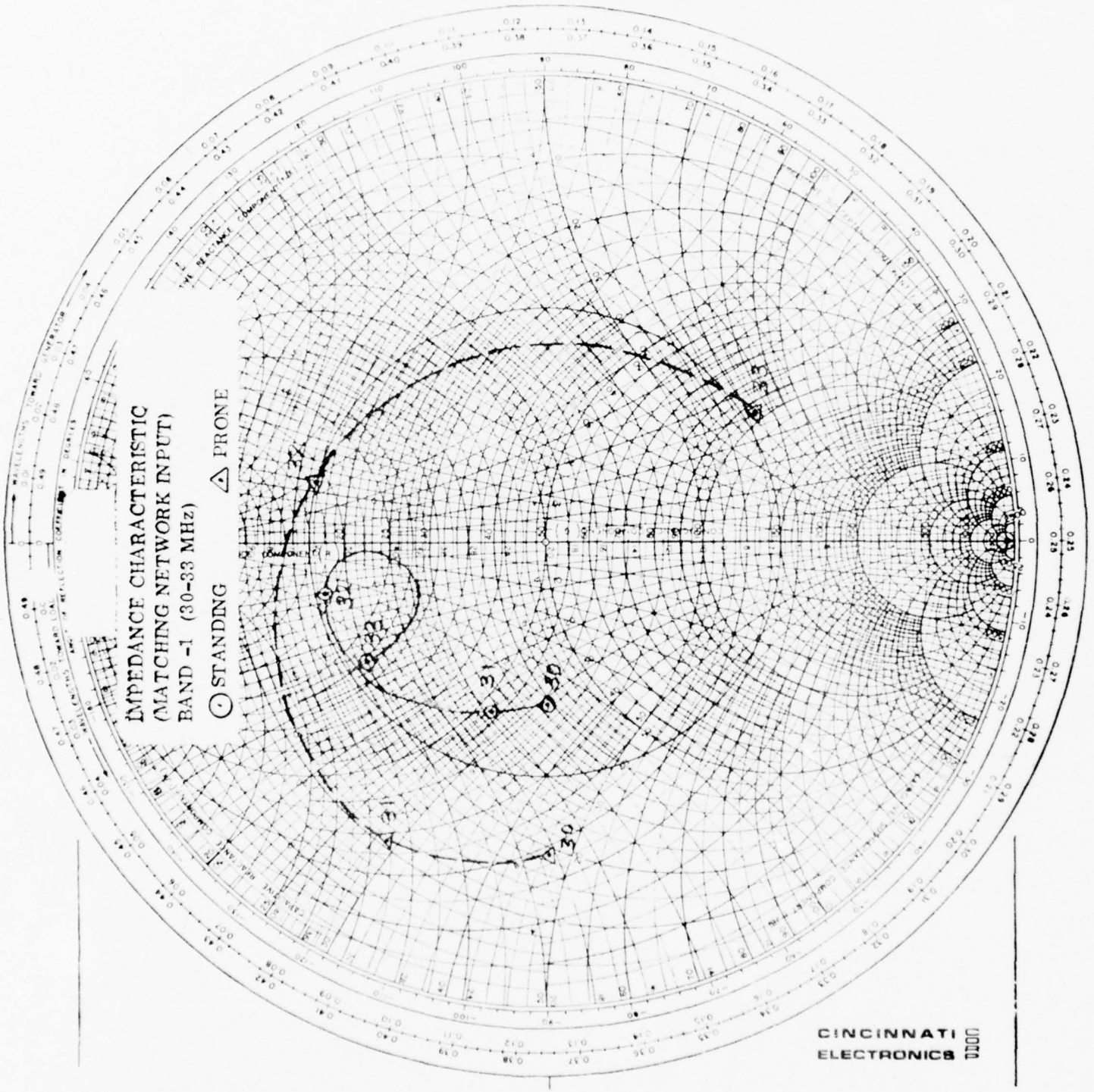
IMMITTANCE CHART
IMPEDANCE COORDINATES — 50 OHM CHARACTERISTIC IMPEDANCE
ADMITTANCE COORDINATES — 20 MILLIMHO CHARACTERISTIC ADMITTANCE
IMPEDANCE CHARACTERISTIC
(MATCHING NETWORK INPUT)
BAND -1 (30-33 MHz)
STANDING
PRONE
CINCINNATI ELECTRONICS CORP

FIGURE 22

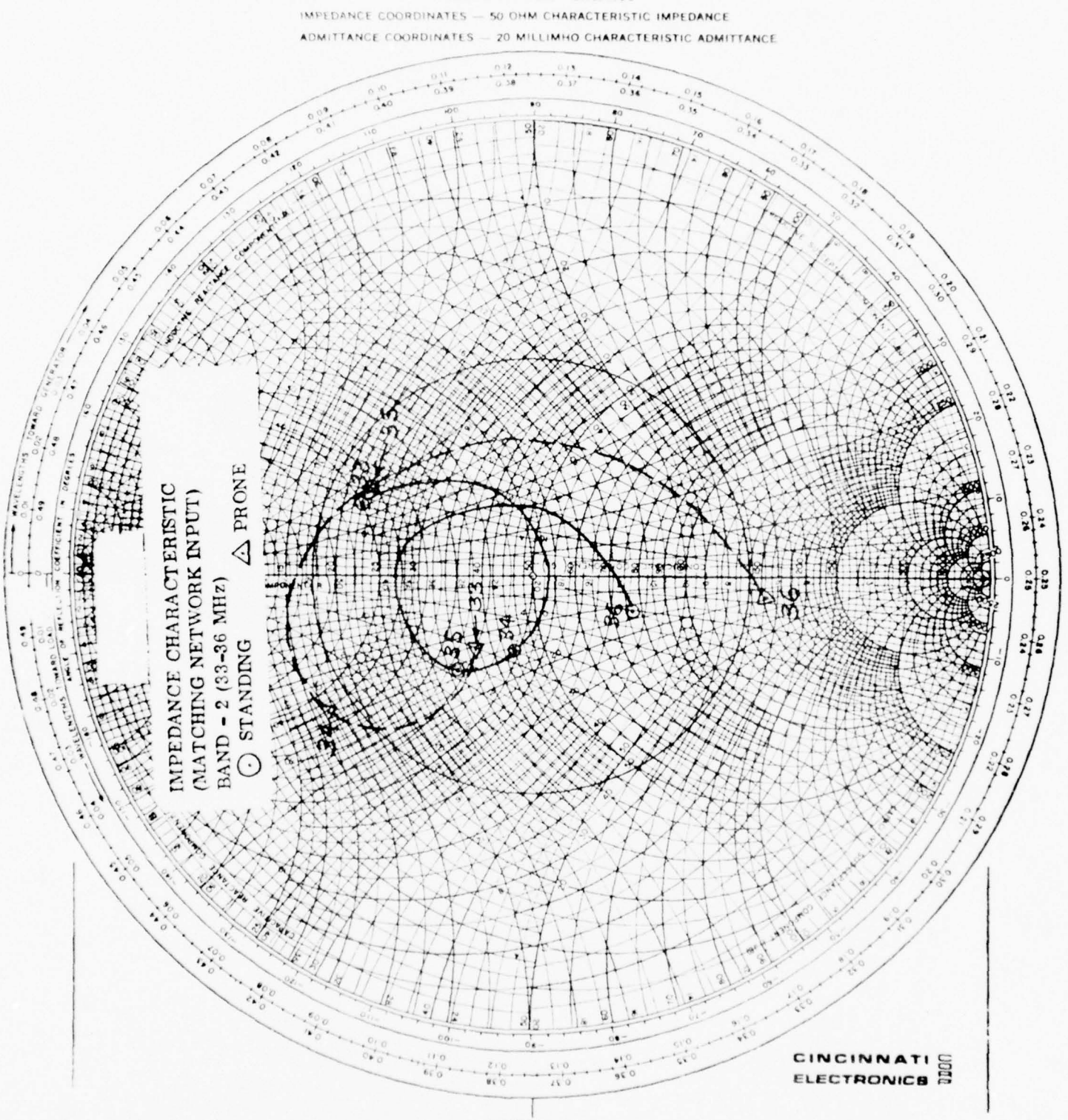
IMMITTANCE CHART
IMPEDANCE COORDINATES — 50 OHM CHARACTERISTIC IMPEDANCE
ADMITTANCE COORDINATES — 20 MILLIMHO CHARACTERISTIC ADMITTANCE
IMPEDANCE CHARACTERISTIC
(MATCHING NETWORK INPUT)
BAND - 2 (33-36 MHz)
△ PRONE
⊙ STANDING
CINCINNATI ELECTRONICS

FIGURE 23

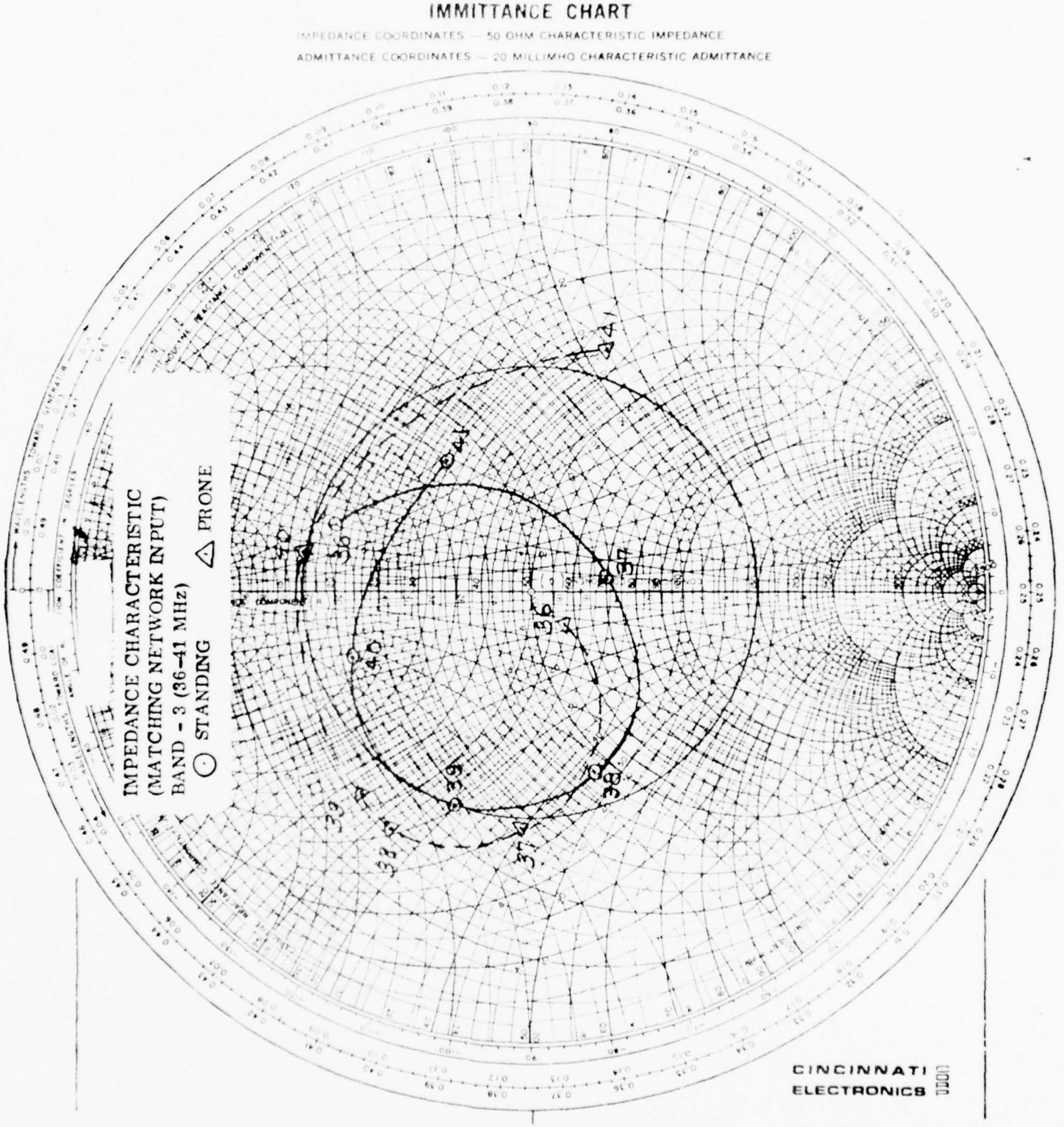
IMMITTANCE CHART
IMPEDANCE COORDINATES — 50 OHM CHARACTERISTIC IMPEDANCE
ADMITTANCE COORDINATES — 20 MILLIMHO CHARACTERISTIC ADMITTANCE
IMPEDANCE CHARACTERISTIC
(MATCHING NETWORK INPUT)
BAND - 3 (36-41 MHz)
STANDING
PRONE
CINCINNATI
ELECTRONICS

FIGURE 24

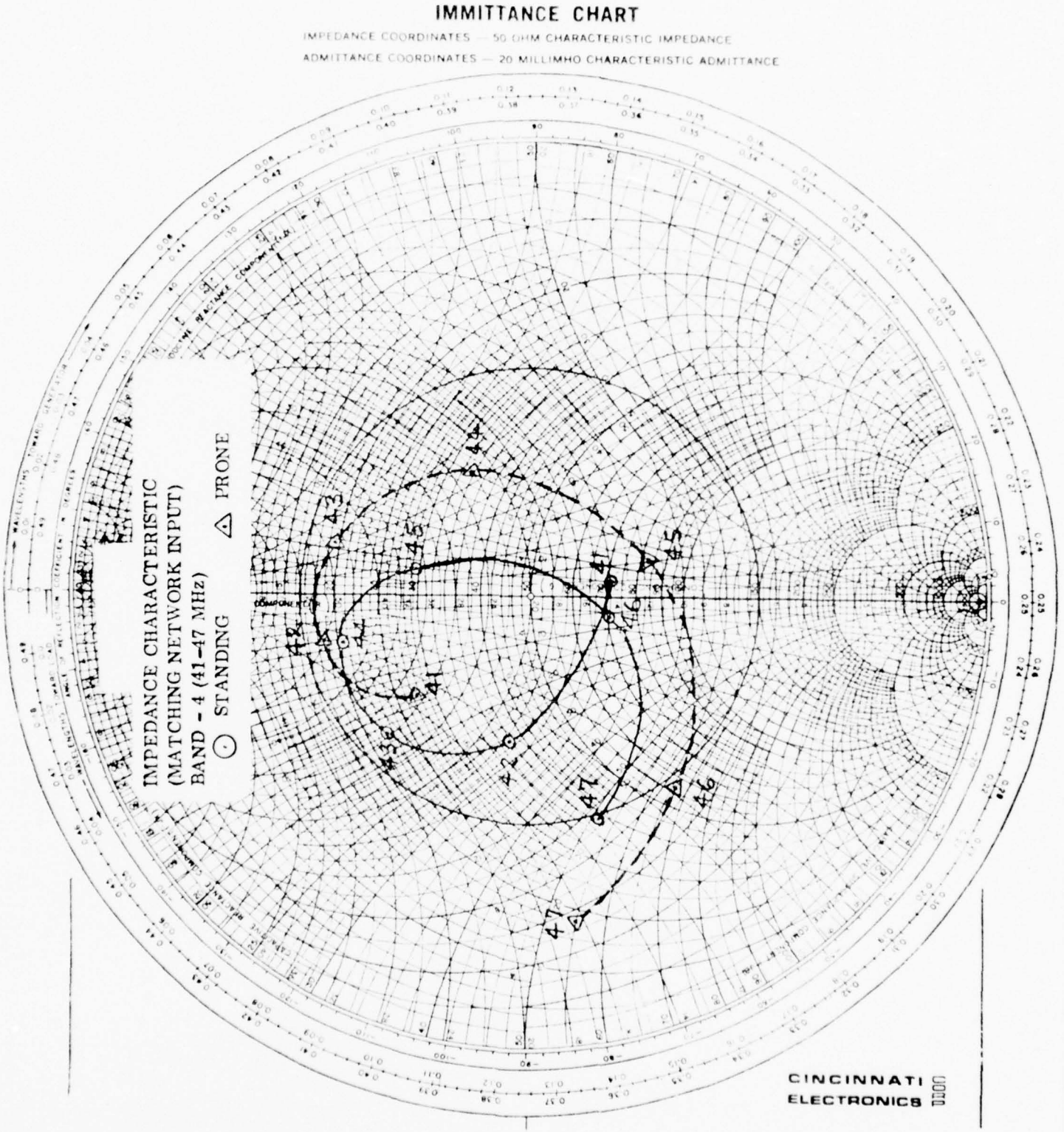
IMMITTANCE CHART
IMPEDANCE COORDINATES — 50 OHM CHARACTERISTIC IMPEDANCE
ADMITTANCE COORDINATES — 20 MILLIMHO CHARACTERISTIC ADMITTANCE
IMPEDANCE CHARACTERISTIC
(MATCHING NETWORK INPUT)
BAND - 4 (41-47 MHz)
STANDING
PRONE
CINCINNATI
ELECTRONICS

FIGURE 25

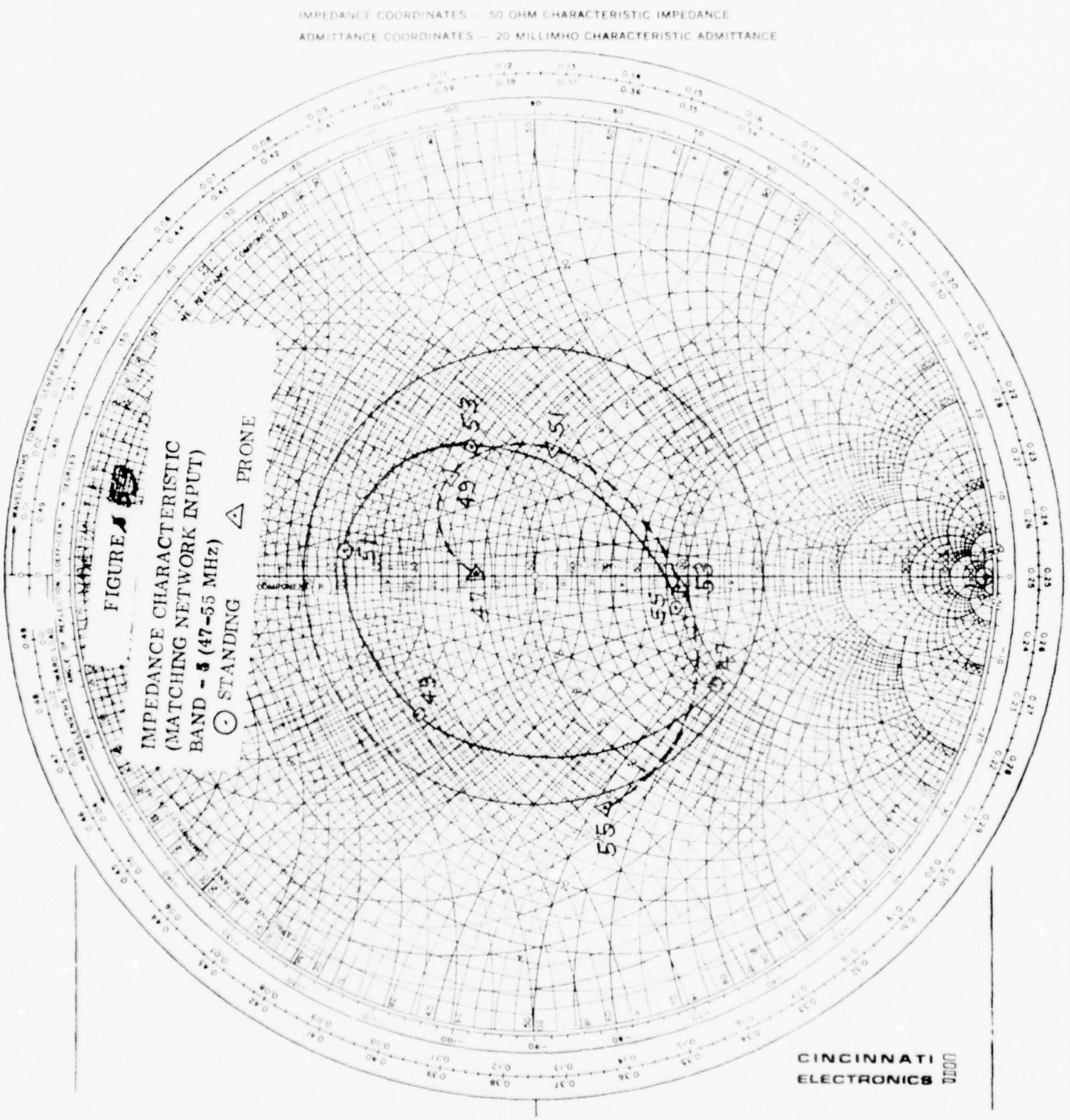
IMMITTANCE CHART
IMPEDANCE COORDINATES — 50 OHM CHARACTERISTIC IMPEDANCE
ADMITTANCE COORDINATES — 20 MILLIMHO CHARACTERISTIC ADMITTANCE
FIGURE 5
IMPEDANCE CHARACTERISTIC
(MATCHING NETWORK INPUT)
BAND - 5 (47-55 MHz)
STANDING
PRONE
CINCINNATI ELECTRONICS

FIGURE 26

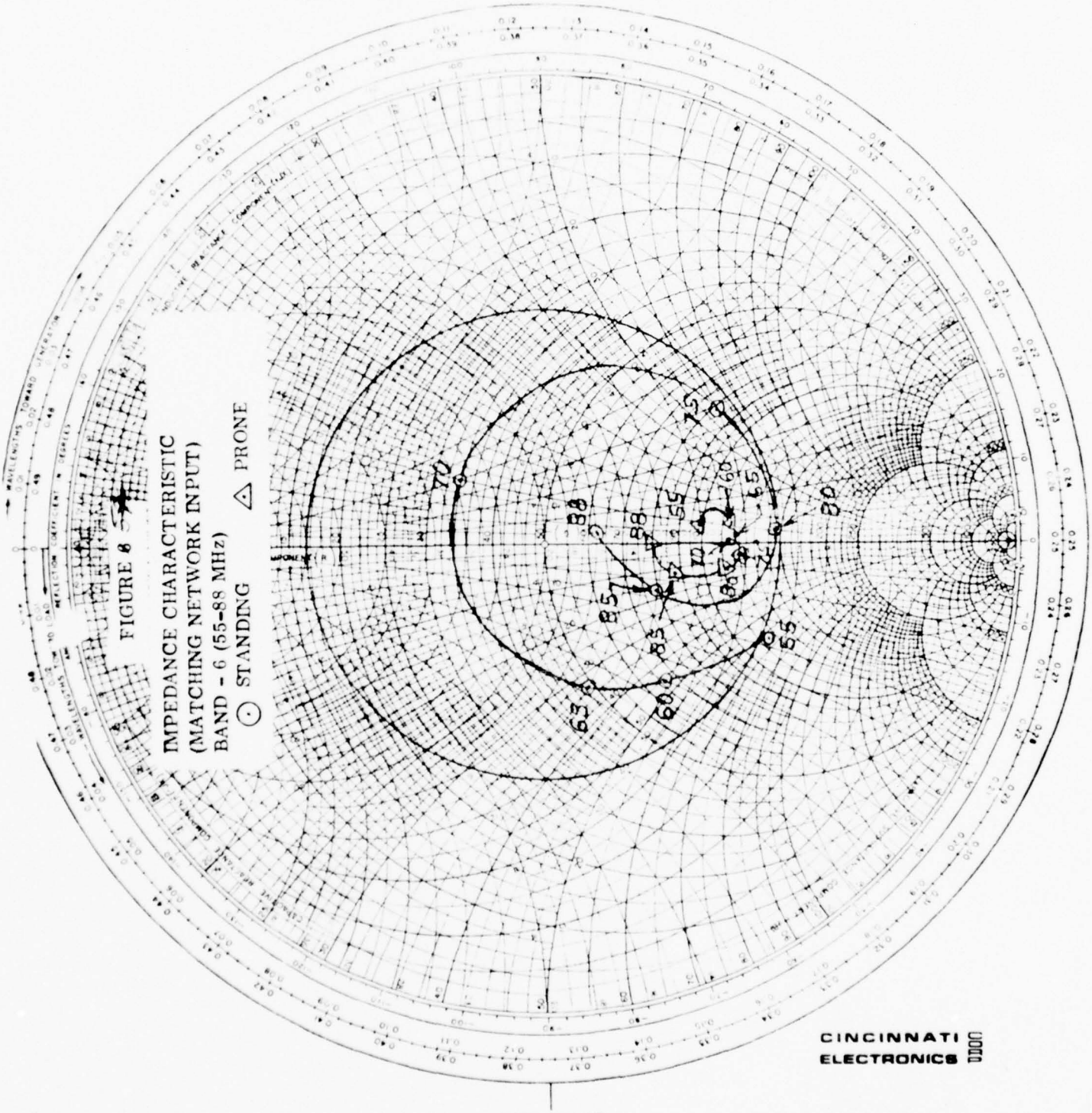
IMMITTANCE CHART
IMPEDANCE COORDINATES - 50 OHM CHARACTERISTIC IMPEDANCE
ADMITTANCE COORDINATES - 20 MILLIMHO CHARACTERISTIC ADMITTANCE
FIGURE 8
IMPEDANCE CHARACTERISTIC
(MATCHING NETWORK INPUT)
BAND - 6 (55-88 MHz)
STANDING
PRONE
CINCINNATI ELECTRONICS

FIGURE 27

4.2 Efficiency

Efficiency of the centerfed whip, with associated matching networks, was measured relative to a resonant half-wave dipole at the upper and lower frequency end of each sub-band. The reference dipole antenna was mounted on a fiberglass mast with its center 10-feet above ground, as described in the Test Plan. Measurements were performed for both standing and prone positions with the centerfed whip mounted on a modified AN/URC-78 radio. Also, efficiency of a basefed 4-foot whip mounted on the same AN/URC-78 radio was measured. Results of these measurements are shown in Table IV. Since the input VSWR varies over the frequency range, as shown in the impedance plots, all measurements are normalized to unity VSWR for better comparison. In other words, reflection loss for both base and centerfed whips was corrected using the relation:

$$\text{VSWR LOSS FACTOR} = 10 \log_{10} (1-\Gamma_i^2) \text{ (dB)}$$

where: Γ_i is the input reflection coefficient.

Since dissipative insertion loss of the various networks was not measured, the results of Table IV do include this factor.

TABLE IV

EFFICIENCY RELATIVE TO HALF WAVE DIPOLE

Band	Frequency (MHz)	Efficiency Centerfed Whip/dipole (dB) Standing	Efficiency Centerfed Whip/dipole (dB) Prone	Efficiency Basefed Whip/dipole (dB) Standing	Efficiency Basefed Whip/dipole (dB) Prone
(1)	30	-6.1	- 4.4	-9.6	-8.8
	33	-9.8	-13.6	-9.6	
(2)	33	-7.5	- 6.2	-9.4	
	36	-7.6	- 4.2	-9.4	
(3)	36	-7.6	- 7.2	-9.1	
	41	-5.6	- 5.4	-9.1	
(4)	41	-5.3	- 3.9	-9.7	
	47	-5.3	- 4.1	-9.7	
(5)	47	-6.9	- 6.4	-4.4	
	55	-5.3	- 3.5	-4.4	-4.1
(6)	55	-3.7	- 3.2	-3.8	
	80	-5.5	- 8.0	-3.9	-3.0

Due to some day-to-day variation in the efficiency data, the results presented in Table IV represent the average of several measurements. In general, the centerfed antenna appears to be several dB better than the basefed antenna over the lower portion of the band. At the higher end of the band, the basefed and centerfed performance tends to converge. The sizeable difference between band 1 and band 2 at 33 MHz has not been resolved. It would appear that the band 1 network has a high insertion loss at 33 MHz; however, computation of insertion loss using measured inductor Q's and measured antenna impedance does not show this to be the case.

One unexpected result shown by the efficiency measurements, is that efficiency of both whips in the prone position is in general slightly better than for the standing position. This may be due to the fact that a stronger surface-wave is launched when in the prone position. In other words, the ground reflection coefficient becomes closer to unity due to a lower angle of incidence. The receiving antenna used in all cases was a quarterwave monopole driven against a radial-wire counterpoise which was resting on the ground.

4.3 Radiation Patterns

Azimuth radiation patterns, measured with both the centerfed and basefed antennas are shown in figures 28 through 62. In all cases the person carrying the manpack radio was facing in the 0° - chart direction, marked forward (FWD), on the polar charts. In the prone position, the operator's head corresponds to the 0° direction. Patterns were recorded automatically as the operator, with radio and antenna, was rotated on a motor-driven azimuth pedestal. Height of this pedestal was about 15 inches above ground level.

Over the lower end of the band (30-36 MHz) the azimuth patterns are omnidirectional within approximately 1 dB for either the basefed or centerfed configurations. From 35 to 50 MHz both antenna configurations exhibit increased directivity in the forward (0° -direction) for the standing condition and increased directivity in the 180° direction for the prone position. However, the centerfed whip pattern exhibits better symmetry about the 0-180° axis. At 60 MHz the basefed whip pattern exhibits deep nulls for both standing and prone conditions while the centerfed patterns remain reasonably well behaved, except for some accentuation of the forward and rearward directivity associated with the standing and prone positions respectively.

At 70 MHz the centerfed whip prone-pattern is almost totally directed toward the rear (180° -direction); a second pattern taken with the operator crouching also exhibits this characteristic. Apparently the operator's body and legs act as a counterpoise causing the pattern to be directed to the rear. This effect occurs to some degree at lower frequencies but the extreme case probably occurs when the operator's body is near resonance in the prone position; 70 MHz in this case. A similar condition is observed in the case of vehicular antennas, in other words; if a whip antenna is mounted on the left rear side of a vehicle the major pattern lobe is directed toward the right front quadrant and the degree of directivity is a function of frequency.

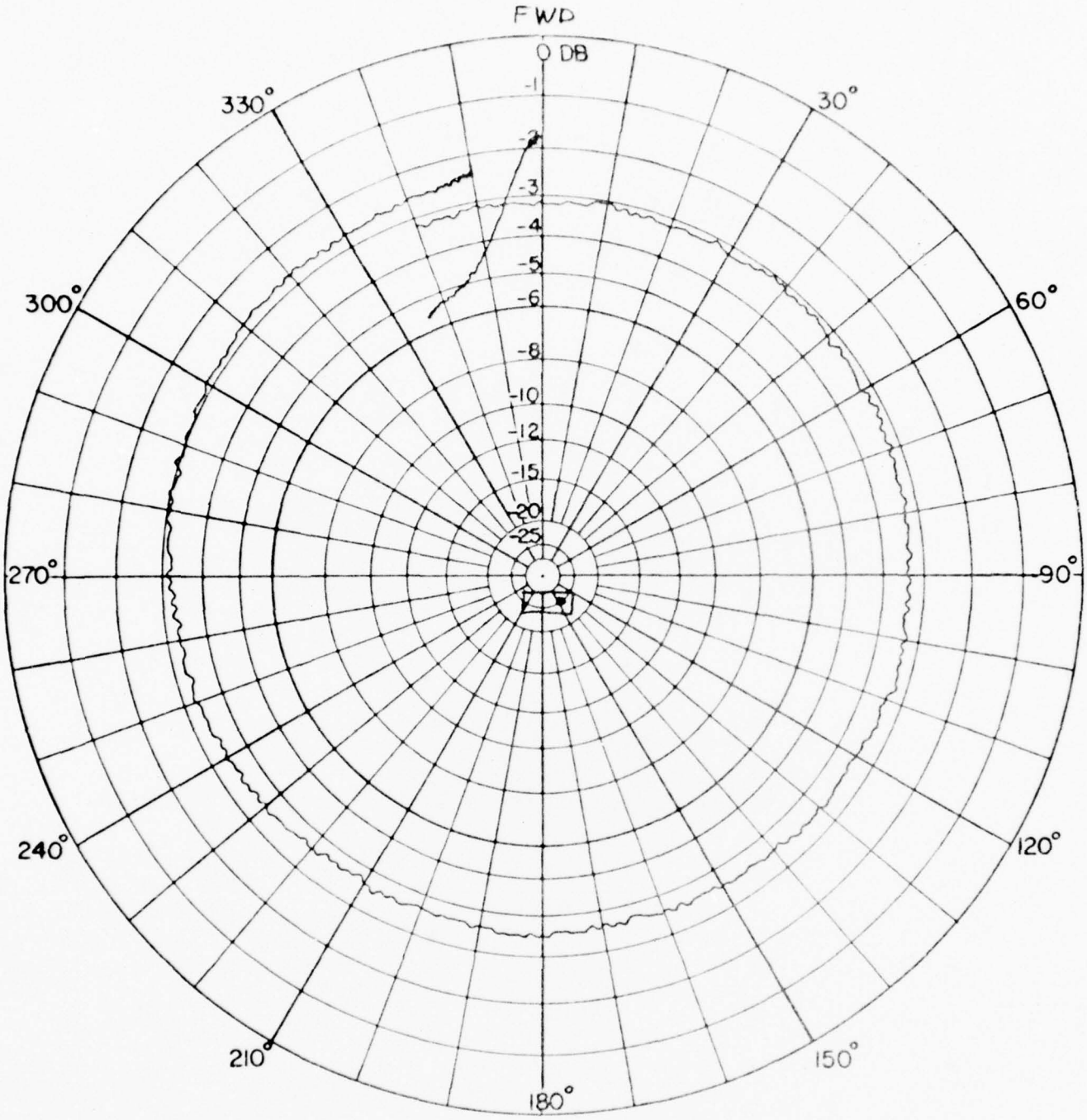

DIAGRAM	TITLE VHF MANPACK ANTENNA
	ANTENNA 4ft Centerfed Whip
	FREQ. 30MHz POLARZ Vert
	MODEL SCALE EΦ= EΘ=
	DATE 4-29-77 BY SCA
	REMARKS STANDING

FIGURE 28

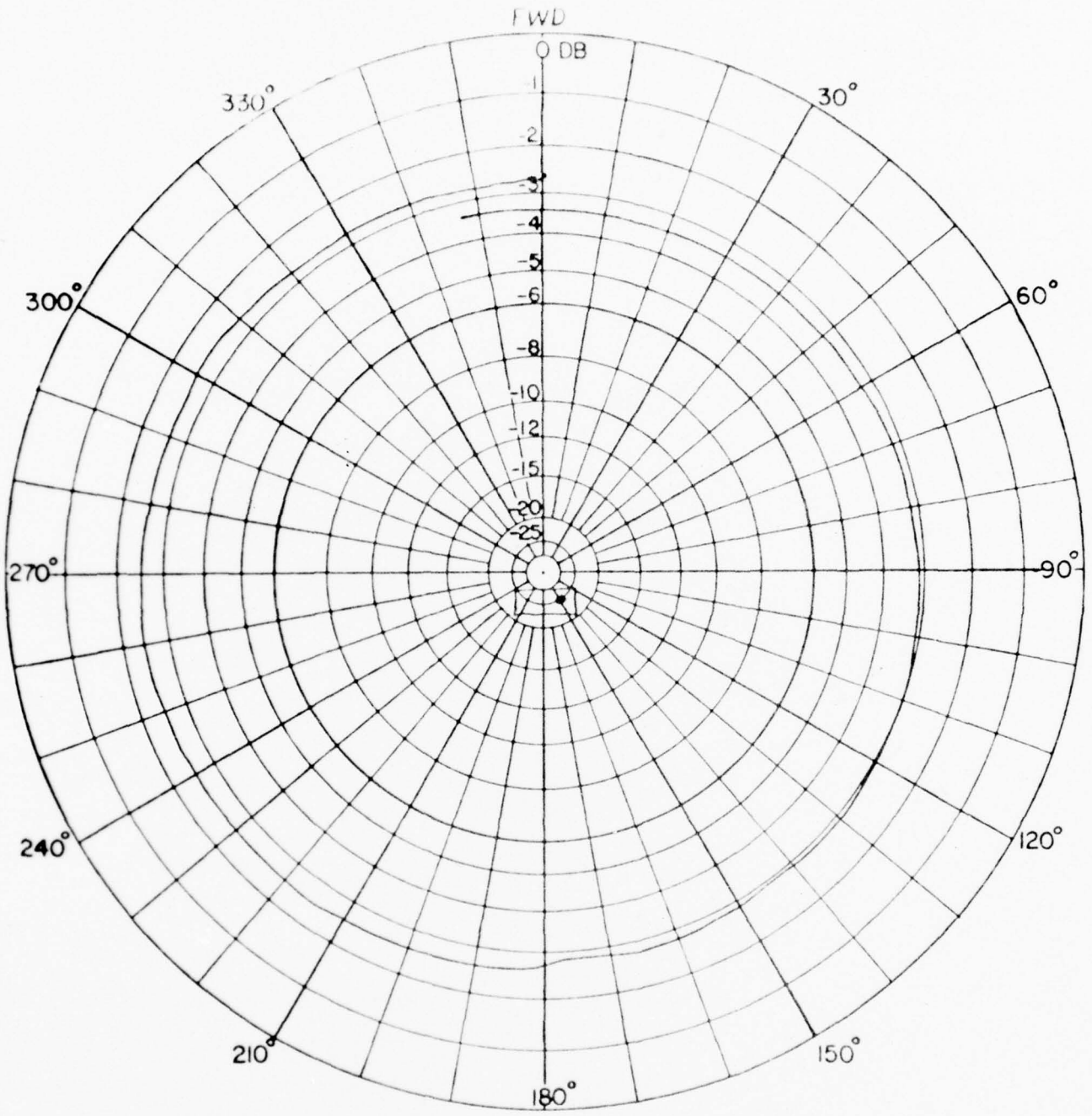

DIAGRAM	TITLE VHF MANPACK ANTENNA	
	ANTENNA 4-ft Centerfed Whip	
	FREQ. 30 MHz	POLARZ Vert
	MODEL SCALE	EΦ= EΘ=
	DATE 4-29-77	BY [illegible]
	REMARKS PRONE	

FIGURE 29

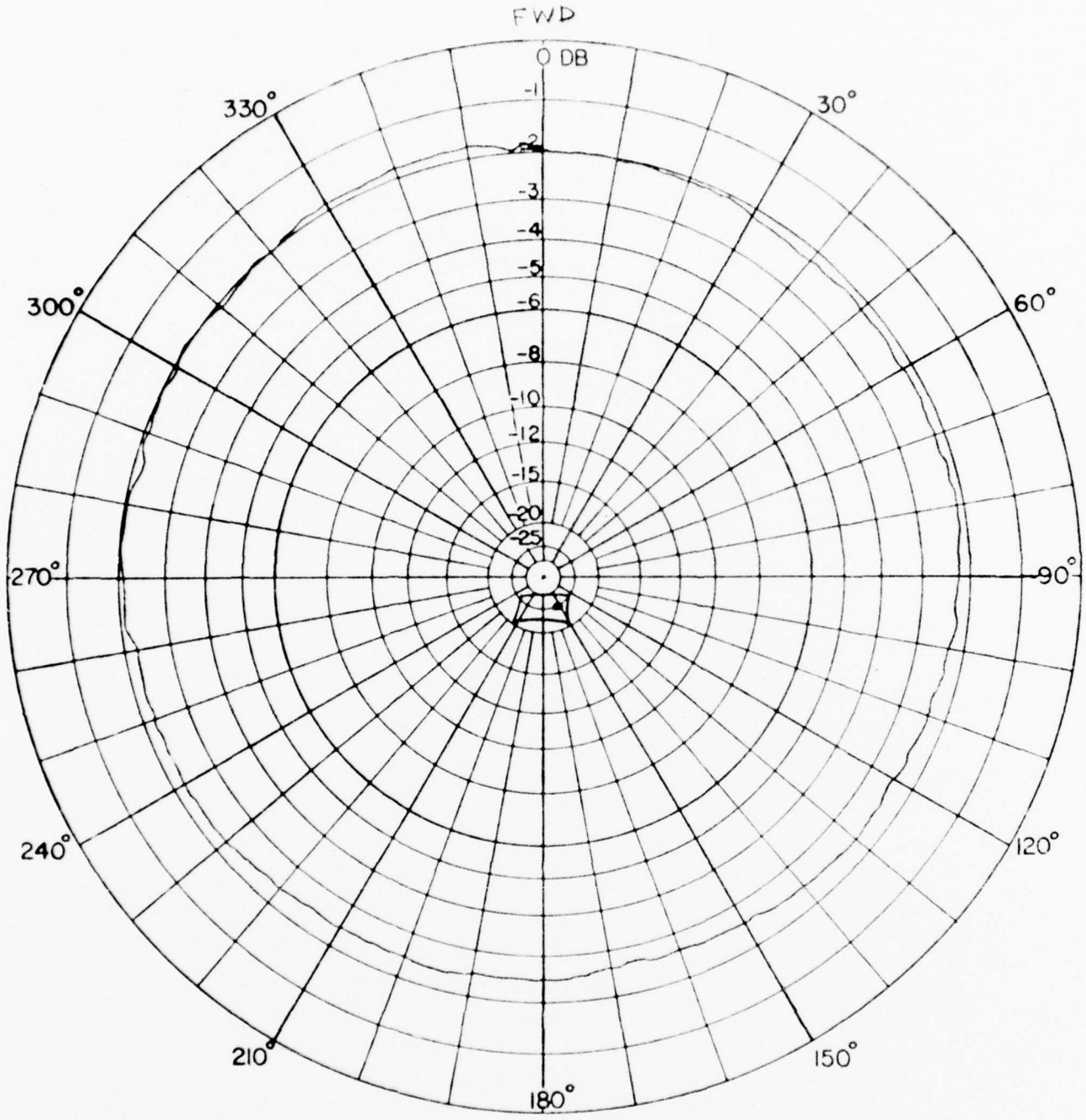

DIAGRAM	TITLE VHF MANPACK ANT	
	ANTENNA Base fed Whip	
	FREQ. 30 MHz	POLARZ Vert
	MODEL SCALE	EΦ= EΘ=
	DATE 4-29-77	BY
	REMARKS STANLINE	

FIGURE 30

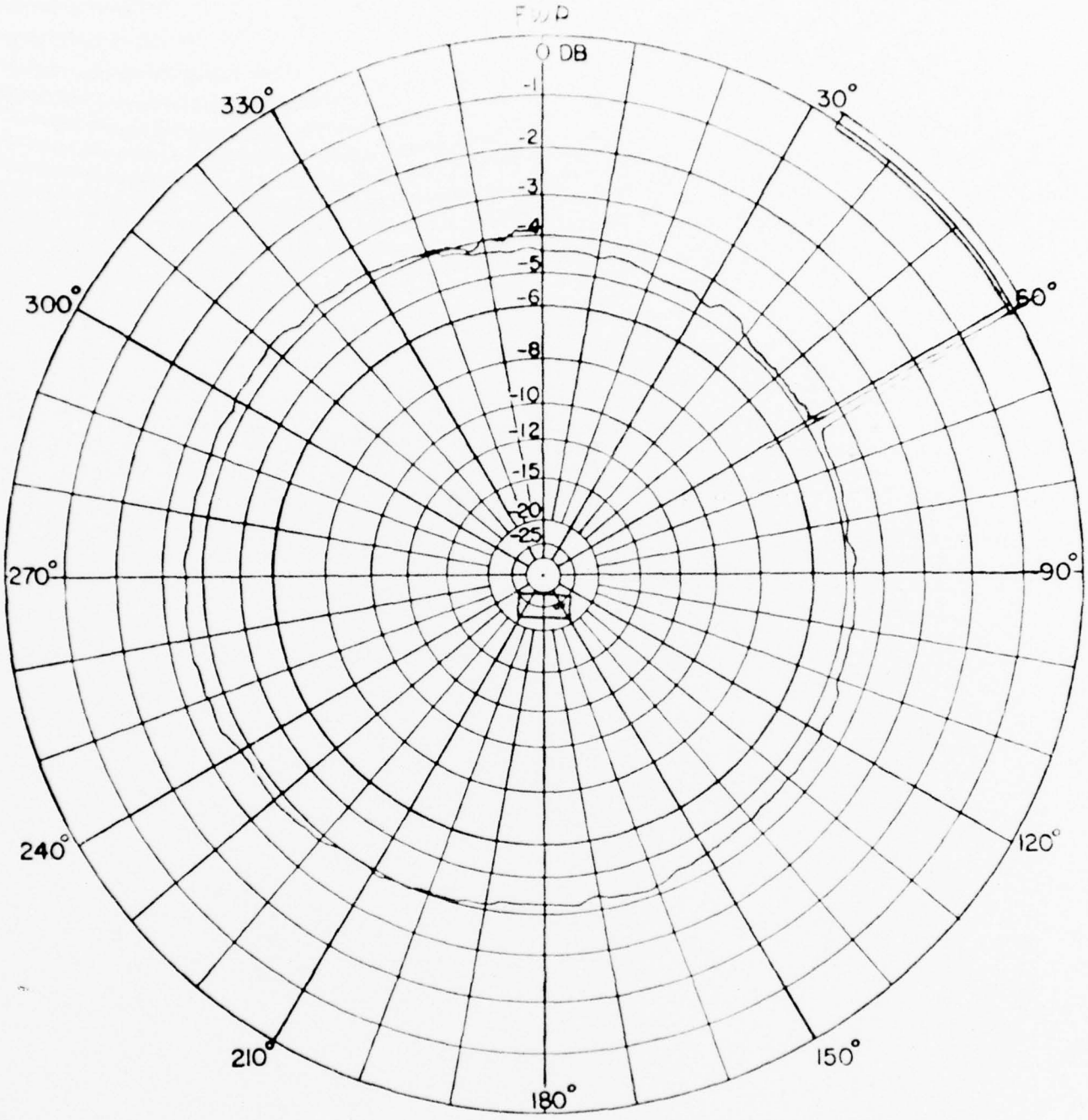

DIAGRAM	TITLE VHF MANPACK ANT
	ANTENNA Basefed Whip
	FREQ. 30 MHz POLARZ Vert
	MODEL SCALE EΦ= EΘ=
	DATE 4-25-77 BY
	REMARKS PROBE

FIGURE 31

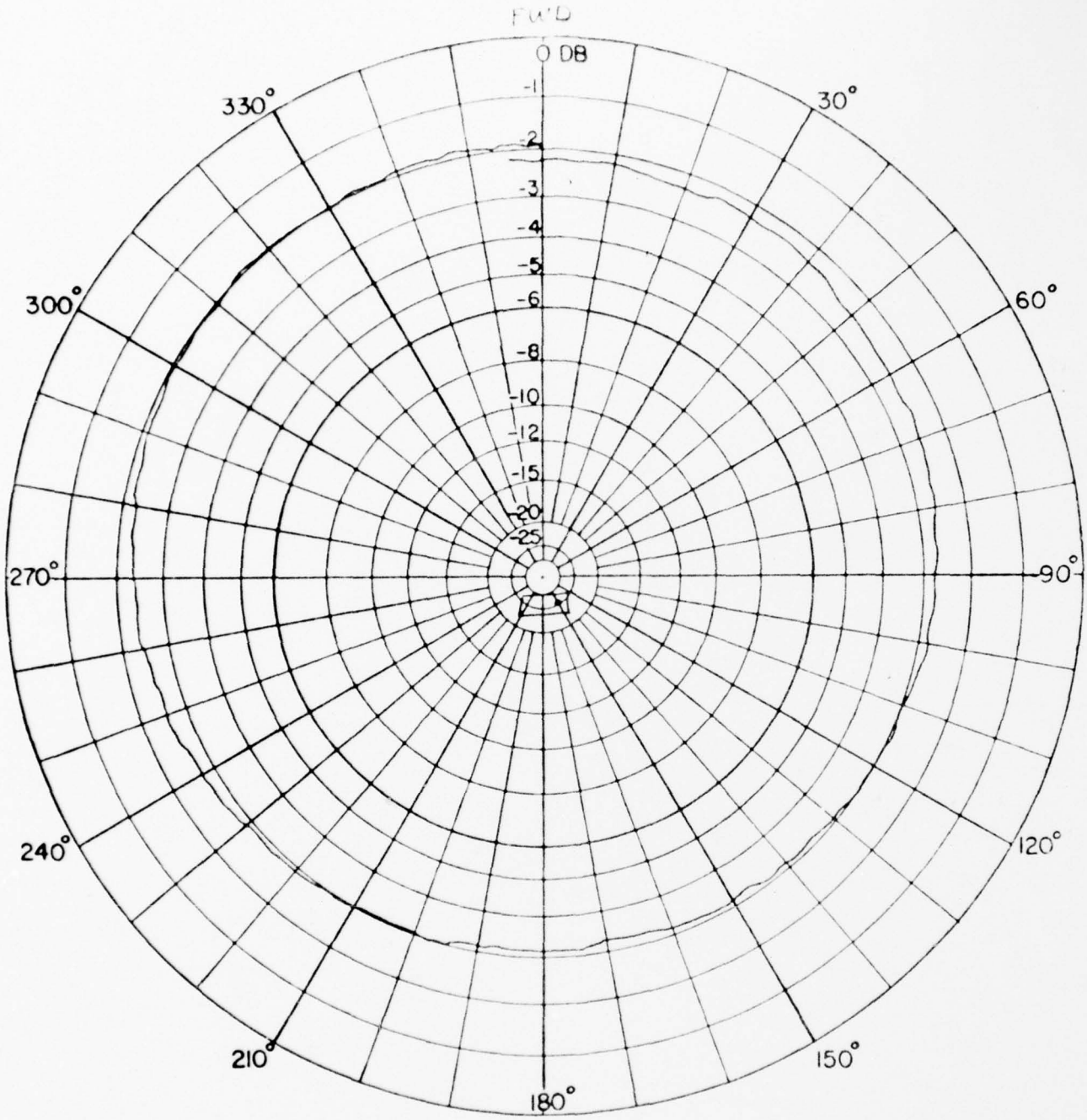

DIAGRAM	TITLE VHF MANPACK ANT.
	ANTENNA 4 ft Centerfed whip
	FREQ. 33 MHz POLARZ Vert
	MODEL SCALE EΦ= EΘ=
	DATE 4-29-77 BY
	REMARKS

FIGURE 32

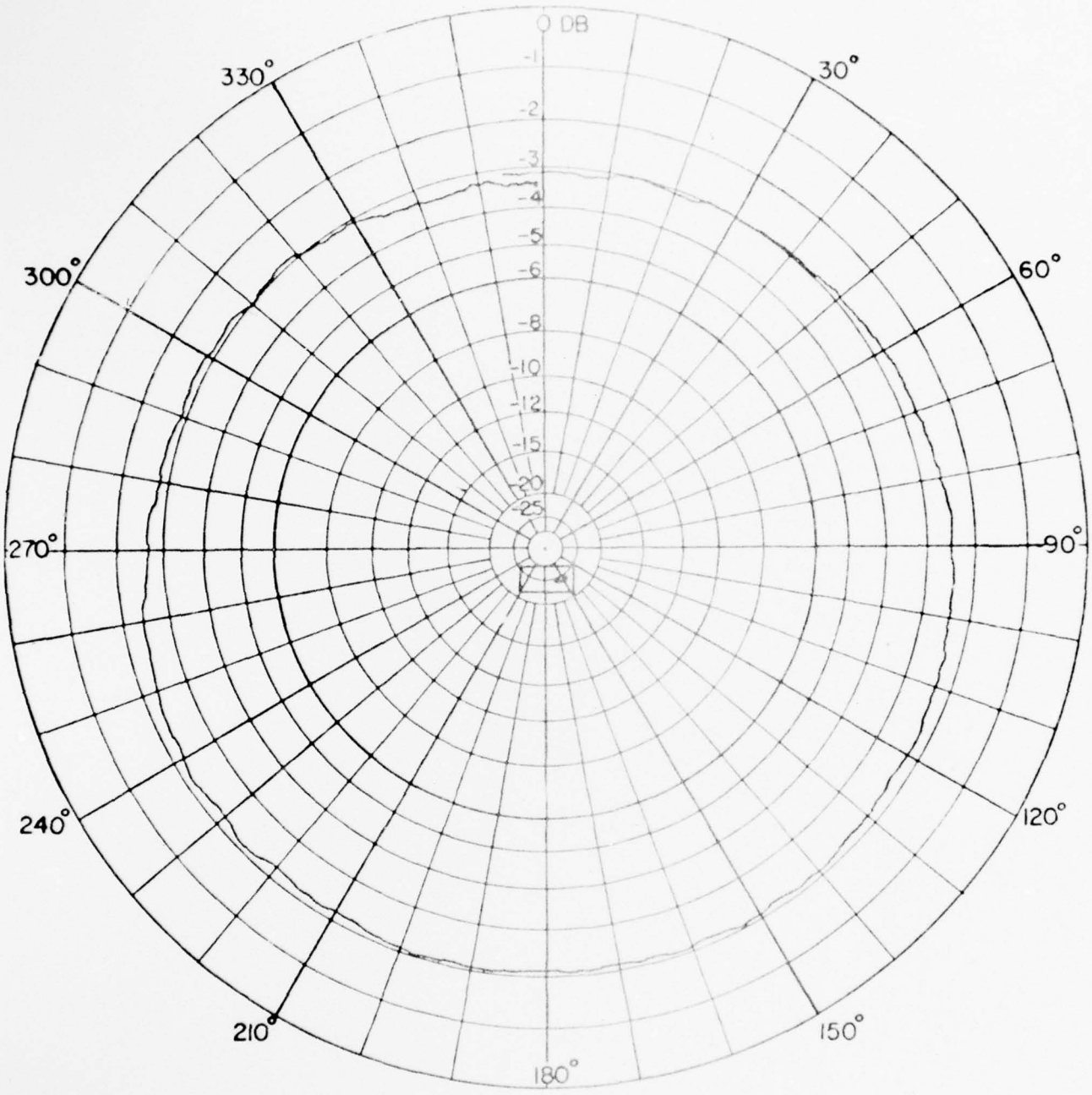

DIAGRAM	TITLE VHF MANPACK ANT
	ANTENNA 4-ft Centerfed Whip
	FREQ. 33 MHz POLARZ V
	MODEL SCALE EΦ= EΘ=
	DATE 4-29-77 BY
	REMARKS PROBE

FIGURE 33

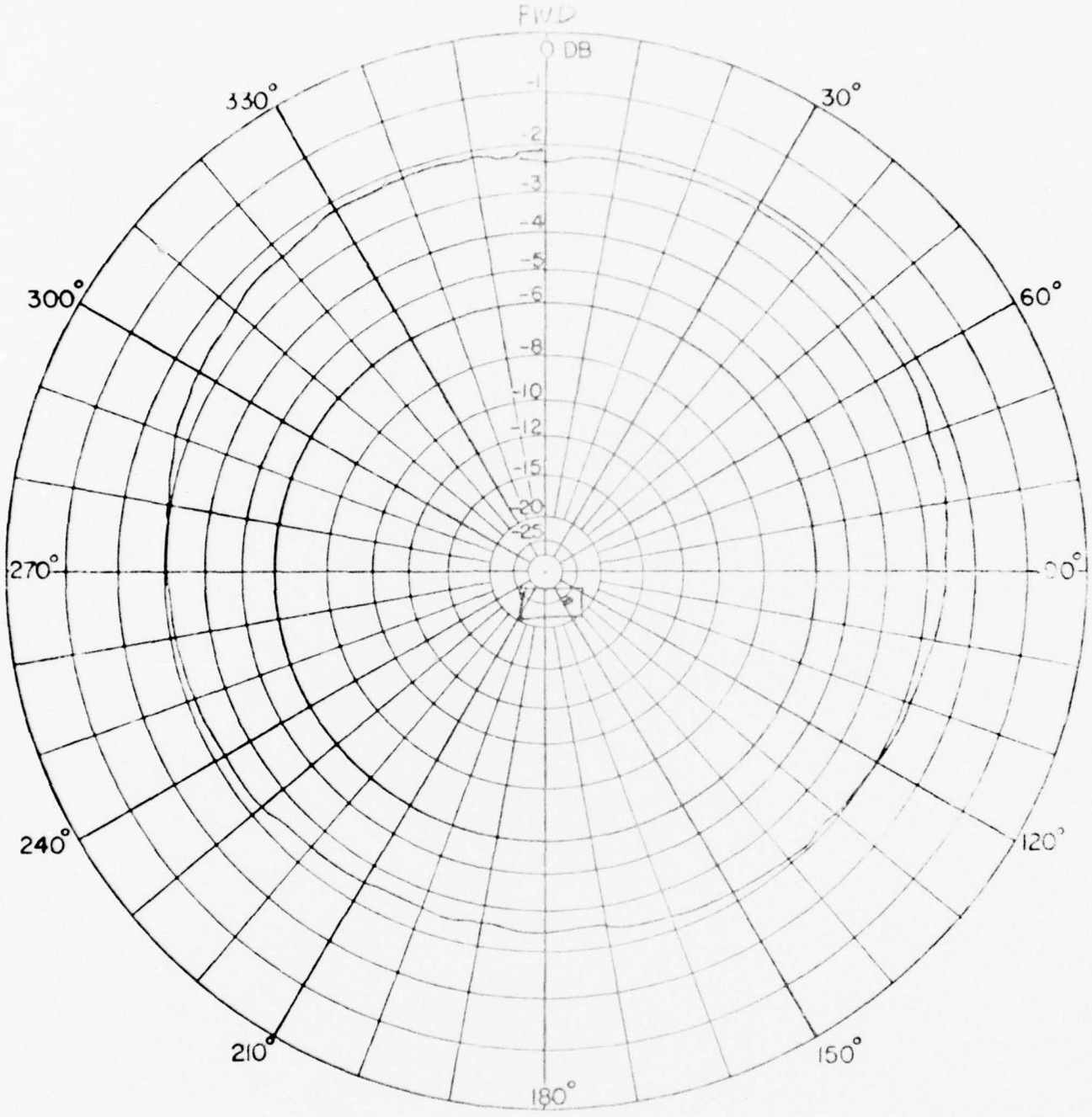

DIAGRAM	TITLE VHF MANPACK ANT
	ANTENNA 4 ft Centerfed Whip
	FREQ. 36 MHz POLARZ
	MODEL SCALE EΦ= Eθ=
	DATE 2-28-77 BY
	REMARKS

FIGURE 34

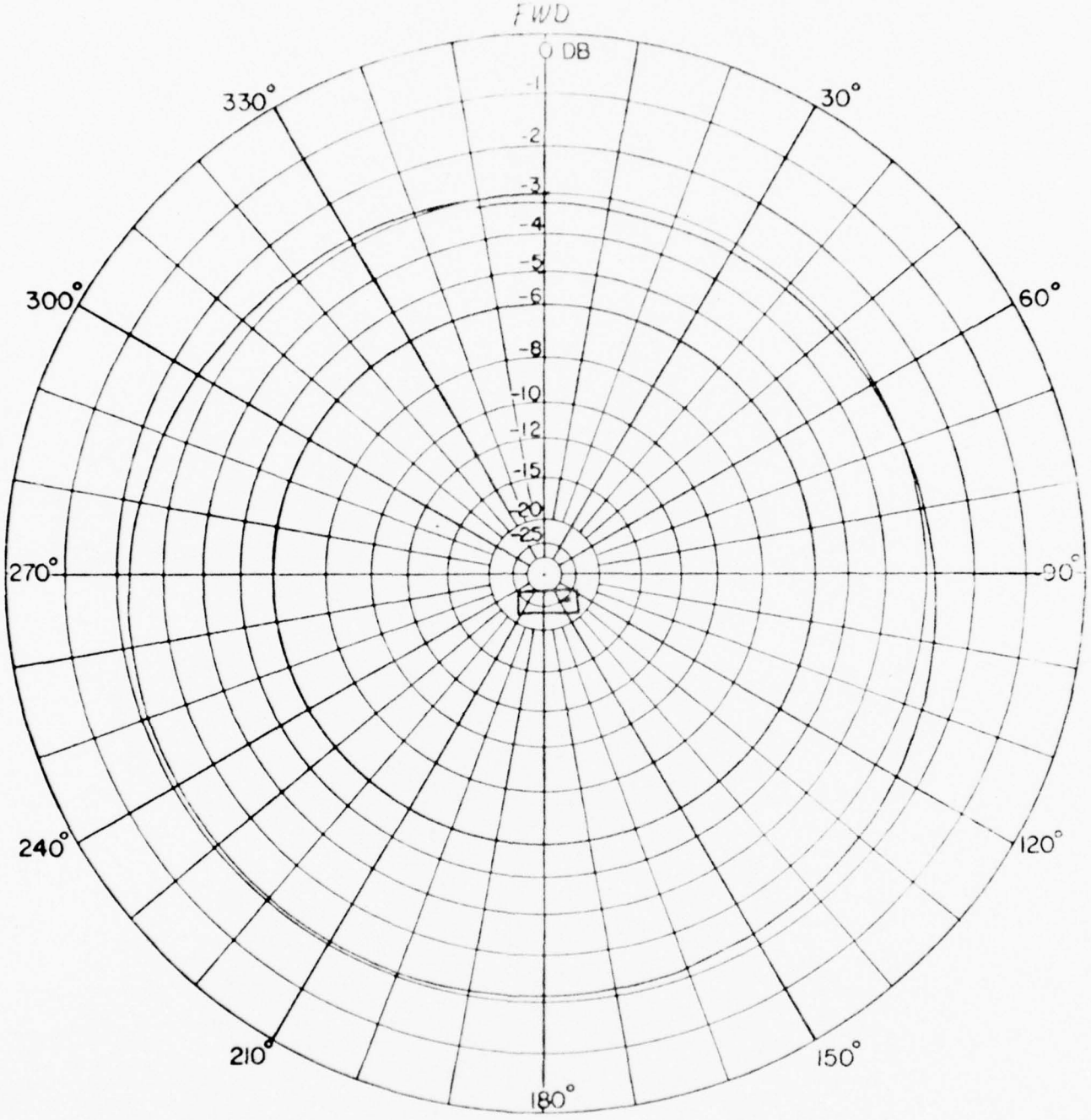

DIAGRAM	TITLE VHF MANPACK ANT
	ANTENNA 4-ft Centerfed Whip
	FREQ. 36 MHz POLARZ Vert
	MODEL SCALE EΦ= EΘ=
	DATE 4-25-77 BY
	REMARKS PRONE

FIGURE 35

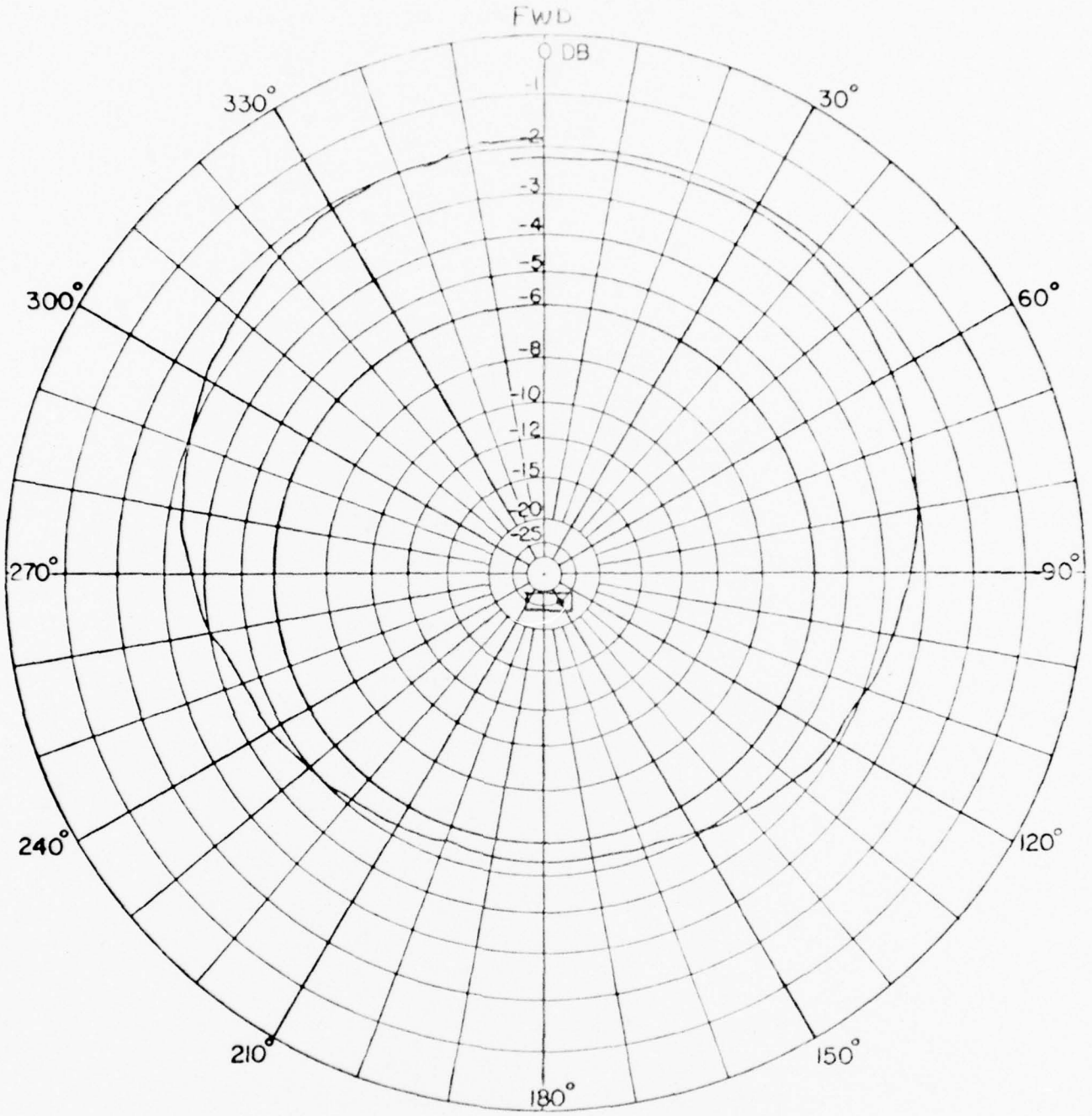

DIAGRAM	TITLE VHF MANPACK ANT
	ANTENNA 4-ft Centerfed Whip
	FREQ. 41 MHz POLARZ Vert
	MODEL SCALE EΦ= EΘ=
	DATE 4-29-77 BY
	REMARKS STANDING

FIGURE 36

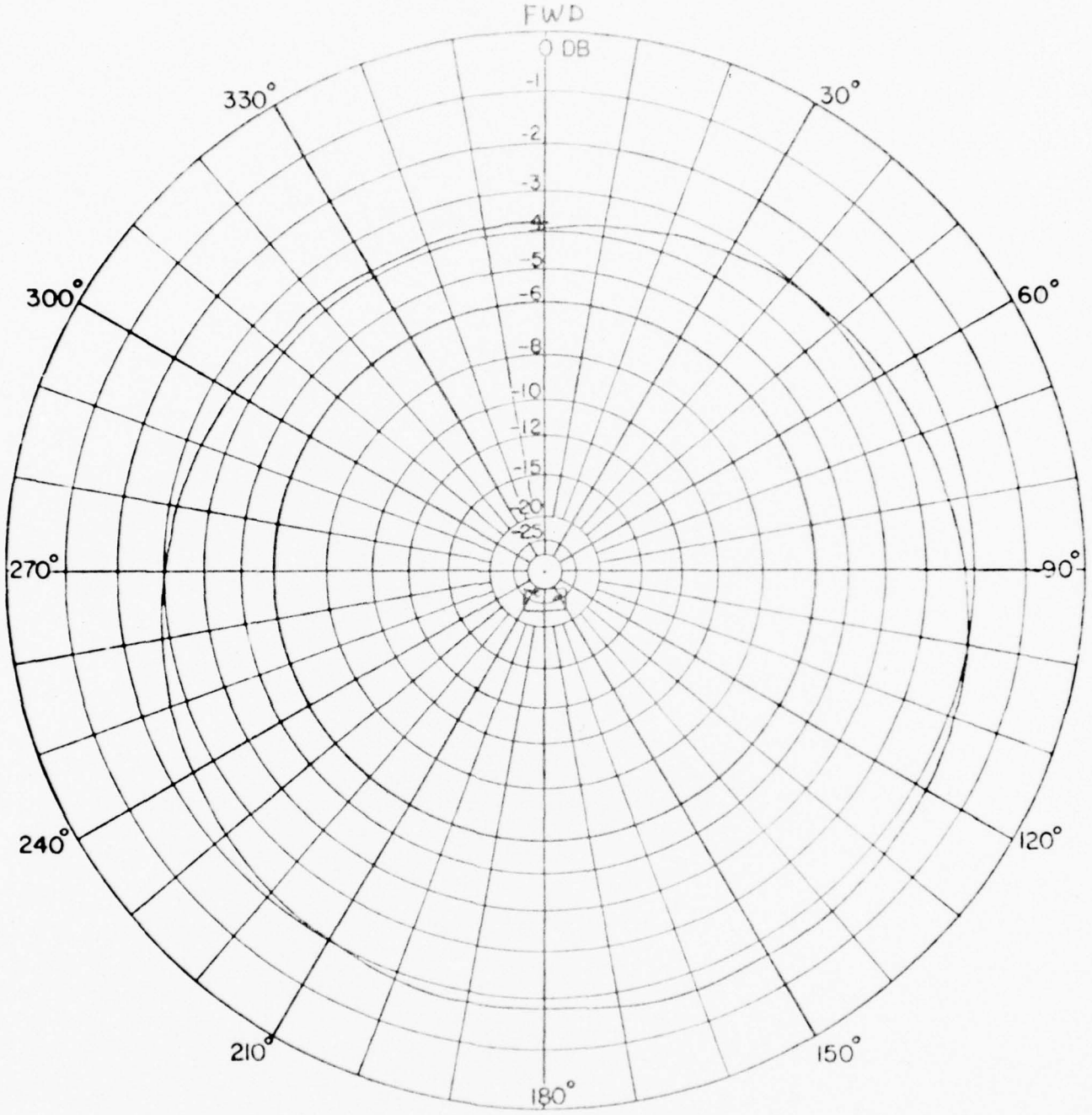

DIAGRAM	TITLE VHF MANPACK ANT
	ANTENNA 4-ft Centerfed Whip
	FREQ. 41 MHz POLARZ Vert
	MODEL SCALE EΦ= EΘ=
	DATE 4-29-77 BY
	REMARKS PRONE

FIGURE 37

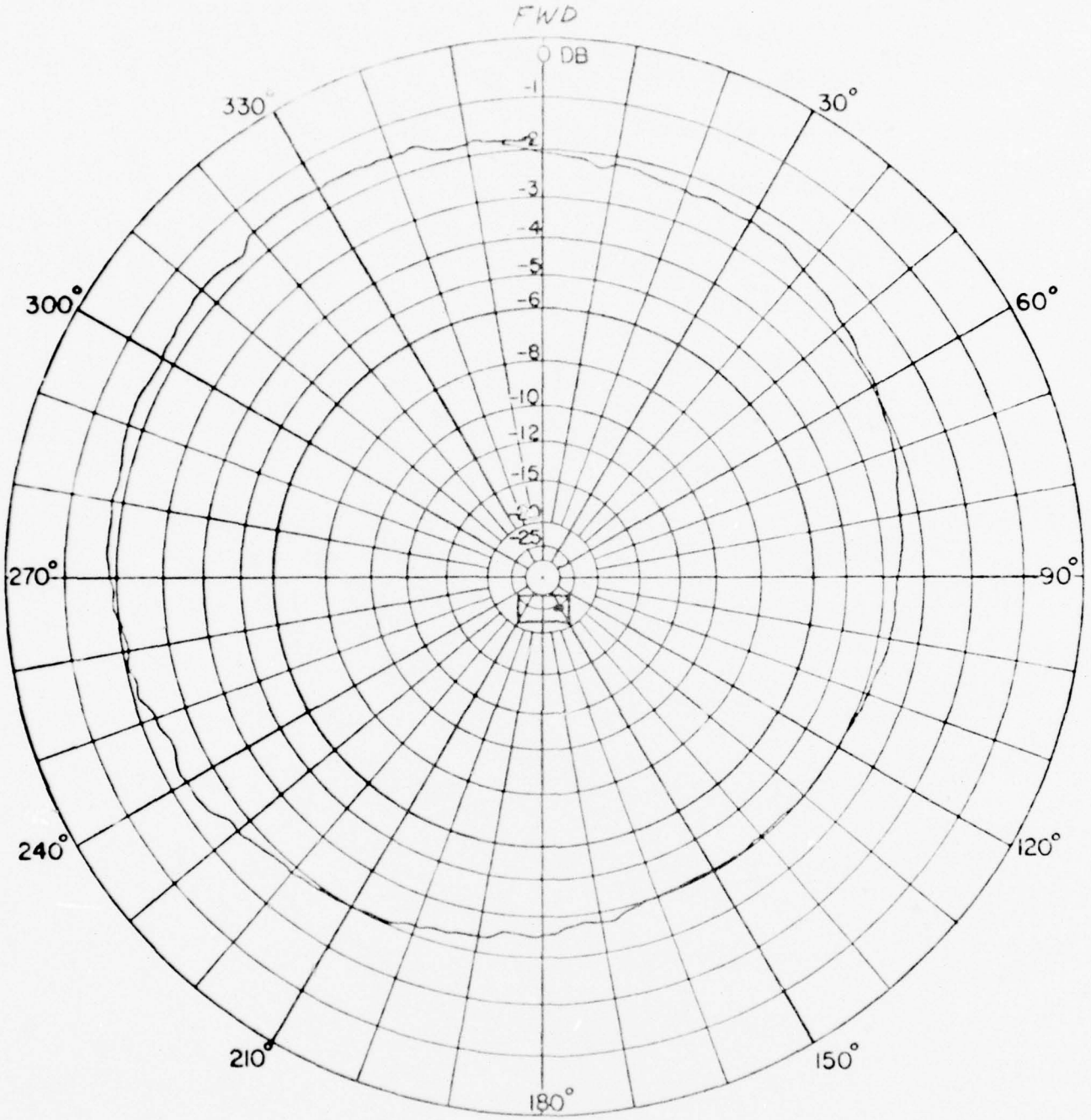

DIAGRAM	TITLE VHF MANPACK ANT	
	ANTENNA Basefed Whip	
	FREQ. 40 MHz	POLARZ Vert
	MODEL SCALE	EΦ= EΘ=
	DATE 4-29-77	BY
	REMARKS STAMSEW=	

FIGURE 38

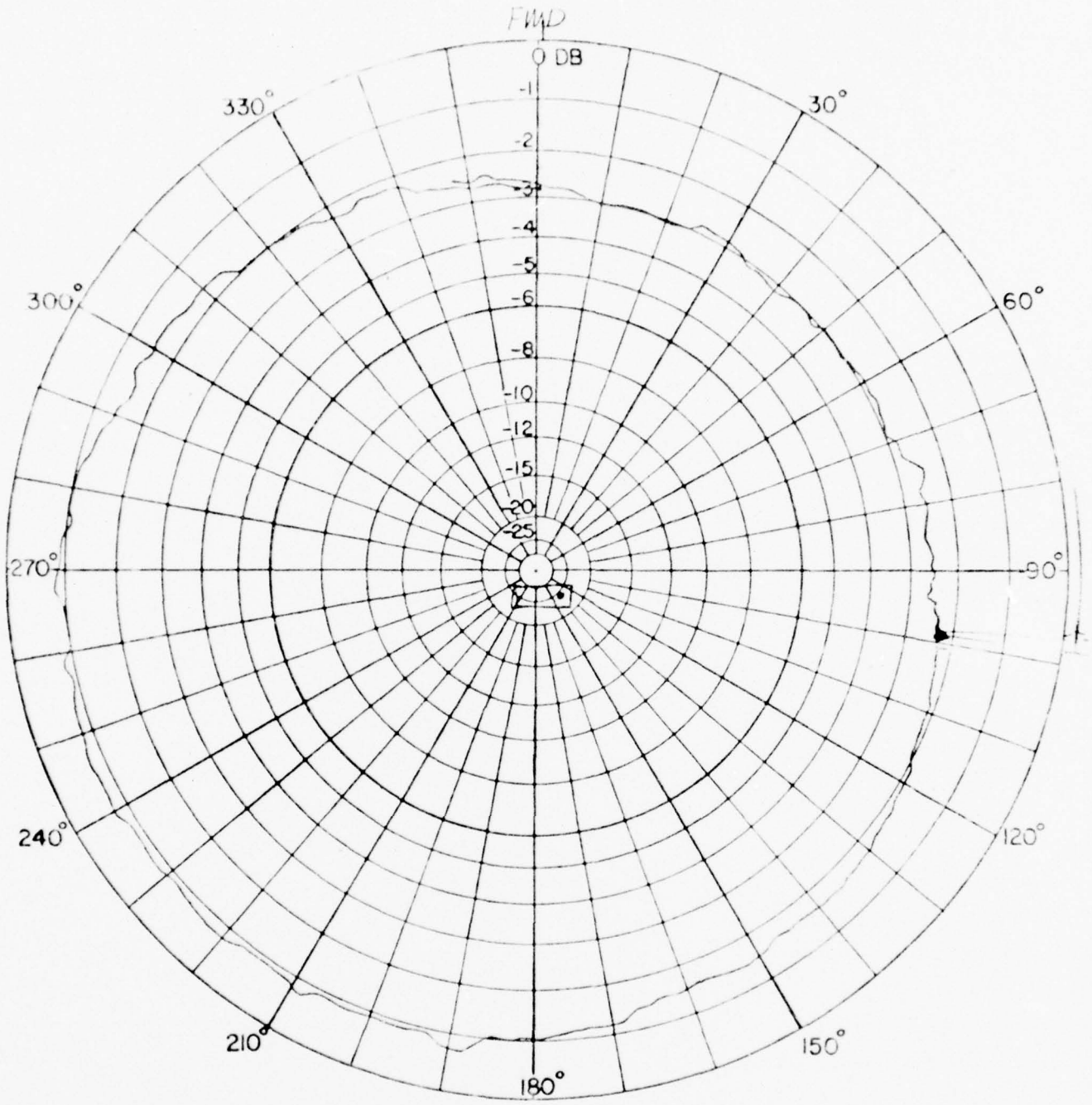

DIAGRAM	TITLE VHF MARPACE ANT
	ANTENNA Base fed Whip
	FREQ. 40 MHz POLARZ
	MODEL SCALE EΦ= EΘ=
	DATE 4-27-77 BY
	REMARKS PHONE

FIGURE 39

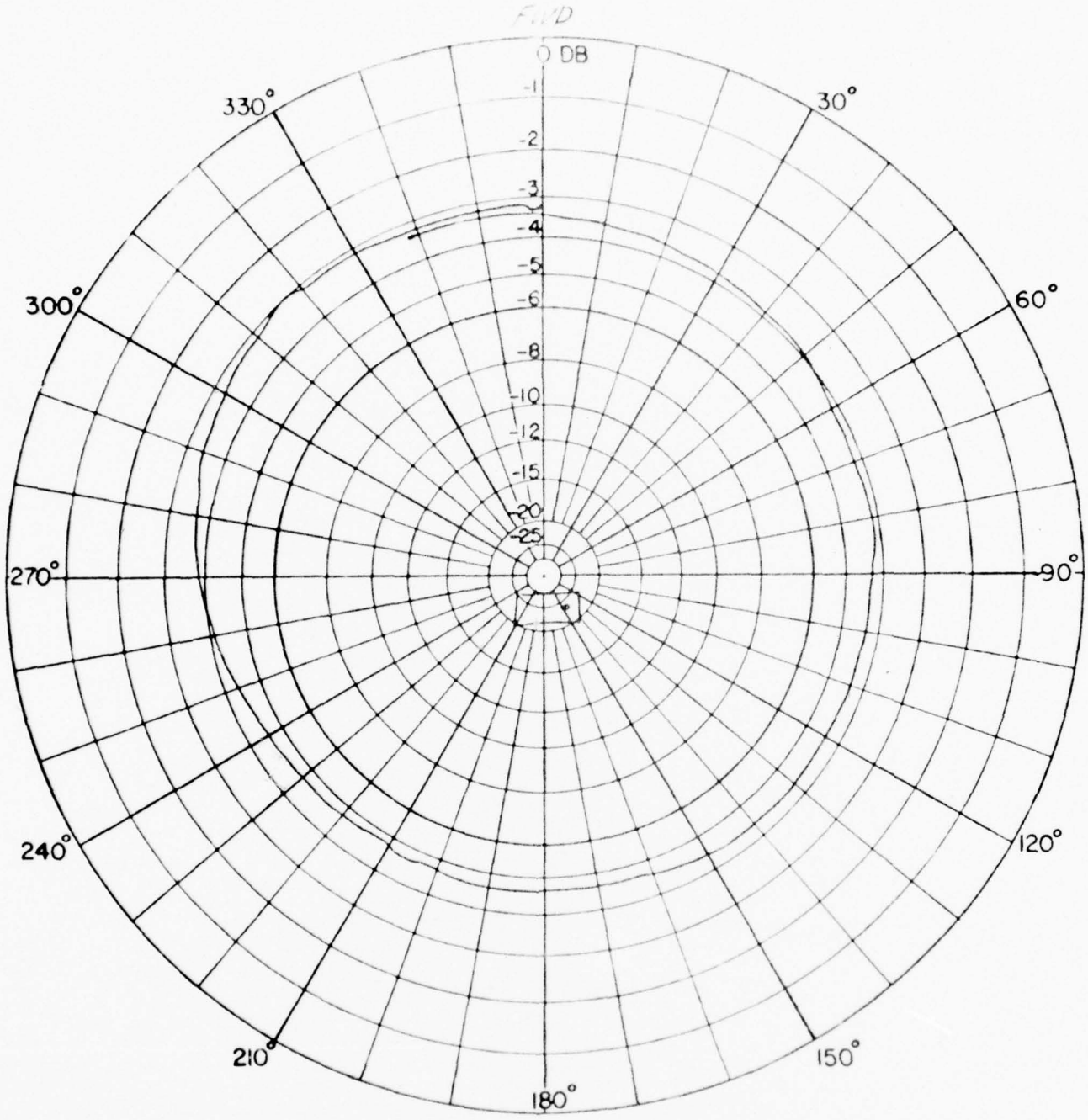

DIAGRAM	TITLE VHF MANPACK ANT	
	ANTENNA 4 ft Centerfed Whip	
	FREQ. 44 MHz	POLARZ Vert
	MODEL SCALE	EΦ= EΘ=
	DATE 7-29-77	BY
	REMARKS STANDARD	

FIGURE 40

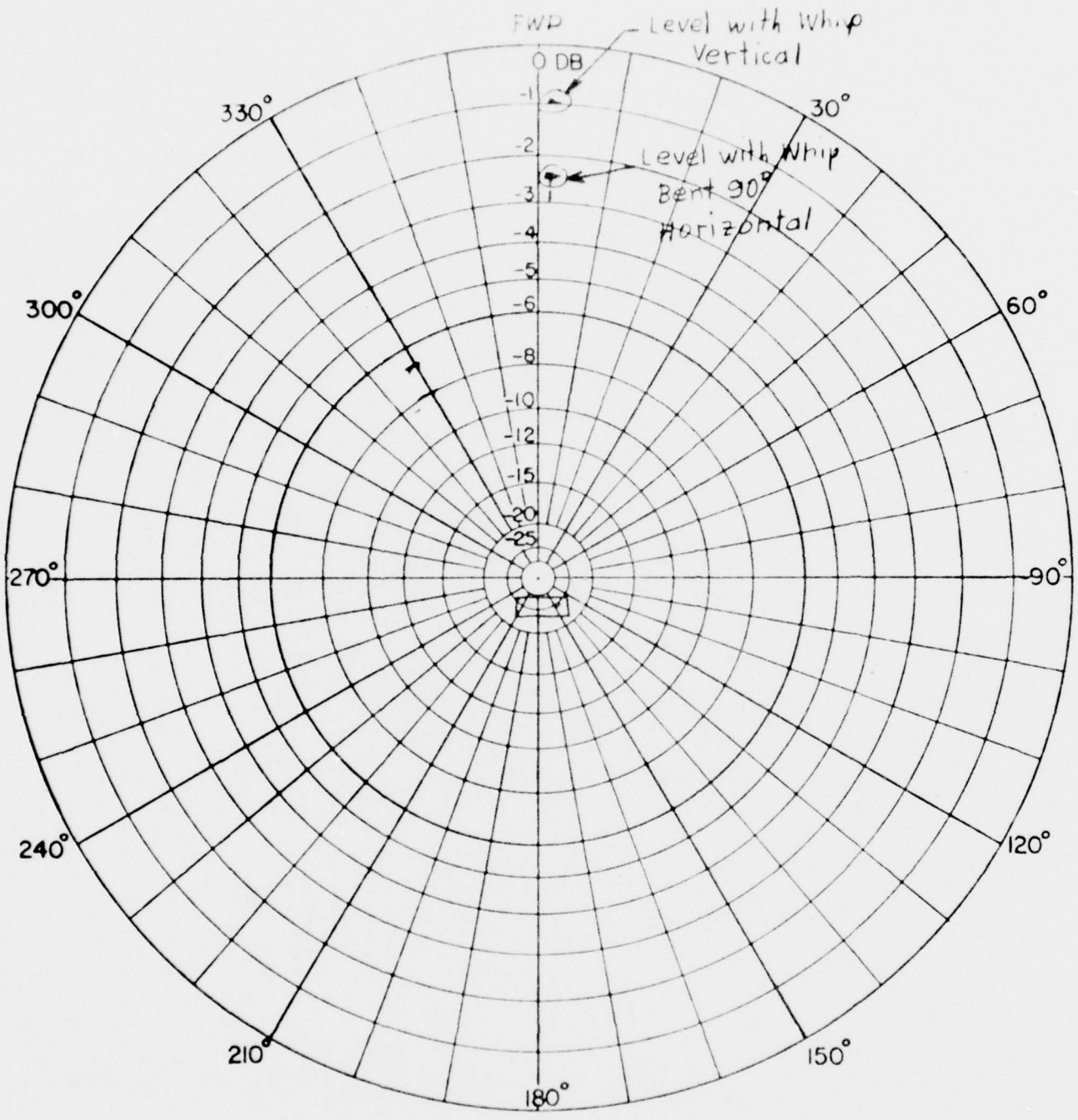

DIAGRAM	TITLE VHF MANPACK ANT	
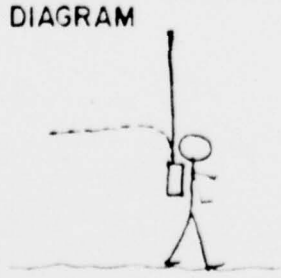	ANTENNA 4-ft Centerfed Whip	
	FREQ. 44 MHz	POLARZ Vert
	MODEL SCALE	EΦ= EΘ=
	DATE 4-27-77	BY
	REMARKS STANDING	

FIGURE 41

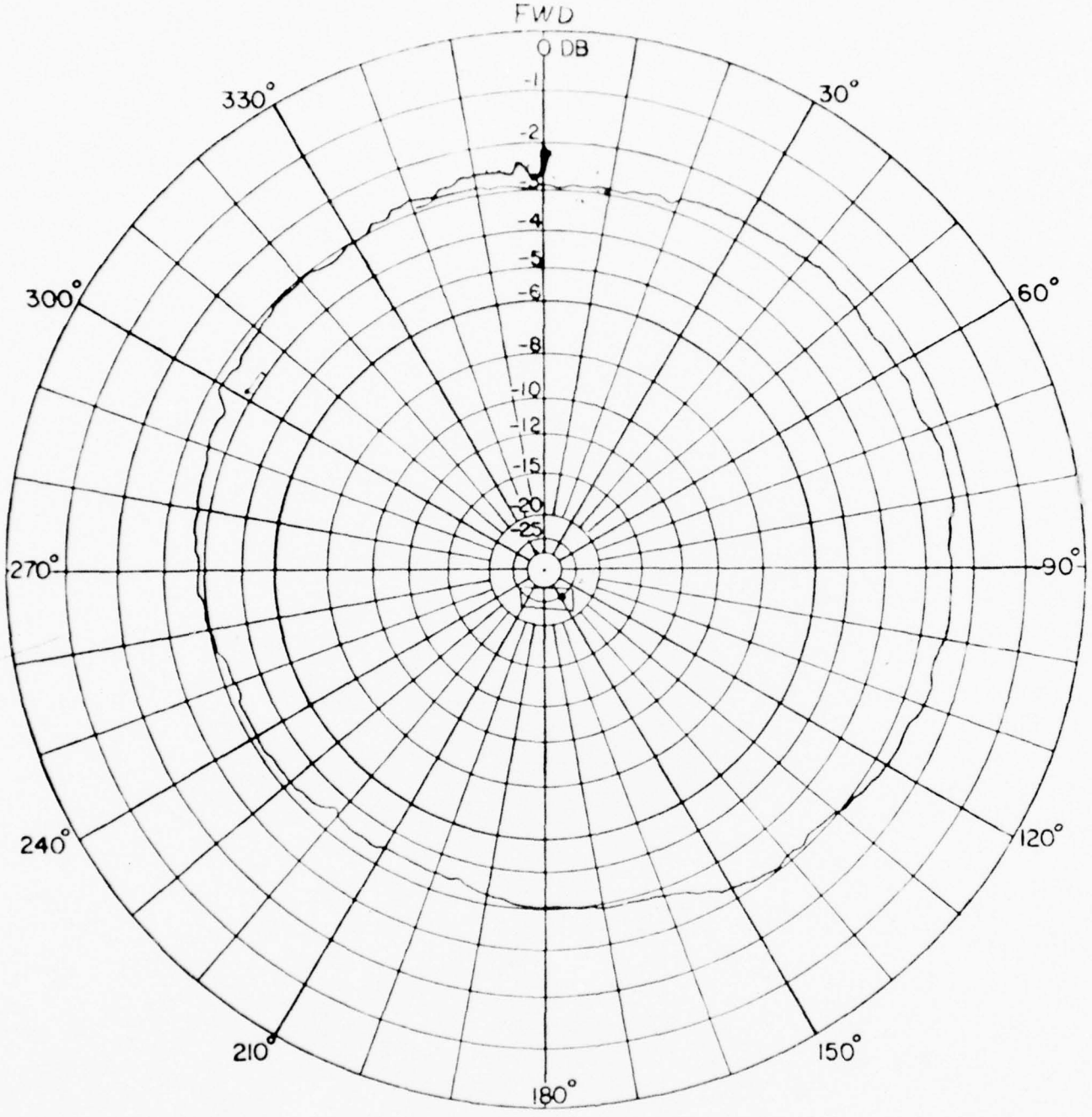

DIAGRAM RECEIVING MONOPOLE

MANPACK

ANT

$\phi = 0$

180'

TITLE VHF MANPACK (URC-78)	
ANTENNA 4-ft Centerfed Whip	
FREQ. 47 MHz	POLARZ Vert
MODEL SCALE	EΦ= EΘ=
DATE 4-27-77	BY JCA
REMARKS Standing - Right Arm extended	

FIGURE 42

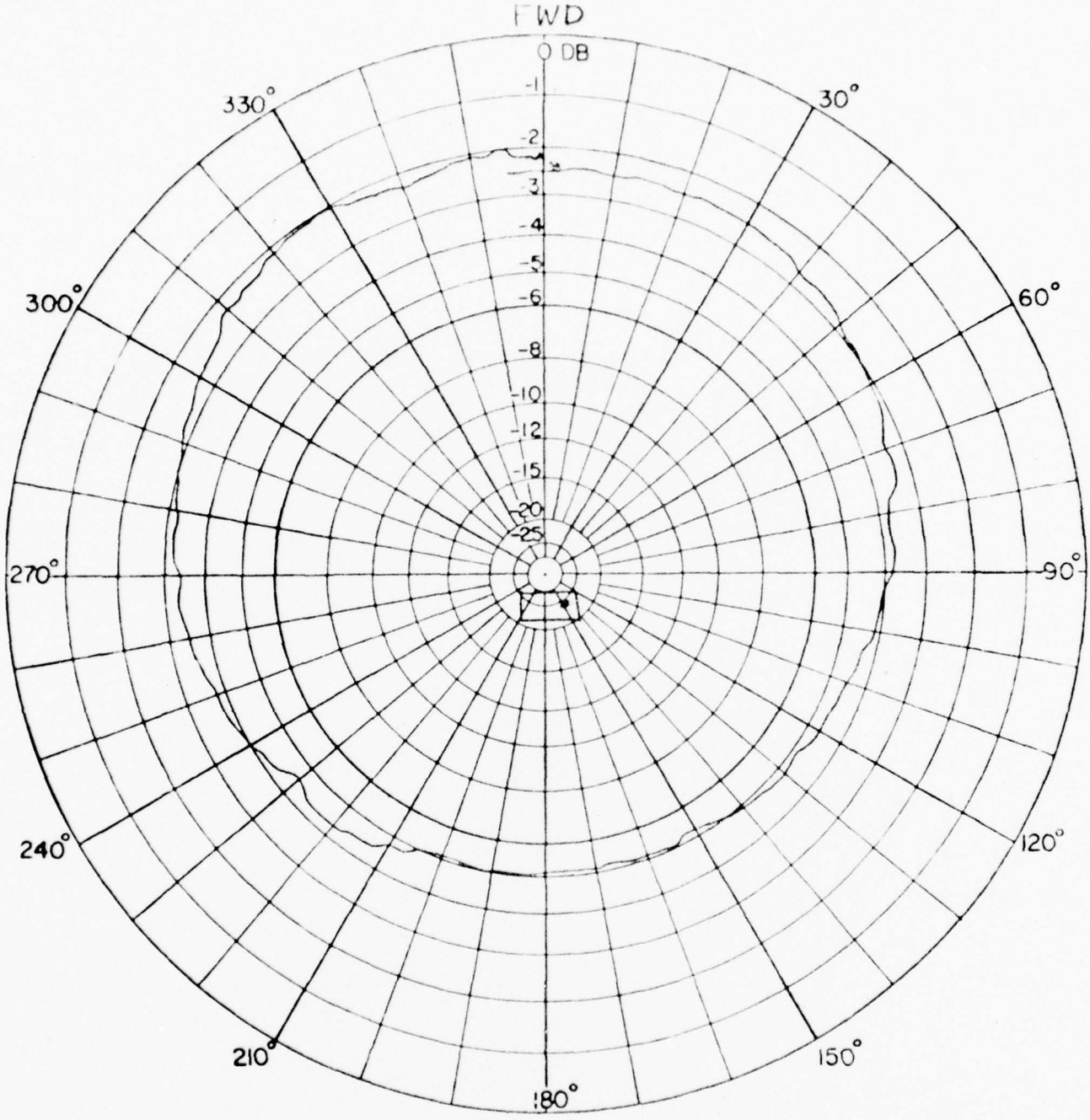

DIAGRAM	TITLE VHF MANPACK ANT	
	ANTENNA 4ft Centerfed whip	
	FREQ. 47 MHz	POLARZ Vert
	MODEL SCALE	EΦ= EΘ=
	DATE 4-2?-77	BY
	REMARKS STANDARD	

FIGURE 43

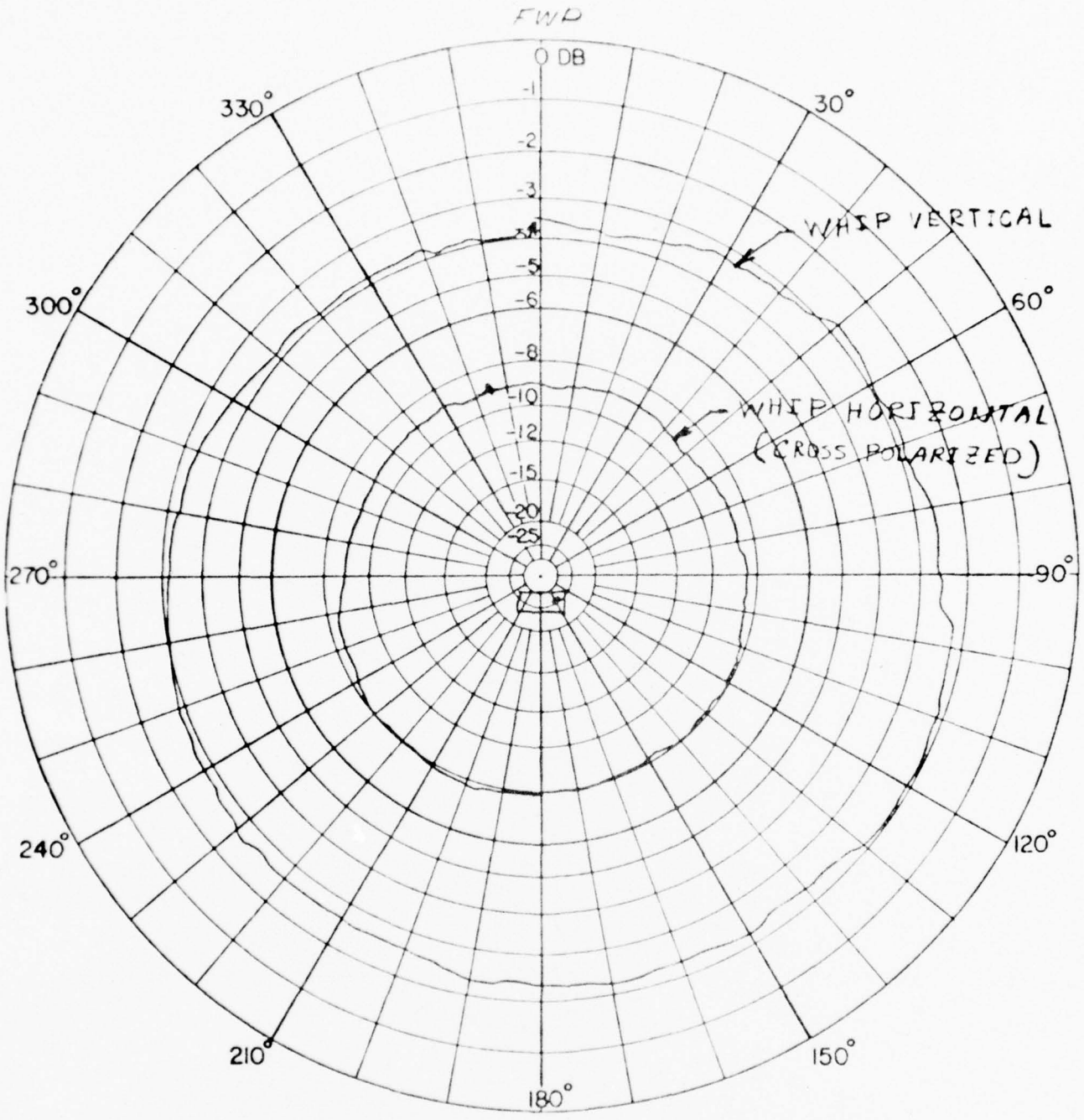

DIAGRAM	
	TITLE VHF MANPACK ANT
	ANTENNA 4-ft Centerfed Whip
	FREQ. 47 MHz POLARZ Vert
	MODEL SCALE Eϕ= Eθ=
	DATE 4-27-77 BY
	REMARKS PRONE

FIGURE 44

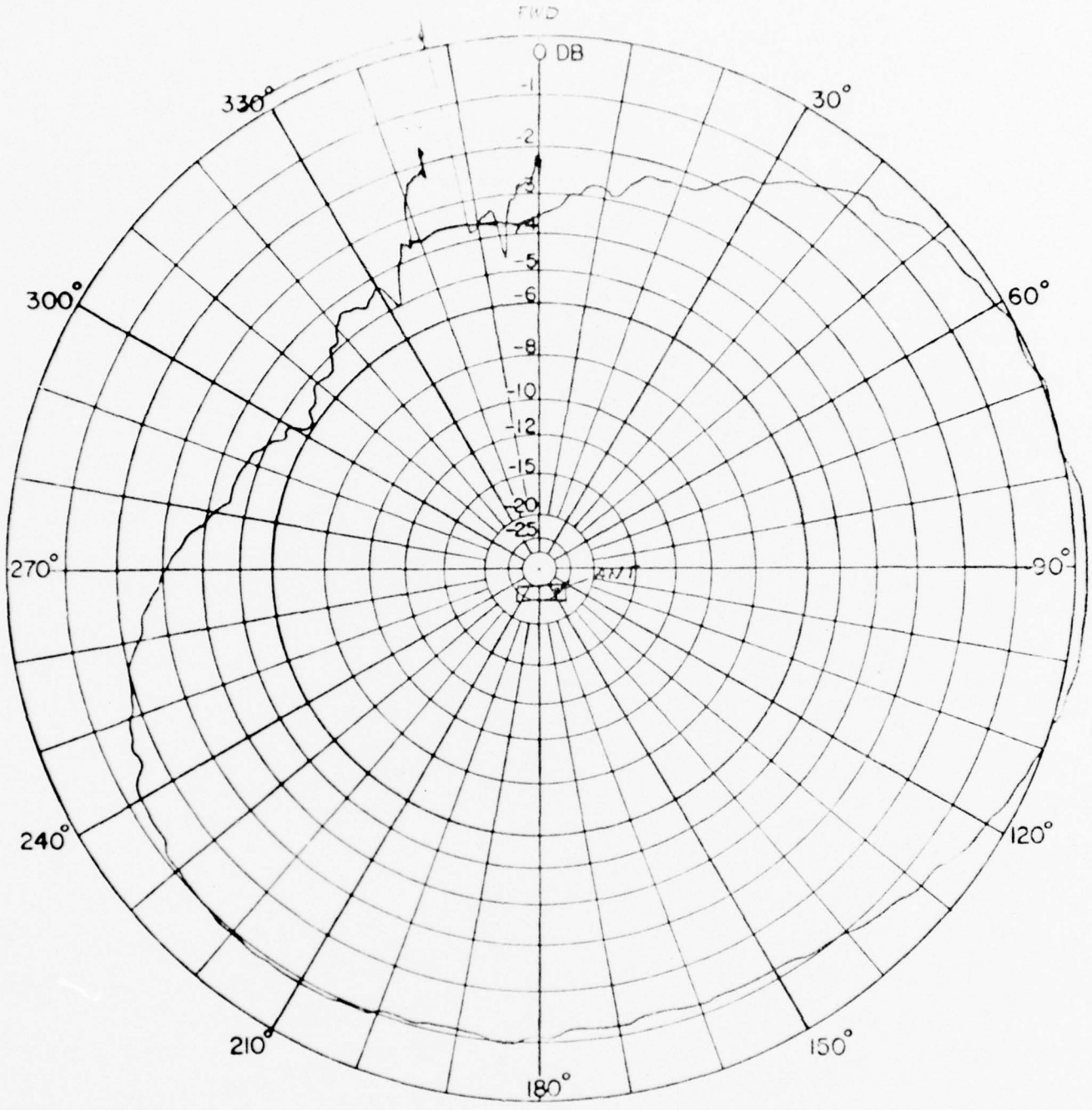

DIAGRAM	TITLE VHF MANPACK URC-78
	ANTENNA 4-ft Centerfed Whip
	FREQ. 51 MHz POLARZ Vert
	MODEL SCALE EΦ= EΘ=
	DATE 4-28-77 BY
	REMARKS Standing

FIGURE 45

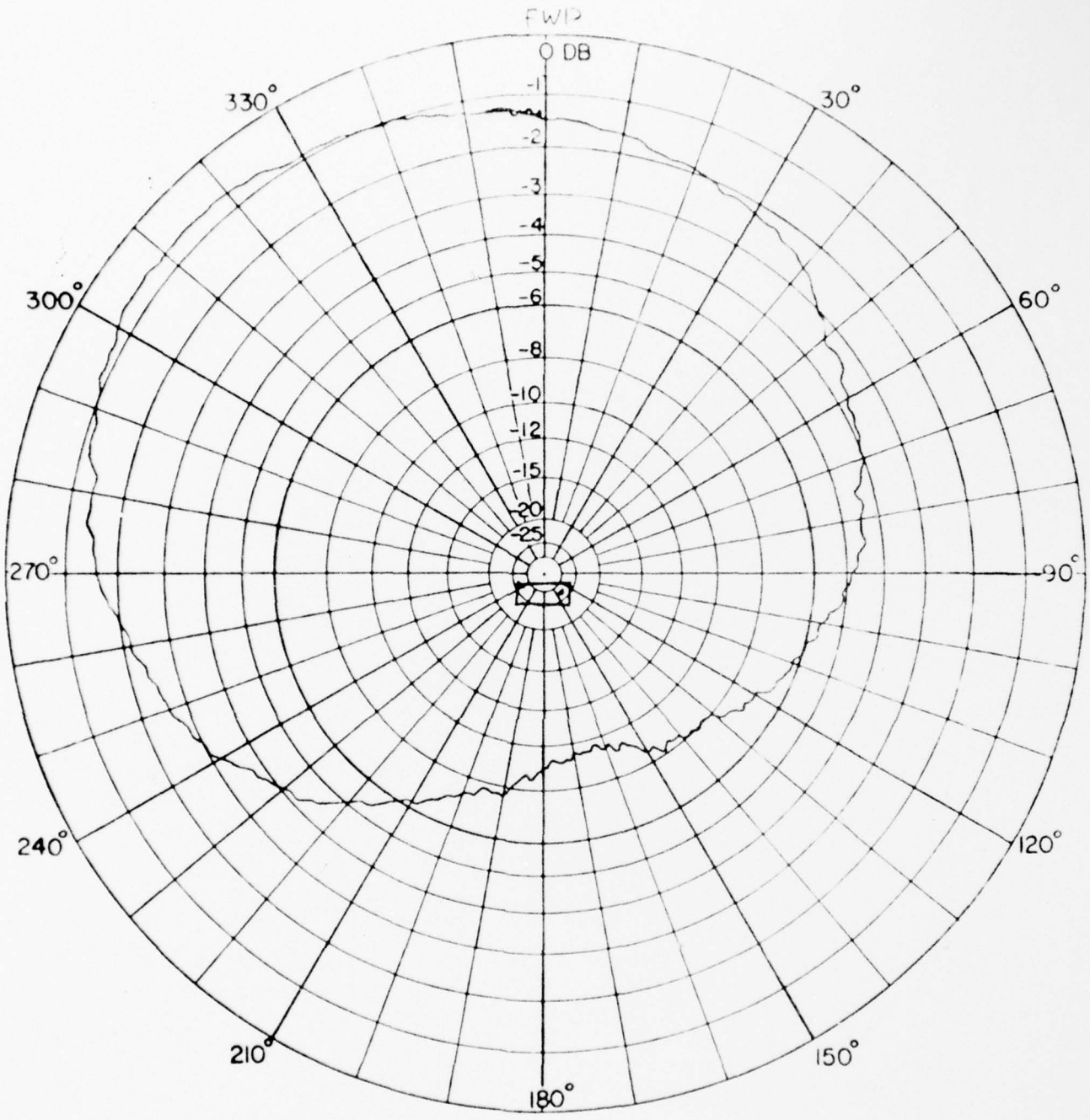

DIAGRAM	TITLE VHF MANPACK ANT	
	ANTENNA Basefed Whip	
	FREQ. 50 MHz	POLARZ Vert
	MODEL SCALE	EΦ= EΘ=
	DATE 4-29-77	BY
	REMARKS STANDARD	

FIGURE 46

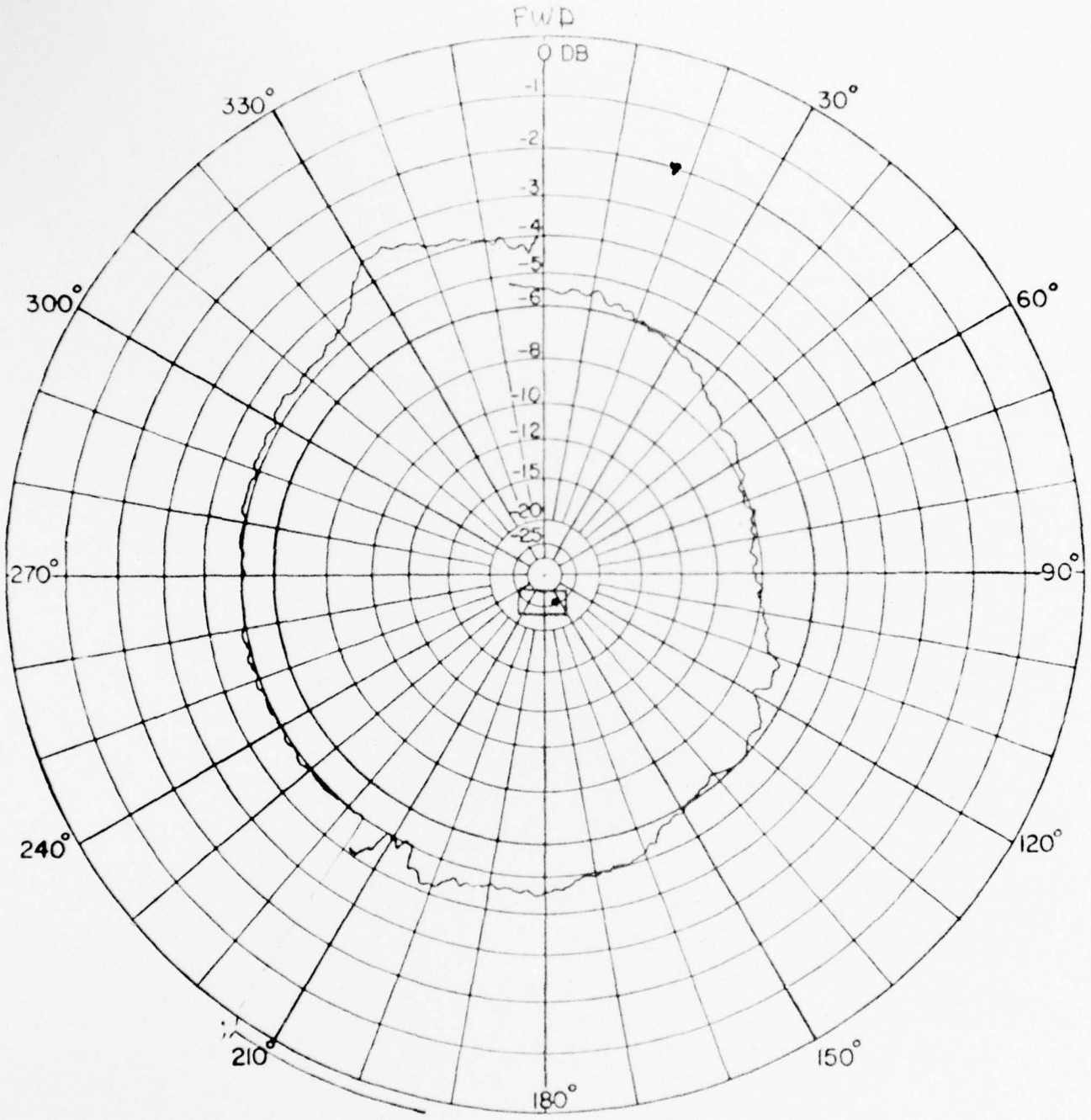

DIAGRAM	TITLE VHF MANPACK ANT
	ANTENNA Basefed Whip
	FREQ. 50 MHz POLARZ Vert
	MODEL SCALE EΦ= EΘ=
	DATE 4-5-77 BY
	REMARKS PRONE

FIGURE 47

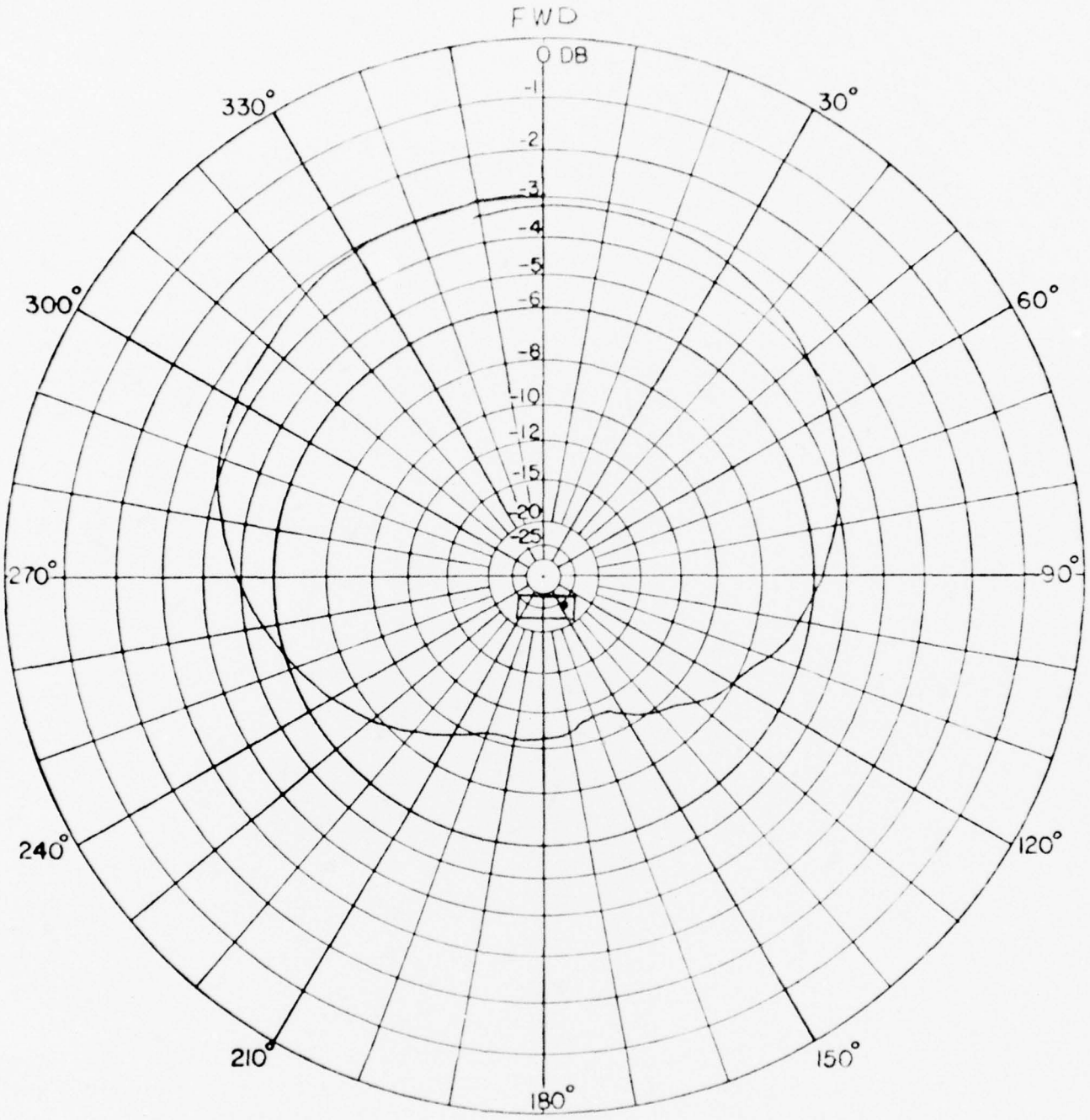

DIAGRAM	TITLE VHF MANPACK (URC-78)	
	ANTENNA 4-ft Centerfed Whip	
	FREQ. 55 MHz	POLARZ Vert
	MODEL SCALE	EΦ= EΘ=
	DATE 4-27-77	BY L.
	REMARKS Standing	

FIGURE 48

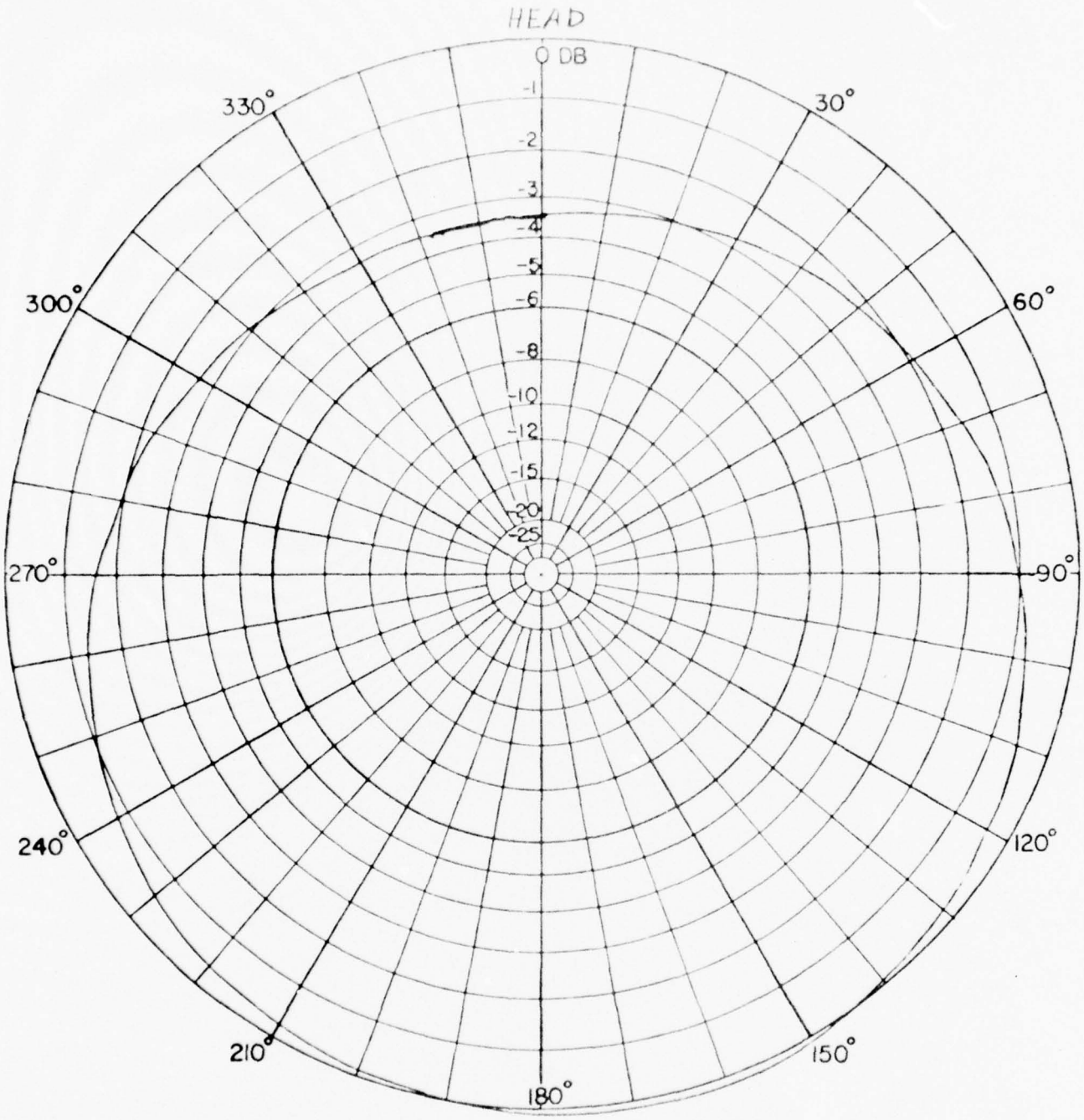

DIAGRAM	TITLE VHF MANPACK (URC-78)
	ANTENNA 4ft Centerfed Whip
	FREQ. 55 MHz POLARZ Vert
	MODEL SCALE EΦ= EΘ=
	DATE 4-27-77 BY [illegible]
	REMARKS Prone

FIGURE 49

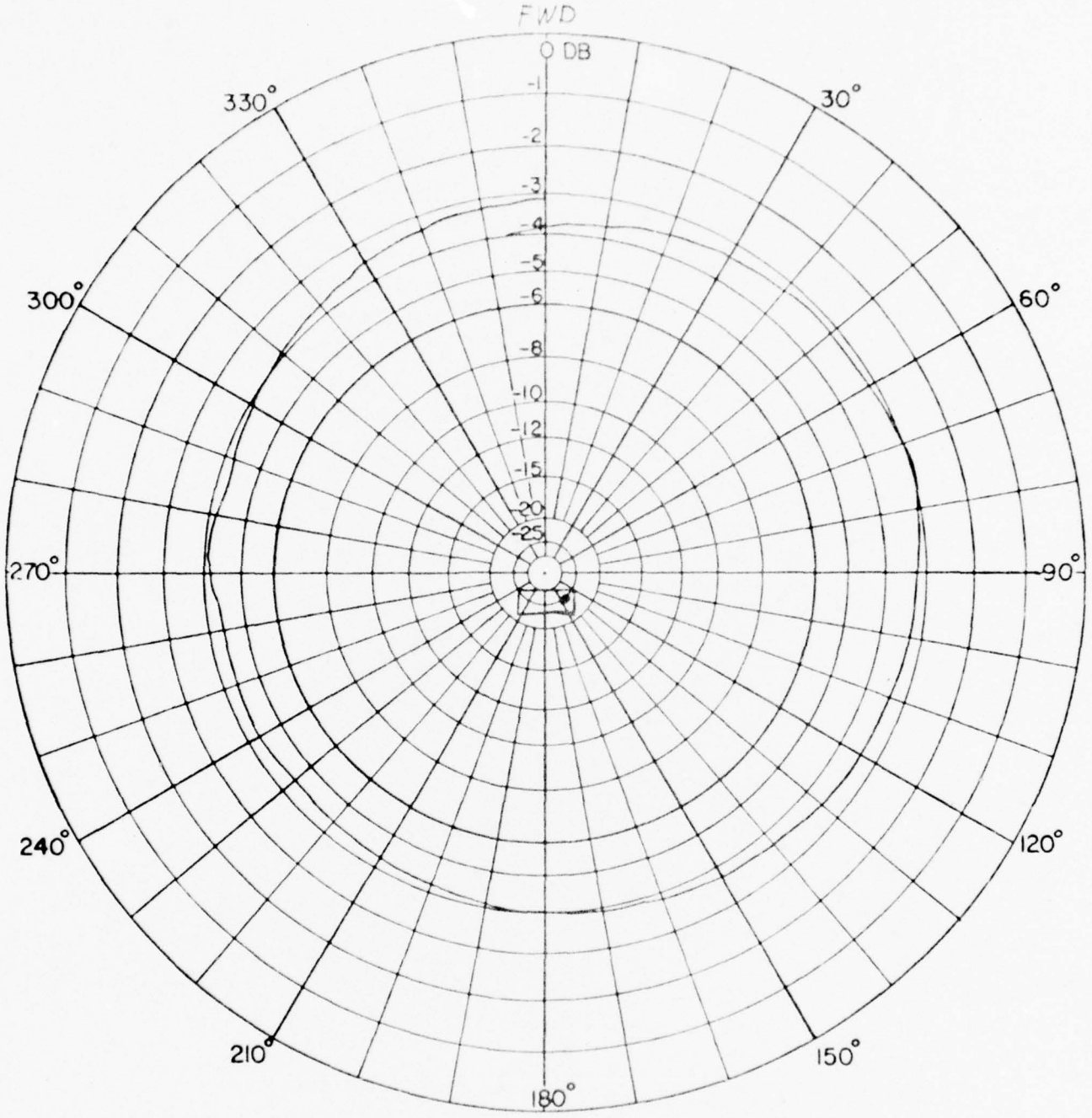

DIAGRAM	TITLE VHF - MANPACK (URC-78)
	ANTENNA 4 ft Centerfed Whip
	FREQ. 60 MHz POLARZ Vert
	MODEL SCALE EΦ= EΘ=
	DATE 4-27-77 BY [illegible]
	REMARKS Standing

FIGURE 50

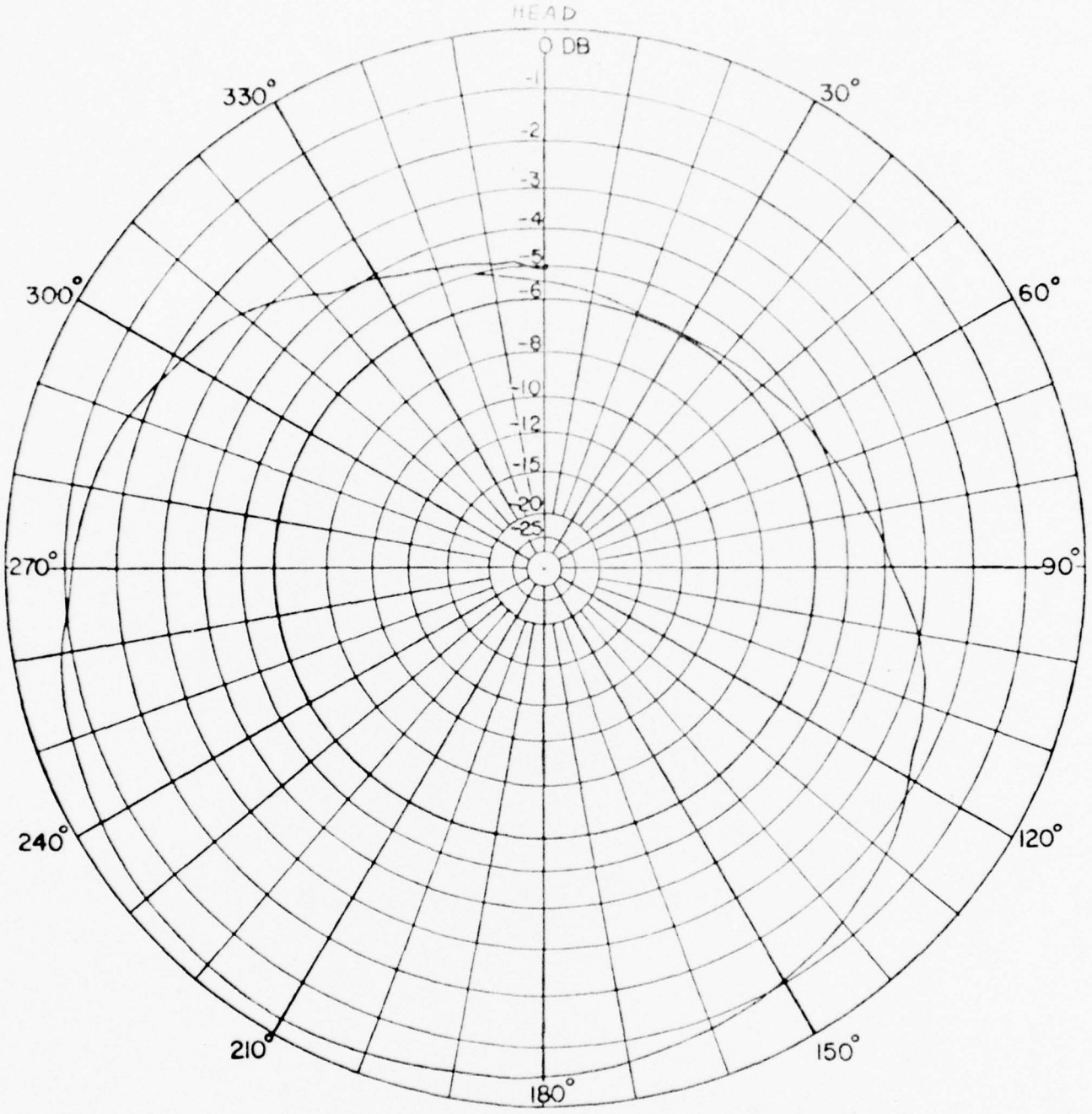

DIAGRAM	TITLE VHF MANPACK (URC-78)
	ANTENNA 4-ft Centerfed Whip
	FREQ. 60 MHz POLARZ Vert
	MODEL SCALE EΦ= EΘ=
	DATE 4-27-77 BY
	REMARKS Plane

FIGURE 51

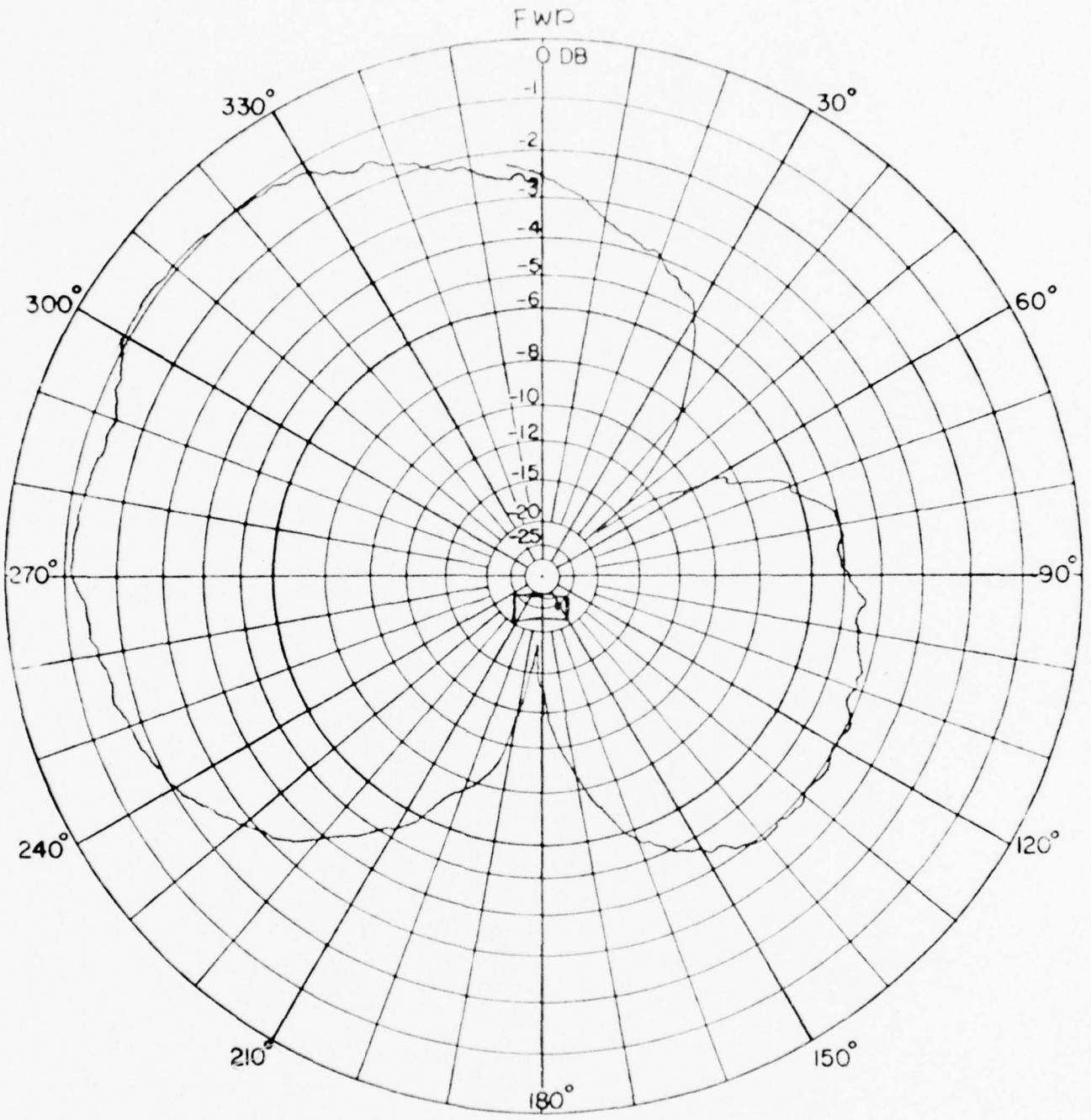

DIAGRAM	TITLE VHF MANPACK ANT
	ANTENNA Basefed Whip
	FREQ. 60 MHz POLARZ Vert
	MODEL SCALE EΦ= EΘ=
	DATE 4-27-77 BY
	REMARKS STA...

FIGURE 52

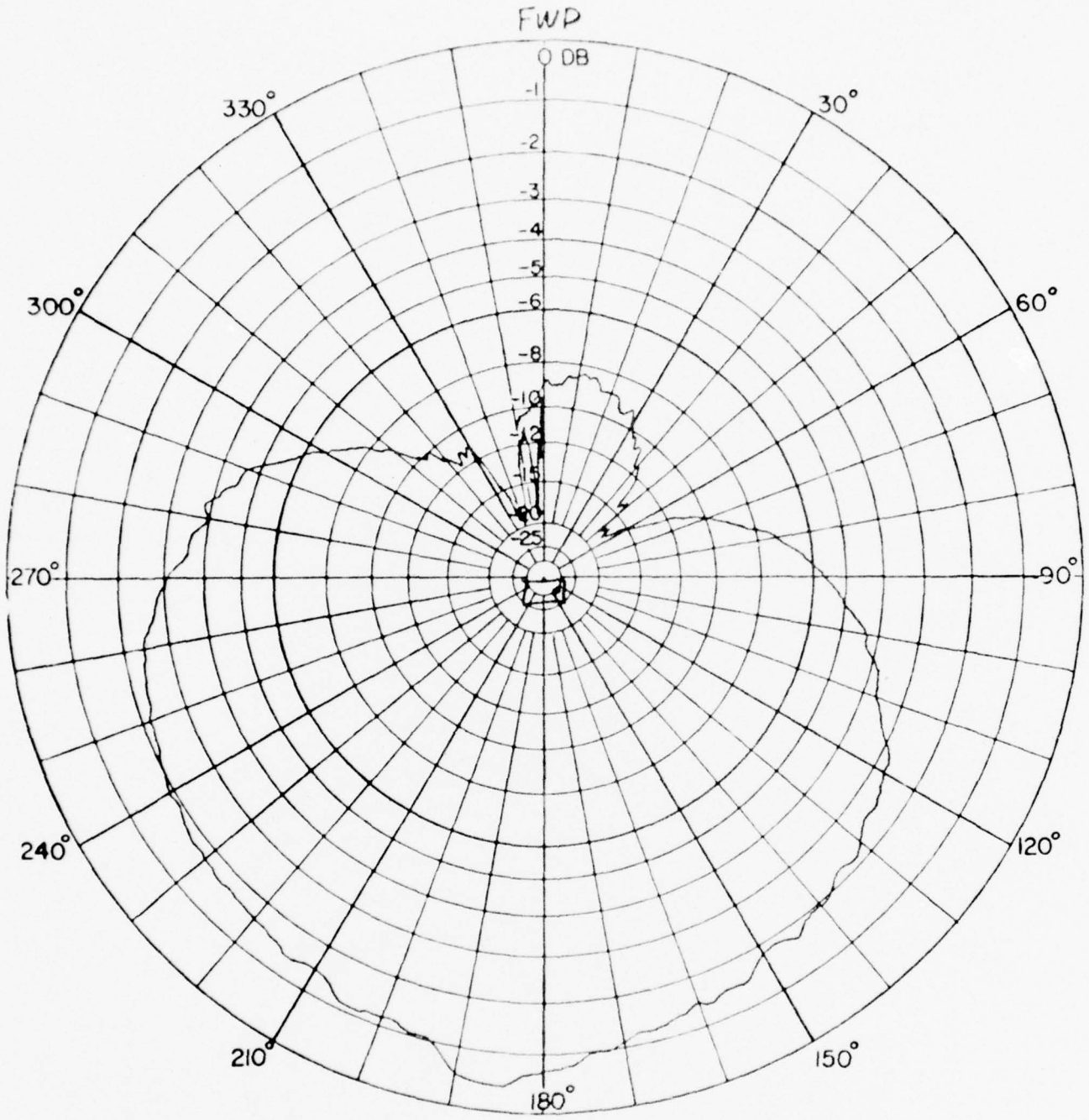

DIAGRAM	TITLE VHF MANPACK ANT
	ANTENNA Basefed Whip
	FREQ. 60 MHz POLARZ Vert
	MODEL SCALE EΦ= EΘ=
	DATE 4-27-77 BY
	REMARKS DRONE

FIGURE 53

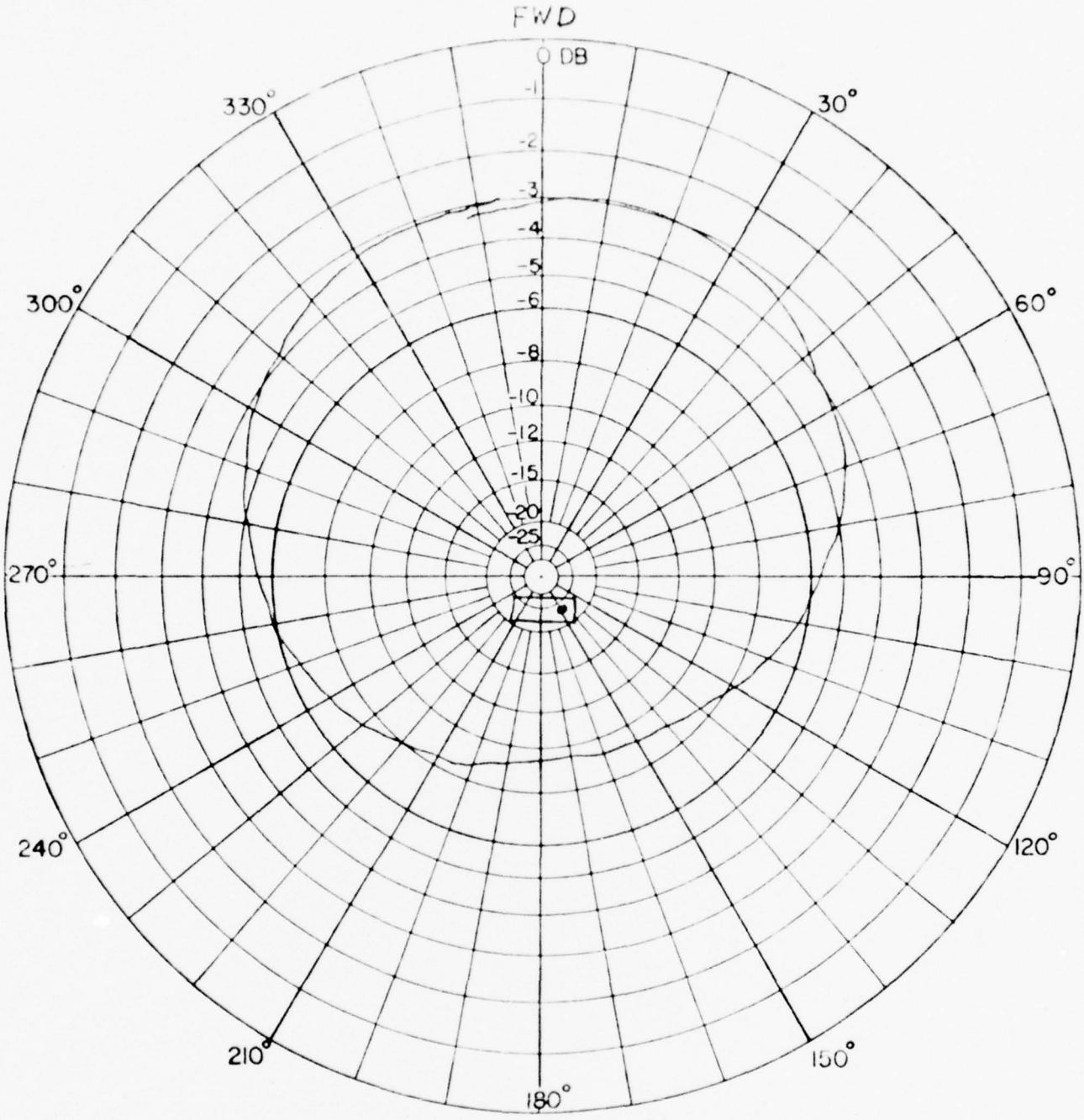

DIAGRAM	TITLE VHF MANPACK (URC-78)
	ANTENNA 4 ft Centerfed Whip
	FREQ. 70 MHz POLARZ Vert
	MODEL SCALE EΦ= EΘ=
	DATE 4-27-77 BY [illegible]
	REMARKS Standing

FIGURE 54

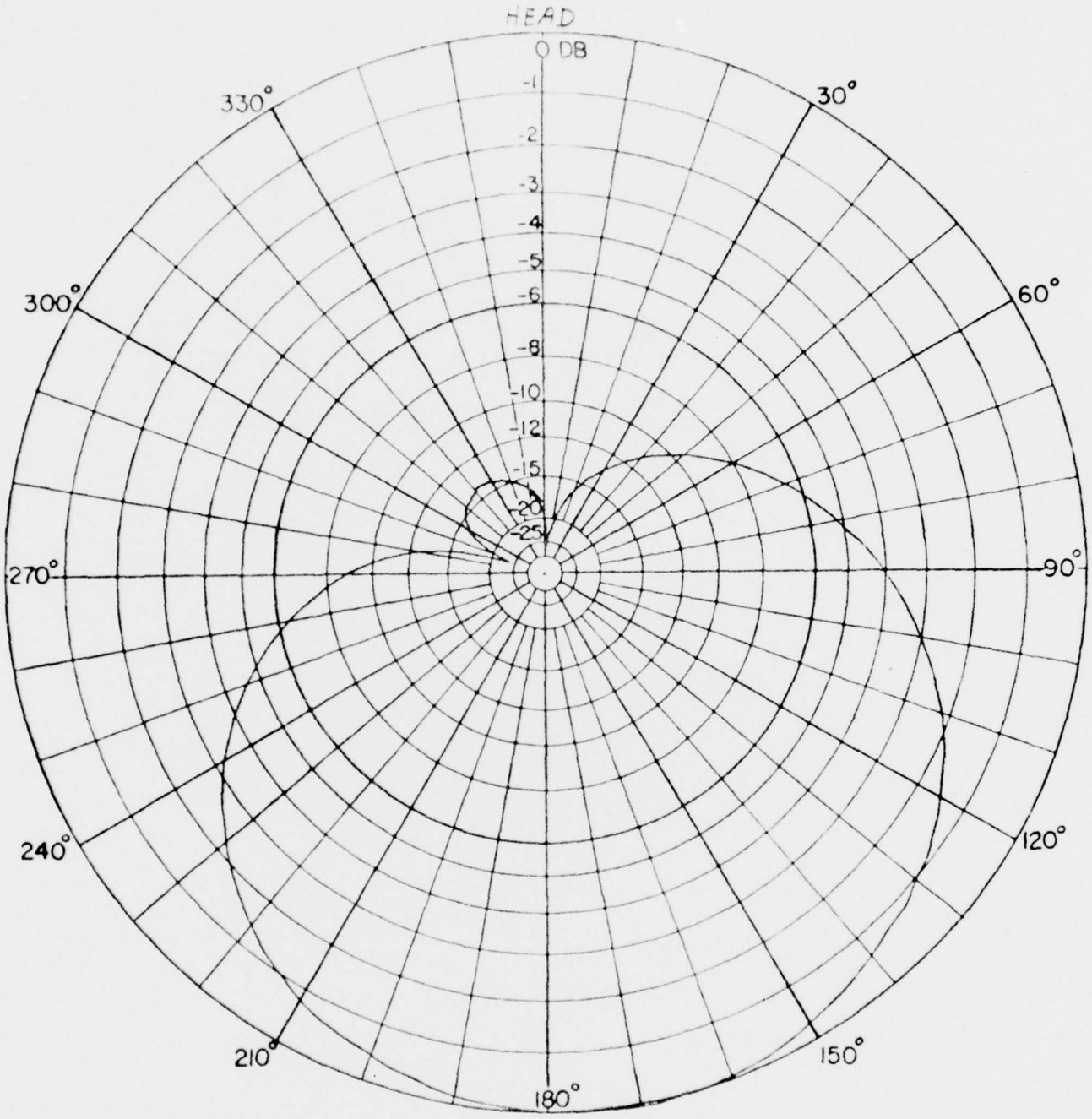

DIAGRAM	TITLE VHF MAVERICK (VHC-75)
	ANTENNA 4-ft Centerfed Whip
	FREQ. 70 MHz POLARZ Vert
	MODEL SCALE EΦ= EΘ=
	DATE 4-28-77 BY
	REMARKS Roof

FIGURE 55

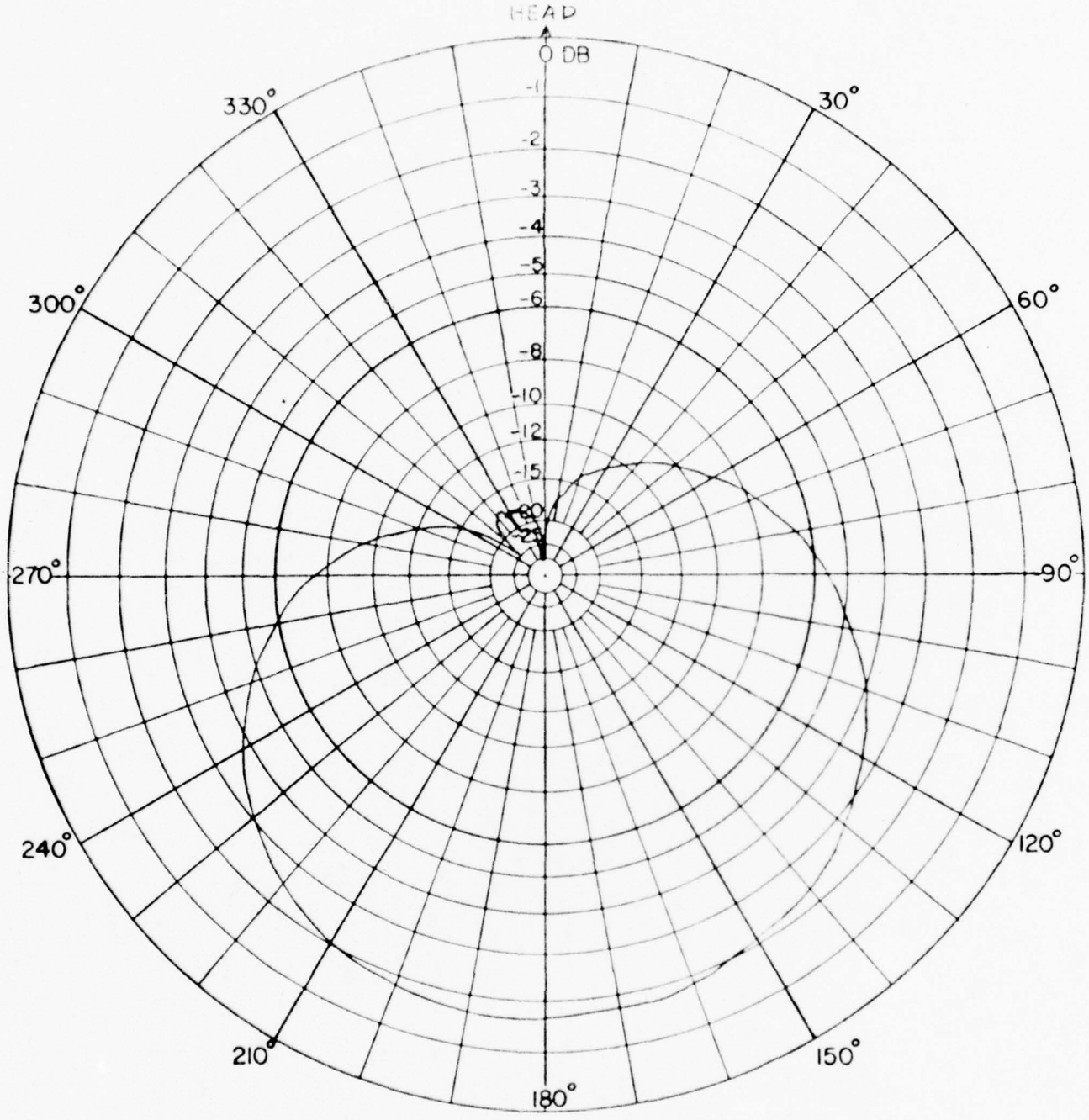

DIAGRAM	TITLE VHF MANPACK	
	ANTENNA 4-ft Centerfed Whip	
	FREQ. 70 MHz	POLARZ Vert
	MODEL SCALE	EΦ= EΘ=
	DATE 4-28-77	BY
	REMARKS Crouching	

FIGURE 56

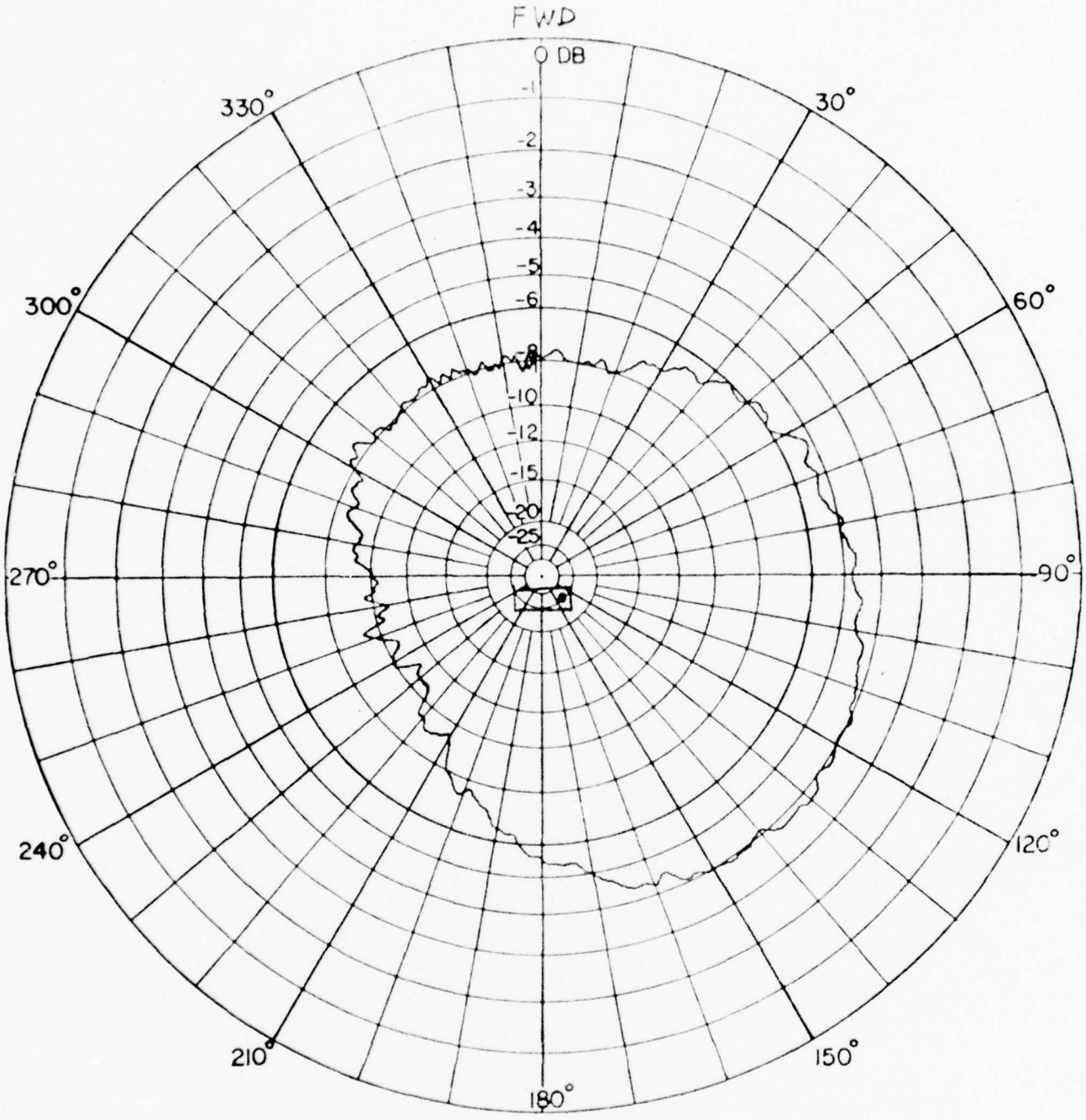

DIAGRAM	TITLE VHF MANPACK A/T	
	ANTENNA Basefed Whip	
	FREQ. 70 MHz	POLARZ Vert
	MODEL SCALE	EΦ= EΘ=
	DATE	BY
	REMARKS	

FIGURE 57

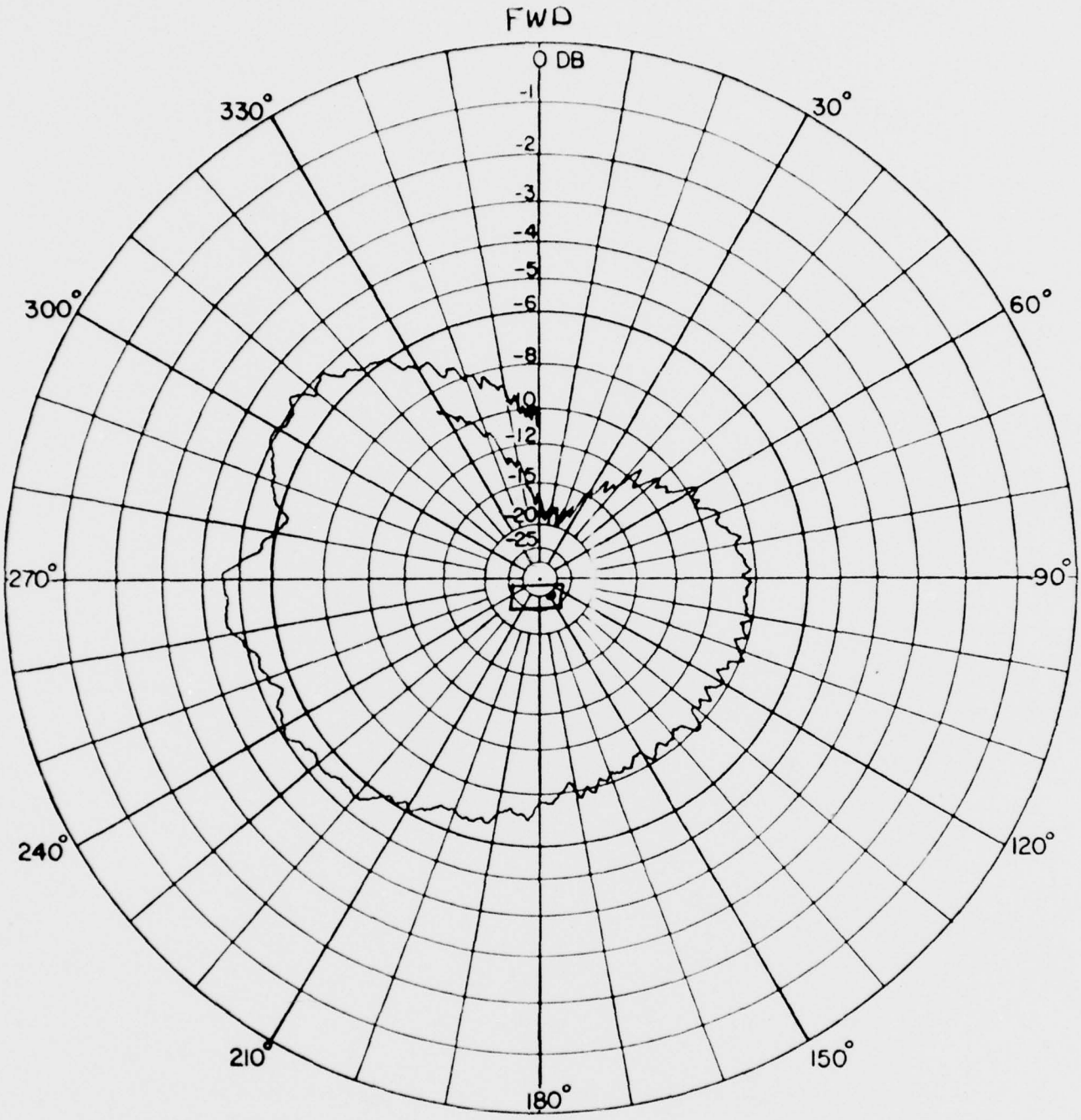

DIAGRAM	TITLE VHF MANPACK ANT	
	ANTENNA Basefed Whip	
	FREQ. 70 MHz	POLARZ Vert
	MODEL SCALE	EΦ= EΘ=
	DATE 9-27-72	BY
	REMARKS PRONE	

FIGURE 58

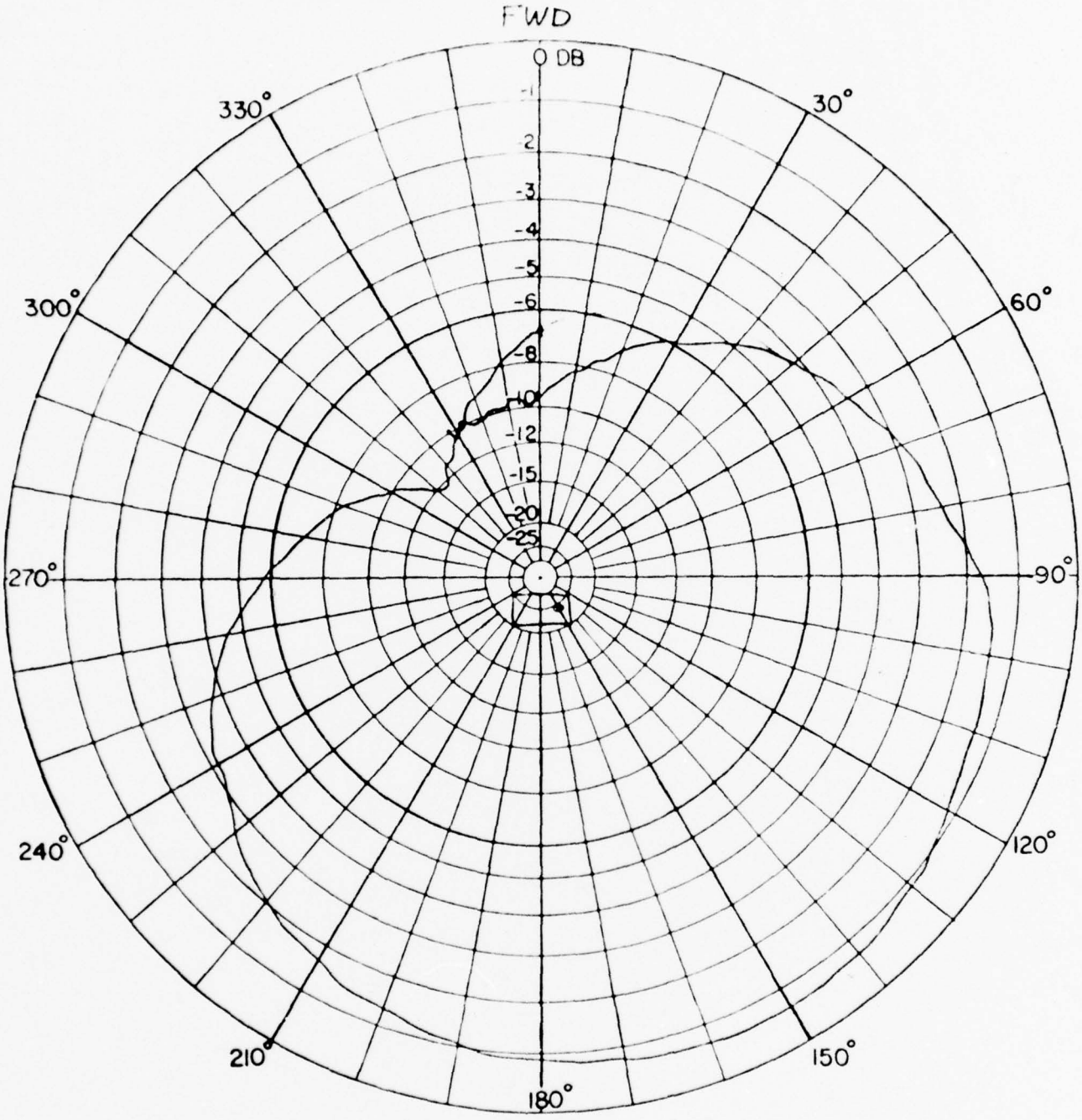

DIAGRAM	TITLE VHF MANPACK (URC-78)
	ANTENNA 4 ft Centerfed Whip
	FREQ. 80 MHz POLARZ Vert
	MODEL SCALE EΦ= EΘ=
	DATE 4-27-77 BY [illegible]
	REMARKS Standing

FIGURE 59

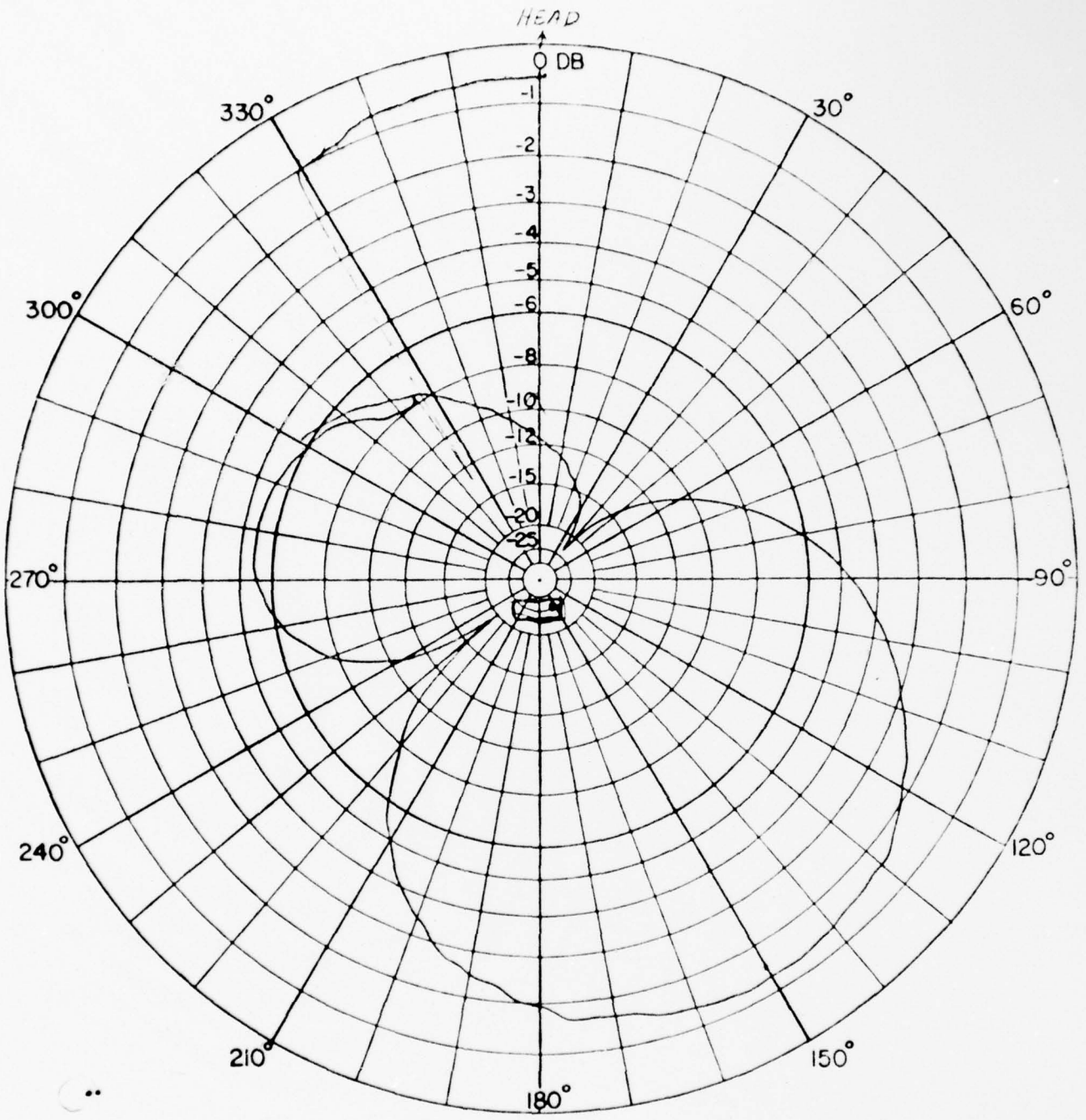

DIAGRAM	TITLE VHF MANPACK (78)
	ANTENNA 4 ft Centerfed Whip
	FREQ. 80 mc POLARZ Vert
	MODEL SCALE EΦ= EΘ=
	DATE 4/28/77 BY
	REMARKS Prime

FIGURE 60

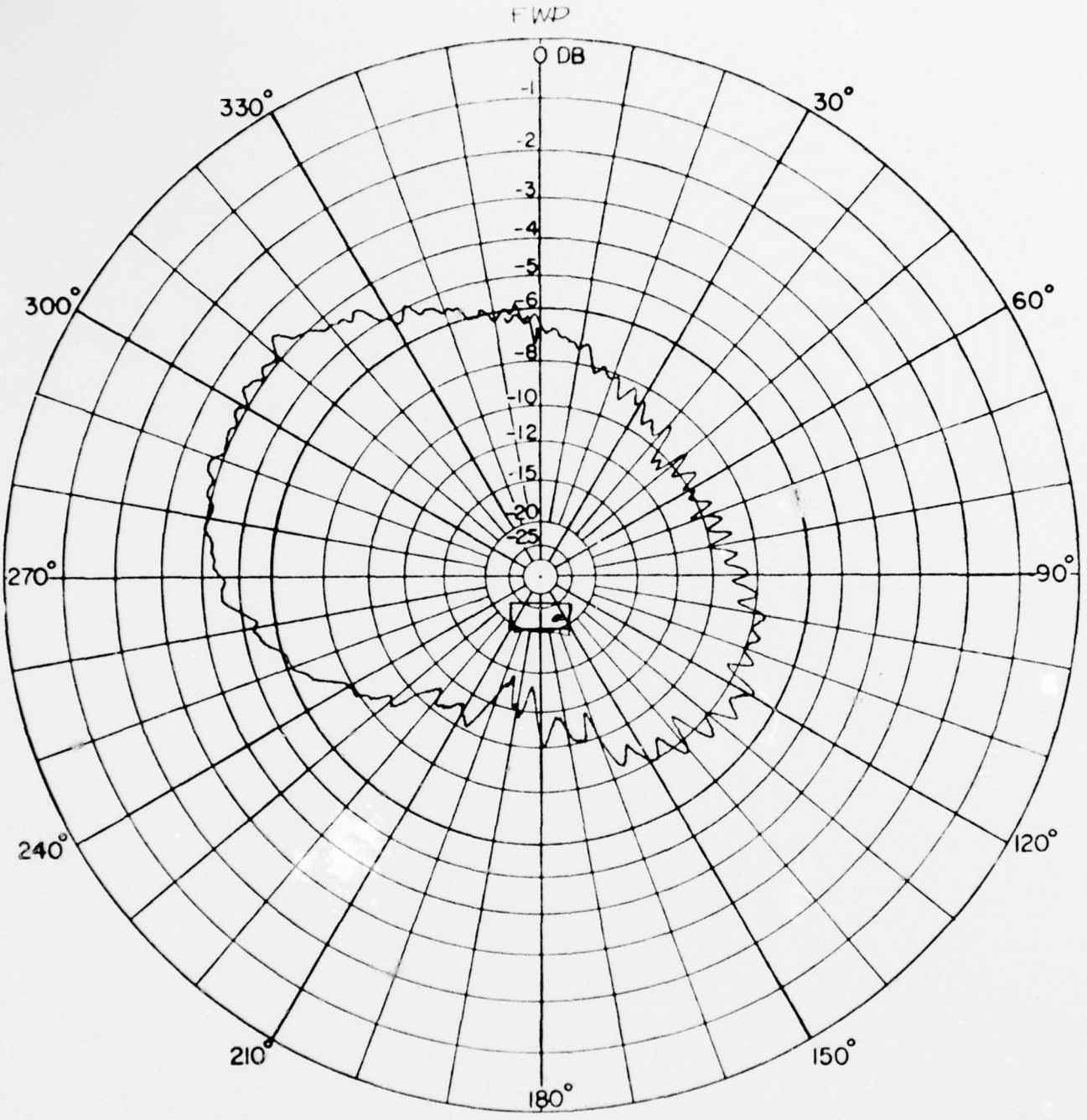

DIAGRAM	TITLE VHF MANPACK ANT
	ANTENNA Baseted Whip
	FREQ. 75 Mhz POLARZ Vert.
	MODEL SCALE EΦ= EΘ=
	DATE 4-21-72 BY
	REMARKS STD.

FIGURE 61

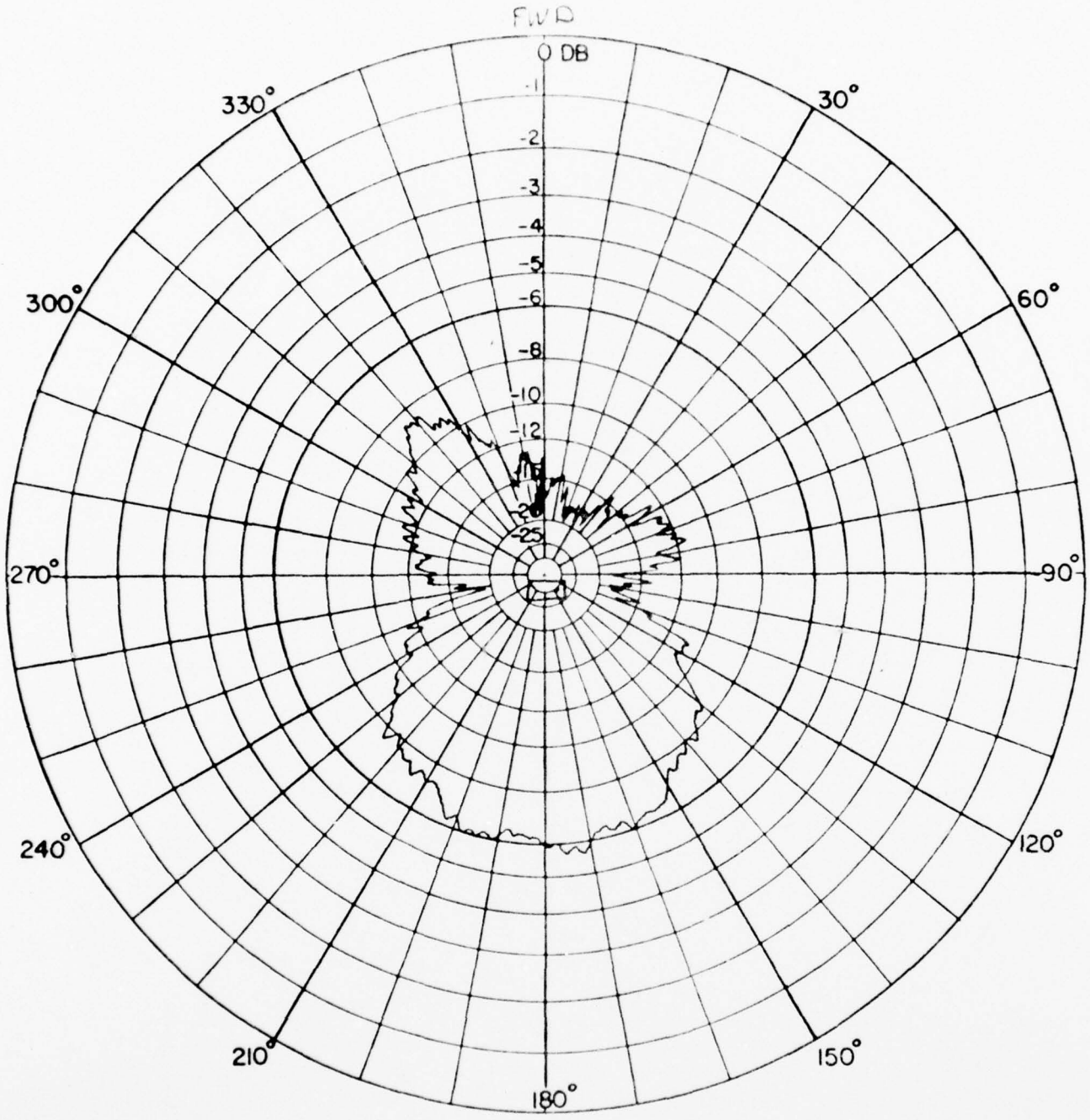

DIAGRAM	TITLE VHF MANPACK ACJT	
	ANTENNA Basefed Whip	
	FREQ. 75 MHz	POLARZ Vert
	MODEL SCALE	EΦ= EΘ=
	DATE 4-2-22	BY
	REMARKS PLOTTED	

FIGURE 62

As shown in figures 57, 58, 61 and 62 the basefed whip patterns are also rather asymmetrical at 70 MHz and 75 MHz.

The 80 MHz centerfed whip prone-pattern somewhat resembles the 60 MHz basefed whip standing pattern (see figures 52 and 60). Both of these patterns could be simulated by an array of two closely spaced elements fed in anti-phase with unequal amplitudes. For the present case these elements would be represented by the driven whip and parasitically excited operator. Apparently the excitation coefficients required to generate the observed patterns exist only over a small frequency range.

An auxiliary measurement was conducted at the center of band 4 (44 MHz) to determine the level of radiation fromthe operator's body. Referring to figure 41, a measurement was taken in the standing position with the whip vertical and bent 90°, the difference in received signal was only 1.5 dB as shown. This would indicate that significant energy is radiated by the operator's body at 44 MHz and probably at all other frequencies with variable magnitudes depending on coupling and the operator's size. Investigations of this type were not conducted at other frequencies due to time limitations; however, the measurement does indicate the significance of radiation from the operator's body.

In order to determine the effect of letting the whip drop to a horizontal orientation when in the prone position, another short test was performed at 47 MHz. With the operator in prone position on the azimuth rotator, a pattern was measured with the whip antenna oriented in the normal vertical position. The whip was then oriented horizontally, so that radiation from both the whip and operator's body would be cross-polarized relative to the vertical receiving antenna and another pattern was measured. Results of this test, as shown in figure 44, indicates that a relatively strong vertical component is radiated (only 5 to 6 dB below the vertical whip pattern) even though the operator and whip are both horizontal. It is also of interest to note that the horizontal condition pattern is nearly omnidirectional.

5.0 Summary and Conclusions

Based upon review of all test results, it is concluded that the centerfed whip antenna offers a number of advantages relative to the basefed configuration. These are as delineated below:

1. Relative to the basefed whip, centerfeeding results in a much smaller reactive antenna impedance component over the lower portion of the 30-88 MHz band. This results in less impedance dispersion when the antenna input impedance is transformed by addition of the matching network; hence, fewer subbands are required. Also, impedance variation between standing and prone positions, for the centerfed whip, is less than encountered with the basefed antenna. This allows a reasonable impedance match to be maintained for both conditions.

2. Efficiency of the centerfed whip is several dB better than the basefed whip over the lower frequency range and about equal to the basefed whip at the high end of the band. Also, the centerfed whip exhibited very good performance in the prone position.

3. Azimuth radiation patterns of both the centerfed and basefed configurations were reasonably omnidirectional over the lower (30-50 MHz) portion of the band. At 60 MHz however, the basefed whip exhibited a double lobed patrern with deep nulls in two directions. The centerfed whip showed a similar pattern for the prone position, but at 80 MHz.

In general, both antenna configurations exhibited increased directivity in the direction the operator was facing when standing and in the direction of the operator's feet when prone. This characteristic is minimal at 30 MHz (near omni pattern) and becomes increasingly pronounced at higher frequencies.

REFERENCES

(1) Z. Krupka, "The Effect of the Human Body on Radiation Properties of Small-Sized Communications Systems", IEEE Transactions on Antennas and Propagation AP-16, No. 2, March 1968.

(2) R.L. Tanner, "Theoretical Limitations of Impedance Matching", Electronics Vol. 24 pp. 234-242, February 1951.

(3) R.M. Fano, "Theoretical Limitations on the Broadband Matching of Arbitrary Impedances", Research Lab. Electronics, MIT, Tech. Rept. 41, Cambridge, Mass., January 1948.

(4) J. W. Mink, "Studies on VHF Manpack Whip Antennas"; Technical Memorandum dated 13 January 1975, Comm/ADP Laboratory USAECOM, Fort Monmouth, N.J.

APPENDIX A

HYBRID BRIDGE ACCURACY CONSIDERATIONS

When using a 180°-hybrid for impedance comparison, as indicated in the sketch below, it is of interest to investigate the difference port null as a function of reference load R & X-component variation relative to the unknown load R & X components which one desires to measure. In other words, it is desirable to determine how measurement accuracy is related to null depth for various unknown load impedance components.

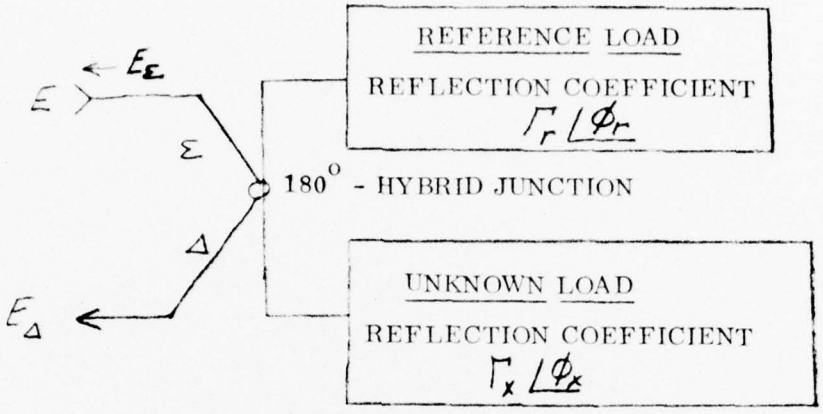

Referring to the above sketch, a voltage "E" applied to the sum port of the hybrid results in reflected voltages at the sum and difference ports given by:

$$E_\Sigma = \frac{E}{2}\left[\Gamma_r e^{j\phi_r} + \Gamma_x e^{j\phi_x}\right] \tag{A1}$$

$$E_\Delta = \frac{E}{2}\left[\Gamma_r e^{j\phi_r} - \Gamma_x e^{j\phi_x}\right] \tag{A2}$$

Expanding equations (1) and (2) yields:

$$|E_\Sigma|^2 = \frac{E^2}{4}\left[\Gamma_r^2 + \Gamma_x^2 + 2\Gamma_r\Gamma_x \cos\delta\right] \tag{A3}$$

$$|E_\Delta|^2 = \frac{E^2}{4}\left[\Gamma_r^2 + \Gamma_x^2 - 2\Gamma_r\Gamma_x \cos\delta\right] \tag{A4}$$

Where: $\delta = (\phi_r - \phi_x)$

The difference port output is maximum when $\Gamma_r = \pm 1$, $\Gamma_x = \mp 1$ and $\phi_r = \phi_x$; in other words, the voltage reflected to the difference port is equal to "E" the voltage applied to the sum port. Defining null depth as the ratio of the difference port output to the maximum possible difference port output "$E_{\Delta m}$" one obtains:

$$\text{Null Depth (dB)} = 10\log_{10}\left|\frac{E_\Delta}{E_{\Delta m}}\right|^2 = 10\log_{10}\left[\frac{1}{4}\left(\Gamma_r^2 + \Gamma_x^2 - 2\Gamma_r\Gamma_x\cos\delta\right)\right] \tag{A5}$$

If $\delta = 0$, equation (A-5) reduces to:

$$\text{Null (dB)} = 20\log_{10}\left[\frac{1}{2}\left(\Gamma_r - \Gamma_x\right)\right] \tag{A6}$$

Conversely, if $\Gamma_r \equiv \Gamma_x = \Gamma$ & $\delta \neq 0$ or $(\phi_r \neq \phi_x)$ equation (A-5) becomes:

$$\text{Null (dB)} = 20\log_{10}\left[\frac{\Gamma}{2}\sin\delta/2\right] \tag{A7}$$

Equation (A-7) shows that ϕ_r and ϕ_x must be accurately matched ($\phi \rightarrow 0$) to obtain a good null when (Γ) is large ($\Gamma \rightarrow 1$). Conversely, when Γ is small a good null can be achieved with a rather large difference between φ_r and φ_x resulting in poor accuracy. For example, if $\delta = (\phi_r - \phi_x) = 20°$ and Γ = unity equation (A-7) yields a -18 dB null, but if Γ = -10 dB a -28 dB null results, for the same 20° angular error.

The R and X impedance components are related to the reflection coefficient by the following experssions:

$$R = \frac{(1-\Gamma^2)\, Z_o}{(1+\Gamma^2) - 2\Gamma \cos\phi} \tag{A8}$$

$$X = \frac{2\Gamma Z_o \sin\phi}{(1+\Gamma^2) - 2\Gamma \cos\phi} \tag{A9}$$

If one assumes $\phi_x = -80°$, and $\phi_r = -100°$ ($\delta = 20°$) with $\Gamma = -10$ dB, the resultant measured R and X components as given by equation (A-8) and (A-9) are R = 37.2 ohms and X = 25.74 ohms; whereas the correct values are $R_x = 45.45$ ohms and $X_x = -31.45$ ohms. This represents an 18% error for both components. If ϕ_r and ϕ_x are matched within 10°, which corresponds to a null of -39 dB, the error is reduced to 10% for the R-component and 8.6% for the X-component.

The above discussion indicates that careful adjustment of the reference load reflection coefficient angle is necessary to achieve good accuracy when $|\Gamma_x|$ is small. Also, equation (A-6) shows that adjustment of the reference load reflection coefficient magnitude is not quite as critical, in terms of achieving a good null, when Γ_x is small. For example, if $\Gamma_x = -10$ dB and $\Gamma_r = \Gamma_x \pm 1$ dB a -35 dB null is realized assuming $\phi_x \equiv \phi_r$. However, the good null is misleading because a large error in the measured reactive component can result even though the resistive component error remains reasonably small. Therefore, accurate adjustment of $|\Gamma_r|$ is also necessary.

When the unknown reflection coefficient magnitude is large ($\Gamma_x \rightarrow$ unity), the bridge null is most sensitive to adjustment of ϕ_r and accurate reactive component measurements result. However, large errors in the resistive component will occur if $|\Gamma_r|$ does not accurately match the unknown load reflel tion coefficient magnitude, even though a deep null is achieved.

If the variable reference load is constructed by placing a variable attenuator in series with a variable reactance, as sketched below; the attenuator insertion loss (practical values being 0.2 to 0.5 dB) becomes the limiting factor when measuring high reflection coefficient loads.

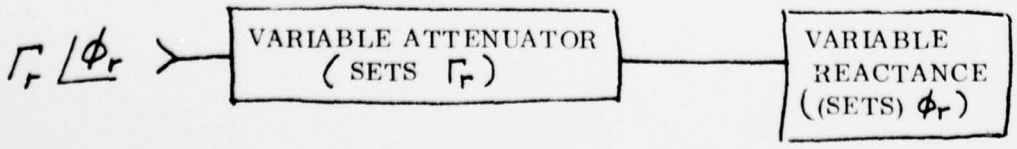

For example, if $|\Gamma_x|$ is 1% less than $|\Gamma_r|$ a 45 dB null can be achieved by setting $\phi_r = \phi_x$, but the error in the measured **R**-component will be 50% for $\phi_r = \phi_x = \pm 45$ degrees. Therefore, when measuring high $|\Gamma|$ loads it is advisable to make sure that the attenuator is not set at minimum even though a good null is achieved; because, there may be a small difference between $|\Gamma_r|$ and $|\Gamma_x|$ resulting in large R-component error, as discussed above. In other words, the attenuator adjustment should allow the null indicator to pass through a minimum before reaching the lower limit of attenuation adjustment. If this cannot be directly accomplished, a reactance of known value can be placed in series with the unknown impedance to transform the reflection coefficient to a lower value. The impedance thus measured can then be corrected by deducting the known reactance.

APPENDIX B

IMPEDANCE CHARACTERISTIC PLOTS

FOR

STANDING, STANDING WITH HANDSET EXTENDED

AND PRONE CONDITIONS

FEED LINE CHARACTERISTIC IMPEDANCES

(75, 95 and 125 Ohms)

FEED POINT LOCATIONS

(17 Inch, 19 Inch and 21 Inch)
ABOVE BASE OF WHIP

IMPEDANCE COORDINATES — 50-OHM CHARACTERISTIC IMPEDANCE

ENG. DEV. MOD.
FP = 17"
$Z_0 = 75\Omega$
STANDING

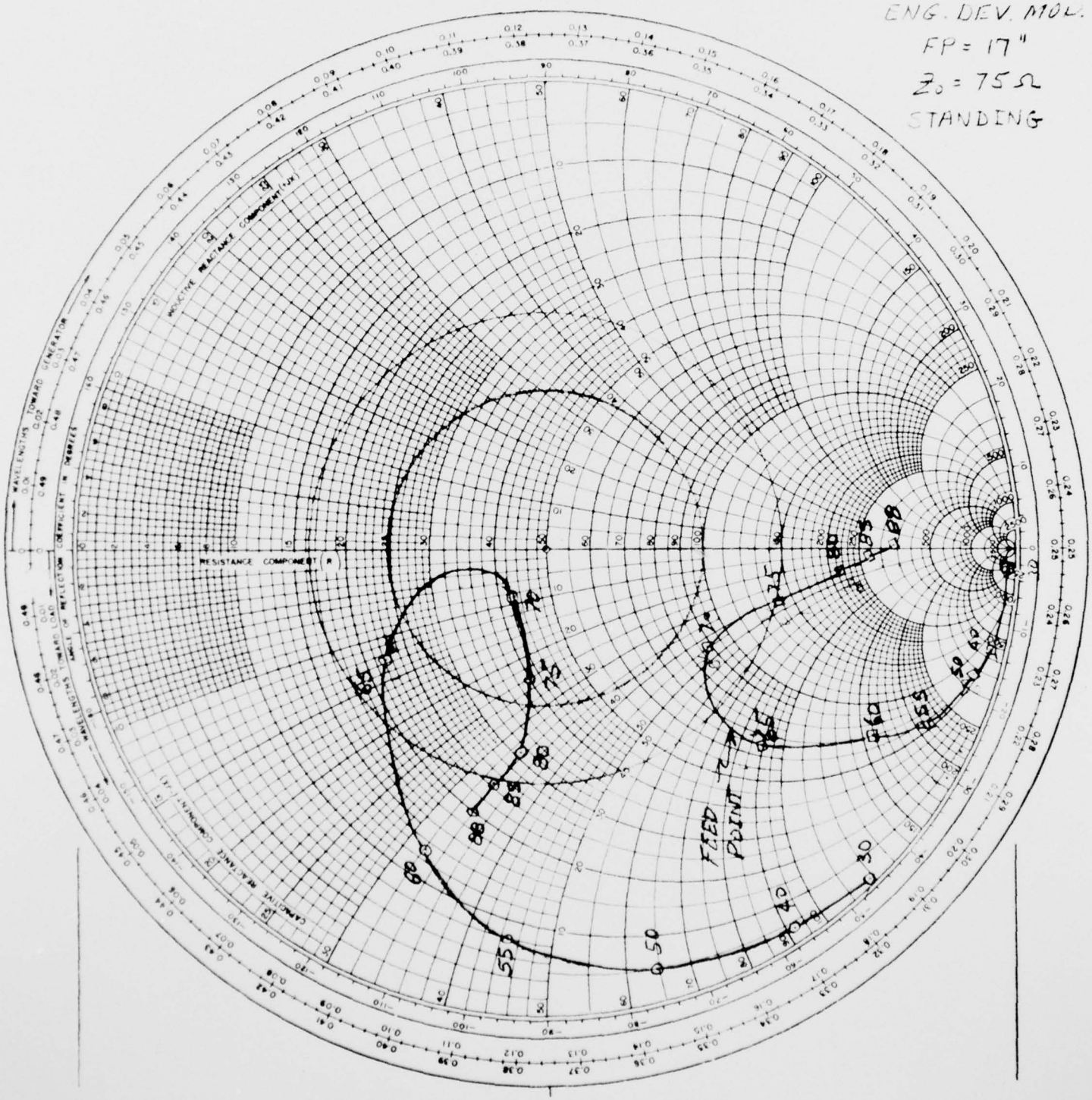

FIGURE B-1

EXP. DEV. MODEL
E.P. = 17"
$Z_0 = 75\,\Omega$
STANDING
HANDSET EXT

IMPEDANCE COORDINATES—50-OHM CHARACTERISTIC IMPEDANCE

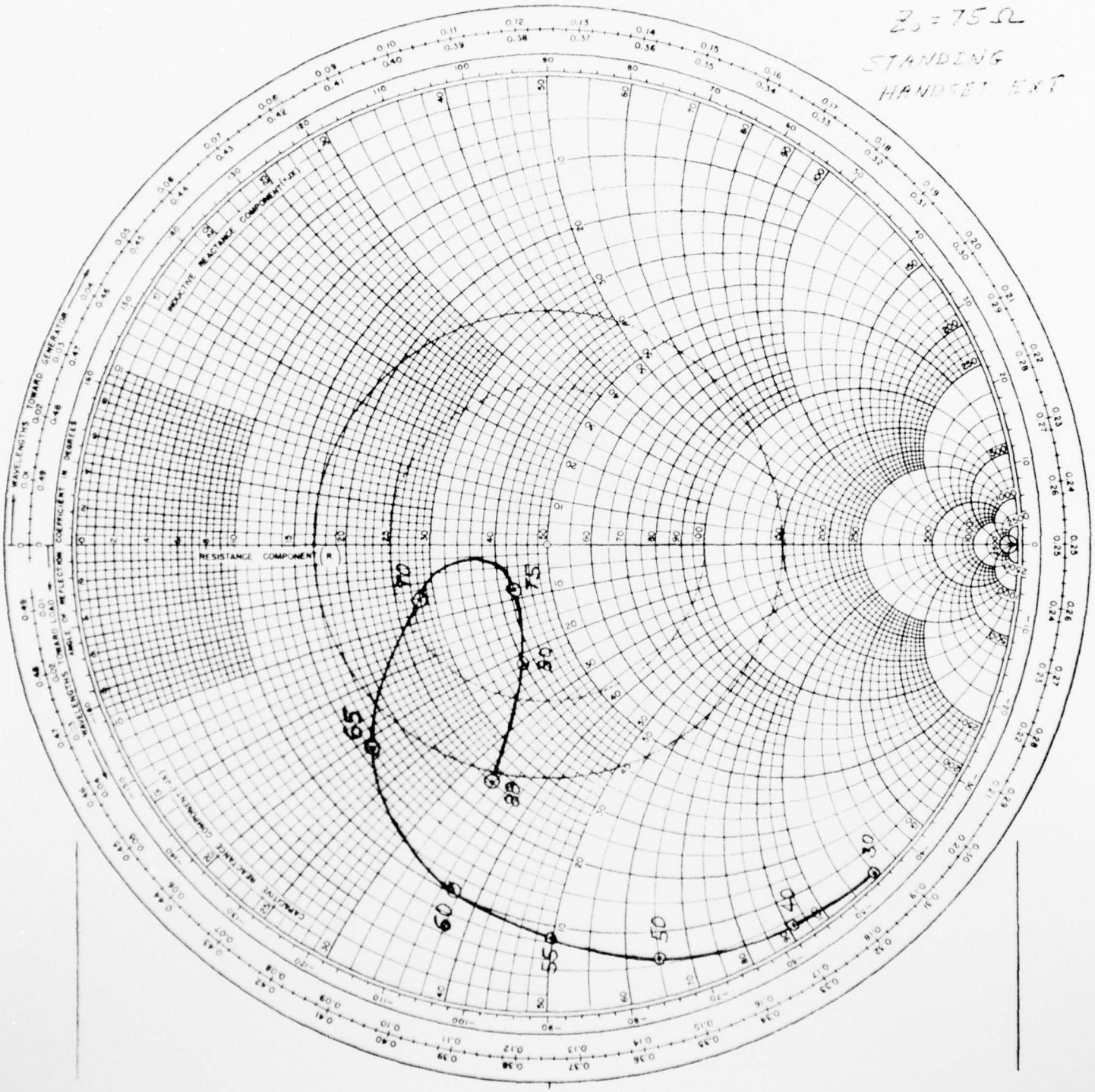

FIGURE B-2

ENG DEVELOP. MOD
FP = 17"
$Z_0 = 75\,\Omega$
PRONE

IMPEDANCE COORDINATES — 50-OHM CHARACTERISTIC IMPEDANCE

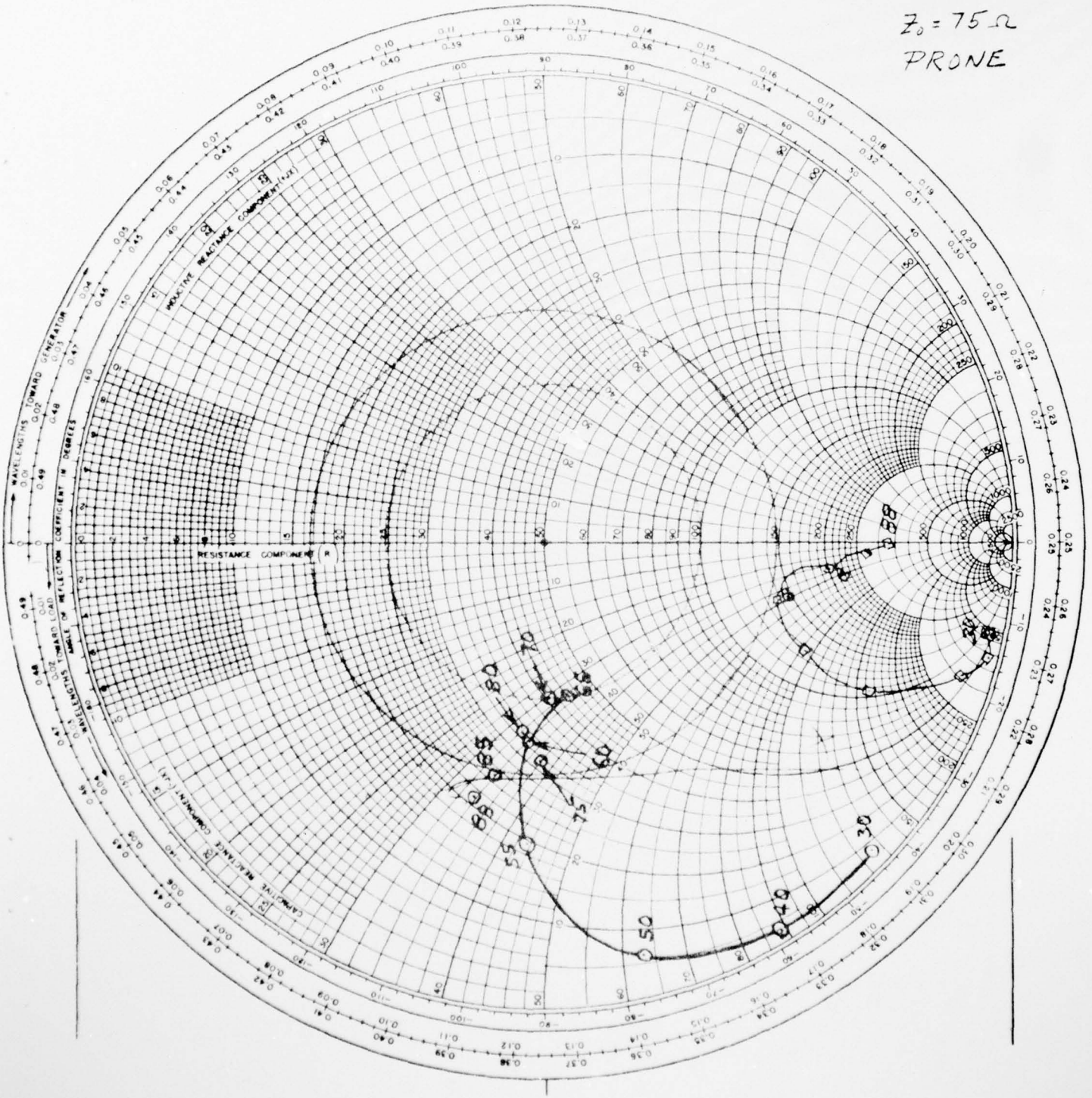

FIGURE B-3